

2015-08-10

Growth, Mortality, and Availability of Eastern Pacific Sailfish

Mark Daniel Fitchett

University of Miami, mfitcett@rsmas.miami.edu

Follow this and additional works at: https://scholarlyrepository.miami.edu/oa_dissertations

Recommended Citation

Fitchett, Mark Daniel, "Growth, Mortality, and Availability of Eastern Pacific Sailfish" (2015). *Open Access Dissertations*. 1506.
https://scholarlyrepository.miami.edu/oa_dissertations/1506

This Embargoed is brought to you for free and open access by the Electronic Theses and Dissertations at Scholarly Repository. It has been accepted for inclusion in Open Access Dissertations by an authorized administrator of Scholarly Repository. For more information, please contact repository.library@miami.edu.

UNIVERSITY OF MIAMI

GROWTH, MORTALITY, AND AVAILABILITY OF EASTERN PACIFIC SAILFISH

By

Mark Daniel Fitchett

A DISSERTATION

Submitted to the Faculty
of the University of Miami
in partial fulfillment of the requirements for
the degree of Doctor of Philosophy

Coral Gables, Florida

August 2015

©2015
Mark Daniel Fitchett
All Rights Reserved

UNIVERSITY OF MIAMI

A dissertation submitted in partial fulfillment of
the requirements for the degree of
Doctor of Philosophy

GROWTH, MORTALITY, AND AVAILABILITY OF EASTERN PACIFIC SAILFISH

Mark Daniel Fitchett

Approved:

Nelson M. Ehrhardt, Ph.D.
Professor of Marine Biology and Fisheries

Jerald S. Ault, Ph.D.
Professor of Marine Biology
and Fisheries

Andrew Bakun, Ph.D.
Professor of Marine Biology and Fisheries

Elizabeth A. Babcock, Ph.D.
Associate Professor of Marine
Biology and Fisheries

David J. Die, Ph.D.
Research Associate Professor of Marine
Biology and Fisheries

Dean of the Graduate School

Christopher M. Legault, Ph.D.
Supervisory Research Fishery Biologist
National Marine Fisheries Service
Woods Hole, Massachusetts

FITCHETT, MARK DANIEL
Growth, Mortality, and Availability of
Eastern Pacific Sailfish

(Ph.D., Marine Biology and Fisheries)
(August 2015)

Abstract of a dissertation at the University of Miami.

Dissertation supervised by Professor Nelson M. Ehrhardt.
No. of pages in text. (185)

The Indo-Pacific sailfish, *Istiophorus platypterus*, has significant ecological and socioeconomic importance in the tropical eastern Pacific Ocean (EPO). It is caught as bycatch in tuna commercial fisheries, but targeted in economically important catch-and-release recreational fisheries. The sustainability of this valuable resource had not been successfully assessed due to poor fishery landings and effort data with unreliable demographic estimates for sailfish. The goal of this dissertation was to assess lifetime demographics and stock mortality rates of sailfish and to infer ecosystem dynamics that drive availability of sailfish to recreational fisheries. This dissertation developed a new age and growth model for sailfish in the EPO. An improved set of growth parameters representing the regional distributional range of sailfish in the EPO were obtained by mixture distribution analyses on a large length frequency database and by incorporating size-at-age results from existing studies. A numerical algorithm, Statistical Age-Length Key (StALK), was developed using the new growth parameters and variance of sizes-at-ages to compute expected probabilities of ages-at-size. The StALK algorithm was validated with known simulated fishery age-structured data under varying levels of recruitment, exploitation, size selectivity, and random error. Simulation experiments showed the statistical robustness and limitations of StALK at producing reliable age frequency distributions at size from observed length-frequency distributions. StALK was

applied to annual sailfish length-frequencies from 1991-2010 from the non-selective EPO purse seine fishery. Age frequencies resulting from StALK were used to estimate total mortality rates for a data-poor EPO sailfish fishery using catch curve analysis of resulting age frequencies and compared well with length-based methods. Age frequencies resulting from StALK for sailfish produced instantaneous fishing mortality rates that exceeded precautionary benchmarks ($F_{0.1}$) for fishing mortality for all but two years. These results indicate that sailfish in the EPO are experiencing overfishing, indicating the need for urgent fishery management. Generalized multiple linear model analysis reveal that recruitment of EPO sailfish is dependent on time-delayed ocean current indices (e.g., intensity of northern equatorial currents). Ocean current indices significantly predict recruitment of age 5 sailfish, the first fully recruited age class into recreational fisheries. Sailfish CPUE in recreational fisheries appear to be driven by oceanographic variables such as sea surface height and ocean currents. These variables are responses to local upwelling and shallowing of the oxygen minimum layer which concentrates fish in limited areas, inflating sailfish catch rates in regional recreational fisheries. Satellite logbook systems installed on recreational vessels in Guatemala and Costa Rica demonstrated the negative effects of vessel crowding relative to the sailfish catch efficiency (fishing success). It is concluded that expansion of tourism-based recreational fisheries in the region could have deleterious effects on fishing success if these fisheries are not cooperatively managed throughout the Central American Isthmus.

DEDICATION

I dedicate this work to my mother and father, Donna and Reid Fitchett, and to my older “big” brother Paul Fitchett- for their unconditional love and support throughout my life and always encouraging me in all that I do. They always fostered my curiosity for the ocean and taught me to do what is right, to not be selfish, and to remain diligent.

ACKNOWLEDGEMENTS

First and foremost, I would like to thank and extend my most sincere gratitude to Dr. Nelson Ehrhardt for his guidance and mentorship. When we began working together in 2004, the idea for a billfish research program was just a dream and it started from scratch. It all began from our first trip together in Guatemala in 2007 with just a clipboard and a pen walking around marinas and collecting cursory data on fishing boats and catch information in 100 degree heat. Less than eight years later, we have a full team of four, we have implemented state-of-the-art technologies to collect data, we have deployed 60 satellite tags on billfish throughout the entire Central American region, we were the impetus for political action on billfish conservation in Central America, our presence is known throughout the region, and our work lead to the first-ever national commission for the conservation of sailfish. Nelson has taught me to think big, persevere, and be resourceful. And in the last several years, we have done just that. Most importantly, Nelson had faith in me and that is the greatest gift one can give another.

I sincerely thank my committee members for their advice, guidance, and insights: Drs. Jerry Ault, David Die, Beth Babcock, Andy Bakun, and Chris Legault.

I would also like to thank my fellow lab mates for their help, advice, and friendship. I thank Vallierre Deleveaux for tolerating years of sharing an office with me. I thank Bruce Pohlot for making tagging trips more enjoyable and Julie Brown for the entertaining banter.

I thank my fellow graduate student fisheries friends (“2nd Floor Crew”) past and present: Nathan Vaughan, Mike Larkin, Nick Farmer, Ashley McCrae-Strub, Marc

Nadon, Mike Feeley, Dominique Lazarre, Elizabeth Council, Holly Perryman, Molly Adams, Steve Saul, and Francesca Forrestal. As well as non-fisheries friends over the years- Adam Greer, Andrew Kough, Will Komaromi, Lyza Johnston, Rebecca Albright, Monica Arienzo, Brian Giebel, Chelsea Pederson, Paul Jones, Michelle Harangody, and Tara Baris. I thank fellow Wetlab staff for all the great memories and fellowship.

I also especially thank friends who were always supportive and there for me even when I didn't deserve it- Ian Zink, Crawford Drury, Eli Langford, Scott Eaddy, Kristine Stump, Dan Goethel, Rolando Santos, Quinn Devlin, and Stephanie Schopmeyer.

The work completed in this dissertation was partially supported by the NOAA/Sea Grant Population Dynamics Fellowship Program. I thank all those involved with the Fellowship Program. Other fellowships contributing financial support include: The Manasquan River Marlin and Tuna Club George Burlew Scholarship, Miami Billfish Tournament, The International Light Tackle Tournament Association, and the International Women's Fishing Association.

The Central American Billfish Association provided support for activities that lead to this Dissertation. I thank Casa Vieja Lodge in Guatemala for their unwavering support and their captains for contributing time and data. I thank Guatemalan Billfish Adventures and Pacific Fins for providing data and information. I thank Crocodile Bay Lodge in Costa Rica for all the support and for providing data and information. I thank George and Anna Beckwith of the Dragin Fly in Costa Rica. Thanks to the crew of the Typhoon in Golfito, Costa Rica.

Last but not least, I thank Tim Choate for his everlasting support, vision, and belief in us to put our ideas into fruition.

TABLE OF CONTENTS

	Page
LIST OF FIGURES	viii
LIST OF TABLES	xiv
Chapter	
1 INTRODUCTION	1
1.1 Indo-Pacific Sailfish Biology.....	1
1.2 Notable Billfish Sportfisheries in the EPO.....	4
1.3 Exploitation and Significance of Billfish in the EPO.....	7
1.4 Habitat Compression Impacts on EPO Sailfish.....	12
1.5 Problem Identification, Goals, Objectives	16
2 GROWTH OF SAILFISH IN THE EASTERN PACIFIC OCEAN	18
2.1 Background and Existing Information on Growth.....	18
2.2 Materials and Methods.....	20
2.3 Results of New Growth Analyses.....	33
2.4 Discussion and Significance	40
3 DETERMINATION OF EXPLOITATION AND MORTALITY	49
3.1 Motivation and Background	49
3.2 New Methods, Model Testing, and Application.....	55
3.3 Results	74
3.4 Discussion and Novelty	91
4 DYNAMICS OF LOCAL AVAILABILITY AND FISHING SUCCESS OF RECREATIONAL FISHERIES	104
4.1 Background.....	104
4.2 Materials and Methods.....	107
4.3 Implementation and Results	123
4.4 Discussion	137
5 CONCLUSIONS.....	147
Recommendations and Future Work	152
REFERENCES.....	155

APPENDIX A. Profiles of Residuals by Adjusting Mean Size at Age in MIX Analyses.....	168
APPENDIX B. Introducing a Selectivity Pattern Estimation Methodology.....	170
APPENDIX C. Red Snapper Growth, ALKs, and Estimated ALKs.....	174

List of Figures

- Figure 1.1.1. Mapping of nominal CPUE (# fish per 1000 hooks) for sailfish and shortbill spearfish from high seas longline gear (IATTC, 2001). The EPO is defined by red border. “Area 2” is within the EPO where Joseph et al. (1974) found catch composition to be nearly entirely sailfish.....2
- Figure 1.2.1. Recreational catch rates of sailfish (per day) in destinations within the EPO (from: Ehrhardt and Fitchett, 2006).....5
- Figure 1.2.2. Notable locations for billfish sportfisheries in Central America: 1) Puerto San Jose, Guatemala, 2) Guanacaste, Costa Rica 3) Jaco/Herradura/Quepos, Costa Rica 4) Gulfo Dulce, Costa Rica 5) Chiriqui, Panama and 6) Darien, Panama.....6
- Figure 1.3.1. Annual average catch rates for: (A) Iztapa, Guatemala; and (B) Costa Rican locations in recreational catch-and-release fisheries (Ehrhardt and Fitchett, 2008).....9
- Figure 1.3.2. Historical trophy size (lbs) and Japanese longline CPUE (Fish/100 Hooks) by year for sailfish in the EPO (Ehrhardt and Fitchett, 2006). Trophy size data from International Gamefish Association (IGFA) and CPUE data from IATTC.....11
- Figure 1.3.3. Billfish landings, billfish exports to the USA, and Mahi mahi landings from Costa Rica, 1997 to 2007 (From: Ehrhardt and Fitchett, 2009, *unpublished report*).....12
- Figure 1.4.1. Color contour plot of depth of dissolved oxygen minimum layer (1 mg/L seawater) in waters within the EPO. (Data from: World Ocean Atlas, 2009; Estimated and interpolated in R, R Statistical Environment, 2014).....14
- Figure 1.4.2. Monthly variability of the thermocline, mixed layer and minimum (1ml/l) of dissolved Oxygen (DO₂) off the coast of Guatemala (adapted from NORAD UNDP/FAO, 1988 in Ehrhardt and Fitchett, 2006) during Non-El Nino year.....15
- Figure 2.2.1. Sailfish length-frequency sample sizes from the EPO purse seine fishery by 5° x 5° degree latitude-longitude grid. Outside thick black border indicates range of length observations and red border indicates area of high sailfish relative densities per exploratory longline surveys in the 1960’s prior to heavy fishing in the region (Joseph et al. 1974).....22
- Figure 2.2.2 Length frequency distribution of sailfish lengths, aggregated from 1991 to 2010. Length frequencies were weighted by catches (in numbers) in 5° x 5° degree grids, months, and years for which they originated.....24

Figure 2.2.3. Color map of average length (cm, EFL) of observed sailfish from IATTC observer program, 1991-2010.....	25
Figure 2.2.4. Flowchart for analysis of length frequency data to estimate parameters for MIX, simulating lengths and age, and fitting a growth model of EPO sailfish.....	29
Figure 2.3.1. Mixture distributions for age groups versus length (red line) adding to an integrated probability distribution (green) versus a length frequency distribution from the years 1991-2010.....	36
Figure 2.3.2. Length frequency distributions of size at age for Age 3 (red) and 4 (blue) sailfish used in MIX analyses and those estimated by Cerdaneres-Ladrón De Guevara et al. (2011).....	37
Figure 2.3.3. Simulated age class 0 sailfish lengths at age (n =1000) generated from size at age parameters by Sponaugle et al. (2010).....	38
Figure 2.3.4. Fan plot of EPO sailfish von Bertalanffy growth function with 95% confidence interval of length at age fitted to 1100 simulated lengths at age for sailfish ages 0, 2 to 11 years. Observed Age 3 and 4 sailfish from Cerdaneres-Ladrón De Guevara et al. (2011) plotted as white circles.....	39
Figure 2.4.1. Length frequency data histogram from region wide growth analyses for EPO sailfish with an estimated von Bertalanffy growth function (solid line) slicing through the distribution with 95% confidence intervals (dashed lines) of size at age estimated by the growth equation.....	41
Figure 2.4.2. Histograms of length-frequency data used in notable growth analyses for sailfish (green: Cerdaneres-Ladrón De Guevara et al., 2011, blue: Chiang et al., 2004, red: this study) with fitted von Bertalanffy growth trajectory. Primary response axis is frequency of fish in 5 cm bins, secondary response axis is age.....	45
Figure 2.4.3. Simulated theoretical length distribution of an unexploited population of EPO sailfish for ages 2 to 11 using growth parameters estimated in this chapter.....	48
Figure 3.1.1. Redrawn from Legault (1996): Depiction of three growth trajectories (circle, triangle, and square) passing through age and size bins, increasing in finite a+1 ages groups and by L+i size groups depending on growth parameters selected from a known distribution.....	54
Figure 3.2.1- Fish with an assigned, heritable “size predisposition” deviance, a z-score equal to 1 from a surrogate Gaussian distribution (solid line) subjected to a size-dependent exploitation pattern and age-specific mortality throughout time (ages 0 to 3, dashed lines).....	58

Figure 3.2.2. Cumulative densities of selected observed length-frequencies (black) and corresponding fitted cumulative densities from estimates of StALK (red)	63
Figure 3.2.2. A color image plot of a theoretical ALK constructed for sailfish for ages 2 to 11 in catches	64
Figure 3.3.1. CPUE index (red) from <i>SimCatch</i> and recruitment (black) for a simulated sailfish fishery. Recruitment is 20 % random variability, +/-10%.....	75
Figure 3.3.2. CPUE index (red) from <i>SimCatch</i> and recruitment (black) for a simulated sailfish fishery. Recruitment is 40 % random variability, +/-20%.....	76
Figure 3.3.3. Total mortality, Z , estimated through age-structured catch curve by StALK and from simulated age compositions, 20% random recruitment	79
Figure 3.3.4. Total mortality, Z , estimated through age-structured catch curve by StALK and from simulated age compositions, 40% random recruitment	79
Figure 3.3.5. Age frequencies estimated in Year 14 by StALK and from a simulated fishery for Year 14 in a fishery experiencing 20% random recruitment	80
Figure 3.3.6. Age frequencies estimated in Year 14 by StALK and from a simulated fishery for Year 14 in a fishery experiencing 40% random recruitment	81
Figure 3.3.7. Selectivity used in simulator and misspecified selectivity that estimate age frequencies in StALK versus simulated age frequencies at 90% confidence	82
Figure 3.3.8. Growth model used in simulator and misspecified growth that estimate age frequencies in StALK similar to simulated age frequencies at 90% confidence	83
Figure 3.3.9. Time series (1991-2007) of total mortality (Z) estimates from the Ehrhardt-Ault (1992) direct estimation of total mortality, Pauly's (1980) LCCC slicing procedure, and mortality estimated from the StALK algorithm.....	84
Figure 3.3.10. Histograms of purse seine-caught eastern Pacific Sailfish caught in 2 cm bin length frequencies by year and corresponding selectivity pattern estimated using the LCCC method (black) and selectivity under constraints of EA method (green)	85-87
Figure 3.3.11. Age frequencies for sailfish in the EPO estimated by StALK by year.....	88-90
Figure 3.4.1. Time series (1991-2007) of fishing mortality (F) estimates from the Ehrhardt-Ault (1992) method and derived from age frequencies using StALK algorithm compared with estimates of $F_{0.1}$ (red) equaling 0.28.....	92

Figure 3.4.2. Percent error in total mortality, Z , estimated by age frequencies derived from StALK , length-based Z estimations, LCCC methods by year versus Z estimated by ACC in known simulated age frequencies with 40% interannual recruitment.....	94
Figure 3.4.3. Comparisons of total mortality, Z , estimated by age frequencies from StALK, LCCC, and ACC of known simulated age frequencies.....	95
Figure 3.4.4. Average age (years) for sailfish in the EPO by 5°x5° grids as estimated by StALK algorithm.....	103
Figure 4.1.1. Flowchart and hierarchy of goal and objectives for this chapter	107
Figure 4.2.1. The Iridium satellite constellation system offers satellite GPS and data transmission capabilities from vessels to the Iridium Processing Center (IPC) and CLS America servers transmit the information to individual users as well as a centralized project laboratory (University of Miami) for data assimilation and integration with oceanographic and habitat data	110
Figure 4.2.2. Components of the hardware necessary to operate an electronic satellite logbook system.....	111
Figure 4.2.3. An Android phone, Motorola Defy, with the Billfish Catch Reporter mobile application, used from Fall 2011 to present	112
Figure 4.2.4. Depiction of nearest neighbor, averages of r (in blue) and distance searched, P (red) used in determining indices for aggregation and clustering (R-ratio) for the vessel indicated by the red dot	119
Figure 4.3.1. Oceanographic conditions (SSH and geostrophy) conducive to high catch rates (red dots). February 12-14, 2011, with strong zonal currents and a powerful anticyclonic eddy	125
Figure 4.3.2. Oceanographic conditions (SSH and geostrophy) conducive to poorer fishing conditions (catch in red dots), January 31- February 2, 2011, with an absence of dominant zonal current as a divergent transition zone.....	125
Figure 4.3.3. Seasonal trends in sailfish availability, showing a gradual increase in local abundance from August to April (red) with a decrease from May to August (blue)	127
Figure 4.3.4. 3D Principal Component Analyses plot of orthogonal sea surface temperature (SST), sea surface height (SSH), and Upwelling. Red observations denote months in which sailfish are entering the recreational fishery from the late summer and winter (September to April) months and blue denotes observations taken in summer months (May to August) where sailfish are exiting the fishery.....	128

Figure 4.3.5. Monthly averages of standardized availability and the first principal component of a PCA of sea surface height (SSH), sea surface temperature (SST), and upwelling129

Figure 4.3.6. Evans-Clark R-ratios as a function of average predicted availability (raises per day) for daily vessels fishing 2011-2012 when three or more other vessels were fishing simultaneously, $R\text{-ratio} = \frac{1}{666.27(1 - e^{-0.00019*(Y\text{raises}-7.57)})}$ 130

Figure 4.3.7. Estimation of catch efficiency per hour, Q_b as a linear function of bites with respect to raises (discrete). $\text{Bites} = 0.6948*\text{Raises}$ with an $R^2 = 0.754$ 131

Figure 4.3.8. Estimation of catch efficiency per hour, Q_c as a linear function of caught and released fish (discrete) with respect to Bites. $\text{Caught} = 0.5875*\text{Bites}$ with an $R^2 = 0.60$ 131

Figure 4.3.9. Relationship of Bites as a function of Raises with discrete points colored relative to natural log scale of aggregation (red = low τ , blue = high τ)132

Figure. 4.3.10. Estimated Q_b as a function of aggregation, τ 133

Figure 4.3.11. Estimated Q_c as a function of aggregation, τ 133

Figure 4.3.12. Standard error of Q as power function of aggregation, τ , $y=0.15\tau^{0.77}$, $R^2=0.75$ 134

Figure 4.3.13. Plotted time series of standardized indices (mean = 0, standard deviations=1) of five-year lagged NEC (solid black), catch per day (dashed black), and year 5 strength (solid red)135

Figure 4.3.14. Predicted recruitment of age 5 sailfish by year as a multiple regression of NEC lagged 5 years and MEI at present with 95% CI (multiple $R^2=0.66$)136

Figure 4.4.1. Catchability versus sportfishing effort capacity in four controlled scenarios in which stock size, effort, impoundment area, density, and catch are known. Data provided is from: A) Walleye Lake Oneida, NY (DeWalk et al, 2005), B) Largemouth bass (Issak et al, 1992), C) Rainbow trout Mt. Mitchell, NC (Ratledge and Cornell, 1952), D) California brown trout (Vestal et al, 1954; Butler and Kabel, 1959)140

Figure 4.4.2. DO minimum depth (in meters) color shaded in blue hues (deeper) to white (shallower) in the eastern tropical Pacific. Data from World Ocean Atlas 2013, processed in R.....143

Figure 4.4.3. Illustration of the northern equatorial current (red) and equatorial countercurrent (yellow) with bathymetry of the eastern Pacific basin. Currents in white represent coastal currents, including the Costa Rican Current and California Current...144

Figure 4.4.4. Geostrophic currents and eddies during a period of high zonal currents.
Data: AVISO, January 2010146

Figure 4.4.5. Geostrophic currents and lessen eddies during a period of low zonal
currents. Data: AVISO, June 2010146

List of Tables

Table 1.1.1. Spawning activity of sailfish observed by time of year, region, and source in scientific literature.....	4
Table 2.1.1. von Bertalanffy growth function parameters (t_0 , k , L_∞) in peer-reviewed literature: by region, sex, authors, and L_∞ converted to eye forklength (EFL) by lower-jaw forklength (LJFL) conversion functions by Prince (1986)	20
Table 2.2.1. Descriptive statistics of IATTC length (EFL in cm) frequencies for sailfish by year: sample size, mean, median, quartiles, minimum, and maximum used in analyses	23
Table 2.3.1. Results from analyses applied to data from Cerdaneres-Ladrón De Guevara et al. (2011) under known age distributions, under various distributions, and under assumptions regarding variance of length at age.....	34
Table 2.3.2. Parameter estimates from mixture distribution analyses of IATTC sailfish length frequency data from 1991-2010.....	36
Table 2.3.3. Variance-covariance matrix for von Bertalanffy growth function parameters for sailfish in the eastern tropical Pacific	39
Table 2.3.4. Estimates of mean lengths at age from fitted von Bertalanffy model with parameters 207.46 cm for L_∞ , 0.37 cm/yr for K , and -0.004 years for t_0 , 95% confidence intervals for estimates with a CV = 10.1%.....	40
Table 3.2.1 Terms, definitions, and units for variables and subscripts.....	56
Table 3.3.1 Simulated sailfish fishery with 20% random recruitment, resulting Z values from age structured catch curves (ACC) of simulated versus StALK estimates.	77
Table 3.3.2. Simulated sailfish fishery with 40% random recruitment, resulting Z values from age structured catch curves (ACC) of simulated versus StALK estimates	78
Table 4.2.2. Annual indices (1994-2010) of NEC lagged five years, MEI, catch per trip, proportion of age 5 fish from StALKS analyses on length frequencies, and a year 5 strength index	122
Table 4.3.1. Multiple regression ANOVA table of monthly “raises per day” (1994-2010) power transformed (0.38) to a Normal distribution using Box-Cox Powers (Box and Cox, 1964) and partitioned by month, vessel, sea surface height (SSH) and a month*SSH interaction term. Multiple $R^2 = 0.34$	126

Table 4.3.2. ANOVA table of a multiple regression model predicting recruitment of year 5 sailfish as a function of NEC lagged 5 years and MEI at present136

Chapter 1

Introduction

Highly migratory billfishes, of the family *Istiophoridae*, inhabit the world's temperate and tropical oceans and have fascinated scientists, fishermen, and laypersons alike. Author Zane Grey, whose novels captivated imaginations worldwide, likened his encounters with billfish to a religious experience in his 1925 book, *Fishing the Virgin Seas*, which vividly documented his sportfishing adventures all over the world, notably in the tropical and sub-tropical eastern Pacific Ocean (EPO). This dissertation examines the Indo-Pacific sailfish (*Istiophorus platypterus*), the most common billfish in the EPO, and their population dynamics. More specifically, this dissertation introduces methods and concepts to estimate population demographics, lifetime growth, and stock mortality within a dynamic oceanic ecosystem.

1.1 Indo-Pacific Sailfish Biology

The Indo-Pacific sailfish is a coastal migratory epipelagic billfish found in all temperate and tropical oceans, most commonly found in the EPO: a region defined in this dissertation as the waters in the Pacific latitudinally from 15°S northward to 25°N and longitudinally 150°W eastward to the coast of the American continents (Figure 1.1.1). This cosmopolitan billfish species is genetically similar to its Atlantic counterpart (*Istiophorus albicans*, Latreille, 1804) based on its mitochondrial DNA such that designation of species between oceans is most likely unnecessary (Graves and McDowell, 1995). Indo-Pacific sailfish within the EPO are notably larger than the

Atlantic sailfish. This size difference could be attributed to increased food availability in highly productive upwelling regimes in the EPO, a common oceanographic trait along western continental boundaries. A comparison of worldwide sailfish catch rates indicated that the species is more abundant and relative densities are greatest in the EPO, particularly offshore of the Central American isthmus. While migratory, sailfish are most often associated with coastal regions from 35°N to 25°S within all oceans. Typically it occupies the upper 100 m of the water column with apparent preferred residence from the surface to 25 m depth, and within water temperatures ranging from 14° to 32°C, preferring waters between 28° and 30°C (Prince et al., 2006). Habitat preference results in increased availability and vulnerability to surface fishing gears and sailfish are significant bycatch in industrial fisheries targeting tropical tunas (Ehrhardt and Fitchett, 2006).

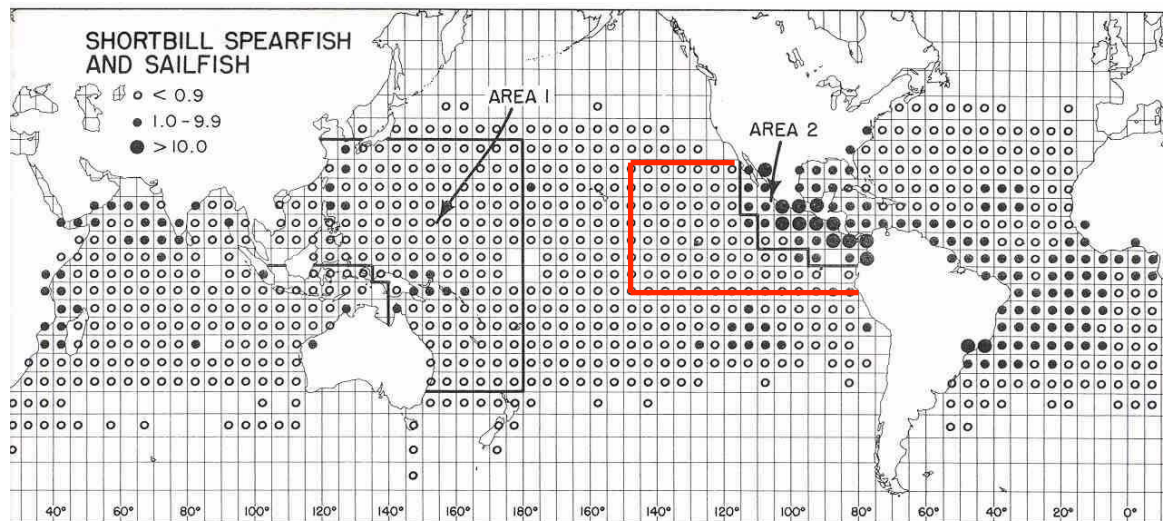


Figure 1.1.1. Mapping of nominal CPUE (# fish per 1000 hooks) for sailfish and shortbill spearfish from high seas longline gear (IATTC, 2001). The EPO is defined by red border. “Area 2” is within the EPO where Joseph et al. (1974) found catch composition to be nearly entirely sailfish.

Relatively little is understood about billfish population dynamics in the EPO, particularly within the Pacific Central American Coastal Large Marine Ecosystem (PCAC LME). This unique ecosystem extends from offshore waters along the coast of the southern Mexico, south to the Central American Isthmus, and west to the Galapagos Islands (Bakun et al, 1999)

Analyses of sailfish gut contents off the Mexican Pacific coast found that cephalopods (dart squid *Loliolopsis spp.* and pelagic octopuses *Argonauta spp.*) and small pelagic fish were the major prey items (Evans and Wares, 1972). Eldridge and Wares (1974) and Rosas-Alayola et al. (2002) found a different species composition in sailfish gut contents with clupeid fishes and paper nautilus comprising a large portion of gut contents. Bendik et al. (1988) and Hernandez et al. (1998) found threadfin sardines, *Opisthonema spp.* to be the dominant prey off Central America and that each observation of sailfish gut contents showed a notably high degree of satiation. Hernandez et al. (1998) noted that sailfish within the off the coast of Central America were in an apparent feeding mode with little sign of spawning activity. All of these findings lead to a conclusion that sailfish are not only voracious predators, but opportunistic feeders; and elect to occupy the waters off Central America to feed in this highly productive region. Ehrhardt and Fitchett (2006) concluded that sailfish occupy this region due to ecosystem forced high densities of prey in a vertically compressed habitat due to the surfacing of the dissolved oxygen minimum depth.

Sailfish spawning has been reported in various nearshore regions off Central America in the scientific literature (Table 1.1.1). Hernandez-Herrera et al. (2000) found that sailfish likely have intervals between spawning that are less than 3.6 days. Evident

differences and variability in temporal spawning activity among regions and studies is an indication that the species may be broadcast spawning when seasonal environmental conditions are propitious to oceanic enrichment and retention. The times of recorded spawning activity by Joseph and Kume (1969), Eldridge and Wares (1974), and Yurow and Gonzales (1971) coincide with a high frequency of eddies along the Central American coastline and circulatory patterns associated with seasonal wind stress and large scale currents (Chang et al., 2012).

Table 1.1.1. Spawning activity of sailfish observed by time of year, region, and source in scientific literature.

Time of Year	Region	Source
Winter (December-February)	Central America	Joseph and Kume (1969), Eldridge and Wares (1974)
Winter to Spring (February-April)	Southern Mexico	Yurow and Gonzales (1971)
Summer (June-September)	Panama	Shingu et al. (1974)
Autumn (September-November)	Mexico	Hernandez-Herrera and Ramirez-Rodriguez (1998)

1.2 Notable Billfish Sportfisheries in the EPO

High catch-and-release rates of billfish, particularly sailfish, generate a high demand for recreational fishing services by anglers from all over the world in nearshore waters off Central America. Guatemala, Costa Rica, and Panama exhibit the highest recreational catch rates of any region along the EPO (Figure 1.2.1). Ehrhardt and Fitchett (2006) postulated that seasonal high catch rates are indicative of high seasonal densities

due to fish entering the region under a compressed habitat within this region, and not necessarily true stock abundance.

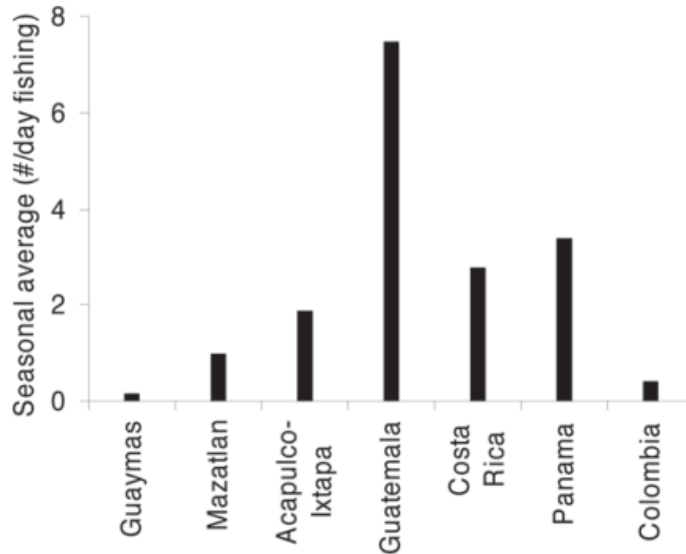


Figure 1.2.1. Recreational catch rates of sailfish (per day) in destinations within the EPO (from: Ehrhardt and Fitchett, 2006).

In Costa Rica, sportfishing operations are commonly available for anglers and tourists through the large and fully developed tourism industry there. These operations extend along the entire coast from Guanacaste-Flamingo, along the southwestern coast to Golfito, along the coast near the border with Panama. However, the largest recreational fishing operations in Central America occur near the localities of Jaco and Quepos along the central Pacific coast. This area is home to approximately 400 vessels and is considered to be an epicenter of sportfishing activity. About 50 sportfishing vessels are located in the Golfo Dulce region along the southern Pacific coast.

In contrast, Guatemala has a much smaller fleet centralized in one locality, Puerto San Jose, the major deepwater port and only marina access for sportfishing yachts

in this country. At any given time, there are a maximum of 38 known sportfishing vessels fishing out of Puerto San Jose. In spite of its relatively small fleet size and smaller tourism infrastructure, sportfishermen experience the highest sailfish catch rates in the world in this region (Figure 1.2.2).

Panama is home to over 200 sportfishing vessels associated to numerous hotels and fishing lodges from Pacific coast localities near Chiriqui in the border with Costa Rica to Darien near the Colombian border. Operations in the Darien coastline are well known for high catches of black marlin comingled with sailfish and blue marlin.

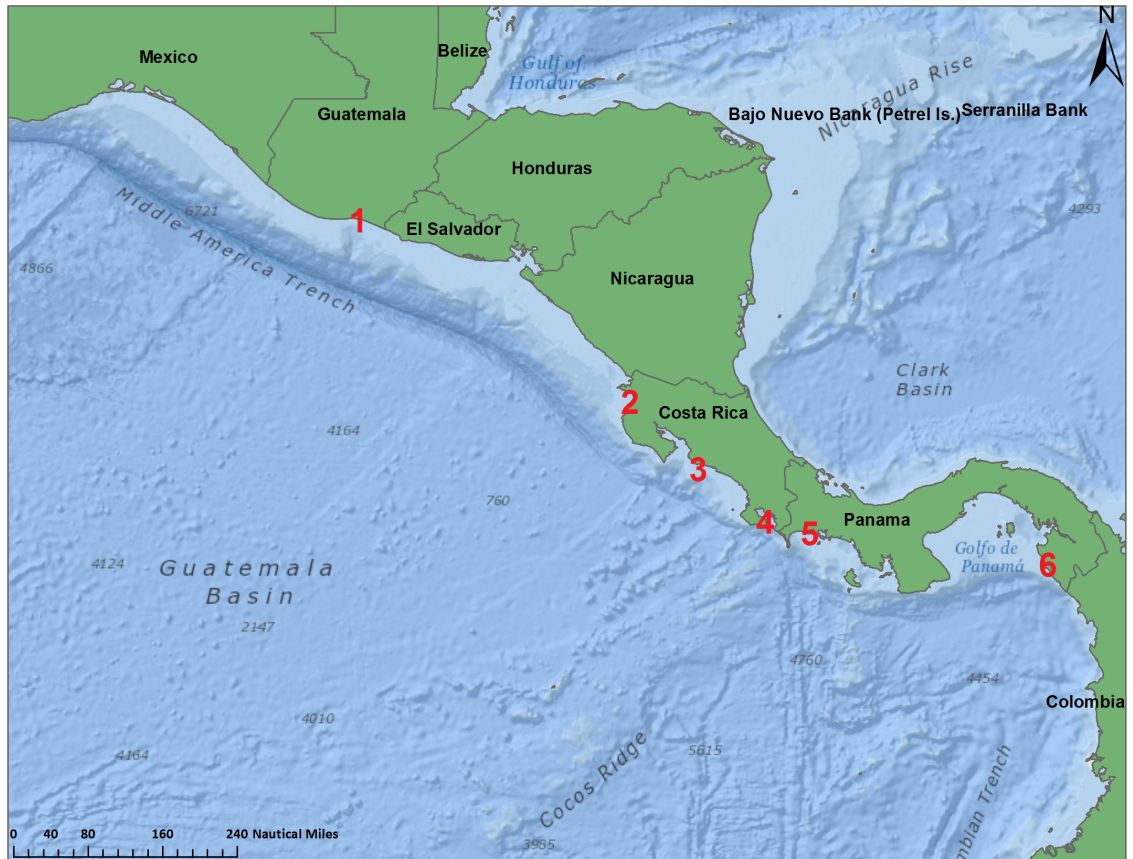


Figure 1.2.2. Notable locations for billfish sportfisheries in Central America: 1) Puerto San Jose, Guatemala, 2) Guanacaste, Costa Rica 3) Jaco/Herradura/Quepos, Costa Rica 4) Golfo Dulce, Costa Rica 5) Chiriqui, Panama and 6) Darien, Panama

1.3 Exploitation and Significance of Billfish in the EPO

High catch rates of sailfish off the Pacific coast of Central America allow this billfish resource to be one of the most important resources in the region for tourist industries through catch-and-release recreational fisheries. Central American communities rely on tourism to generate revenue. According to Gentner (2008), 2.2 million tourists visit Costa Rica annually and contribute \$2.0 Billion USD to Costa Rican tourism revenue each year. Ehrhardt and Fitchett (2009, *report to Government of Costa Rica*) carried out a socioeconomic analysis to determine the value of sailfish resource to the local recreational fishing industry. These authors estimate that a 100 pound sailfish caught once in catch-and-release fisheries is worth approximately \$822 to local economies when caught on conventional bait and over \$2000 when caught once on fly-fishing gear. In contrast, a 100 pound sailfish sold locally or exported sells for typically \$0.50-\$0.60 per pound, contributing \$50-\$60 to local economies with no added value since it may not be caught again. Recreational fishing is oriented to the catch and then release of live animals; therefore, many released fish will contribute to future catches, escalating its value relative to the value as landed fish. Clearly, sailfish is worth more monetarily alive than dead. In July, 2015, stakeholders and scientists within the region met for a first-ever meeting to develop a management plan for tourism-based fisheries in Central America and successfully requested support from the regional fishery management organization, Organización del Sector Pesquero y Acuícola de Centroamerica (OSPESCA). Successful management of the billfish resource can materialize into social and economic opportunities to citizens living in Central America and Panama.

Catch rates of sailfish (# fish/fishing day) vary regionally and through time. In Guatemala, sailfish annual catch rates have been consistent throughout the available time series (1994-present), except during years exhibiting El Niño events (e.g.1997-8, 2006-7) (Figure 1.3.1A). Catch rates off Costa Rica show a rapidly decreasing trend over time (2000-present) to just below 1 sailfish per trip on average (Figure 1.3.1B). These regional differences are likely due to the fact that competition among recreational vessels and local depletion from commercial longline fisheries in Guatemala is significantly lower than in Costa Rica- where commercial longline fleets and recreational fisheries operating through the country are much larger, exhibiting greater fishing capacity having spatially extended fishing operations. These fundamental operational differences between the two countries are contrasting scenarios of a low degree of local depletion versus a situation of local depletion negatively impacting recreational fisheries. Local depletion and vessel interference in recreational fleets may impact fishing success, thus affecting the probability of repeated demand for services. Low catch rates can prevent or discourage anglers from visiting the region to participate in tourism-based fishing- leading to negative economic consequences.

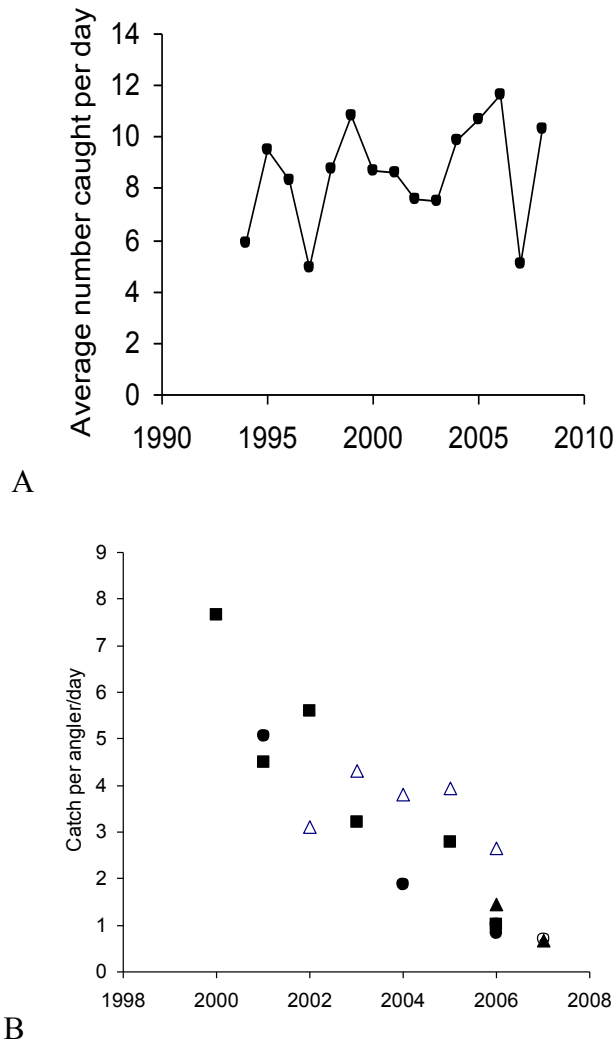


Figure 1.3.1. Annual average catch rates for: (A) Iztapa, Guatemala; and (B) Costa Rican locations in recreational catch-and-release fisheries (Ehrhardt and Fitchett, 2008)

Studies have found that worldwide large pelagic marine resources, particularly in the Pacific, are depleted (Myers and Worm, 2003; Sibert et al., 2006). Myers and Worm (2003) found that predatory large pelagic fish populations are at about 10% of nascent abundance by reviewing trends in catch-per-unit effort (CPUE). Sibert et al. (2006), using a suite of stock assessment techniques, found that top predators (including bycatch species) in the Pacific Ocean have declined 36% to 91% from biomass levels prior to

fishery expansion in the 1950s. Sibert et al. (2006) also note that many highly migratory stocks have experienced substantial decreases among larger fish and a decrease in the trophic level of animals comprising commercial catch.

Historically, high seas longline operations have been a major source of fishing mortality for billfishes and tunas in the EPO. Billfishes that occupy the same habitat niche as tunas (Musyl et al, 2003) have been more susceptible to non-directed fisheries. Since 1970, sailfish relative abundance index from Japanese high seas CPUE follows a decreasing trend with a reduction of 82% by 2006. Concomitantly, registered trophy sized sailfish (data by the International Gamefish Association, IGFA) decreased by 64% in that same time period (Figure 1.3.2; Ehrhardt and Fitchett, 2006). Trophy size, albeit subjective, is a baseline size defined by the IGFA for a fish to be considered extraordinarily large- approaching a maximum size or winning fishing tournaments- for the time in which it was caught. Absence of large individuals and declines in average size is a tell-tale sign of overexploitation (Ault et al., 1998; Pauly et al., 1998). As marine ecosystems are subjected to exploitation, they experience a dramatic decline in trophy sized animals (Ault et al., 1998; McClenachan, 2009).

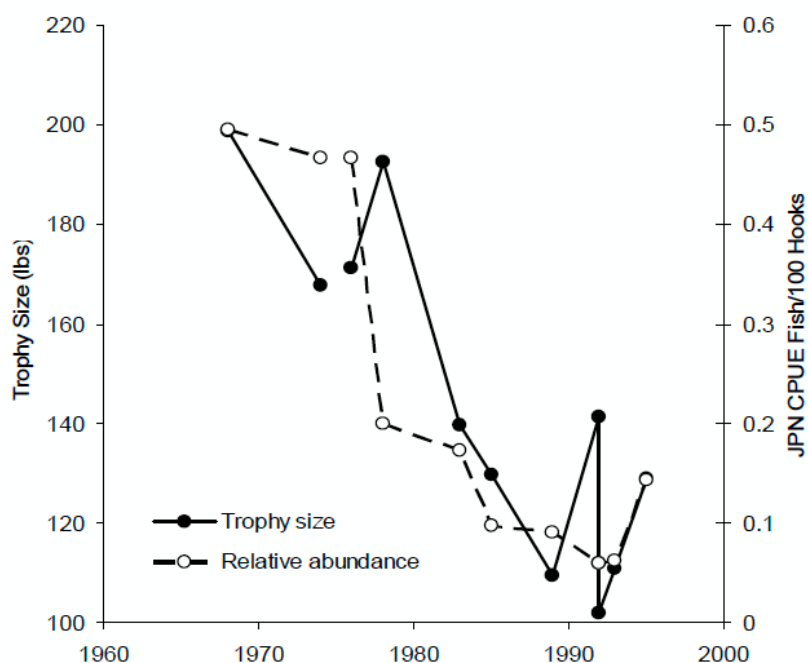


Figure 1.3.2. Historical trophy size (lbs) and Japanese longline CPUE (Fish/100 Hooks) by year for sailfish in the EPO (Ehrhardt and Fitchett, 2006). Trophy size data from International Gamefish Association (IGFA) and CPUE data from IATTC.

Despite historical decreasing trends in sailfish abundance, artisanal and semi-industrial coastal longline fisheries targeting mahi mahi (dolphinfish), tunas, sharks, and billfishes have expanded throughout the region since the early 1990's. This was a result of increased demand for mahi mahi and fresh tuna in the world markets. Therefore, those fisheries in Central America and Panama responded quickly to the increased demand with increased fishing intensity that has indirectly impacted billfish as bycatch. This indirect exploitation of billfish increased to a point where nearly 35% of all longline landings in Costa Rica were comprised of billfishes during peak months (Ehrhardt and Fitchett, 2009 unpublished report to the Government of Costa Rica) and sailfish commercial catch rates

were higher than all target species in commercial fisheries, with catch rates of 10 fish per 1000 hooks. Despite growing fleet sizes and increasing effort by semi-industrial longline fisheries in the region, landings of mahi-mahi and billfishes have decreased rapidly in Costa Rica since 2004 (Figure 1.3.3).

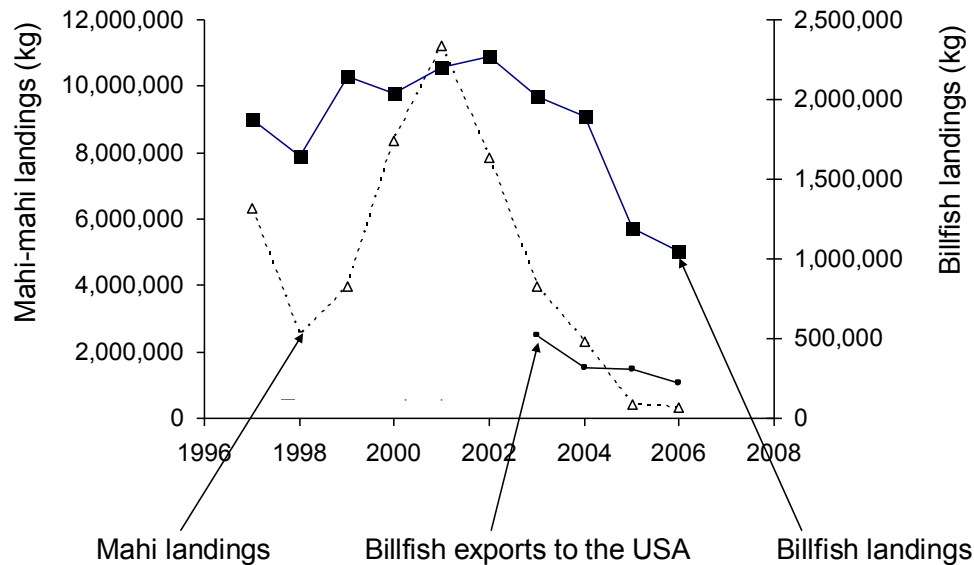


Figure 1.3.3. Billfish landings, billfish exports to the USA, and Mahi mahi landings from Costa Rica, 1997 to 2007 (From: Ehrhardt and Fitchett, 2009, *unpublished report*)

1.4 Habitat Compression Impacts on Sailfish

Assessment methods often assume spatial homogeneity given the data used to assess a fishery. Ocean conditions contribute to variability in the catchability and abundance of billfish within their habitat. These dynamics lead to a violation of assumptions in assessment methods when not taking into consideration the spatial and temporal structure of habitat relative to fishery data. Dissolved O₂ levels that can sustain life (> 1 mg/L seawater) vary from 100 m to just 5 m from the surface in waters east of

120°W, which is a prominent, spatially dynamic oceanographic feature of the EPO (Figure 1.4.1). Western boundary currents along continents force Ekman-induced upwelling along coastlines from wind-induced surface water displacements westward (Xie. et al., 2005). Upwelling brings cooler and nutrient-rich water to the surface and forces water column strata- such as the thermocline, mixed layer, and O₂ minimum layer (>1.0 mg/L seawater) toward the surface (Wyrski, 1967). The end result is increased biological productivity in near-surface waters where light, nutrients, and dissolved oxygen are biologically sufficient. However, in the EPO and especially within the PCAC LME, these conditions are quite pronounced and have seasonal extremes. Easterly winds called “gap winds”, pass from the Gulf of Mexico and Caribbean Sea through the Tehauntepec lowlands, Nicaragua Lake District, and through the Panama Canal region, causing wind-induced upwelling in the Pacific off the Central American coast (Wyrski, 1965; Wyrski, 1967; Stumpft, 1975; Bakun et. al, 1999, Xie et al., 2005). These “gap winds” are the strongest during northern winter months and coincide seasonally with strengthening of west-flowing equatorial currents. These processes strengthen wind-driven upwelling and Ekman upwelling simultaneously (Bakun et al., 1999, Xie et al., 2005). The result is surfacing of the mixed layer, thermocline, and dissolved O₂ minimum. These physical processes bring about a condition in which prey species for billfishes and other top predators are confined in a vertically compressed upper ocean (Ehrhardt and Fitchett, 2006;). Prince and Goodyear (2006) used data from 13 pop-off satellite archival tags (PSAT) to demonstrate that sailfish within the PCAC LME inhabit almost entirely in the upper 25m in the water column. This is in contrast to much deeper occupancy of billfish in other regions of the western Pacific Ocean (Sippel et al., 2011).

Ehrhardt and Fitchett (2006) found that the availability of seasonal high density groupings of pelagic prey resources correlate highly with high density groupings of sailfish that congregate into the region for feeding purposes. Because of this, sailfish exhibit a highly seasonal trend of high density along Central American nearshore waters from the months of December to April.

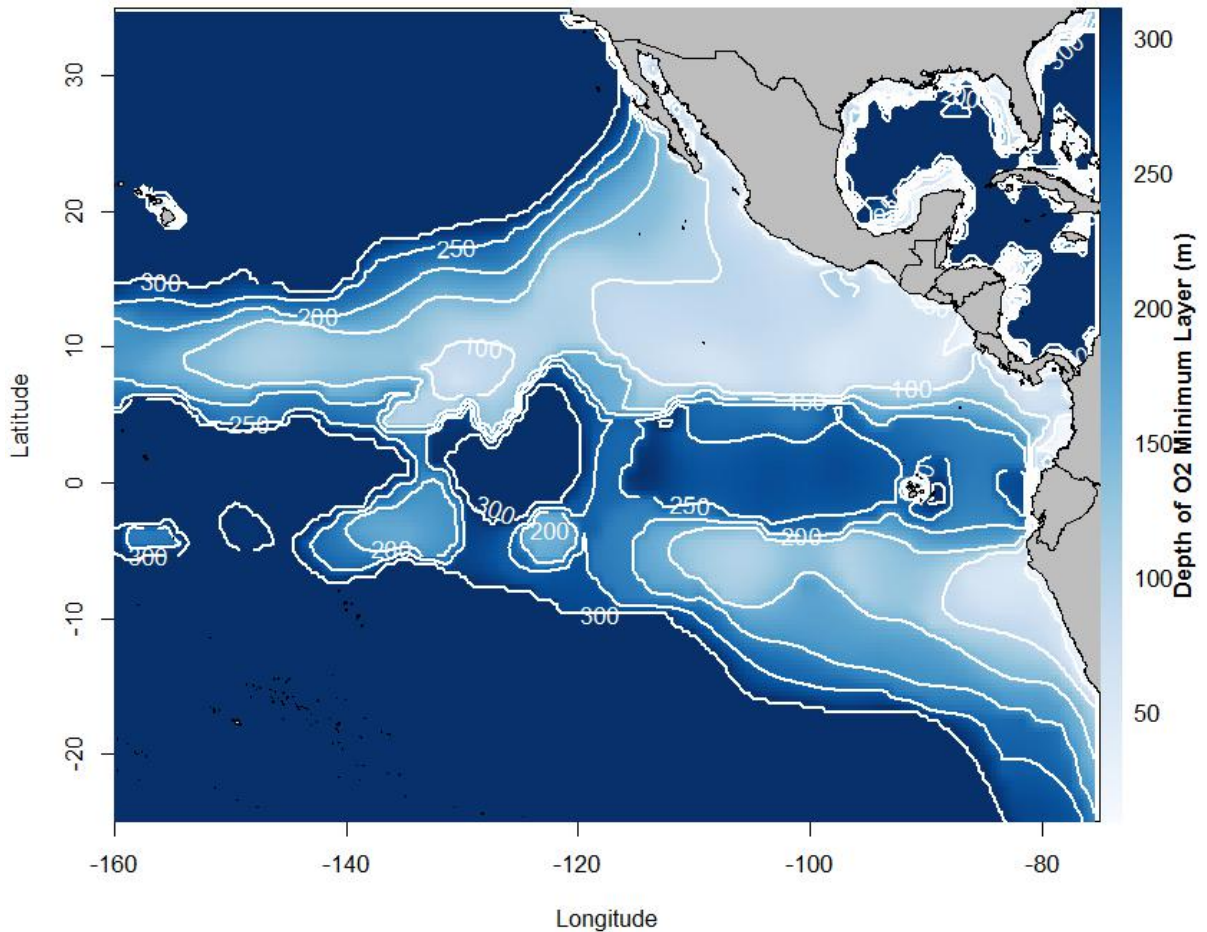


Figure 1.4.1. Color contour plot of depth of dissolved oxygen minimum layer (1 mg/L seawater) in waters within the EPO. (Data from: World Ocean Atlas, 2009; Estimated and interpolated in R, R Statistical Environment, 2014)

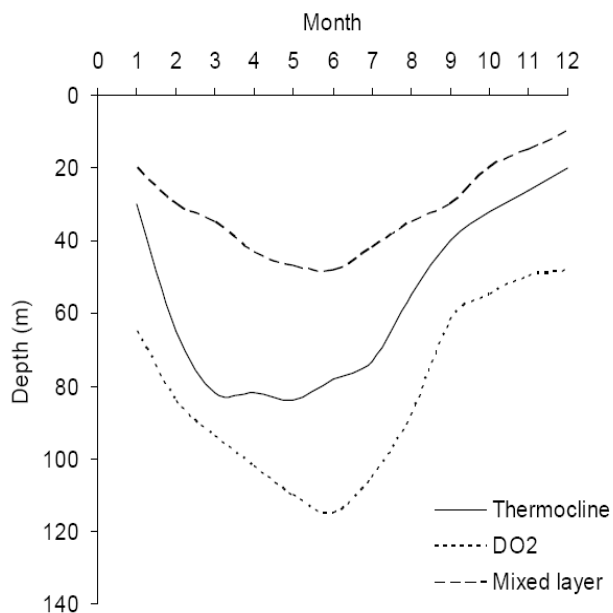


Figure 1.4.2. Monthly variability of the thermocline, mixed layer and minimum (1 ml/l) of dissolved Oxygen (DO_2) off the coast of Guatemala (adapted from NORAD UNDP/FAO, 1988 in Ehrhardt and Fitchett, 2006) during Non-El Nino year

Habitat compression creates a quality of habitat favorable to billfishes through concentrating prey while physically limiting vertical habitat due to oxygen limitations at depth. The attractive qualities and restrictions in volume of livable habitat most likely create a two-fold impact on catchability of billfishes for recreational fisheries. Baranov (1918), Gulland (1964, 1983) and Caddy (1979) found that catchability is a function inversely related to the area (or volume) for which a fish resource is available. In the nearshore waters off Central America and Panama, the volume of habitat decreases drastically during episodic habitat compression, thus increasing density of individuals- and hypothetically creating favorable conditions for catchability.

1.5 Problem Identification, Goals, Objectives

Sailfish have yet to be assessed in the EPO. Hinton and Maunder (2013) reported that the Inter-American Tropical Tuna Commission (IATTC) was unable to assess sailfish in the eastern Pacific. They tried to assess the population with an unstructured surplus production model, but incomplete catch and effort data, low contrast in data through time, and unreliable parameter estimates prevented model convergence.

At present, sailfish growth is based on observations from limited spatial coverage, which also limits the range of ages covered. While these studies present credible age at size estimates, they do not truly represent population-wide size structure. Misspecification of growth in stock assessment models can lead to serious errors in assessment methods (Maunder, 2014; Chang and Maunder, 2012).

There is also an immediate need to estimate sailfish fishing mortality rates relative to fishing mortality benchmarks. Most of these benchmarks depend on growth parameters that must cover the extent of the life span of the species. In the absence of catch data, a full stock assessment is not possible, but developing indices of exploitation (such as fishing mortality estimates) in data-poor stocks is possible under certain assumptions. Furthermore, understanding the role of the ecosystem forcing on the local availability of billfish to recreational fisheries and understanding the impacts of fleet dynamics on catch rates of recreational fisheries is imperative. Because of these necessities for billfish conservation in the region, there is a need to understand what drives sailfish population densities and availability. Moreover, there is an immediate need to determine the status of exploitation of the sailfish resource in the eastern tropical Pacific.

The goal of this Dissertation is to determine the sustainability status of EPO sailfish. To achieve the proposed goal based on certain core population dynamic characteristics and availability of sailfish in the tropical EPO, four broad objectives are:

- (1) To develop a reliable lifetime growth model that reflects the entire sailfish stock in the EPO (Chapter 2)
- (2) To develop a new demographic estimation method that can be used to quantify mortality of the EPO sailfish stock from length frequencies (Chapter 3)
- (3) To explore ocean ecosystem dynamics that may influence sailfish recruitment, survivorship, and availability to regional sportfisheries (Chapter 3 and 4)
- (4) To determine specific oceanographic conditions that drive sailfish availability to recreational fisheries and fishing behavior through historical data and remote fishery data acquisition (Chapter 4).

Chapter 2

Growth of Sailfish (*Istiophorus platypterus*) in the Eastern Pacific Ocean

2.1 Background and Existing Information on Growth

Population processes for EPO sailfish are relatively unknown, and there is no population-wide growth model that could be used in assessments of exploitation. The goal of Chapter 2 is to estimate new reliable lifetime growth parameters that are representative of the entire EPO sailfish stock. Age and growth models are a fundamental building block of fishery assessment methods such as yield-per-recruit, sequential population analyses, and other models that can estimate fishery management benchmarks for sustainability. Growth models for sailfish must take consideration of the heterogeneous spatial distribution of size at age data and must be estimated from unbiased sampling across all ages. Therefore, objectives to estimate growth parameters representing the entire range of the stock are: (1) to obtain length frequencies of a non-size-selective fishing fleet from the entire distributional range; (2) to infer size at age variability patterns across ages; (3) to implement mixture distribution analyses to estimate size at age parameters; and (4) to fit a growth equation with new size at age distribution data to estimate new growth model parameters.

Summary for Growth Information for Sailfish in the Pacific

Past studies on the sailfish have been constrained by relatively limited sampling and spatial coverage in particular regions and not the entire stock. A summary of resultant growth parameters are given in Table 2.1.1. Koto and Kodama (1962) used

length-frequency distribution data to estimate the growth of western Pacific sailfish in the 1950's from longline catch data obtained from the Japanese longline fleet throughout the western and central Pacific. Chiang et al. (2004) were the first to use bony hard parts, specifically dorsal fin spines, to back calculate size-at-age to develop an age-and-growth model of western Pacific sailfish off the coast of Taiwan.

Age and growth studies in the EPO (waters east of 180°W) by Alvarado-Castillo and Félix-Uraga (1996, 1998) found very fast growth to age 3 and a significant slowing of growth towards older ages. Their study used specimens collected in a relatively narrow size range from sportfisheries operating in the Gulf of California, Mexico. Cerdanarés-Ladrón De Guevara et al. (2011) and Ramírez-Pérez et al. (2011) developed age and growth models from specimens from spatially stratified samples collected from recreational fisheries in Mazatlan and Tehuantepec, Mexico, respectively. These showed a large negative t_0 estimate for the von Bertalanffy growth function, which indicates the absence of small (i.e. young) animals in their samples. Estimated parameters of the von Bertalanffy growth function for sailfish found in the literature exhibit high variability, even within geographical regions (Table 2.1.1). Some of these discrepancies within regions may not be related to the biology of the species but due to statistical artifacts of the data that may preclude portions of, or truncate, size at age distributions. To sample hard parts for growth from throughout the geographical range of the population would require widespread sampling. This sampling procedure for incidental species such as the sailfish would likely be very difficult and cost ineffective in many of the directed fisheries targeting tunas and mahi-mahi. In contrast, occurrence data and length samples of bycatch billfish species from Inter-American Tropical Tuna Commission (IATTC)

observers in tuna purse seiners are available over most of the habitat range of the sailfish in the EPO.

Table 2.1.1 – von Bertalanffy growth function parameters (a_0 , K , L_∞) in peer-reviewed literature: by region, sex, authors, and L_∞ converted to eyeforklength (EFL) by lower-jaw forklength (LJFL) conversion functions by Prince (1986).

Region	Sex	L_∞	K	a_0	Converted L_∞ EFL	Source
Gulf of California, Mexico	Both	203.6	0.80	-0.002	178.9	Alvarado-Castillo and Felix-Uraga (1998)
Mazatlan, Mexico	Both	180.6	0.36	-0.240	180.6	Cerdenares-Ladrón De Guevara et al (2011)
Mazatlan, Mexico	Both	190.6	0.21	0.480	190.6	Cerdenares-Ladrón De Guevara et al (2011)
Tehautepec, Mexico	M	256.7	0.16	-1.370	226.1	Ramírez-Pérez et al (2011)
Tehautepec, Mexico	F	251.4	0.18	-1.080	224.3	Ramírez-Pérez et al (2011)
Taiwan	F	261.4	0.11	-4.210	233.6	Chiang et al (2004)
Taiwan	F	250.3	0.14	-2.990	223.3	Chiang et al (2004)
Taiwan	M	252.6	0.12	-3.910	222.4	Chiang et al (2004)
Taiwan	M	240.4	0.15	-2.781	211.3	Chiang et al (2004)
Atlantic US	F	221.0	0.62	0.000	196.2	Ehrhardt and Deleveaux (2006)
Atlantic US	M	160.8	0.58	0.000	138.9	Ehrhardt and Deleveaux (2006)
Atlantic Florida	F	183.0	0.16	-3.312	183.0	Hedgepeth and Jolley (1983)
Atlantic Florida	M	147.0	0.30	-1.959	147.0	Hedgepeth and Jolley (1983)

2.2 Materials and Methods

MacDonald and Pitcher (1979) introduced statistical methods (MIX) to follow the modal progression of age classes through a length-frequency time series by fitting finite mixture distributions representing age groups. Similarly, Brothers (1980) used temporal changes in modes of finite distributions to extract information on fish growth rates. These studies led to computer programs that estimate growth parameters from temporally stratified length-frequency data such as ELEFAN (Pauly and David, 1981;

Pauly, 1987) and MULTIFAN (Fournier et al., 1990; Fournier and Sibert, 1998). These collective statistical methodologies can be used to estimate age and growth parameters that agree with model fits from biological hard parts (Hammers and Miranda, 1991). However, the efficacy of using modal progression analyses and/or mixture distribution analyses depends on use of a large sample of size observations throughout the entire population range and relative to the population distribution. The resulting length at age estimates will be used to estimate the parameters of a von Bertalanffy growth curve. A comprehensive, non-size-selective length frequency database was used for analyses in following sections.

Sailfish length frequencies were collected (1991-2010) by Inter-American Tropical Tuna Commission (IATTC) observers stationed aboard tuna purse seiners operating in the tropical eastern Pacific Ocean. The purse seine fishery incidentally captures a large size range of sailfish as bycatch and is considered to non-selective. For this purpose, purse seine length-frequencies were used to determine information on growth and total mortality rates. Because of the spatial extent of the tuna fishery, these data are likely representative of the population distribution in EPO (Fig. 2.2.1). The spatial distribution of the purse seine fishery include the entire spatial range of sailfish identified by longline experimental surveys conducted in the years prior to heavy regional exploitation (Joseph et al., 1974; Figure 2.2.1).

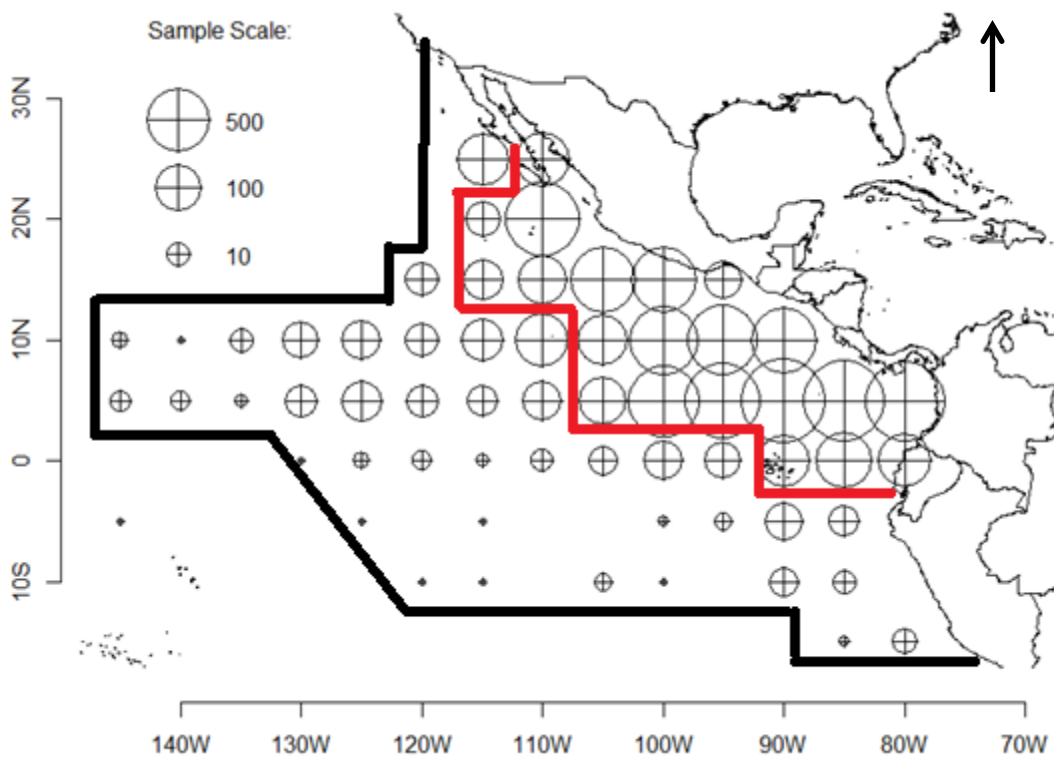


Figure 2.2.1. Sailfish length-frequency sample sizes from the EPO purse seine fishery by 5° x 5° degree latitude-longitude grid. Outside thick black border indicates range of length observations and red border indicates area of high sailfish relative densities per exploratory longline surveys in the 1960's prior to heavy fishing in the region (Joseph et al. 1974).

The database (Table 2.2.1 and Figure 2.2.2) was comprised of eye-forklength (EFL) measurements in centimeters (cm). The IATTC Observer Program (Bayliff, 2010) collected this data starting in 1991 covering nearly 100% of the vessels greater than 363 registered tons. Length frequency data are stratified by 5° latitude and 5° longitude from the location of the set that captured the sample- with month and year provided. Generally, all billfish caught in these purse seine hauls are counted and samples are taken from each

haul; however, in hauls in which billfishes are caught in exceptionally large numbers, a subsample of total billfish catch is measured by EFL in cm. The data spans a longitudinal range from 145° W eastward to the coastal Americas and from 10° S northward to 25° N. A total of 11,086 sailfish lengths were recorded from 1991 to 2010 and were made available to this study by the IATTC. Length frequencies were expanded by total catch of sailfish also provided by the IATTC observer program. Length frequencies were expanded by corresponding 5° x 5° degree grid location, year, and month of origin. After expanding recorded lengths by landings, a total of 19,702 EFL observations resulted.

Table 2.2.1. Descriptive statistics of IATTC length (EFL in cm) frequencies for sailfish by year: sample size, mean, median, quartiles, minimum, and maximum used in analyses

Year	# Samples	Mean	Mean	25% Quartile	75% Quartile	Minimum	Maximum
1991	436	182.26	182	166	200	98	246
1992	621	174.27	176	165	186	108	218
1993	817	171.60	174	161	184	85	224
1994	770	162.42	163	152	172.75	95	228
1995	631	170.98	172	159	183.5	82	234
1996	591	166.01	169	157.5	180	71	238
1997	623	169.24	172	160	185	80	220
1998	1526	175.47	177	166	186	102	249
1999	908	166.00	167	156	177	92	225
2000	1358	170.25	171	160	180	102	220
2001	829	172.15	174	166	182	95	235
2002	991	177.54	178	167	190	99	245
2003	2598	174.80	176	166	186	88	230
2004	836	174.34	177	163	188.25	71	240
2005	1099	176.40	177	163	194	73	247
2006	1146	170.25	172	158	186	72	213
2007	1207	169.69	172	158	187	71	237
2008	816	174.71	175	163	186	93	248
2009	651	176.26	176	164	189	96	248
2010	1177	173.28	175	157	190	93	248

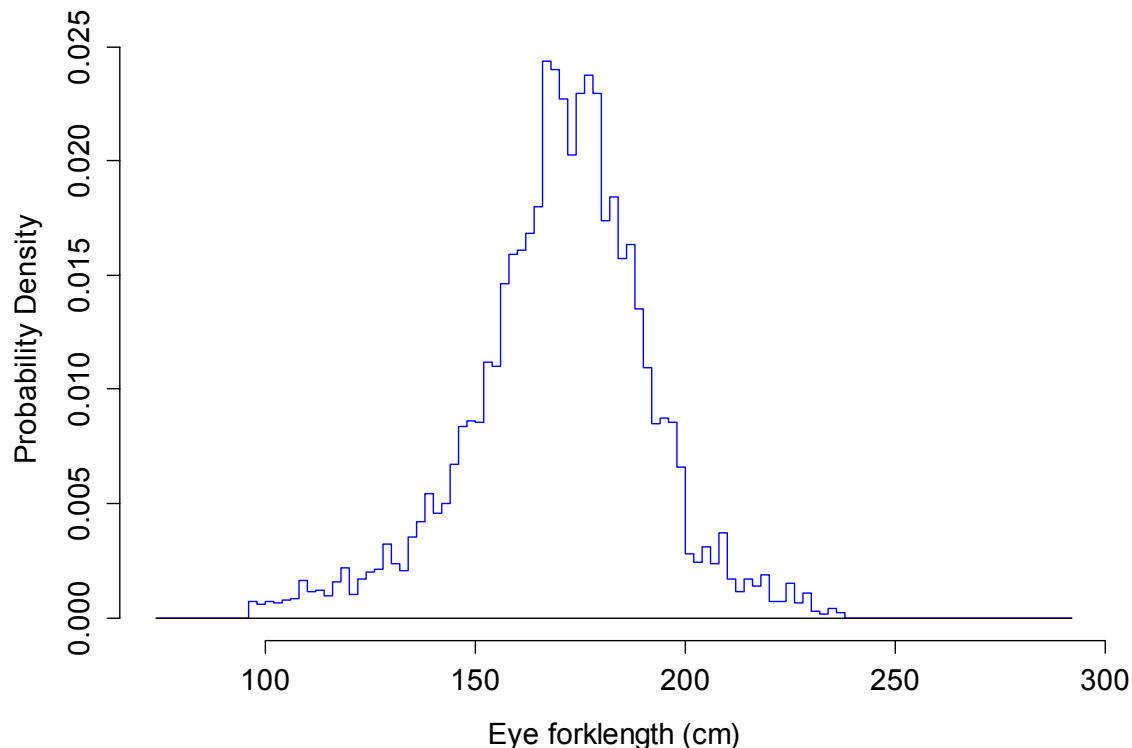


Figure 2.2.2 Length frequency distribution of sailfish lengths, aggregated from 1991 to 2010. Length frequencies were weighted by catches (in numbers) in $5^{\circ} \times 5^{\circ}$ degree grids, months, and years for which they originated

Within the database, a high frequency of smaller specimens (< 120 cm) were found in waters west of 110° W, suggesting high occurrence of younger sailfish in the western range of the population distribution. Specimens from waters extending southward from the Gulf of Panama (south of 5° N) exhibited a larger variance in size composition, with a high frequency ($\sim 20\%$) of specimens over 180 cm in size in addition to a relatively high frequency of small specimens (< 120 cm). Despite a large sample size ($n=3041$), specimens from nearshore waters extending from southern Mexico to Costa

Rica exhibited a narrow range of sizes, with the vast majority of the specimens ranging from 120 cm to 180 cm. Differences in average lengths between regions (Figure 2.2.3) suggest ontogenetic movements of sailfish.

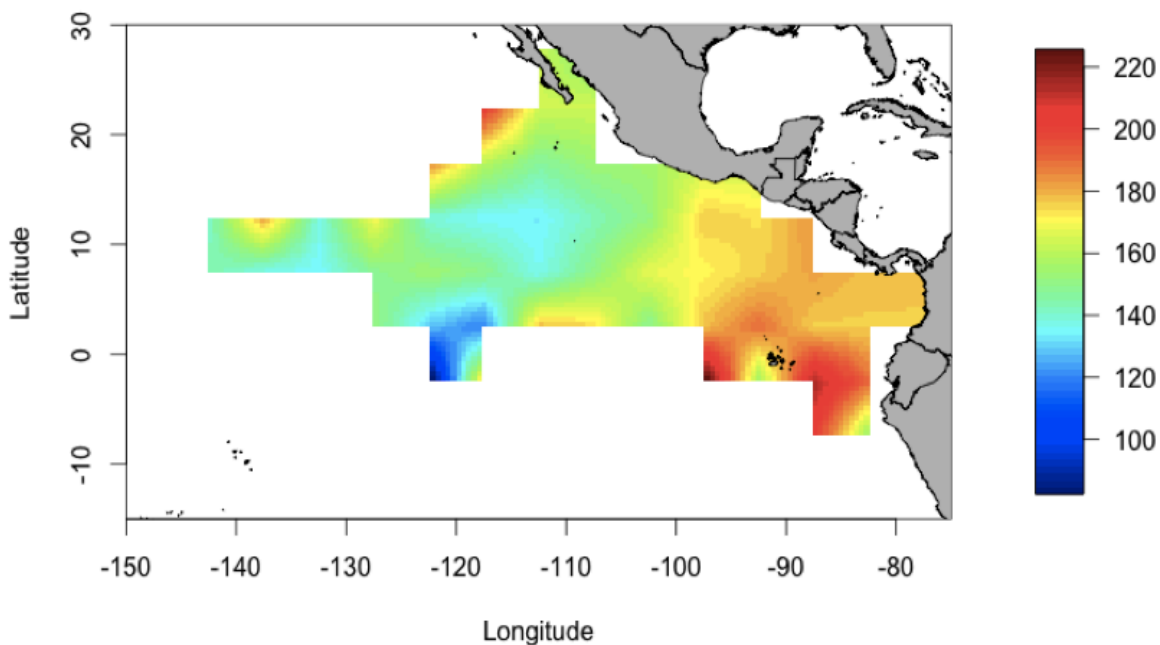


Figure 2.2.3. Color map of average length (cm, EFL) of observed sailfish from IATTC observer program, 1991-2010.

Selection of an Appropriate Bin Size for Length Frequency Data

To estimate age-and-growth from observed length frequency distributions, sailfish lengths required binning into intervals (or size classes). This is needed because incorrect assignments of bin widths may mask otherwise discernible age groups. Appropriate size class intervals must be clearly defined prior analysis of length frequency data to determine growth parameters.

Paucity of data in bins adjacent to bins with exceptionally large numbers are not likely to be reflective of the population probability density function. These discrepancies

could be an artifact of sample sizes or of possible measurement errors caused by rounding. Shimizaki and Shinomoto (2007) introduced an algorithm to estimate optimal bin sizes in frequency data. This algorithm assumes data are sampled independent of each other and does not make any assumption of the underlying density function of the data. The method can be used for binning data under any probability density. For example, this method was found to be the most reliable method for (1) bin optimization of observed pixels in satellite data by Stilla and Hedman (2010), (2) precipitation observations by Teegavarapu (2013), and (3) DNA fragment sizes (Manching et al., 2014). Optimal size class intervals for sailfish used in growth studies were selected using the methodology of Shimizaki and Shinomoto (2007). A bin size (ΔL) is selected and thus length data is divided into N total of i bin groups with k observations in each bin group. This is achieved by first calculating mean and variance (\bar{k} and v) of the count across candidate bin size classes:

$$\bar{k} = \frac{1}{N} \sum_{i=1}^N k_i \quad \text{and} \quad v = \frac{1}{N} \sum_{i=1}^N (k_i - \bar{k})^2 \quad (2.1)$$

Resulting in an cost function $C(\Delta L)$ given by

$$C(\Delta L) = \frac{2\bar{k} - v}{(\Delta L)^2} \quad (2.2)$$

Size class interval (ΔL) for length (L) is optimized by minimization of $C(\Delta L)$ through an iterative process scanning through possible candidate intervals. The resultant optimized size class interval was the optimum bin width for length frequency data.

MIX Algorithm Procedure to Define Size-at-Age Groupings

MIX uses an expectation-minimization (EM) algorithm with starting parameters mean size at age (μ_a) and standard deviation of size at age (σ_a) for each of a predetermined number of statistical normal distributions of lengths corresponding to ages. Alternative distributions, such as the lognormal and gamma distribution may also be used. The combined normal frequency distributions are fitted using the EM algorithm to the observed frequency distribution. These distributions for ages (a) were combined into a summed total frequency distribution at all values of length L ($f(L)$) by:

$$f(L) = \sum_{a=1}^{a_\lambda} \omega_a p_a(L|\mu_a, \sigma_a) \quad (2.3)$$

Where $p_a(L|\mu_a, \sigma_a)$ is fitted as a normal distribution for each a normal distribution,

$$p_a(L|\mu_a, \sigma_a) = \frac{1}{\sigma_a \sqrt{2\pi}} e^{-\frac{(L-\mu_a)^2}{2\sigma_a^2}}, L > 0 \quad (2.4)$$

And ω_a is a coefficient representing the proportion of fish of age a to the total frequency distribution being analyzed; hence the sum of all ω_a equals 1.

Modal progression methods like MIX require knowledge of the number of year classes most likely present in length-frequency samples. Studies examining directly observed ages of Pacific sailfish (Cerdenares-Ladrón De Guevara et al. , 2011; Ramirez-Perez, 2011; Chiang et al., 2004) did not observe sailfish that were older than 11 years, therefore terminal age, a_λ , was set to 11 years. Also, lengths of sailfish older than age 10 are not likely to change much from year to year as individuals are reaching terminal age. Definitions of Age 1 sailfish fish using hard parts were equivocal and inconsistent among studies, likely due to the difficulty in reading first annuli demarcations and due to error in back-calculation of ages to Age 1 (Cerdenares-Ladrón De Guevara et al. , 2011; Ramirez-

Perez, 2011; Chiang et al., 2004). Very few individuals (i.e. less than 0.1%) in the data used for this analysis were within 20 cm of estimates of Age 1 fish from the literature, implying that Age 1 sailfish were virtually absent in our samples. Therefore, ten age classes were assumed in the statistical analyses of length frequencies, beginning with estimates of year class ii and ended with estimates of terminal year class xi. Hinton and Maunder (2013) also adopted this assumption in the attempted sailfish assessment using IATTC data with Stock Synthesis 3 (Methot and Wetzel, 2013).

To estimate candidate size at age parameters for each age group, MIX is applied on length frequencies. Figure 2.2.4 provides a flowchart of how length frequencies are processed and analyzed in MIX. To avoid an influence of arbitrary initial conditions on results, MIX was run with randomly assigned initial mean values for 10 ages. Starting estimates of mean size at age used were mean size at ages comparable to those estimated in the literature, particularly Cerdaneres-Ladrón De Guevara et al. (2011), Ramirez-Perez et al. (2011), and Chiang et al. (2004) since each of these studies offer mean size at age for multiple methods of back-calculation with confidence intervals. For each of the runs, estimation of the 10 size at age distributions was carried out with no constraints on mean (μ_a) and specified constraints on standard deviation (σ_a) - assuming constant coefficient of variation (CV). A constant CV of length with respect to age suggests increasing linear uncertainty of size at age, which is biologically expected due to heritable, phenotypic variability (Sainsbury, 1980; Russo et al., 2009) and is verified in following sections to be a valid assumption for sailfish. Additionally, a constant CV of length with respect to age is a commonly accepted assumption in fish stock assessments (Fournier, 1998) and also widely assumed for istiophorid stock assessments in the Pacific Ocean. For example:

eastern Pacific sailfish (Hinton and Maunder, 2013, CV=0.09), striped marlin (Davies et al., 2012 CV=0.08), and blue marlin (ISC, 2013; Kleiber et al., 2003; Hill, 1986). Lastly, mean values for length at age should be less dispersed for older ages.

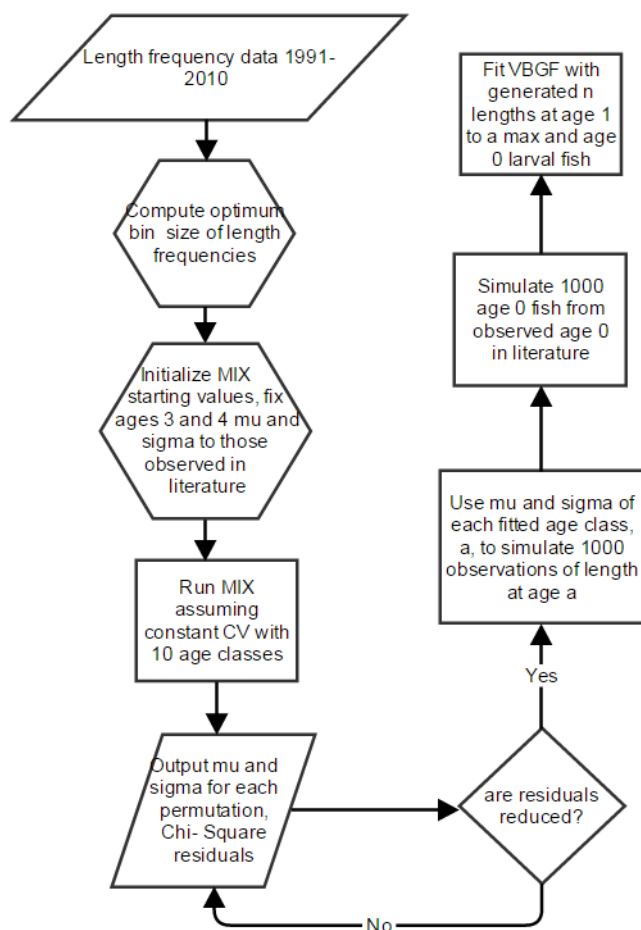


Figure 2.2.4. Flowchart for analysis of length frequency data to estimate parameters for MIX, simulating lengths and age, and fitting a growth model of EPO sailfish.

Probabilistic Simulations of Sailfish Lengths

Stochastic simulations were used to generate expected length distributions at ages using MIX results (Figure 2.24). Mean (μ_a) and standard deviations (σ_a) at age a estimated by the MIX algorithm were used to develop hypothetical statistical

distributions of lengths drawn at random for a given age group, assuming a normal distribution truncated at length 0 and given by Equation 2.4.

Simulated sizes-at-age of sailfish were generated in the R Statistical Environment (R Development Core Team, 2014). Each simulated age group was given an equal sample size so that the fitted growth curve would not be biased due to disproportionate sampling. Each age group was given an arbitrary sample size of 1000 sailfish lengths.

Simulations of Young-of-the-Year (Age 0) Sailfish

Lack of data for ages 0 and 1 will undoubtedly result in inflating the estimation of age when size equals 0 (t_0). This will affect estimation of the Brody growth coefficient (K), which jointly estimated with L_∞ as von Bertalanffy growth equation parameters. To ameliorate the situation, data on age 0 Atlantic sailfish caught in plankton nets (Sponaugle et al., 2010) were incorporated into these analysis. To accomplish this, differences between Atlantic and Pacific sailfish postlarval-juvenile growth were assumed to be negligible. These data were fitted to a simple exponential function to express length at age for postlarval juveniles by Sponaugle et al. (2010). From this model, length at absolute hatch age 0 was estimated at 1.87 mm (standard error [SE] +/- 0.106 mm) with a daily growth rate of 0.134 mm/day (SE +/- 0.004 mm/day) for sailfish between 2 and 18 days of age.

Generated “age 0” specimens were developed through simulating length at age of postlarval and juveniles sailfish. Age 0 fish (3 days post hatch) were simulated from a normal distribution using post hatch growth parameters estimated by Sponaugle et al. (2010). These 1000 simulated “age 0” specimens were combined with the 10000

simulated “adult” sailfish of ages 2 to 11+. A von Bertalanffy growth function was fitted to the simulated data (Figure 2.2.4).

Fitting a von Bertalanffy Growth Function to Simulated Sailfish

The simulated sailfish lengths at age for adults and age 0 sailfish described in the previous section were used to estimate the parameters of the von Bertalanffy growth function (Beverton and Holt, 1957) through a non-linear maximum likelihood estimation:

$$\hat{L}_a = L_\infty [1 - e^{-K(a-t_0)}] \quad (2.5)$$

Where \hat{L}_a is estimated length (in cm) at age a (in years), L_∞ is asymptotic size, K is the Brody growth coefficient, and t_0 is fitted age (time) at size 0 cm. Von Bertalanffy function parameters were jointly estimated using a maximum likelihood procedure in the R Development Core Team (2014) assuming $\varepsilon_{L_a} \sim N(0, \sigma_a^2)$, such that maximizing likelihood (MLE) for all observations from 0 to maximum observed age, a_i :

$$MLE(L_\infty, K, t_0, \sigma_a | L_a) = \sum_{a=0}^{a_i} \frac{1}{\sigma_a \sqrt{2\pi}} e^{-\frac{(L_a - \hat{L}_a)^2}{2\sigma_a^2}}, L_a - \hat{L}_a \cong 0 \quad (2.6)$$

and such that standard deviation of residual error is proportional to estimated mean size at age times a coefficient of variation, CV:

$$\sigma_a = \hat{L}_a \times C.V. \quad (2.7)$$

Calibration of Model Assumptions for MIX Application

The most complete study on eastern Pacific sailfish to provide length and age data from direct age observations is Cerdaneres-Ladrón De Guevara et al. (2011, Table I).

Data from these authors included length frequency data in 5 cm bins and a distribution of

directly observed ages. The age distribution from that study rendered the opportunity to construct proportionality factors (ω_t) in mixture distributions. With known fixed proportions of ages in the sample, the nature of the mixture distributions representing size-at-age distributions under varying scenarios of variance or distributions at age. MIX was applied to the length-frequency data provided in Table I of Cerdanarés-Ladrón De Guevara et al. (2011), fixing known observed age proportionality factors (ω_t) to those estimated in their study. Input for starting estimates of mean length-at-age were back-calculated estimates of mean length at age from of Cerdanarés-Ladrón De Guevara et al. (2011) resulting from the preferred power model and used in their study. Means were freely estimated in the analysis. The variance structure of size-at-age was estimated under varying scenarios: including constant variance at age, constant coefficient of variation (CV) at age (proportional uncertainty at length), constant variance at younger ages (1 to 5) with a fixed CV at older ages (6 to 11). Normal distributions and lognormal distributions were also tested. MIX scenarios were evaluated by examining residuals between the mixture distributions and the surrogate distribution. Resulting von Bertalanffy growth parameters for sailfish under each of these conditions should also resemble those estimated through back-calculation in Cerdanarés-Ladrón De Guevara et al. (2011). Scenarios that both reduce residuals in fitting and also yield similar growth parameters as those estimated in Cerdanarés-Ladrón De Guevara et al. (2011) should be considered in fitting mixture distributions to the regional length frequency data series.

Cerdanarés-Ladrón De Guevara et al. (2011) also provided directly observed size at age for sailfish although their analyses of growth parameters relied on back-calculated size at age. Observed size at age distributions for certain age classes, presumably those

ages in earlier years, may be statistically representative of the entire EPO population and could be used to fix mean size at age for those particular age classes. These age classes may be normally distributed (Pearson's test for normality) and be symmetrical with no signs of truncation at larger sizes due to either selection biases or lack of available individuals resulting from spatial stratification of samples.

2.3 Results of New Growth Analyses

Analyses exhibit that the assumption of normality and a constant coefficient of variation for size at age distributions fit the data the best under known proportions of age groups with resulting growth parameters closely resembling those estimated by Cerdaneres-Ladrón De Guevara et al. (2011). Results from this validation are seen in Table 2.3.1 and serve as a basis to apply the mixture distribution analyses on the IATTC 1991-2010 length frequency database under the same assumptions. Analyses examining the distributions of directly observed sizes at age from Cerdaneres-Ladrón De Guevara et al. (2011) found that ages 3 and 4 were quite robust as normal distributions ($P > 0.5$) in both Pearson's test for normality and Shapiro-Wilk tests (package *nortest*, R Statistical Computing Language, 2014). Distributions of ages 5 and older were observed to exhibit truncation, which could be due to size-selection in the sampling for the study or due to availability of larger sizes. Application of MIX to sailfish length frequencies fixed age classes iii and iv (presumably 3 and 4 years of age) to directly observed mean size at age from Cerdaneres-Ladrón De Guevara et al. (2011) in those year classes.

Table 2.3.1. Results from analyses applied to data from Cerdaneres-Ladrón De Guevara et al. (2011) under known age distributions, under various distributions, and under assumptions regarding variance of length at age.

Distribution	Constraint on σ	σ at age or CV	Residuals (χ^2)	L_{∞}	K
Normal	Freely estimate CV	CV = 6.4%	30.852	181.91	0.38
Normal	Freely estimate constant σ	σ = 10.67 cm	40.090	184.7	0.35
Normal	Set fixed CV	CV= 6%	35.602	186.32	0.3
Normal	Set fixed CV	CV= 7%	42.567	180.1	0.37
Normal	Set fixed CV	CV= 8%	59.833	178.5	0.39
Normal	Set fixed CV	CV= 9%	80.429	173.3	0.44
Normal	Freely estimate constant σ Age 1-5, Constant CV Age 6-11	σ Age 2-5 = 10.67, CV Age 6-11 = 6.4%	40.418	180.8	0.38
Lognormal	Freely estimate a constant CV CV	CV = 6.9%	33.257	179.6	0.4
Lognormal	Freely estimate a constant CV σ	σ = 10.9 cm	42.696	183.26	0.36
Lognormal	Freely estimate constant σ Age 1-5, Constant CV Age 6-11	σ Age 2-5 = 10.92, CV Age 6-11 = 6.9%	39.770	181.4	0.38

Application of the method of Shimizaki and Shinomoto (2007) to optimize histogram bin widths found an optimal size class interval of 2 cm. This corresponds to Hinton and Maunder's (2013) decision to use bins of 2 cm for analyzing the same dataset. The most prevalent length interval was 168 to 170 cm. The length-frequency distribution data in 2cm bins (Figure 2.3.1) was partitioned into size-at-age statistical distributions using the MIX algorithm by MacDonald and Pitcher (1979).

Running MIX with the binned length frequency data found that means estimated for the first age distribution, age ii (115 cm), were statistically similar with estimates of back-calculated lengths at age 2 from Cerdaneres-Ladrón De Guevara et al. (2011), who estimated Age 2 fish to have mean lengths of 102.8 to 124.8 cm, and Ramirez-Perez et al. (2011), who estimated back-calculated lengths of Age 2 sailfish to be 109 cm to 130.6 cm

eye forklength (lower-jaw forklenghts in this study converted to eye-forklengths using a conversion function in Prince (1986). Age 1 sailfish were seldom observed in studies by Cerdanarés-Ladrón De Guevara et al. (2011) and Chiang et al. (2004) and absent in Ramirez-Perez et al. (2011). Hence, the first fully identified age distribution by MIX is presumed to be a second age class, age class ii.

Length distribution analyses by the MIX algorithm on the for the entire time series 1991-2010 found a continual progression in size at age with a coefficient of variation equal to 0.101 (Table 2.3.1 and Figure 2.3.2). Age 3 and 4 with fixed means from Cerdanarés-Ladrón De Guevara et al. (2011) and standard deviations estimated by MIX are shown in Figure 2.3.2 to resemble distributions of direct estimation in the literature. The fifth age group, v, comprised the largest proportion of the frequency distribution ($\omega = 0.30$) with a mean equal to 166 cm (standard deviation = 16.6 cm) while the oldest assigned age class was xi(11+), with a mean size ($\mu_{11} = 212$ cm) and standard deviation ($\sigma_{11} = 21.2$ cm). According to a Kolmogorov-Smirnov goodness of fit test performed between combined fitted mixture distributions at age and the total observed length-frequency distribution, determined that the MIX fit is sufficient ($P > 0.05$). Error profiles of mean size at age estimated in MIX are provided in Appendix A.

Table 2.3.2 Parameter estimates from mixture distribution analyses of IATTC sailfish length frequency data from 1991-2010.

Age Class	ω_a	μ_a	σ_a
ii	0.03	115	11.5
iii	0.03	144	14.3
iv	0.15	158	15.7
v	0.29	166	16.5
vi	0.30	176	17.5
vii	0.14	185	18.4
viii	0.05	192	19.2
ix	0.01	201	20.0
x	0.002	208	20.7
xi	0.002	212	21.2

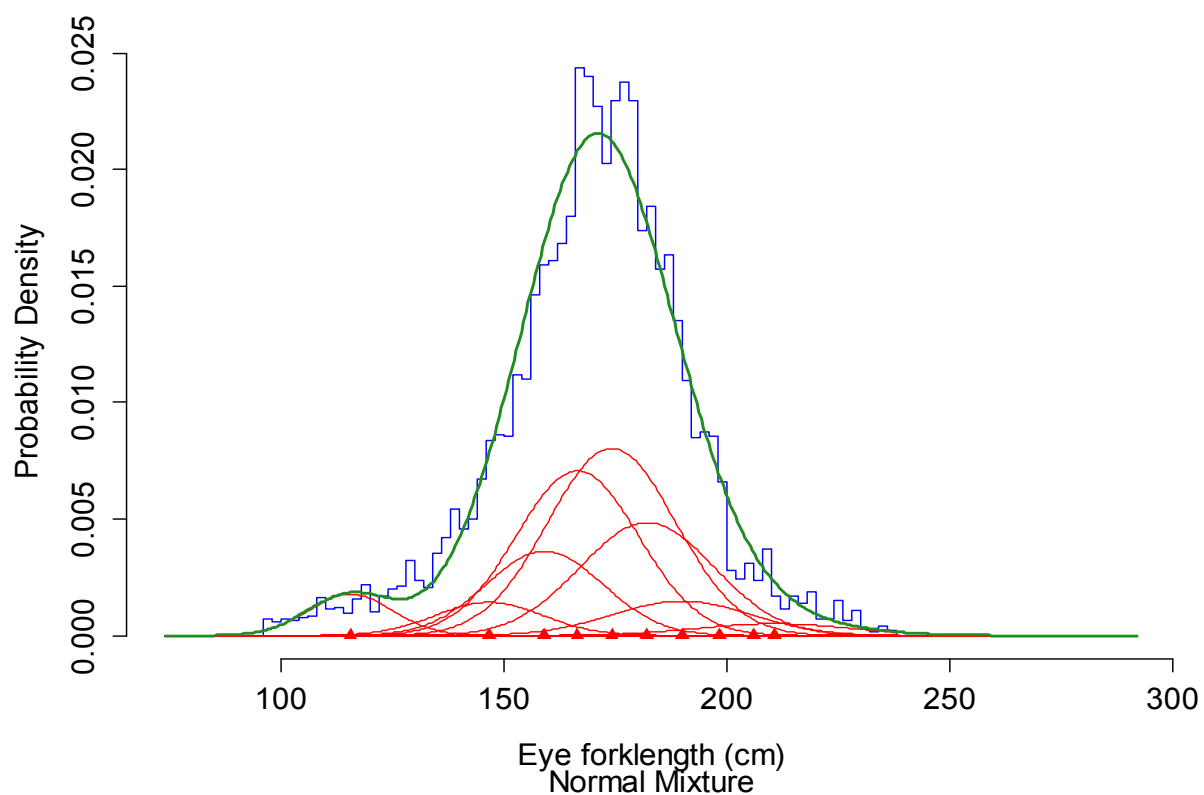


Figure 2.3.1. Mixture distributions for age groups versus length (red line) adding to an integrated probability distribution (green) versus a length frequency distribution from the years 1991-2010.

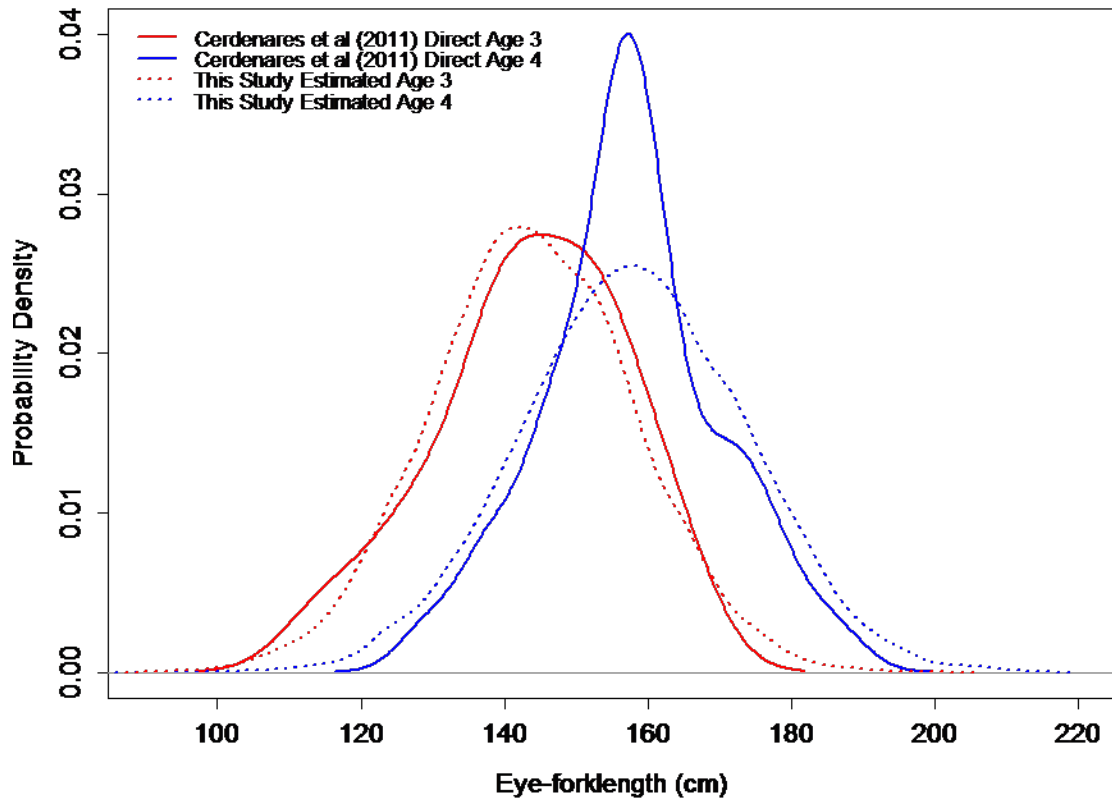


Figure 2.3.2. Length frequency distributions of size at age for Age 3 (red) and 4 (blue) sailfish used in MIX analyses and those estimated by Cerdenares-Ladrón De Guevara et al. (2011)

Monte Carlo simulations of outputs from mixture distribution analyses resulted in a distribution of 11000 fish. This distribution of fish are coupled with 1000 simulated Age 0 fish. Ages of simulated very young age 0 sailfish were converted from ages in days to years and lengths from millimeters to centimeters and are shown in Figure 2.3.3.

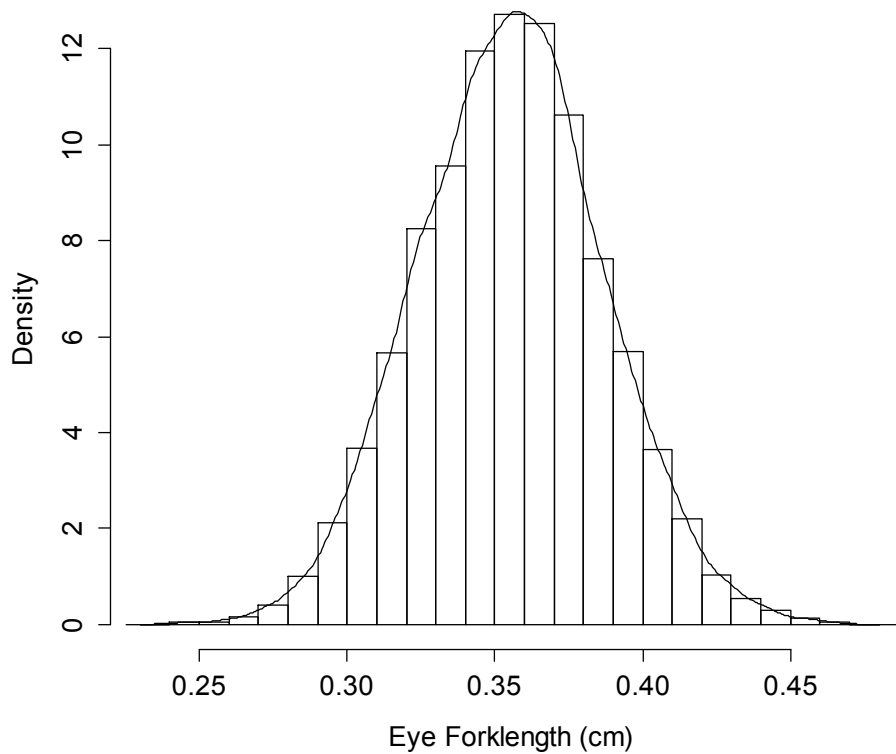


Figure 2.3.3. Simulated age class 0 sailfish lengths at age ($n=1000$) generated from size at age parameters by Sponaugle et al. (2010)

Parameter estimates from the von Bertalanffy growth function using the entire time series are 207.4 cm for L_{∞} , 0.37 yr^{-1} for K , and -0.004 years for t_0 . A variance-covariance matrix for these parameters is given in Table 2.3.3. The fitted von Bertalanffy growth function and the simulated data are shown in Figure 2.3.4. Estimates of size at age, 95% confidence intervals for size at age are included in Table 2.3.4.

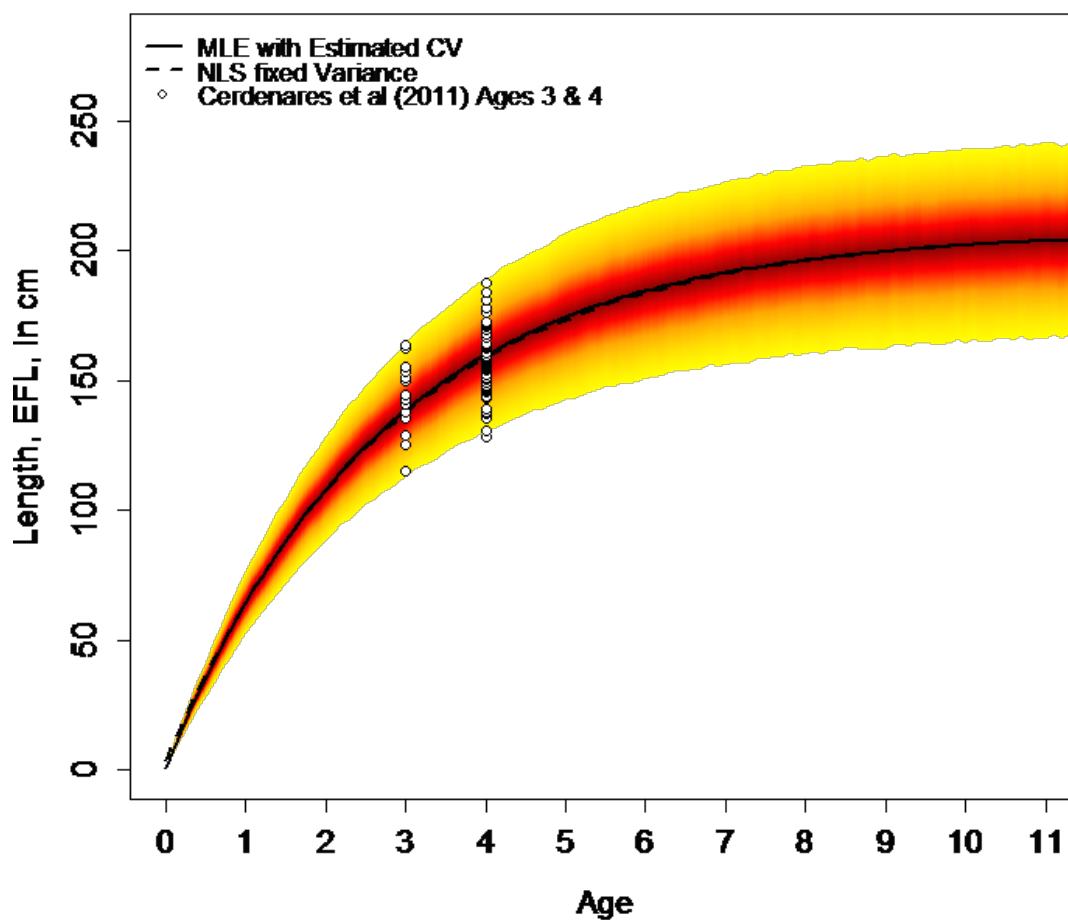


Figure 2.3.4. Fan plot of EPO sailfish von Bertalanffy growth function with 95% confidence interval of length at age fitted to 1100 simulated lengths at age for sailfish ages 0, 2 to 11 years. Observed Age 3 and 4 sailfish from Cerdenares-Ladrón De Guevara et al. (2011) plotted as white circles.

Table 2.3.3. Variance-covariance matrix for von Bertalanffy growth function parameters for sailfish in the eastern tropical Pacific.

	L_{∞}	K	t_0
L_{∞}	428.49	2.59	0.54
K	-2.59	0.14	0.0013
t_0	-0.53	0.0015	0.000002

Table 2.3.4. Estimates of mean lengths at age from fitted von Bertalanffy model with parameters 207.46 cm for L_{∞} , 0.37 cm/yr for K , and -0.004 years for t_0 , 95% confidence intervals for estimates with a CV = 10.1%

Age a	Fitted L_a	+/- 95% CI
2	108.4	21.5
3	138.9	27.5
4	169.9	31.7
5	174.5	34.5
6	184.6	36.5
7	191.5	37.9
8	196.3	38.9
9	199.6	39.5
10	201.9	40.0
11	203.5	40.5

2.4 Discussion and Significance

Due to size composition differences throughout the region, it is important to draw statistical inferences on size at age and growth parameters from a database that includes the entire spatial and ontogenetic range of the species. The new growth analysis yielded a growth curve and variances of size at age that adequately represent the region-wide sailfish population. The growth trajectories and corresponding confidence intervals encompass the entire range of observed lengths for sailfish (Fig. 2.4.1). Applying a growth equation that only represents a part of a stock generates misspecified stock assessment results that can have profound consequences on estimates of mortality and production (Maunder and Piner, 2015; Chang and Maunder, 2012). Age-structured surplus production methods are sensitive to inputs and error in individual growth rate, K , while age-based methods are highly sensitive to errors in L_{∞} (Chang and Maunder, 2012).

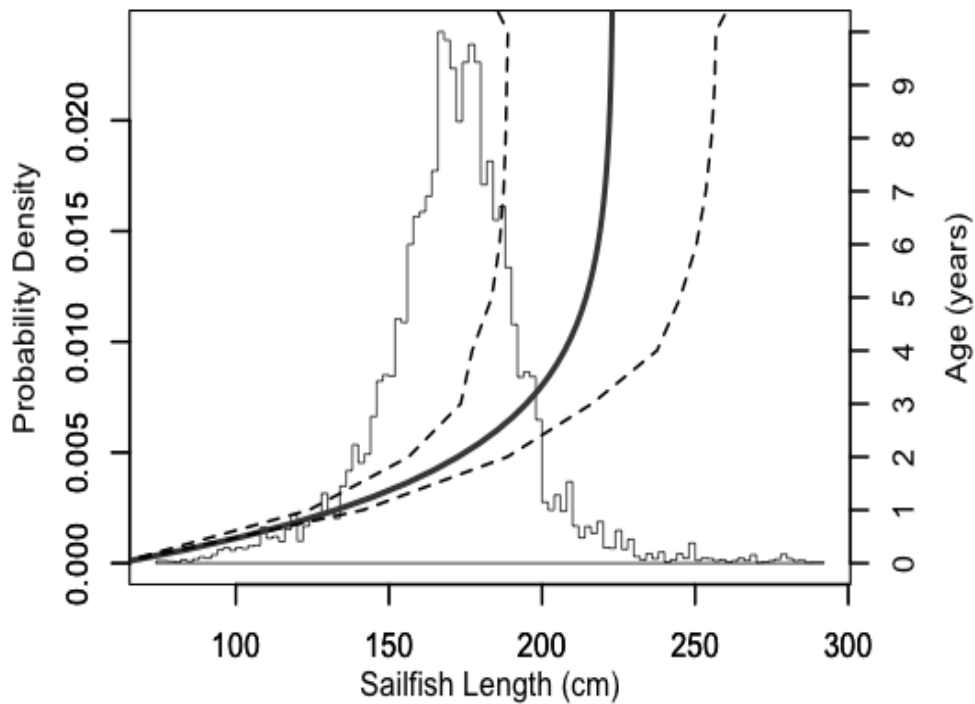


Figure 2.4.1. Length frequency data histogram from region wide growth analyses for EPO sailfish with an estimated von Bertalanffy growth function (solid line) slicing through the distribution with 95% confidence intervals (dashed lines) of size at age estimated by the growth equation.

Partitioning an overall length-frequency distribution into size at age groups by the MIX algorithm yielded distributions for length at age that include estimates of mean size-at-age estimated by Cerdaneres-Ladrón De Guevara et al (2011) from samples from Tehauntepec, Mexico and Ramirez-Perez et al (2011) from samples from Mazatlan, Mexico. The distribution of observed and simulated sizes at age are most similar for ages 3 through 6 for which Cerdaneres-Ladrón De Guevara et al (2011) and Ramirez-Perez et al (2011) recorded heavy sampling (Figure 2.3.4). Age 3 and 4 mean size-at-age

distributions match nearly exactly those between this study and those in the former-mentioned study (Figure 2.3.2). Estimates of mean size at age for sailfish estimated by Cerdanarés-Ladrón De Guevara et al (2011) using a linear back-calculation method are fairly consistent with the estimates of mean size at age from this study. Cerdanarés-Ladrón De Guevara et al (2011) preferred their growth trajectory using estimates from power model back-calculations, citing a slightly higher coefficient of determination in the power model versus the linear model. However, the residual pattern exhibited by these models in Cerdanarés-Ladrón De Guevara et al (2011, Figure 7) do not suggest a consistent, predictive fit about the estimated line, most likely due to absence of larger sampled individuals. Estimates of the growth coefficients (K) in this study (0.37yr^{-1}) were similar to those observed by Cerdanarés-Ladrón De Guevara et al. (2011) (0.36), although they estimated a lower L_{∞} (180.6 cm EFL compared to 207.4 cm EFL). Disparities in L_{∞} and in size at age distributions between Cerdanarés-Ladrón De Guevara et al (2011) and those estimated in this chapter may be due to the small sample size of larger fish available in their sample. In data provided by Cerdanarés-Ladrón De Guevara et al (2011, Table I), 6.7% of length data exceeded their estimated L_{∞} of 180.6 cm EFL. In the data used in the analyses for this chapter, 30.5% of length data exceeded 180.6 cm EFL. Only 4 % of length frequency samples used in this study exceed it the new estimate.

However, size at age distributions and estimated growth parameters in the analyses presented in this chapter are quite different from those reported by Alvarado-Castillo and Felix-Uraga (1998) and Ramirez-Perez et al., (2011). Growth parameters from these studies yielded growth trajectories that either approached L_{∞} within the first year due to an overestimated growth coefficient (Alvarado-Castillo and Felix-Uraga,

1998) or yielded a quasi-linear growth curve with a highly negative t_0 (Ramirez-Perez, 2011). Alvarado-Castillo and Felix-Uraga (1998) aged sailfish from a highly size selective recreational fleet where large individuals were sampled, leading to likely overestimation of K . Additionally, vascularization in billfish spines may bias direct observation of early age rings when spine sections are for older age individuals (Chiang et al, 2004; Cerdaneres-Ladrón De Guevara et al., 2011; Ramirez-Perez et al., 2011) and methods to correct for missing annual rings in spine readings may not have been widely available at the time of the Alvarado-Castillo and Felix-Uraga (1998) study.

Variance within presumed age groups from the mixture distribution analyses in this study show an increase in variance in length at age ($CV = 0.101$) which is consistent to the rate assumed by Hinton and Maunder (2013, $CV=0.09$) and to the ratio of variance to mean length at age exhibited by Cerdaneres-Ladrón De Guevara et al. (2011) as demonstrated by Hinton and Maunder (2013). Low sample sizes due to availability, selectivity, and exploitation patterns could prevent estimation of size-at-age distributions of certain age classes. Such issues with size-at-age variance in older specimens could possibly lead to truncated estimates of length-at-age distributions- that when fitting a growth function- could lead to biased estimates of K and L_∞ . Truncated length-at-age distributions for older fish and a lack of representation of very young fish can also lead to a lack of curvature of von Bertalanffy growth trajectories for younger specimens, thus estimating highly negative t_0 and unexpectedly low K . For example, Chiang et al. (2004) and Ramirez-Perez et al. (2011) observed a lack of variance for older fish, presumably as a statistical artifact of their low sample size of older fish due to selectivity/availability or low sampling rates of older fish that may not be available. Consequently, both studies

estimated quasi-linear growth curves with asymptotic lengths (L_{∞}) that far exceed observed lengths with highly negative age-at-size 0 parameters (t_0) and low growth coefficients (K). These curves seem unrealistic for a relatively fast-growing pelagic species such as the sailfish.

Growth parameters for sailfish estimated in this study contrast with some of those in the peer-reviewed literature (Alvarado-Castillo and Félix-Uraga, 1998; Chiang et al., 2004; Cerdaneres-Ladrón De Guevara et al., 2011; and Ramírez-Pérez et al., 2011) in that estimates for t_0 are closer to zero due to the use of estimated lengths from age 0, therefore “anchoring” the growth trajectory at age 0 in model fitting. This adds significant biological meaning to the t_0 and K parameters in the von Bertalanffy growth function by using an actual distribution of Age 0.

L_{∞} estimated for sailfish in this study result from a larger sample range of observed length data for sailfish in the EPO while the range of observed larger fish length data used in the studies by Chiang et al., (2004) and Cerdaneres-Ladrón De Guevara et al., (2011) are narrower (Figure 2.4.2). Consequently, the estimates for L_{∞} are significantly different among the studies.

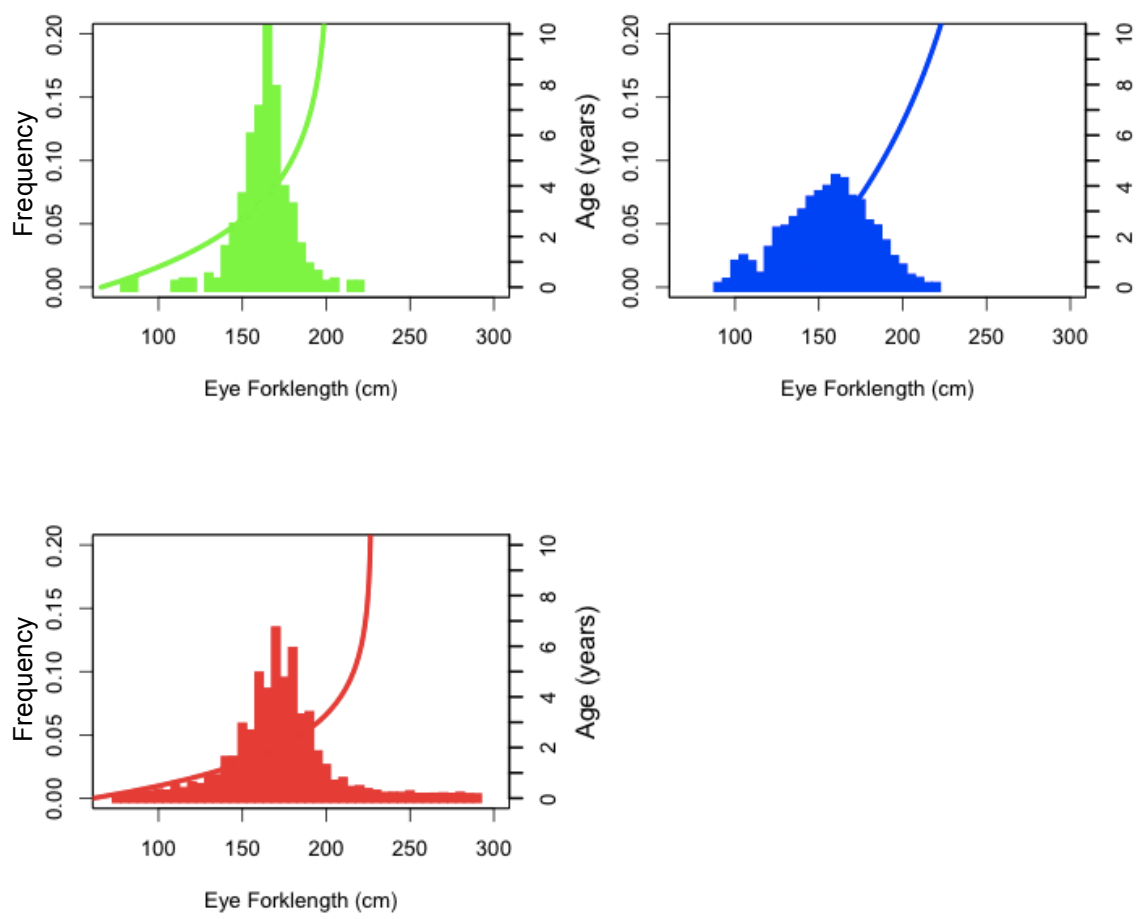


Figure 2.4.2. Histograms of length-frequency data used in notable growth analyses for sailfish (green: Cerdaneres-Ladrón De Guevara et al., 2011, blue: Chiang et al. , 2004, red: this study) with fitted von Bertalanffy growth trajectory. Primary response axis is frequency of fish in 5 cm bins, secondary response axis is age.

The possibility of sexual dimorphism in Pacific sailfish cannot be evaluated from the length frequency data used in this study because fish were not sexed. Dimorphism was also not reported in sailfish in the EPO within the literature. Alvarado-Castillo and Félix-Uraga (1998) found no significant differences in growth between sexes using observed length at age, while Cerdanars-Ladrón De Guevara et al. (2011) used sexes combined in their growth analyses. Ramírez-Pérez et al. (2011) did not find significant differences in the asymptotic lengths estimated for female and male sailfish, indicating an absence of sexual dimorphism. For sailfish examined in the Western Pacific, Chiang et al. (2004) found small differences for male and female growth parameters and males exceeded females in size at age. However, a rigorous statistical test of sexual dimorphism in the western Pacific samples was not included to conclude on differences in growth between sexes.

Direct observation of ages should not be supplanted by use of modal progression analyses. However, directly measuring age of istiophorids from hard parts such as spines is notoriously difficult and results are often inconsistent and methodologies are different between studies (Kopf et al, 2011). Chiang et al (2004) were the first to implement methodologies on billfishes to correct for missing annual rings in spines due to vascularization, which have been major caveats in growth studies on billfishes. In absence of direct observations of age throughout the distributional range of a fish species, analyses of length-frequencies to partition age groups can serve as an alternative or to complement limited observations of age. Prince (1986) recommended departing from the use of spines and to rely more on tag-recapture methods to assess growth of billfishes. However, low recapture rates of tagged billfish and uncertainty in size measurements

(Ehrhardt and Deleveaux, 2006) remain as problems in assessing growth of billfishes. Ideally, modal progression methods outlined in this chapter can serve to supplement better tag-recapture analyses and direct observations of age at growth for sailfish throughout the region when they become available, much like a hierarchical approach introduced by Dortel et al. (2011) who incorporated multiple sources of data to estimate parameters. In addition to observing and partitioning length groups into age groups, morphometric studies of billfishes can be used to infer age classes. Ehrhardt (1996) examined allometry of swordfish and found remarkable patterns in morphometric growth that can be used to assess age classes. Morphometric growth patterns should be tested in future growth studies of istiophorids, and fisheries data collection modified to include additional metrics of body shape, girth, length, etc in sampling by observers.

The use of length frequency distribution analyses without any prior knowledge of directly observed length at age may yield suitable determinations of size at age for a species if sampling is thorough with large sampling rates for many years (Pauley and Morgan, 1987), if length at age distributions are visually conspicuous in length frequencies, or for short-lived and fast growing species (Campana, 2001). In the case of this study, information for existing studies allowed the ability to anchor a growth trajectory of sailfish at Age 0, validate assumptions of variance relative to mean size at age, and provided starting estimates of mean size at age to estimate distributions of size at age from a comprehensive length frequency sample. Additionally, sampling size for sailfish was relatively high.

Estimates of size at age developed from the growth equation presented in this chapter were used to partition length samples into probabilities of age at length and used

to estimate total instantaneous mortality rates for sailfish by year in the following chapter. Length frequencies based on growth parameters under zero exploitation with natural mortality (M) equaling 0.25 (Ehrhardt and Fitchett, 2015, in progress) are depicted in Figure 2.4.3. This theoretical length frequency distribution under no exploitation was not seen in sampled catch due to exploitation patterns and fishing mortalities. These exploitation patterns and mortalities are addressed in Chapter 3.

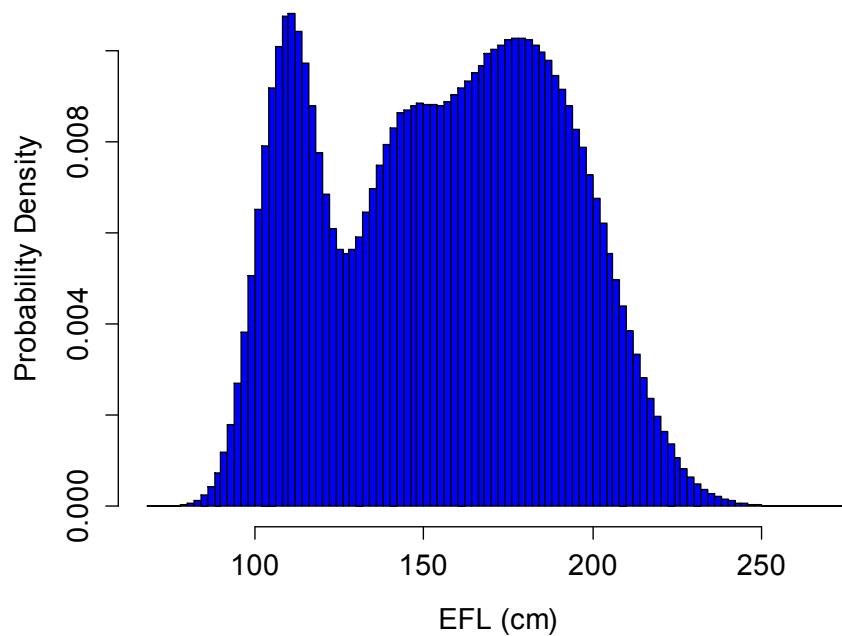


Figure 2.4.3. Simulated theoretical length distribution of an unexploited population of EPO sailfish for ages 2 to 11 using growth parameters estimated in this chapter.

Chapter 3

Determination of Age Composition and Mortality

3.1 Motivation and Background

Sailfish in the eastern Pacific Ocean have yet to be formally assessed, most likely due to incomplete data (Hinton and Maunder, 2013). Landings and fishing effort for eastern Pacific sailfish are incompletely reported from heterogeneous multinational fisheries targeting primarily tunas and mahi-mahi, where sailfish and other istiophorids are caught as incidental bycatch. In April 2013, the Inter-American Tropical Tuna Commission reported (IATTC, 2013) that they had unsuccessfully attempted to assess sailfish in the eastern Pacific Ocean by employing a suite of widely-used stock assessment packages commonly used by the Commission to assess tuna species. Estimation of mortality and abundance was inconclusive due to dubious growth functions and absence of complete landings for many of the fleets operating in the region. As mentioned in Chapter 2, existing growth equations had estimates of average asymptotic length (L_{∞}) that were exceeded by over 30% of all observed length frequencies in the region. A new set of growth parameters were developed in Chapter 2 that represents the geographic and size range of animals observed in the eastern Pacific Ocean and produced a more plausible estimate of L_{∞} .

The goal of this chapter is to develop a method to elucidate age structure from available length frequencies and then use these data to estimate age structure, and subsequently stock mortality of sailfish in the EPO. A virtue of understanding age structure of a fishery is to have the ability to infer future abundances of the stock, provide

advice on harvest regulations, infer recruitment, and retrospectively estimate prior stock abundances by age. Age-structured assessment methodologies that track cohorts of animals through time to determine population abundance and exploitation rates depend on information on age composition in landings. Murphy (1965) and Gulland (1965) popularized the use of sequential population analysis that estimates annual age-specific abundance and fishing mortality rates based on the frequencies of ages in landings for a given year or fishing period. Pope (1972) coined the term “cohort analysis” for a method that simplified the assumptions of sequential population analyses, but was still based on age composition in landings. Ricker (1958) described yield-per-recruit analysis to be dependent on functional relationships between age, growth, and mortality throughout the life span of the species. A paramount requirement for application of age-based stock assessment methods is to have matrices of catch at age and size. Ideally, empirical observation of ages in landings may be obtained through length frequencies in biological samples and age determinations from a sub-sample of hard-parts (Beverton and Holt, 1957). Ageing is possible because annual or seasonal age demarcations on hard parts (scales, otoliths, spines, vertebrae, or other biological structures) allow processing by biologists to determine age at size. Collecting sufficient biological samples to directly age fish requires a large processing capacity, high associated costs, and much time. This renders the process of collecting random biological samples representative of a population to be logistically unrealistic in many fisheries. Lacking the sampling capacity and the level of funding required to collect and to analyze total age frequencies in landings from fish populations, Age-Length Keys (ALKs) are used. ALKs are probabilities of ages for any observable sets lengths in length frequency samples.

Expanding length frequencies into ages with use of an ALK allows estimation of age composition in a fishery. An avenue to generate a catch at age matrix is to integrate length frequency samples with a corresponding ALK and then expand these to total landings. Therefore, an essential step in generating stock assessment information is to estimate unbiased age-length keys to estimate catches at ages.

Empirical observations of length-at-age from biological hard parts to discern age composition are mostly unavailable for EPO sailfish. When spines are available to age sailfish, vascularization makes it difficult to validate ages. Furthermore, sailfish are caught as bycatch in widespread and diverse tuna and mahi-mahi fishing operations throughout the EPO. Therefore, this chapter introduces a new algorithm to construct ALKs in data poor situations in which total catch and effort is incomplete or unavailable. The algorithm draws from known distributions of size at age (or variance-covariance of growth parameters of a known growth function) and exploitation patterns derived from length frequency samples that are collected at random from the population. The algorithm fits predicted length frequency distributions to field-observed length frequencies through an objective function. These length frequencies are ultimately assigned age at size probabilities in the algorithm.

Constructing Age-Length-Keys (ALKs)

The use of age-structured population assessment methodologies depend on knowledge of age frequencies in size-structured landings - either estimated or empirically observed. Fredriksson (1934) first developed the concept of age-length keys which are distributions of age at size from a two stage sampling where a large size frequency

sample, N_L , is collected as random samples from the landings and a random sub-sample of catch, $C_{a,L}$, containing age a and length L through ageing hard parts is drawn from the previous sample to generate an age-length key. In this way age frequencies in fish landings can be estimated from limited samples of age at size determinations expanded to total estimated age frequencies from available length-frequency samples expanded to total landings. Conceptually, an age-length key may be expressed as

$$p(a|L) = N_{a,L} / \sum_{a=1}^{a_\lambda} N_{a,L} \quad (3.1)$$

such that:

$$ALK_{L,a} = \begin{bmatrix} p(a_1|L_1) & \cdots & p(a_\lambda|L_1) \\ \vdots & \ddots & \vdots \\ p(a_1|L_\lambda) & \cdots & p(a_\lambda|L_\lambda) \end{bmatrix} \quad (3.2)$$

where L is length/size and a is ages from number of samples in the catch. To extrapolate the numbers of individuals at age and length ($\hat{N}_{a,L}$) from a length frequency sample, the computed age-length key matrix is multiplied by the concurrently collected length frequencies, N_L , and individuals are summed across age classes (Fredriksson, 1934),

$ALK_{a,L} \times N_L$:

$$\hat{N}_{L,a} = \begin{bmatrix} \Pr(a_1|L_1) & \cdots & \Pr(a_\lambda|L_1) \\ \vdots & \ddots & \vdots \\ \Pr(a_1|L_\lambda) & \cdots & \Pr(a_\lambda|L_\lambda) \end{bmatrix} \times \begin{bmatrix} N_{L=1} \\ \vdots \\ N_{L=\lambda} \end{bmatrix} \quad (3.3)$$

Age frequencies, \hat{N}_a , are computed by summing through all lengths by age:

$$\hat{N}_a = \sum_{L=1}^{L_\lambda} [ALK_{a,L} \times N_L] = \sum_{L=1}^{L_\lambda} [\hat{N}_{a,L}] \quad (3.4)$$

Growth Transfer Process

Accounting for the transfer of individuals in size groupings from one age to another is a critical process and the basis for the mechanisms within the numerical algorithm discussed further in this work. Legault (1996) developed a concept of a growth transfer matrix from variance-covariance of growth parameters. In this approach, individuals within a population can be transferred as groups of individuals of age (a) and size or length (L) through progressions in age and possible increments in growth (i). As a predetermined number of fish progress in age, they are grouped in numbers of age-size bins, $N_{a,L}$, and are randomly assigned growth parameters from the variance-covariance matrix of growth parameters which yields a numerical distribution of possible growth increments from the present age increment to the next age increment (Figure 3.1.1; Legault, 1996). Numbers of individuals within size-age bins transfer to age-size bins corresponding to the number of growth increments - depending on the proportion of individuals that experience any possible increment in growth. These proportions of incremental growth for each proceeding age and size increment are defined in the growth transfer matrix, $G_{a,L,i}$. Numbers for each age-size bin $N_{a,L}$ can be estimated by multiplying a number of individuals in the prior age and sizes by an appropriate growth transfer matrix, $G_{a,L,i}$, values:

$$N_{a,L} = \sum_{i=0}^n N_{a-i,L-i} G_{a-1,L-i,i} \quad (3.5)$$

Legault's (1996) growth transfer matrix approach follows an expected number of individual fish growing through predetermined trajectories. At each age step, fish transfer to another growth increment and form a new distribution of individuals at the age. This approach allows a growth transfer to be computed at once rather than continuously for

each iteration of age. Furthermore, an advantage of this approach is the possibility to apply any growth function with known variance-covariance or any known size-at-age distributions for any species.

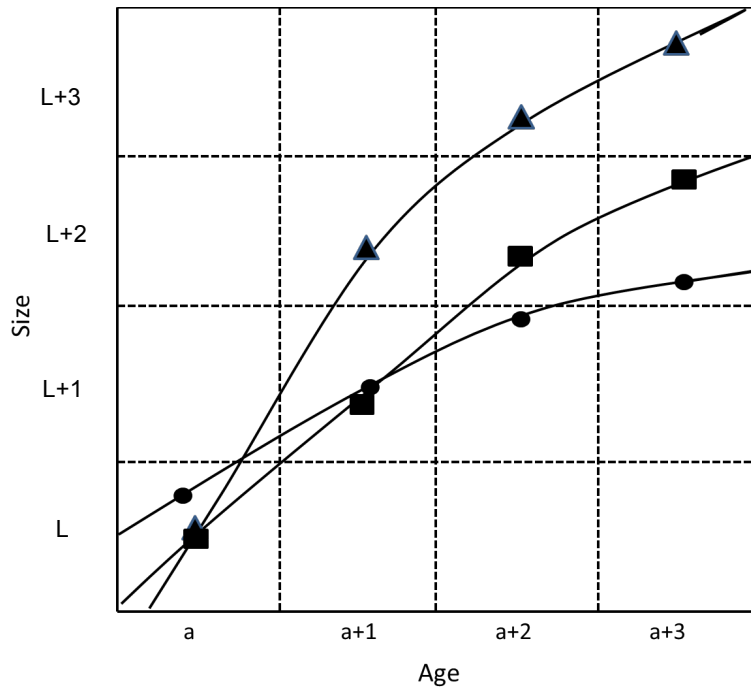


Figure 3.1.1. Redrawn from Legault (1996): Depiction of three growth trajectories (circle, triangle, and square) passing through age and size bins, increasing in finite $a+1$ ages groups and by $L+i$ size groups depending on growth parameters selected from a known distribution.

One limitation in the application of the Legault (1996) transfer matrix is that the groups of individuals in bins of age at size are formed by a combination of individual growth trajectories that differ greatly and the individuals in these bins do not follow a consistent deviation of size within expected size at age distributions as they progress in age. Therefore, individuals may depart from the potential heritable growth deviance

relative to population mean size at age. For this reason, an individual transfer model was developed in the StALK algorithm for the purpose of generating age at size distributions emblematic of heritable growth patterns found in nature (Sainsbury, 1980; Cheverud et al., 1983; Russo et al., 2009; Johnson et al., 2011).

The Statistical Age-Length Key (StALK) algorithm is introduced in this chapter and validated on a simulated sailfish fishery and applied to a known observed red snapper fishery to observe the efficacy and limitations of the algorithm. Validation testing is conducted to ensure that StALK accurately constructs age at size distributions. This new method was used to estimate instantaneous mortality on sailfish and then compared to alternative methods. Testing was conducted in further sections to determine if resulting age compositions at length can be used to estimate total instantaneous mortality rates for data-poor fisheries via simple catch curve analysis.

3.2 New Methods, Model Testing, and Application

The introduced StALK algorithm uses an individual transfer mechanism between size and age based on expected individual, heritable growth patterns. This mechanism is to be used in numerical solutions of expected ALKs that can be applied to length frequencies in data-poor fisheries. The algorithm will estimate age composition in absence of complete catch records. The overall concept of the numerical algorithm is to estimate an age-length key in data-poor fisheries (in which one or more components of landings or effort are unknown) with the flexibility to apply any overall selectivity pattern, any growth trajectory for which mean and variance of sizes at age are known, with any given length-frequency sample that has been thoroughly and randomly collected

from landings with any number of gear types. In ideal situations where landings or CPUE indices are available, the algorithm can track cohort strength through time, even if length frequencies are analyzed independent by year.

Table 3.2.1. Terms, definitions, and units for variables and subscripts

Term	Definition	Units
a	age	yr
L	Length or size	cm EFL
$p(a L)$	probability of age distribution given length	
$N_{a,L,g,y}$	numbers of fish given age a , length L , heritable growth deviance g , or year y	numbers of fish
$C_{a,L,g,y}$	catch of fish given age a , length L , heritable growth deviance g , or year y	numbers of fish
ALK	age-length key; probabilities of age classes for any observable length	dimensionless
g	heritable growth deviances of size distribution	dimensionless
μ	average length at age a , \bar{L}_a	cm EFL
s	standard deviation of size at given subscript, age a	cm EFL
Γ	matrix of size-specific selectivity at age a given length L and predisposed growth deviance g	dimensionless
H	age-specific statistical parameter accounting for mortality and exploitation pattern at age a	yr ⁻¹
Z	instantaneous total mortality	yr ⁻¹
F	annual fishing mortality	yr ⁻¹
F^*	fishing mortality by age, predetermined growth trajectory, and year used in simulation model	yr ⁻¹
M	natural mortality	yr ⁻¹
R	total recruitment by year y	numbers of fish
$Fnom$	annual nominal fishing mortality by year y	yr ⁻¹
U	catch per unit effort (CPUE) in simulator	fish per 1000 hooks

Conceptual Basis for a Numerical Statistical Age-Length Key (StALK)

The primary concept in the numerical algorithm for estimating age-length keys is to follow individual fish through size and age based on a predetermined growth trajectory from age 0 to age of senescence. A growth transfer procedure similar to Legault (1996) is

adopted but with size at age groups ‘tracked’ based on an assigned predisposed growth deviance parameter. Additionally, the algorithm assumes that any fish at any size or age has a genetically-predisposed level of heritable growth deviance, g , that keeps an individual at predetermined level quantile within a size at age distribution as fish pass through ontogeny. The higher the g value, the larger the individual within a given age. The growth deviation values for individuals in the algorithm are numerically seeded z-scores coming from a standard Normal probability distribution at age 0. Since most fisheries do not exploit fish at absolute age 0, the size at age for these fish are inconsequential until they are recruited into the fishery. Therefore, if a fish or group of fishes exhibit an anomaly of +1 at starting age 0, it will continue to have such anomaly at all other ages (Figure 3.2.1). The algorithm is also flexible and can allow adjustment of size transfers in lieu of any introduced extrinsic factors impacting growth, such as environmental impacts or density-dependence.

These individuals of fish, binned in age-size groups, are subjected to one or more size-specific selectivity patterns (either estimated or arbitrarily assigned) and an age/time specific population dynamic process that accounts for both fishing mortality and recruitment effects into the fishery (dotted lines in Figure 3.2.1). This process is modeled as a series of age-specific parameters which are to be estimated, H_a (from $H_{a=1}$ to $H_{a=max\ age}$). Binned fish are also subjected to natural mortality at age, which can be constant or variable. This algorithm relies on known variance at length for a given set of growth parameters, which have been estimated to represent the population. The age-size specific population dynamics process (that reflects recruitment and mortality processes) is estimated through an optimization procedure that minimizes an objective function of the

total sum of squared residuals between length-frequencies yielded by the algorithm and observed length-frequencies. An ALK is produced from the resulting numbers of fish at size and age generated by the algorithm

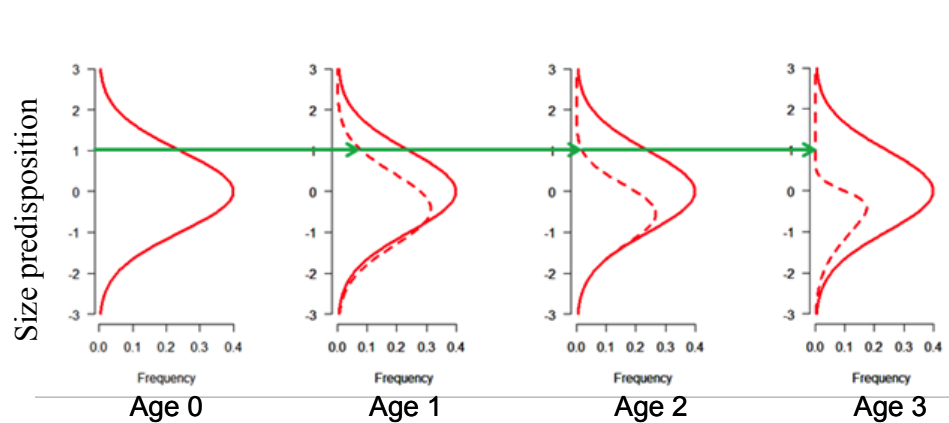


Figure 3.2.1. Fish with an assigned, heritable “size predisposition” deviance, a z-score equal to 1 from a surrogate Gaussian distribution (solid line) subjected to a size-dependent exploitation pattern and age-specific mortality throughout time (ages 0 to 3, dashed lines).

The algorithm assumes that individual age and growth patterns are well understood and fully described by a variance of size at age around a fitted growth function. The algorithm assumes continuous annual population growth and decay with decay terms depending on an age-specific population process statistical fitting parameter, H_a , accounting for fishing mortality, natural mortality, and recruitment into the fishery (if applicable) for each age group. Natural mortality may be accounted for in the fitted parameter H , unless a value for natural mortality is specified otherwise.

A product of using this algorithm in conjunction with an age-structured catch equation could be an estimation of mortality. In absence of complete landings for

sequential population analyses (Gulland, 1965) or standardized abundance indices needed for tuna sequential population analysis (Gavaris, 1988), less complex means of estimating a total annual mortality may be employed such as Ricker's (1958, 1975) age-structured catch curves (ACC) consisting of a regression analysis between fractions of fully recruited ages landed on age for total instantaneous mortality (Z) estimation:

$$\ln\left(\frac{N_a - N_{a-1}}{\Delta a}\right) = b - Za \quad (3.6)$$

Where N_a is the estimated catch at age a in a given year or period and $-Z$ is the total instantaneous mortality rate estimated at a given time period at assumed equilibrium. Numbers of catch at age resulting from StALKS ALK outputs expanded by length frequencies can be inserted in this equation and fitted to estimate total mortality, Z .

Implementation of the Statistical Age-Length Key Solution (StALK)

The algorithm Statistical Age-Length Keys, StALKS, was developed in the R Statistical Computing environment (R Development Core Team, 2014). StALKS begins with seeding the algorithm with an initial recruited population size at age zero, R^* , which is generally a very large number, especially for long-lived stocks with long-term exploitable phases. Additionally, preliminary parameterization includes specifying a pertinent range of sizes in the fishery (maximum and minimum). This is a range of lengths the investigator wishes to fit to, usually the range of lengths and numbers that are fully recruited into a fishery. The user may also specify whether he/she wishes to bin data in a resultant ALK. By default, length at age a distributions are assumed normally distributed with mean length and variance of length (μ_a, σ_a^2) and input into the algorithm.

The StALK algorithm works in the following steps, where $N_{a,g}$ is a matrix of number at age a ($a= 0, 1, \dots a_i$) and growth deviance g ; $N_{a,l}$ is a matrix of frequencies at age a and length bin i ; M_a is time-dependent natural mortality at age (either constant or age-assigned); $\Gamma_{a,g}$ is a matrix of length-specific selectivity derived from growth potential deviance, g ; and H_a are age-specific compounded population recruitment-mortality process coefficients fitted by the algorithm and are initialized to equal 0 for each time step. H_a serves as a coefficient to be multiplied by $\Gamma_{a,g}$ to estimate fishing mortality at age and growth deviance corresponding to size:

1. Following the conceptual frame for the individual transfer model, non-randomly seeded size-specific predisposed heritable growth deviance parameters, g (e.g. $g=-3.00, -2.99 \dots 0.00 \dots 3.00$), are assigned in probability densities as 301 z-scores (from a 99.9% confidence interval) from a standard normal distribution $N(0,1)$ from Equation 2.4. Numbers in corresponding heritable growth deviance parameters at age 0, $N_{a=0,g}$, are these probabilities at g multiplied by R^* . This step creates initial seeded numbers at age 0 for each values of g .
2. For age group, a , there are numbers of individuals at age $N_{a,g}$ with a discrete heritable growth deviance g that are converted to length L .
3. For any age group with known length at age distributions (μ_a and σ_a), individuals of heritable growth deviance g and corresponding age are assigned a computed length from known distributions, such that g is a number of standard deviations from mean value of length at age:

$$L_{a,g} = \mu_a + g\sigma_a. \quad (3.7)$$

From this computation, a matrix of lengths given an age a (0 to a) by heritable growth deviance g (-3.00 to 3.00) is created- this is a growth deviance-length transfer matrix used to convert length at age from respective heritable growth deviance g :

$$L_{a,g} = \begin{bmatrix} L_{a=0,g=-3.00} & \cdots & L_{a=0,g=3.00} \\ \vdots & \ddots & \vdots \\ L_{a=\lambda,g=-3.00} & \cdots & L_{a=\lambda,g=3.00} \end{bmatrix} \quad (3.8)$$

4. Based on a predetermined size specific gear selectivity $F|L$ and exploitation pattern reflected in the sampling of the fish, $F|L$, (application of selectivity discussed in following sections), a matrix of selectivity values, $\Gamma_{a,g}$, is created for each $L_{a,g}$ given any function for selectivity. This matrix is applied for each individual given age a (0 to $a\lambda$) by heritable growth deviance g (-3.00 to 3.00):

$$\Gamma_{a,g} = \begin{bmatrix} \Gamma_{a=0,g=-3.00} & \cdots & \Gamma_{a=0,g=3.00} \\ \vdots & \ddots & \vdots \\ \Gamma_{a=\lambda,g=-3.00} & \cdots & \Gamma_{a=\lambda,g=3.00} \end{bmatrix} \quad (3.9)$$

5. Selectivity at any length is selectivity in Equation 3.9 that shares the respective dimensions of age, a , and growth deviance, g , for length in Equation 3.8.
6. Under conditions of no exploitation, individuals in each bin in a given age are subjected to exponential decay under the conditions:

$$N_{a+1,g} = N_{a,g}e^{-M} \quad (3.10)$$

7. Under exploited conditions, individuals are subjected to size specific exploitation and time-varying mortality. Therefore a size-specific selectivity pattern, $\Gamma_{a,g}$, and age-specific compounded population recruitment-mortality process values, H_a , are applied to population conditions under Step 4, such that

$$N_{a+1,g} = N_{a,g}e^{-M-\Gamma_{a,g}H_a} \quad (3.11)$$

H_a can be negative if availability of a proceeding age class exceeds mortality from the fishery in previous age, depicted in the length frequencies represented by that age class. H_a can account for changes in numbers of fish by size-selective fishing mortality and exploitation pattern by age and length (transferred by heritable growth deviance through age in matrix 3.7), simplified from Equation 3.11:

$$\ln \left(\frac{N_{a,g} - N_{a-1,g}}{\Delta a} \right) = -(M + \Gamma_{a,g} H_a) = Z \quad (3.12)$$

with estimation of total instantaneous mortality, Z , and $\Gamma_{a,g} H_a$ terms

approximates to fishing mortality, F , at a given age and growth deviance.

8. In following age progression, length values L at age $a+1$ and heritable growth deviance g are calculated from the formulation in Step 3.
9. Frequencies of catch derived from population frequencies at length (L) computed in Step 6 and Step 7 are placed in bins corresponding with present age (a) and length (L) in the matrix $N_{a+1,g}$ using conversion matrix, Equation 3.8.
10. Steps 2 through 8 are repeated iteratively from age 1 to maximum age using an optimization procedure, *optim*, that minimizes the sum of square of residuals of fitted length frequencies resulting in Step 7 against observed length frequencies in either biological samples or in total landings. The range of length L used as comparable cumulative density probabilities is subjective but could be from fully selected lengths (where F_L is a high probability) to maximum length L_∞ . The optimization procedure uses a conjugate gradient method (Fletcher and Reeves, 1964) within the *optim* procedure to fit the unknown, time dependent compounded recruitment-mortality population parameter, H_a , through an objective function. The objective function depends on cumulative densities of

estimated length frequencies in Step 8 (\widehat{CDF}_L) and observed cumulative density function of samples (CDF_L). The objective function reduces the total residual sum of squares (RSS) between \widehat{CDF}_L and the cumulative densities of observed length frequencies CDF_L :

$$RSS \cong \min \sum_{l=\min}^{l=\max} (CDF_L - \widehat{CDF}_L)^2 \quad (3.13)$$

Fitting an objective function is depicted in Figure 3.2.2.

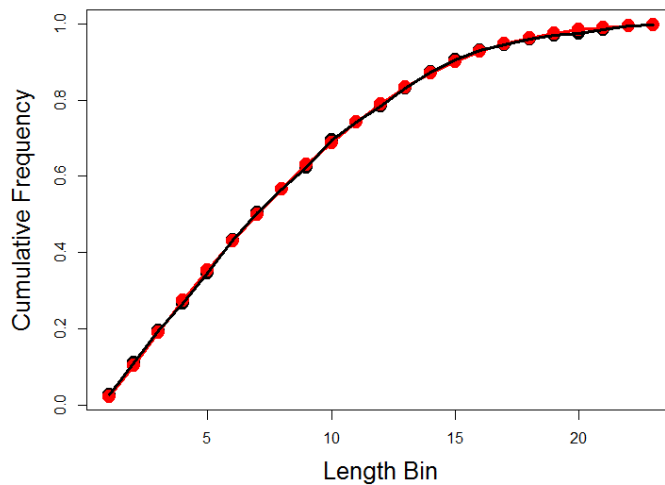


Figure 3.2.2. Cumulative densities of selected observed length-frequencies (black) and corresponding fitted cumulative densities from estimates of StALK (red)

11. A numerical solution for $N_{L,a}$ should emerge from the algorithm at successful convergence of the objective function in Step 9 and fitting optimal values for H_a . An ALK, may be built from the resulting $N_{a,L}$ applying Equation 3.2. A color plot of a resulting ALK is depicted in Figure 3.2.3

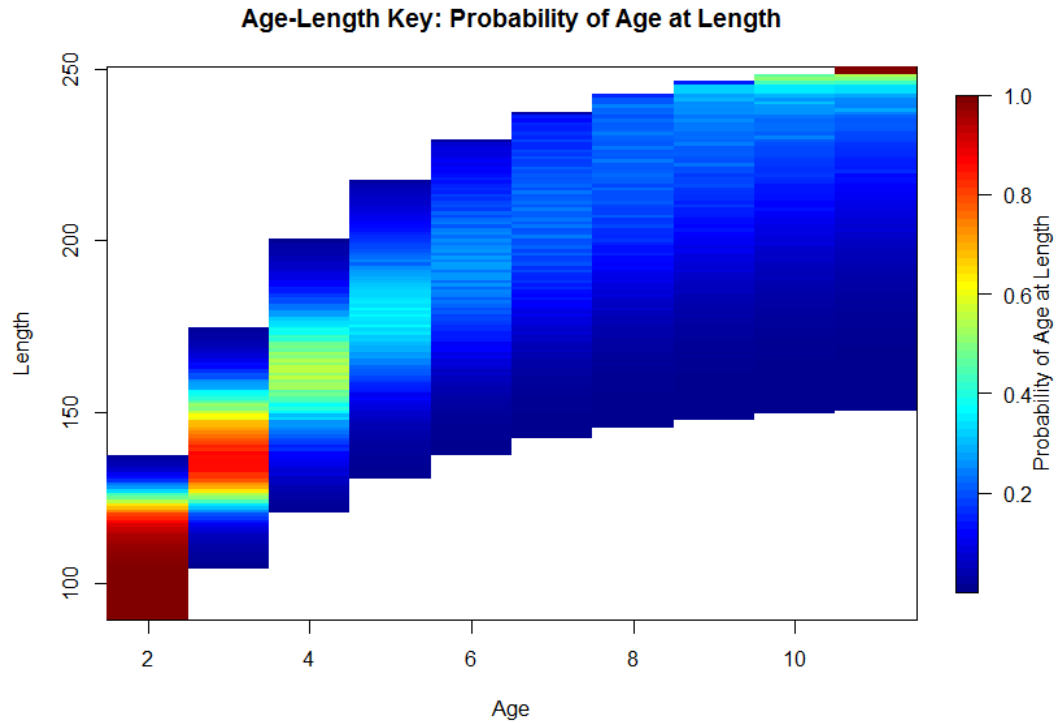


Figure 3.2.2. A color image plot of an ALK constructed by StALK for EPO sailfish for ages 2 to 11.

12. Estimated numbers of individuals at age, \hat{N}_a can be calculated by expanding $ALK_{a,L}$ by observed length frequencies, N_L in Equation 3.5 and summing across lengths by age in Equation 3.5.

The StALK algorithm produces an ALK, $ALK_{a,L}$, and numbers of individuals estimated at age, \hat{N}_a , for each time period or year. StALK is written in the R Statistical Computing environment (R Development Core Team, 2013). The procedural function, ‘StALK’ for Step 2 through Step 9 follows the R-code (available on request).

Validation of StALK Algorithm Through Length at Age Simulation Modeling

In this section, a simulator is developed to construct known size at age distributions on a population withstanding a decreasing relative abundance trend similar to that of the Pacific sailfish- with known growth parameters, known recruitment, and a known selectivity pattern. The StALK algorithm is tested on simulated data under scenarios of varying degrees of exploitation, noisy data found in nature, and in scenarios in which the applied selectivity pattern and growth information is mis-specified to varying degrees (deviations percentages of known selectivity parameters and growth information) to test the sensitivity of StALK in less than ideal situations. The simulation experiment will evaluate how robust StALK is to unknown problems with data and assumptions. Process error is introduced in which 4% of simulated bins of size at age depart from expected size at age values. For the simulations, recruitment is computed to be random with a specified variability (see R code by request). This simulator, referred to as *SimCatch*, is written and packaged in the R Language and is used to validate the StALK algorithm.

Simulation Model (SimCatch)

The *SimCatch* simulator constructs population estimates of size at age per year and catch at age per year, where $N_{a,g,y}$ is a multidimensional array of number at age a ($a=0, 1, \dots, A$), growth deviance g , and year y ; $C_{a,g,y}$ is a multidimensional array of catch at age a and heritable growth deviance bin g per year y ; M_a is natural mortality at age (either constant or age-assigned); q is a catchability coefficient assumed to be constant, $\Gamma_{a,g,y}$ is a matrix of length-specific selectivity per year that applies to mortality due to all

sources of exploitation; and $Fnom_y$ are annual compounded fishing mortality process parameters fitted by an objective function for each time step. The *SimCatch* simulator works as such:

Following the conceptual frame for the individual transfer model in the StALK algorithm, individual groups of fish are seeded as size-specific anomaly values for heritable growth deviance, as shown in Equation 3.7.

1. For any age group with known length distributions (e.g. Normal with μ_a and σ_a), individuals of a seeded value of predisposed growth deviances are assigned a corresponding length. The lengths are then binned. There may be multiple predisposed deviances associated with a single size at age bin. Sizes are rounded to the closest 1cm growth increment.
2. Process error (4%) was added to the simulator to allow departures from expected size at age. Each predisposed size deviance at age bin for each year, $N_{a,g,y}$ is assigned a random number between 0 and 1. Bins drawing values of 0.02 to 0.98 proceed to expected bins of a size i at age, $N_{a,L,y}$. Individuals drawing equal or below 0.01 move down two size increments $N_{a,L-2,y}$, while individuals in bins drawing between 0.01 and 0.02 move down one size increment, $N_{a,L-1,y}$. Bins that draw random numbers 0.98 to 0.99 move up one increment, $N_{a,L+1,y}$, while those drawing between 0.99 and 1 move up two increments, $N_{a,L+2,y}$. Fish in new growth deviance bins remain in those new bins through ontogeny.
3. In the first series of simulated years, individuals in each bin of $N_{a,g,y}$ are subjected to exponential decay under underexploited conditions with instantaneous mortality and a low fishing mortality ($F=0.01$), by year in Equation 3.10 whereas

M is natural mortality and F is assumed to equal near 0, 0.01. The first series of 1 to max age + 1 years. This is to fully construct cohorts from age 0 to maximum age before imposing an initially low level of fishing mortality upon the stock fitted through a CPUE series defined by the user. In the case of sailfish, a monotonically declining Japanese longline CPUE series for sailfish is used.

4. A size-specific selectivity pattern, $\Gamma_{a,g}$ is converted from length by Equation 3.7, and an annual mortality value, $Fnom_y$ are applied to population under unexploited conditions in Step 4, such that $Fnom$ replaces H_a in Equation 3.10 as such:

$$N_{a,g,y} = N_{a-1,g,y-1} e^{-M-\Gamma_{a,g,y-1}Fnom_y} \quad (3.13)$$

A matrix of mortality estimators by age, heritable growth deviance, and year are computed by the multiplication of $\Gamma_{a,g}$ and $Fnom_y$, $F_{a,g,y}^*$.

5. Catches of fish by age, level of heritable growth deviance, and year resulting from $F_{a,g,y}^*$ (by $Fnom_y$) and abundance at the beginning of the year, equaling the abundance of the previous year after instantaneously mortality, $N_{a-1,g,y-1}$ is computed by Baranov Catch Equation:

$$C_{a,g,y} = \frac{F_{a,g,y}^*}{M + F_{a,g,y}^*} \left(1 - e^{-(M+F_{a,g,y}^*)} \right) N_{a,g,y} \quad (3.14)$$

6. All abundances $N_{a,g,y}$ and catches $C_{a,g,y}$ by year age (a), value of heritable growth deviance (g), and year(y) computed in Step 6 and Step 7 are converted from numbers corresponding with heritable growth deviance (g) to length (L) following the conversion described in Equation 3.7. Thus population abundance and catches at age (a), length (L), and year are constructed: $N_{a,L,y}$ and $C_{a,L,y}$, respectively.

7. Annual catch-per-unit-effort (CPUE) indices (U_y) under an assumed constantly catchability, q , are constructed from catches by year:

$$U_y = \sum_{L=1}^{L=\max i} \sum_{a=1}^{a=\max a} C_{a,L,y} / \frac{Fnom_y}{q} \quad (3.15)$$

8. Steps 2 through 8 are repeated iteratively and independently for each year (y), such that adjusting $Fnom_y$ minimizes the sum of square of residuals between annual CPUE resulting in Step 8, \hat{U}_y , against observed CPUE, U_y , used to fit and project abundance and catches at age and size (or predetermined growth), by year. The optimization procedure uses a conjugate gradient method (Fletcher and Reeves, 1964) within the *optim* procedure to fit the $Fnom_y$ annually through an objective function. The objective function is:

$$RSS \cong \min(\hat{U}_y - U_y)^2 \quad (3.16)$$

reducing the residual sum of squares (RSS) by adjusting $Fnom_y$. This estimates a nominal annual fishing mortality given a known CPUE series, known catchability, and known recruitment in the *SimCatch* simulator.

9. For each year, Steps 2 to 9 are repeated such that global fishing mortality $Fnom_y$ is optimized to fit the CPUE series and yield catches at age, size, for each year. From these known catches with known age and size distributions, “port sampling” is simulated for each year by randomly selecting (without replacement) 5000 individuals from catches, with known size information. This is to mimic realistic conditions for how length frequencies are collected by fisheries management agents, assuming their sampling is proportional to the stock.

10. From simulated port samples, simulated biological sampling occurs by randomly selecting (without replacement) 1500 individuals for which size and age are known from the simulator. The sample size of 1500 is per a rule-of-thumb recommendation of Gerritsen and McGrath (2006) that length frequencies be collected at a rate of 100 per length bin. This process mimics how age-length keys are constructed from port-sampled fishes in exploited fisheries. This simulated biological sample is used to construct a “simulator-known” age-length key from simulated data. ALKs from known age-at-size data are constructed for comparisons.

11. For each year, lengths from simulated biological samples are applied to the StALK algorithm. Simulated age-length keys are statistically compared to those numerically constructed by the StALK algorithm by comparing resulting age distributions estimated.

The procedural function, ‘*SimCatch*’ for Step 2 through Step 11 including the sampling of biological samples, follows the R code- which is available on request.

SimCatch is fitted to a CPUE series that emulates that of sailfish caught in the eastern Pacific Japanese longline fleet from 1970 to 2003 (IATTC, 2003). This series is indicative of a stock undergoing heavy exploitation into a fully exploited state in the latter 10 years with over 90% decline in relative abundance. Such a trend is emblematic of catch rate trends for heavily exploited highly migratory top predatory fish stocks since the commencement of industrialized fishing (Maunder et. al, 2006; Polacheck, 2006). Furthermore, this CPUE trend captures a sharp contrast of a fishery undergoing little exploitation to a period of moderate exploitation, followed by several years in a fully

exploited phase to overexploited. Simulations using *SimCatch* were conducted for a 34 year time series: 12 years to fully develop cohorts and then 34 years of exploitation. Simulations were conducted with two common selectivity (Γ) patterns: a knife edge selectivity at 130 cm length and also with a logistic selectivity:

$$\frac{1}{1 + e^{a(L-b)}} \quad (3.17)$$

whereas i is size, a is an assumed logistic rate of increase for selectivity with size equal to -0.075 , and b is an assumed midpoint of 50% selectivity equal to 130 cm. To avoid an exhaustive factorial experimental simulation design, experiments with StALK under varying levels of recruitment, varying degrees of misspecification error from known selectivity, and error in growth parameters were conducted in a multilevel design to draw inferences on StALK's performance.

Sensitivity Analysis of StALK to Varying Exploitation and Recruitment

First, StALK is applied to a time series of simulated fisheries from SimCatch under non-equilibrium conditions and with sampled length frequencies and known age distributions; estimated age distributions and mortality rates from StALK are compared to those known in the simulation. Sailfish fishery simulations using *SimCatch* for the 34 year series are conducted with random +/- 10% variation (20% total variability) in recruitment per year, logistic selectivity as described in the previous section, and 4% process error as described in Step 3. StALKS was applied to each annual simulated sampled length-frequency and the StALK algorithm estimates logistic selectivity with logistic slope equaling $\frac{\ln(4)}{L50-L75}$ where L50 is the length at which the cumulative density function of the length frequency is 50% and L75 is the length corresponding to 75%

cumulative density (Paloheimo and Cadima, 1964). 50% selectivity is estimated to be the mode in the length-frequency. Age distributions and mortality rates from annual StALK run outputs are compared to known simulated distributions and mortalities by age-structured catch curves as shown in Equation 3.6. Analysis of covariance (ANCOVA) was executed annually to test for coinciding linear trajectories of simulated versus estimated age structured curves- which equated to testing for equal total mortality rates in an age catch curve. The simulation and ANCOVA exercise to test for equal mortalities by year between known and estimated data is then repeated - but with increasing “noise” of recruitment to random +/-20% variability (40% total) to test the sensitivity of StALK to high levels of recruitment variation. In this case, both knife edge selectivities and logistic selectivities are used in simulation runs.

Sensitivity Analysis of StALK to Misspecification of Inputs for Selectivity and Growth

To test the StALK algorithm’s sensitivity to misspecification error in selectivity and growth, simulated size at age data and simulated biological sampling data from year 14 in simulation runs with +/-20% (40% total variable) recruitment was selected to be tested with StALK since this simulation year is near the midpoint in the time series and has exhibited a 50% decrease in estimated abundance (CPUE) in a fully exploited phase. Simulated biological samples for year 14 were used to compare an ALK resulting from StALK with an ALK collected by the simulated biological sampling. Length frequencies from the simulated biological samples were used to estimate age frequencies using the StALK algorithm. While ANCOVA is used to compare age-structured catch curves and resulting mortality estimates, estimated age frequencies were compared with known age

frequencies using the Kolmogorov–Smirnov test. Misspecification error resulting within 90% confidence levels between known and estimated age frequencies were used as conservative benchmarks. This is to avoid accepting hypotheses of equal distribution under Type II error, therefore selectivity patterns used in StALK that are within 90% confidence of known age frequencies are used as limits to how much misspecification can be implemented when using StALK to estimate comparable age frequencies to known frequencies. Another source of observation error and misspecification that may create erroneous estimation of age frequencies using StALK are inputs for size at age (growth)- therefore error of size at age distributions were introduced as percentages that underestimated size at age distributions and overestimated size at age distributions from known size at age distributions by adjusting misspecification of L_{∞} . These growth errors were applied jointly with error in selectivity corresponding with 90% confidence bounds of resulting age frequencies from known age frequencies to estimate misspecification conservatively. This simulation design allows to test how robust the StALK algorithm is for age frequency estimation under less than ideal situations. StALK was tested for both logistic selectivity with logistic rate of increase for selectivity with size equal to -0.075 and a midpoint of 50% selectivity equal to 130 cm; and knife-edge selection at 110 cm.

Application of StALK to EPO Sailfish

The IATTC has collected length-frequencies for tunas and billfish species, including sailfish since 1991, as described in Section 2.2 of Chapter 2. This database consists of eye-forklength measurements in centimeters for sailfish caught throughout the eastern tropical Pacific Ocean (Fig. 2.2.1; Chapter 2). Annual length frequencies are used

in the analysis to determine demographics of sailfish in the EPO by year. Fitted von Bertalanffy growth parameters L_∞ , k , t_0 are estimated in Chapter 2 to be 207.4 cm eye forklength, 0.37, -0.004 years, respectively (Table 2.3.4), with a coefficient of variation (CV) for length at age to be 10.1%. Length-frequencies of sailfish caught in the eastern Pacific purse seine fleet by year are analyzed and fitted with a selectivity curve fitted using the “LCCC method” (described in Appendix A) .

Alternative Methods to Estimate Mortality

Length frequencies were also used to estimate total instantaneous mortality using length-based mortality estimators. Beverton and Holt (1956) estimated instantaneous mortality (Z) as a function as average fish length in landings \bar{L} , an assumed known asymptotic length (L_∞) from growth studies, a known growth coefficient for the species (K), and the length of first capture (L_c), assumed a fish could live indefinitely. Ehrhardt and Ault (1992) relaxed the assumption that fish remain indefinitely selected into the fishery, allowing individuals to become unavailable to the fishery at a size below L_∞ and prior to a . Length-based methods have many virtues in that they are estimated from readily available length data (Ault et al 2005). Ault et al (2005) found that methods using average length (Ehrhardt and Ault, 1992; Beverton and Holt, 1956) are insensitive to recruitment shifts and exploitation rates. Ehrhardt and Ault (1992) introduced length for which individuals become unavailable to the fishery (L_λ) in the following formulation:

$$\left[\frac{L_\infty - L_\lambda}{L_\infty - L_c} \right]^{\frac{Z}{K}} = \frac{Z(L_c - \bar{L}) + K(L_\infty - \bar{L})}{Z(L_\lambda - \bar{L}) + K(L_\infty - \bar{L})} \quad (3.18)$$

Furthermore, Ault et al. (2014) proved average length to be a more robust indicator of exploitation than CPUE. For EPO sailfish, recruitment into the fishery (L_c) begins at size 165 cm EFL (eye-forklength) and length at which availability out of the fishery occurs (L_i) is equal to L_∞ , 207 cm EFL.

Pauly (1980) deterministically estimated age frequencies from observed length frequencies by ‘slicing’ ages from von Bertalanffy growth functions through algebraically solving for age at length using a length-converted catch curve (LCCC). The natural logarithm of numbers of fish sampled in length frequencies corresponding to relative ages (converted from lengths) are regressed from the maximum number of samples descending to oldest relative ages. The slope of this line is assumed to be total mortality.

3.3 Results

Simulation Modeling Experiments Using Operating Model, SimCatch

Resulting abundance trends from *SimCatch* analyses depict a drastically declining CPUE trend and recruitment moderately variable for a fishery experiencing 20% random recruitment (Figure 3.3.1) and 40% random recruitment around a base recruitment of 10,000,000 age 0 individuals added per year (Figure 3.3.2).

Age frequencies from known simulation runs for each year were compared to resulting age frequencies through application of StALK for each simulation year (68 years total in 2 time series with differing recruitment). Age structured catch curve analyses between simulated known age frequencies and estimated age frequencies were compared using analyses of covariance (ANCOVA) in the R Statistical Computing

environment (R Development Core Team, 2013) with results depicted in Tables 3.3.3 and 3.3.4.

StALK estimates of age frequency gave total mortality Z estimates (slope of ACC lines) that were statistically comparable to Z estimates estimated by ACC lines from known simulated data for 64 of 68 years, with slopes significantly different at 90% confidence for 1 year in a time series with 20% recruitment variability (Table 3.3.3) and for 3 years in a time series with 40% recruitment variability (Table 3.3.4). Plots of estimated Z from StALK and ACC of simulated age frequencies (Figure 3.3.3 and Figure 3.3.4) depict StALK algorithm estimating total mortality quite accurately, with the exception of some years of high exploitation and highly variable recruitment (Figure 3.3.4) which can cause StALK sensitivity

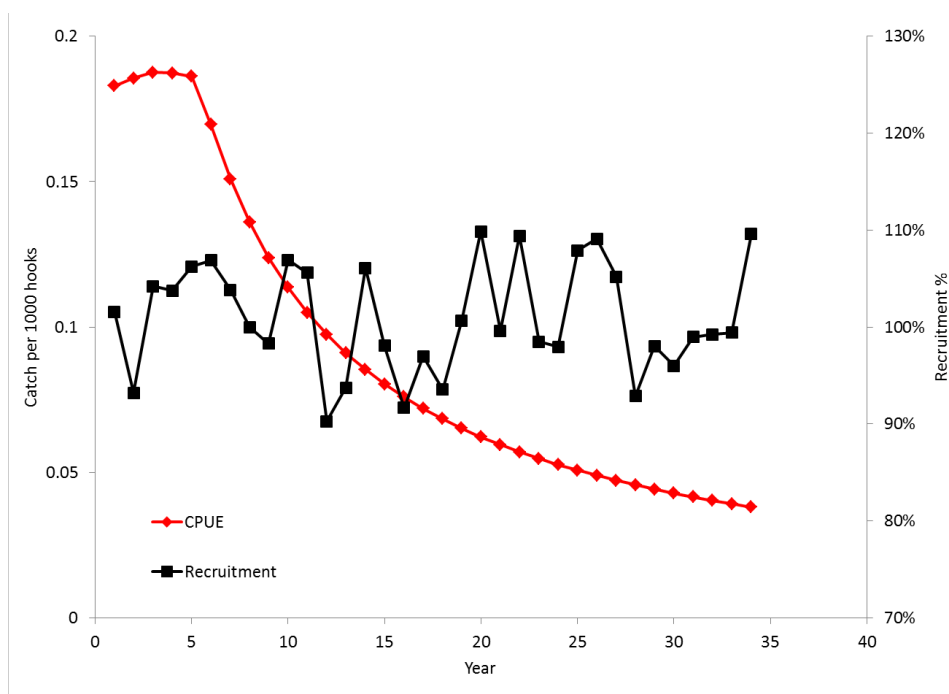


Figure 3.3.1. CPUE index (red) from *SimCatch* and recruitment (black) for a simulated sailfish fishery. Recruitment is 20 % random variability, +/-10%.

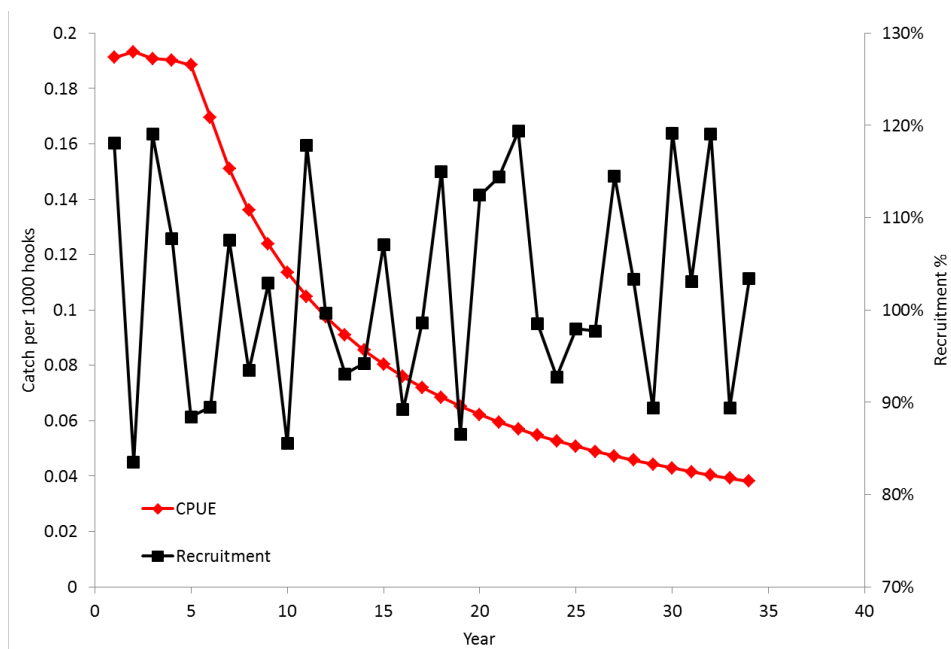


Figure 3.3.2. CPUE index (red) from *SimCatch* and recruitment (black) for a simulated sailfish fishery. Recruitment is 40 % random variability, +/-20%.

Table 3.3.1. Simulated sailfish fishery with 20% random recruitment, resulting Z values from age structured catch curves (ACC) of simulated versus StALK estimates.

Year	Z Simulated ACC	Z Simulated SE	Z StALK Estimate	Z StALK Estimate SE	Error % from Simulated	ANCOVA P-Value Coincidence
1	0.24	0.01	0.24	0.01	-0.03	0.88
2	0.22	0.02	0.24	0.02	0.11	0.80
3	0.25	0.02	0.25	0.01	0.03	0.93
4	0.27	0.02	0.25	0.01	-0.07	0.61
5	0.26	0.03	0.24	0.02	-0.08	0.62
6	0.25	0.02	0.25	0.01	0.00	0.91
7	0.27	0.02	0.26	0.01	-0.04	0.75
8	0.28	0.02	0.27	0.01	-0.04	0.74
9	0.29	0.02	0.24	0.04	-0.20	0.62
10	0.39	0.02	0.35	0.01	-0.08	0.30
11	0.40	0.02	0.43	0.01	0.07	0.58
12	0.44	0.02	0.39	0.02	-0.13	0.14
13	0.47	0.03	0.34	0.07	-0.27	0.10*
14	0.54	0.01	0.51	0.02	-0.06	0.64
15	0.52	0.02	0.53	0.02	0.01	0.91
16	0.55	0.03	0.54	0.02	-0.02	0.90
17	0.62	0.02	0.56	0.02	-0.09	0.19
18	0.61	0.03	0.59	0.02	-0.05	0.60
19	0.69	0.04	0.65	0.03	-0.07	0.62
20	0.64	0.03	0.60	0.03	-0.06	0.71
21	0.71	0.02	0.65	0.03	-0.08	0.36
22	0.88	0.05	0.94	0.05	0.08	0.10
23	0.79	0.05	0.71	0.04	-0.10	0.38
24	0.90	0.03	0.85	0.04	-0.06	1.00
25	0.91	0.09	0.83	0.05	-0.08	0.57
26	0.93	0.03	0.90	0.03	-0.03	0.35
27	1.11	0.09	1.04	0.05	-0.06	0.92
28	1.02	0.02	1.03	0.05	0.01	0.41
29	1.13	0.04	1.13	0.05	0.00	0.32
30	1.11	0.04	1.13	0.06	0.02	0.56
31	1.39	0.22	1.13	0.07	-0.19	0.53
32	1.39	0.11	1.44	0.08	0.03	0.64
33	1.14	0.09	1.19	0.06	0.04	0.83
34	1.25	0.09	1.33	0.07	0.06	0.58

Table 3.3.2. Simulated sailfish fishery with 40% random recruitment, resulting Z values from age structured catch curves (ACC) of simulated versus StALK estimates.

Year	Z Simulated ACC	Z Simulated SE	Z StALK Estimate	Z StALK Estimate SE	Error % from Simulated	ANCOVA P-Value Coincidence
1	0.24	0.01	0.24	0.01	0.01	0.87
2	0.23	0.03	0.23	0.01	0.04	0.94
3	0.24	0.03	0.24	0.01	0.02	0.77
4	0.26	0.03	0.26	0.01	0.00	0.90
5	0.22	0.03	0.21	0.01	-0.04	0.68
6	0.26	0.03	0.24	0.01	-0.07	0.78
7	0.27	0.03	0.26	0.01	-0.05	0.66
8	0.26	0.03	0.28	0.01	0.08	0.97
9	0.35	0.04	0.32	0.04	-0.10	0.59
10	0.34	0.02	0.30	0.01	-0.12	0.32
11	0.37	0.02	0.32	0.03	-0.12	0.16
12	0.43	0.03	0.42	0.01	-0.02	0.61
13	0.46	0.02	0.43	0.01	-0.08	0.18
14	0.50	0.01	0.47	0.02	-0.06	0.51
15	0.60	0.04	0.52	0.02	-0.12	0.10
16	0.57	0.04	0.61	0.03	0.07	0.49
17	0.59	0.02	0.58	0.02	-0.01	0.20
18	0.69	0.03	0.62	0.02	-0.10	0.10
19	0.70	0.04	0.60	0.02	-0.14	0.11
20	0.71	0.04	0.79	0.03	0.11	0.27
21	0.81	0.03	0.72	0.02	-0.12	0.02*
22	0.77	0.03	0.95	0.04	0.23	0.01*
23	0.88	0.03	0.99	0.05	0.12	0.15
24	0.87	0.06	0.80	0.04	-0.08	0.11
25	0.98	0.07	1.14	0.05	0.17	0.40
26	1.10	0.07	1.21	0.06	0.10	0.36
27	0.97	0.07	1.04	0.05	0.07	0.31
28	1.22	0.16	1.37	0.11	0.12	0.32
29	1.14	0.06	1.30	0.09	0.13	0.43
30	1.17	0.08	1.25	0.07	0.06	0.11
31	1.26	0.10	1.23	0.07	-0.03	0.49
32	1.21	0.12	0.96	0.05	-0.21	0.16
33	1.25	0.08	0.93	0.05	-0.26	0.01*
34	1.26	0.09	1.25	0.10	-0.01	0.50

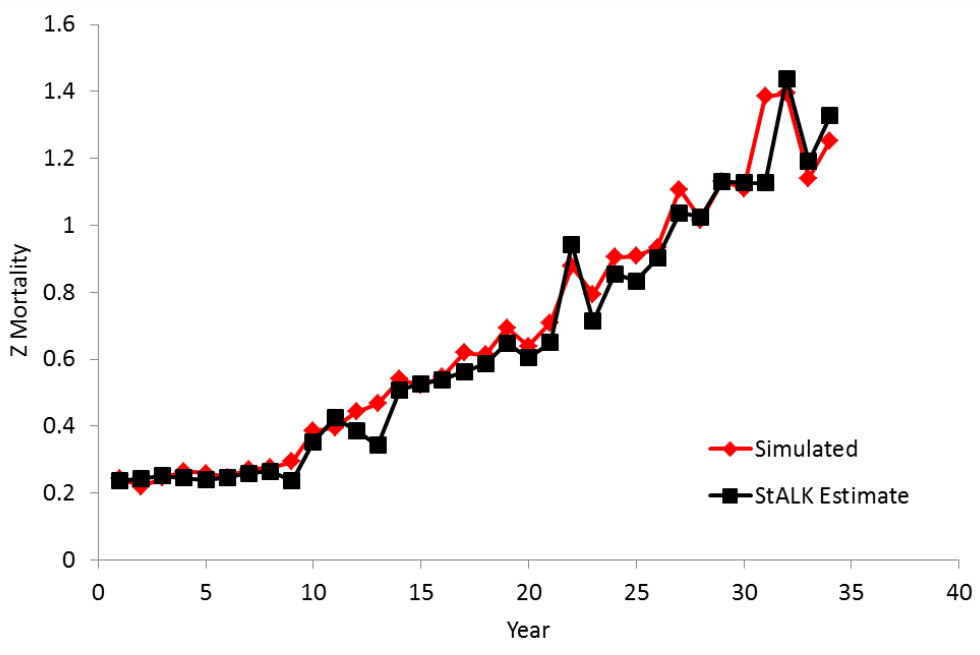


Figure 3.3.3. Total mortality, Z , estimated through age-structured catch curve by StALK and from simulated age compositions, 20% random recruitment.

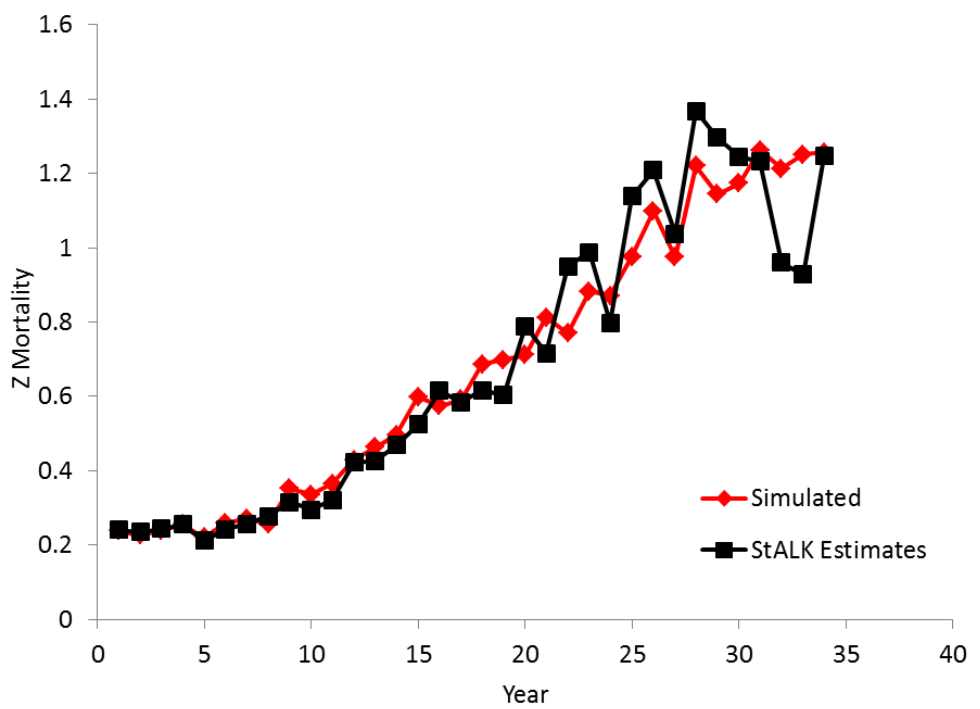


Figure 3.3.4. Total mortality, Z , estimated through age-structured catch curve by StALK and from simulated age compositions, 40% random recruitment

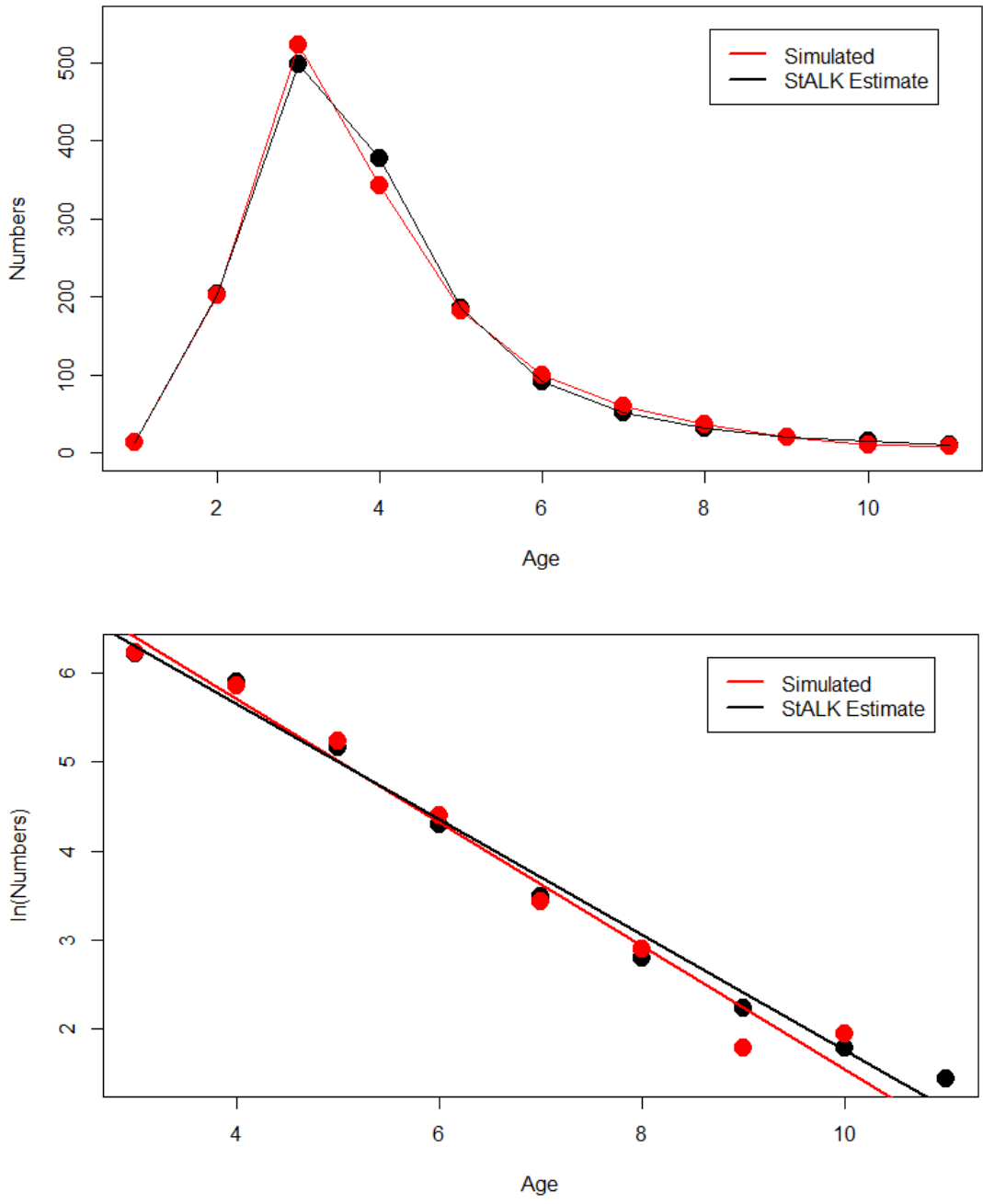


Figure 3.3.5. Age frequencies estimated in Year 14 by StALK and from a simulated fishery for Year 14 in a fishery experiencing 20% random recruitment

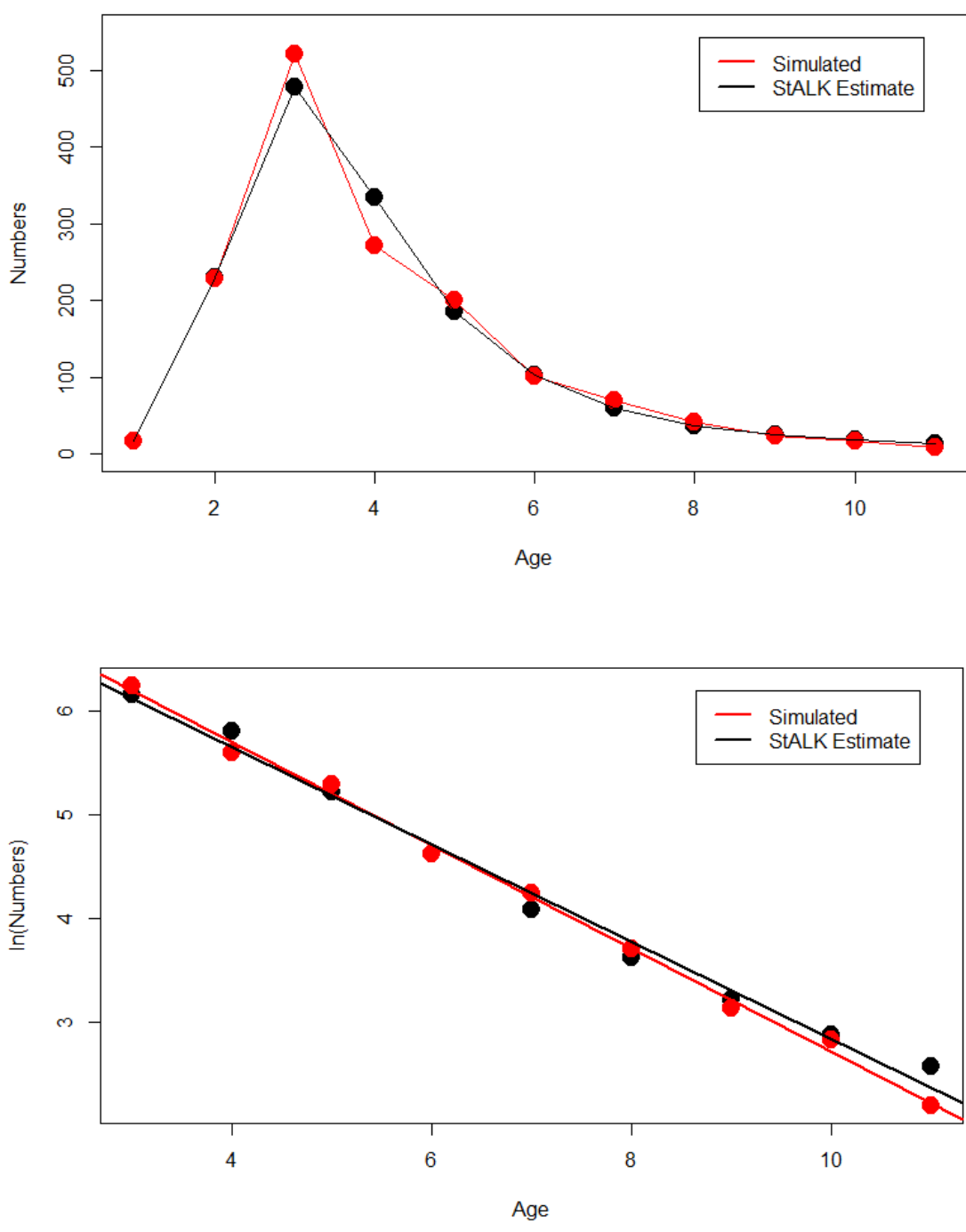


Figure 3.3.6. Age frequencies estimated in Year 14 by StALK and from a simulated fishery for Year 14 in a fishery experiencing 40% random recruitment

Sensitivity of StALK to Misspecification of Selectivity and Growth

The range of misspecification of logistic parameters that yielded age frequencies in StALK equal to known simulated age at 90% significance (KS test, R Development Core Team, 2013) were logistic rate of increase in selectivity: -0.057 to -0.084 (-0.075 in operating model) and a midpoint of selection of 121 cm to 148 cm (130 cm in operating model). Depiction of misspecification yielding comparable results to operating model is in Figure 3.3.7.

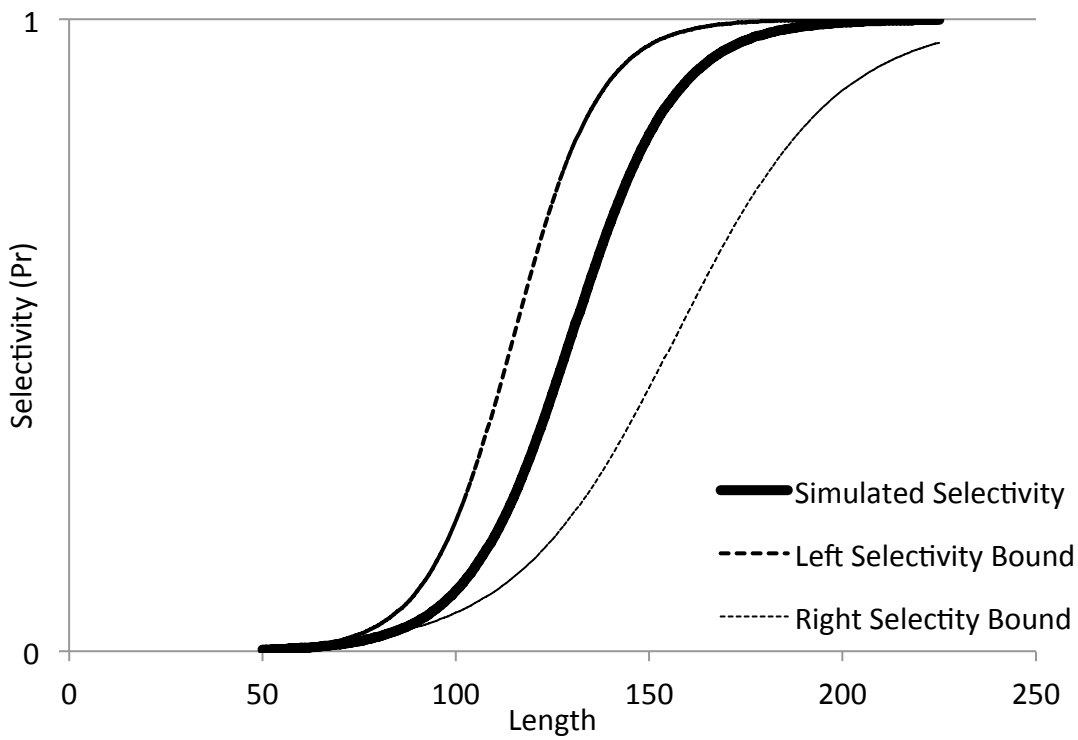


Figure 3.3.7. Selectivity used in simulator and range of misspecified selectivity curves that estimate age frequencies in StALK that were the same as the simulated age frequencies at 90% confidence.

Misspecification of L_{∞} that estimated age frequencies in StALK runs to be equal to those in operating model at 95% confidence was a L_{∞} to be underestimated at 7% and

overestimated at 12% of known asymptotic length used in SimCatch (Figure 3.3.8).

Therefore, StALK can be applicable at 90% confidence under situations of -12% to 24% error in misspecification of logistic selectivity slope estimates, -7% to 14% error in misspecification of logistic selectivity midpoint estimates, and -7% to 12% error in misspecification of L_∞ in growth parameter estimation.

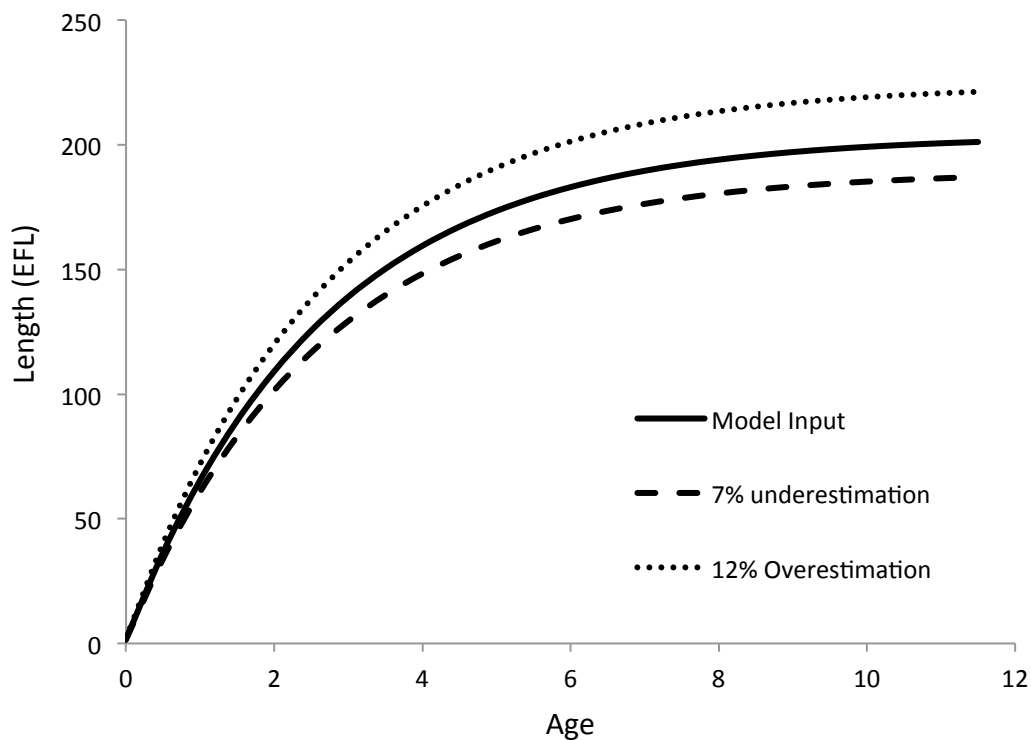


Figure 3.3.8. Growth model used in simulator and misspecified growth that estimates age frequencies in StALK similar to simulated age frequencies at 90% confidence.

Application of StALK to Sailfish in the Eastern Pacific

Estimates of StALK were then compared to alternative methods, including Pauly (1980) slicing method and the Ehrhardt and Ault (1992) (Figure 3.3.9). Resulting age frequencies from StALK algorithm applied to sailfish data from 1991 to 2007 was used to compute total mortality (Z) estimates that follows trends of Z calculated with different

methods including the Ehrhardt and Ault (1992) length-based estimator for mortality and Pauly's (1980) deterministic slicing procedure (Figure 3.3.10). This could further validate the methodology as a useful mechanism to generate age frequencies and mortalities for species that have available length-frequencies. StALK was applied to length-frequencies from 1991 to 2007 using a "LCCC" selectivity pattern which is an estimation procedure introduced in Appendix B (Figure 3.3.10). Age frequencies for each year are provided in Figure 3.3.11.

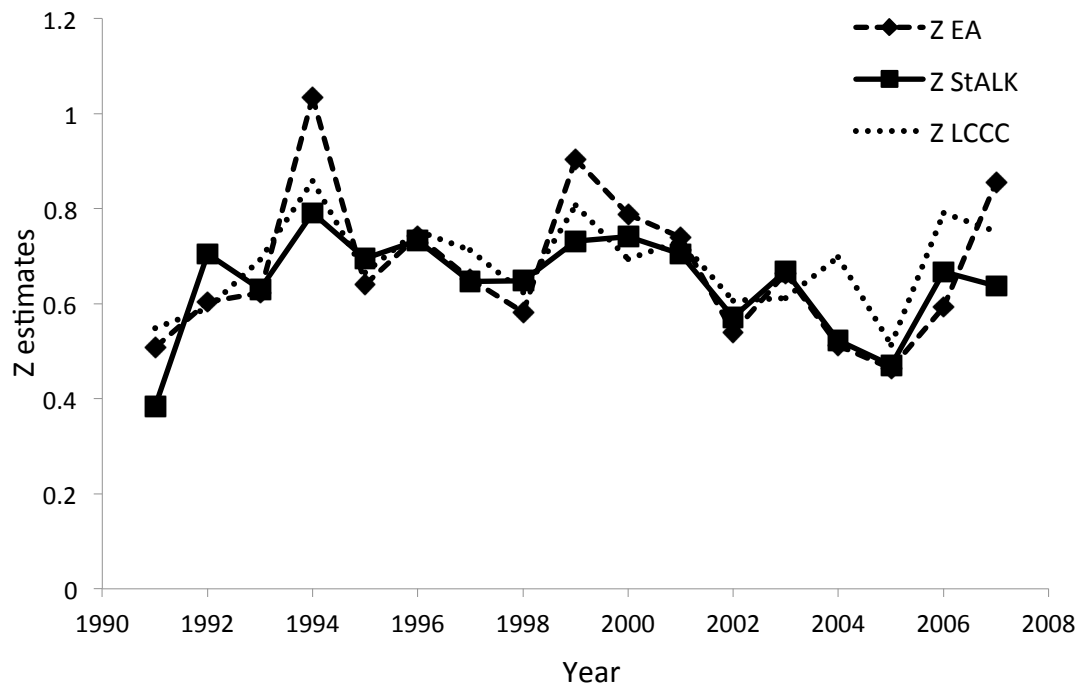


Figure 3.3.9. Time series (1991-2007) of total mortality (Z) estimates from the Ehrhardt-Ault (1992) direct estimation of total mortality, Pauly's (1980) LCCC slicing procedure, and mortality estimated from the StALK algorithm.

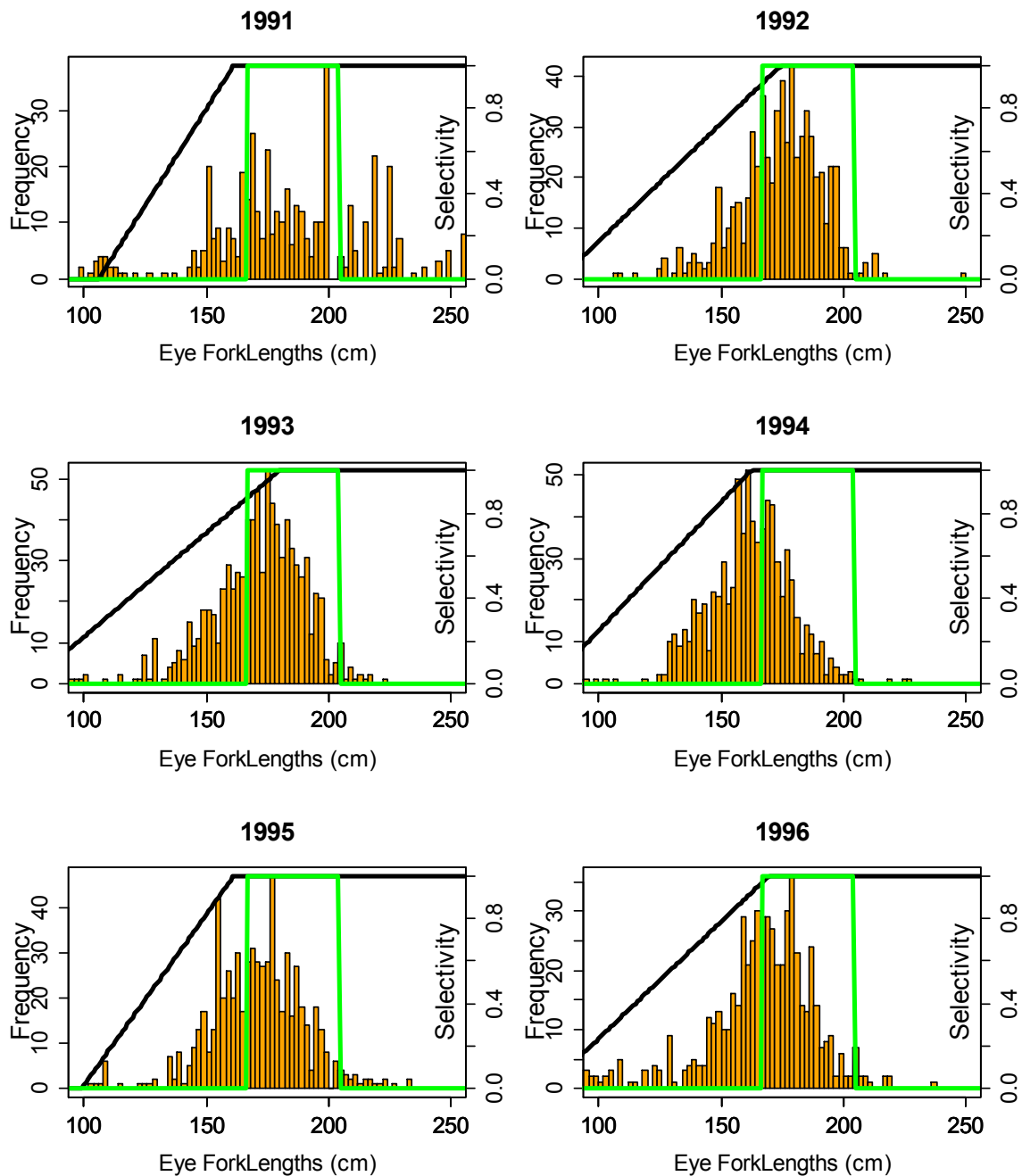


Figure 3.3.10. Histograms of purse seine-caught eastern Pacific Sailfish caught in 2 cm bin length frequencies by year and corresponding selectivity pattern estimated using the LCCC method (black) and selectivity under constraints of EA method (green).

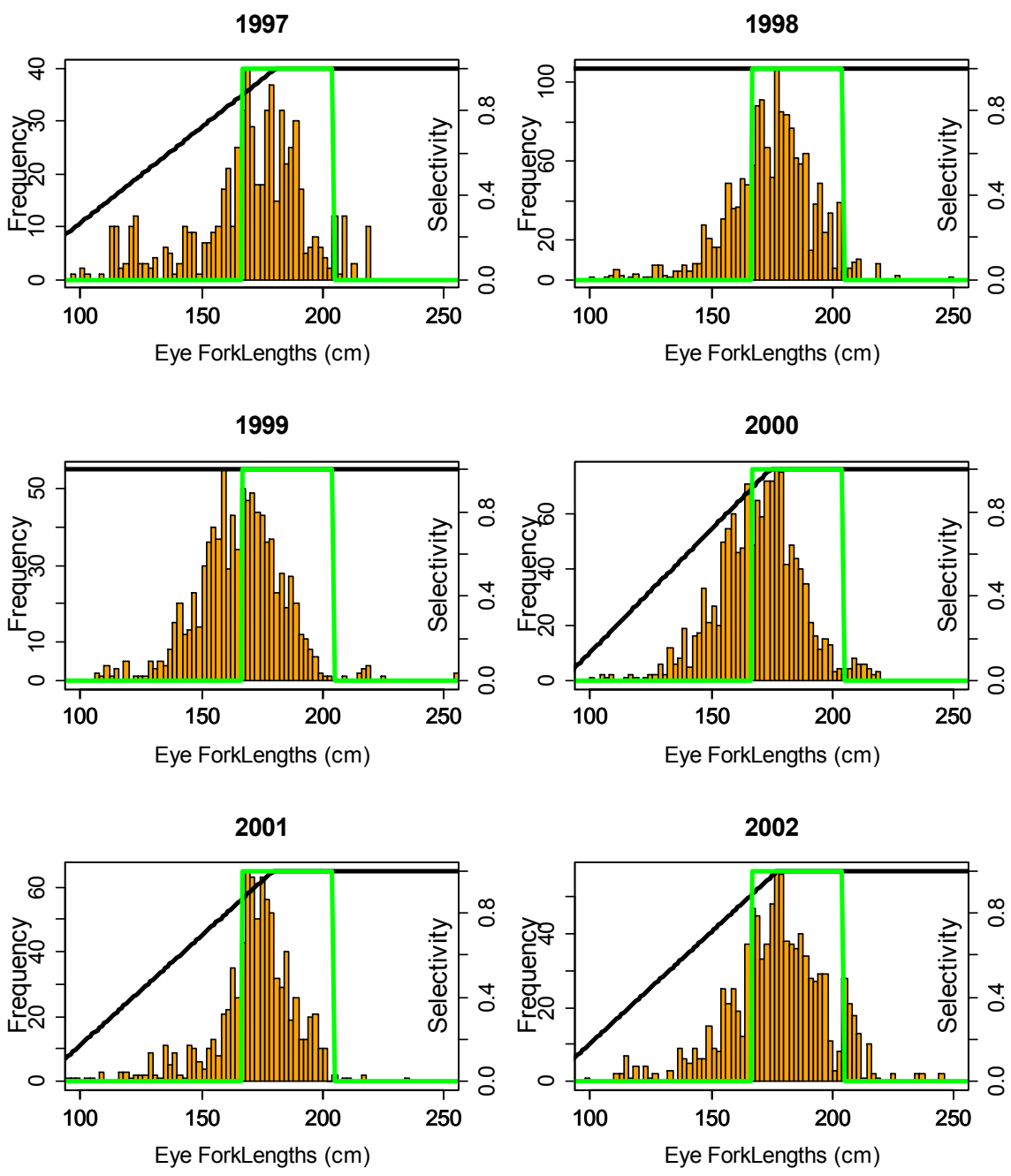


Figure 3.3.10. Histograms of purse seine-caught eastern Pacific Sailfish caught in 2 cm bin length frequencies by year and corresponding selectivity pattern estimated using the LCCC method (black) and selectivity under constraints of EA method (green).

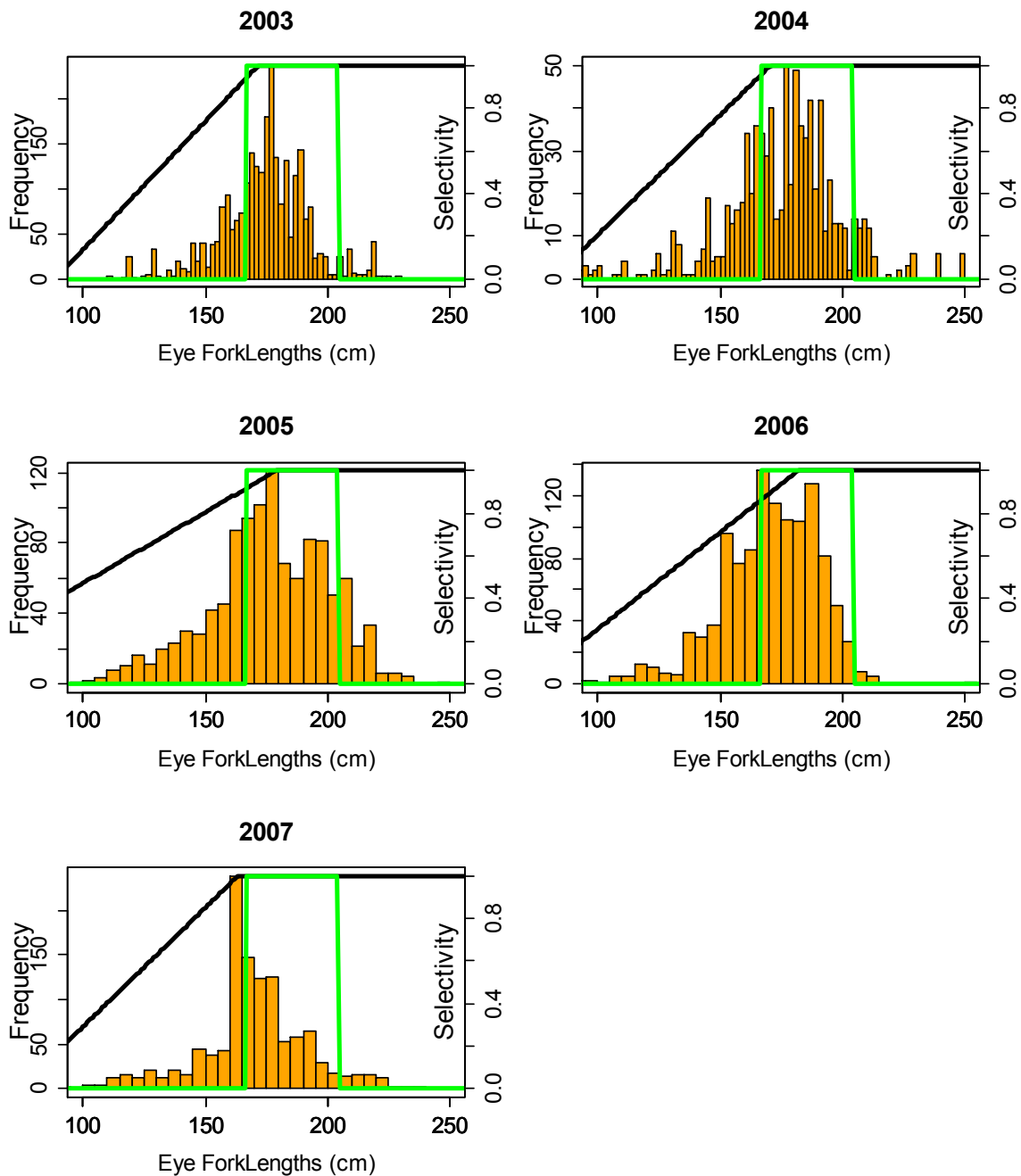


Figure 3.3.10. Histograms of purse seine-caught eastern Pacific Sailfish caught in 2 cm bin length frequencies by year and corresponding selectivity pattern estimated using the LCCC method (black) and selectivity under constraints of EA method (green).

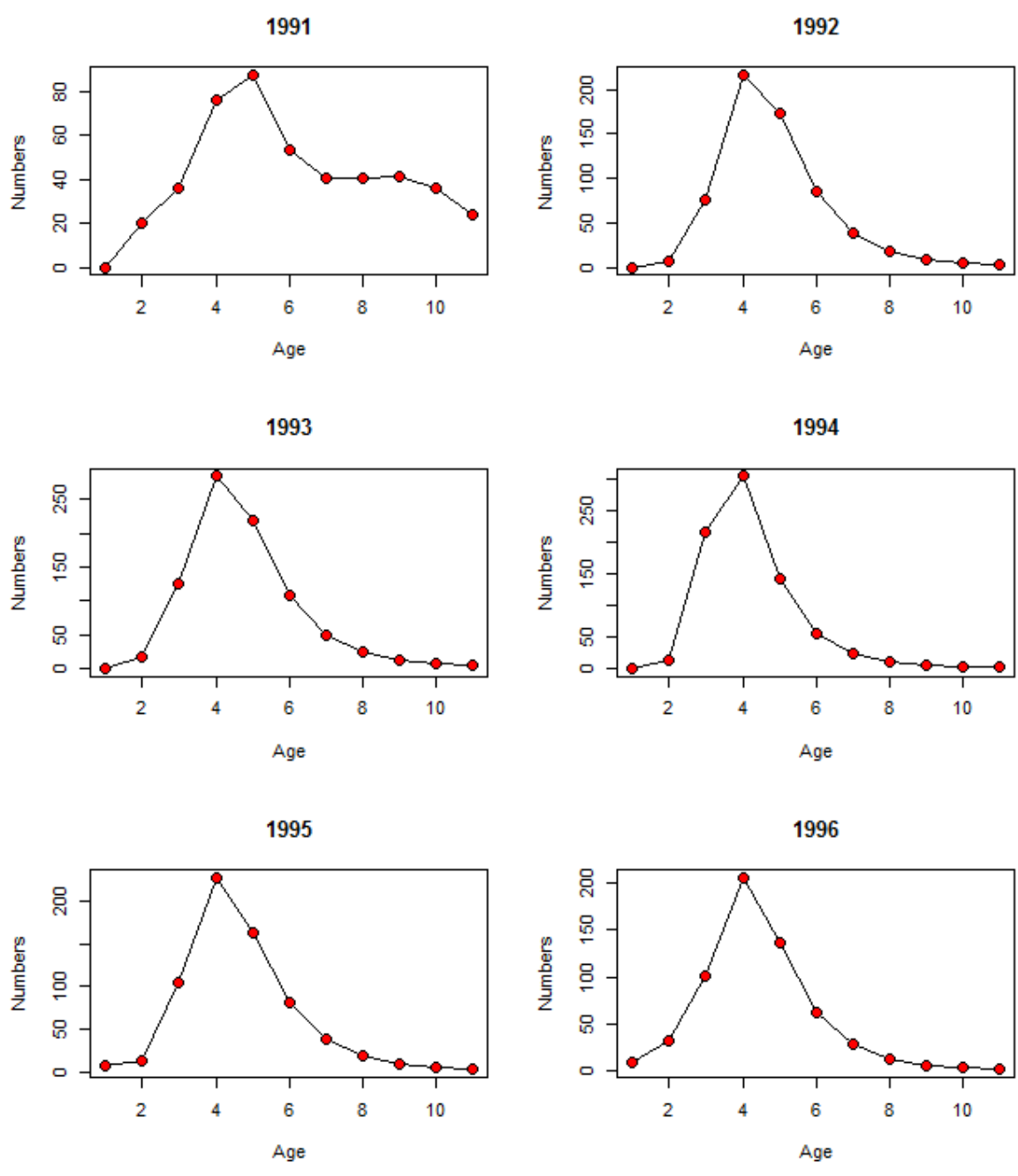


Figure 3.3.11. Age frequencies for sailfish in the EPO estimated by StALK by year.

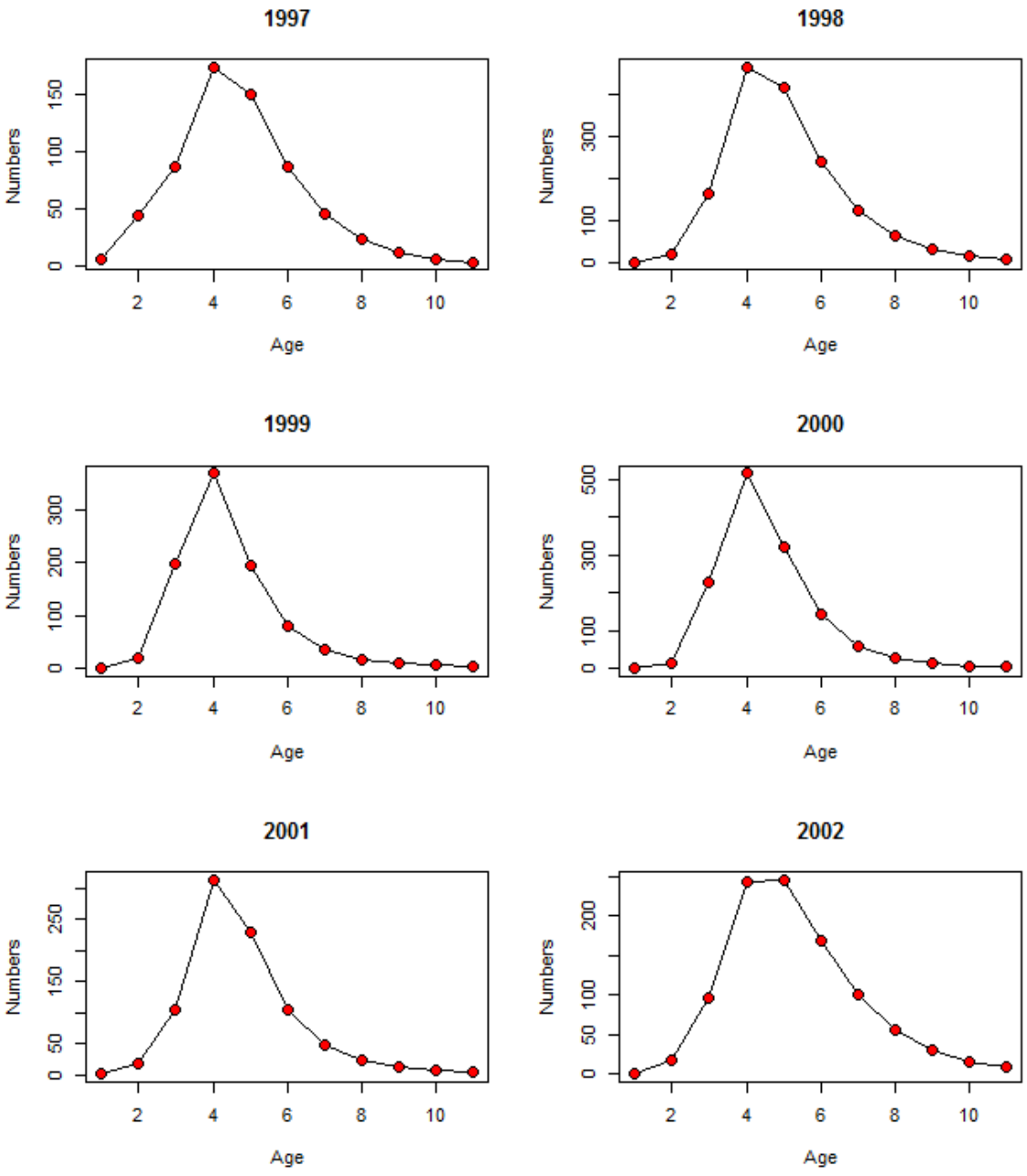


Figure 3.3.11. (cont'd). Age frequencies for sailfish in the EPO estimated by StALK by year.

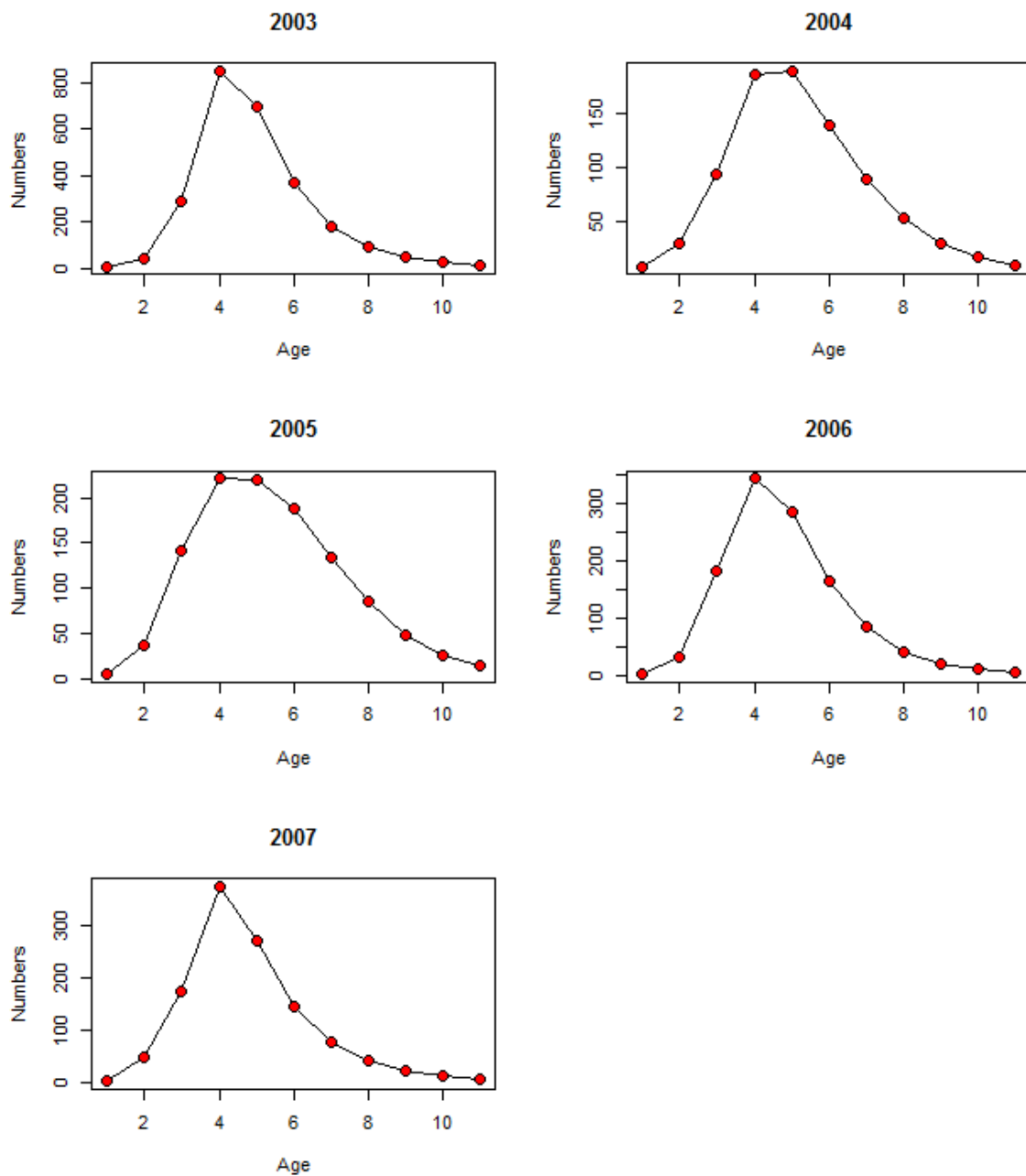


Figure 3.3.11. (cont'd). Age frequencies for sailfish in the EPO estimated by StALK by year.

3.4 Discussion and Novelty

Age-length keys provide critical information to allocate total ages to total length frequencies in the landings and yet they are often not available for stock assessment analysis because age samples are often unavailable. In most instances, collecting unbiased samples for age determination is time-consuming and costly. The StALK algorithm provides an alternative numerical solution to build ALKs.

Estimations of age frequencies and total mortality of StALK from simulation testing reveals that StALK is a robust method. StALK is mildly sensitive to recruitment variability. Estimation of an age-specific population dynamics parameter, H , can account for recruitment differences among cohorts estimated in independent years with StALK while applied under equilibrium conditions. StALK permits significant misspecification of selectivity and growth parameters and still produces age frequencies statistically comparable to known age frequencies. StALK provides adequate estimation of age frequencies for many situations of variable recruitment and exploitation.

StALK and Alternative Popular Methods to Estimate Z

Length-based methods to assess mortality are commonplace due to the frequent availability of length-frequency information in fishery-dependent data. Such methods are oftentimes the only option in the absence of empirical age information. The StALK algorithm bypasses biological sampling for ages when pre-existing growth information is assumed reliable.

Estimates of natural mortality for sailfish in the EPO by Ehrhardt and Fitchett (2014, in progress) lie in a range of 0.23 to 0.28. Assuming a natural mortality rate equal

to 0.25 and recruitment into the fishery at age 4, estimates for a precautionary fishing mortality target, $F_{0.1}$, is computed to be 0.28. Gulland and Boerema (1972) conceptualized $F_{0.1}$ to be a benchmark where $F_{0.1}$ coincides with a value of F on a yield-per-recruit curve to be 10% the slope of yield-per-recruit at virgin conditions. $F_{0.1}$ was selected as a benchmark due to its indication of growth overfishing and the little information needed to estimate it. Estimates of fishing mortality from the Ehrhardt and Ault (1992) method and estimated from StALK outputs are consistently higher than $F_{0.1}$, sometimes double the target fishing mortality rate (Figure 3.4.1). This trend indicates that sailfish may be undergoing heavy exploitation, far exceeding a benchmark or target mortality rate.

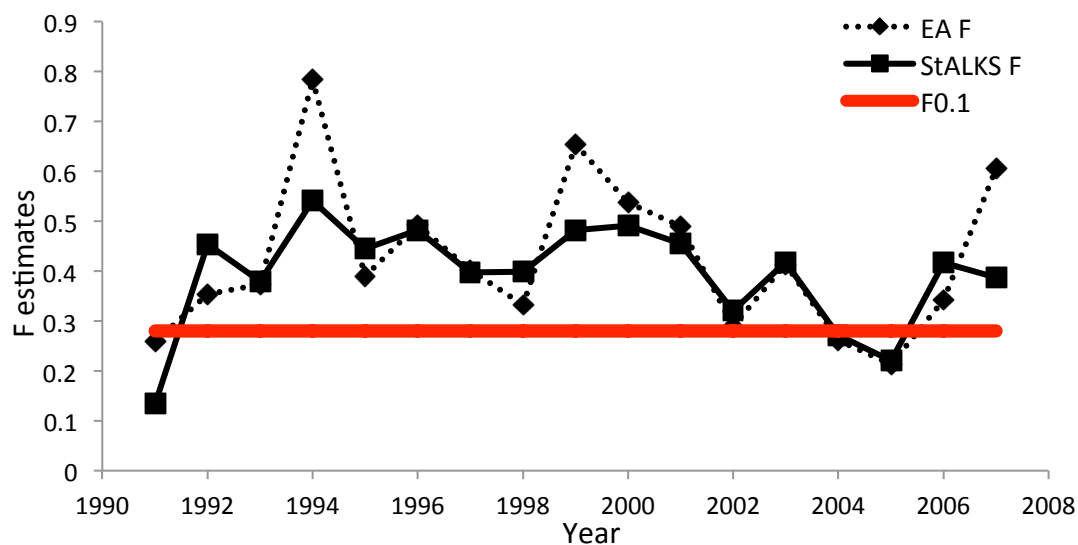


Figure 3.4.1. Time series (1991-2007) of fishing mortality (F) estimates from the Ehrhardt-Ault (1992) method and derived from age frequencies using StALK algorithm compared with estimates of $F_{0.1}$ (red) equaling 0.28.

Estimates of mortality for sailfish using Pauly's (1980) LCCC slicing procedure, the Ehrhardt-Ault (1992) method, and catch curve analyses from ages generated from the numerical solution StALK algorithm yield similar values of total mortality (Z) for each year (1991-2007) in a corresponding pattern (Fig. 3.3.9). Bartoo and Parker (1982) prove that the deterministic nature of Pauly's (1980) LCCC slicing procedure leads to significant biases in age frequency estimation. Animals that are near or equal to asymptotic length, L_{∞} , as fitted by the von Bertalanffy growth function, are estimated to be at ages often unattainable by fish and fish closely below the asymptotic length may be erroneously assigned to much younger ages (Bartoo and Parker, 1982). Additionally, individuals measured to be above L_{∞} must be excluded or arbitrarily assigned to maximum ages (Bartoo and Parker, 1982). When estimates of age frequencies resulting from deterministic estimation of age are used in length-converted catch curve analyses - resulting total mortality (Z) tends to be overestimated (Hampton and Majkowski, 1987).

The efficacy of adopting Pauly's slicing method or LCCC (Pauly, 1980) and the Ehrhardt and Ault (1992) approach versus StALK was evaluated by application of the procedure to simulated data from the operating model *SimCatch* assuming 40% variability in recruitment for 34 years. Error in estimation from the three methods from a known age distribution and resulting ACC are seen as percentages in Figure 3.4.2. Plots of Z estimates using the StALK method versus the two popular alternative methods are shown in Figure 3.4.3. While Pauly's method is quite accurate for a partial duration of the time series (years 20-27, 31-33) as compared to StALK (Figure 3.4.3), the lack of precision throughout the entire time series should be of concern (Figure 3.4.2). Alternatively, StALK provides quite accurate estimates of Z while maintaining much less

variability in its precision. At lower levels of recruitment variability, StALK estimates are even more accurate (Figure 3.3.3). Parrack and Cummings (2003) stated that the LCCC method was most effective with little or no cohort variance, but performed poorly when variance in cohorts were fivefold or more.

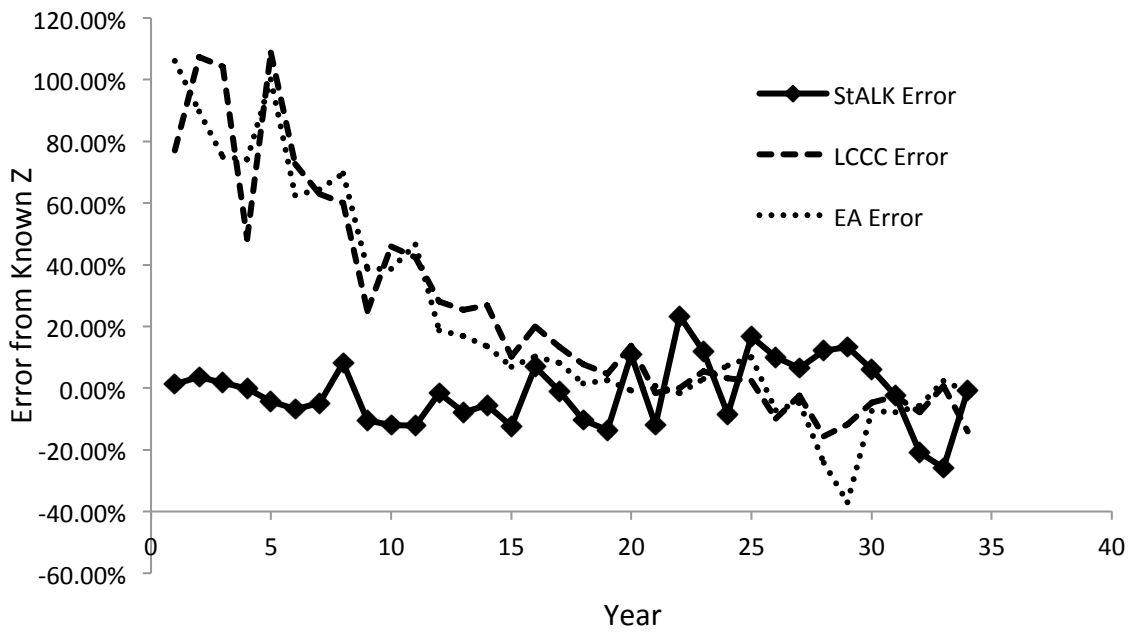


Figure 3.4.2. Percent error in total mortality, Z, estimated by age frequencies derived from StALK , length-based Z estimations, LCCC methods by year versus Z estimated by ACC in known simulated age frequencies with 40% interannual recruitment.

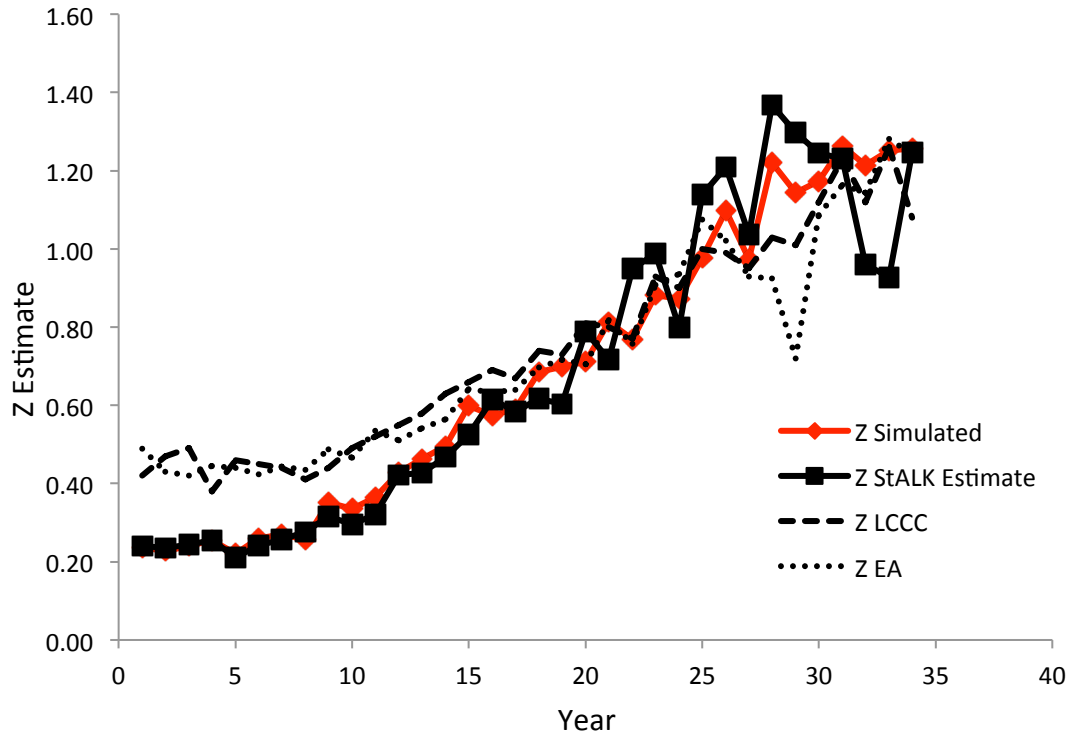


Figure 3.4.3. Comparisons of total mortality, Z , estimated by age frequencies derived from StALK, LCCC, and ACC of known simulated age frequencies 40% interannual recruitment variability

Additionally, Ault et al (1998) showed that total mortality estimators based on average length (Ehrhardt and Ault, 1992) were robust and insensitive to recruitment variability in their simulation studies. However those studies relied on a monotonic change in recruitment versus a high degree of interannual ‘noise’ in recruitment which can be commonly seen in tropical pelagics (Lehody, 2010) and reflected in the simulation experiment. In the case of low exploitation and high interannual recruitment variability, both length-based approaches lead to a positive bias whereas age frequencies and size at age distributions are likely more impacted by recruitment than by exploitation. However,

as total mortality, Z , increases through time and the fishery is fully exploited, the length-based approaches have very low bias in their estimates (Figures 3.4.2 and 3.4.3).

The StALK algorithm to numerically generate age distributions at size estimates distributions that fully cover the age-size range of the species. StALK successfully computed age at size distributions statistically equal to a simulated ALK with known age at size distributions. The combined estimator for recruitment/fishing mortality used in the heritable growth deviance transfer frame also achieved adequate fit of length distributions to observed length frequencies. The complexity of exploitation patterns in multi-gear multi-fleets fisheries could be significantly improved if those exploitation patterns could be estimated via well designed experiments of selectivity/availability. Such studies are less cumbersome and less costly than the generation of directly observed age distributions at size in those fisheries. However, in fisheries with a large portion of catch within a partially recruited size range, selectivity may only be applied to the portion of size ranges where fish are fully recruited into the fishery.

Statistical comparisons of age-length keys are difficult due to many empty cells or missing data and unless some gross assumption are made (i.e. increase size and age bins) (Gerritsen, et. al. 2006). When StALK was applied to Gulf of Mexico red snapper length frequencies and compared to known red snapper ALKs in two fisheries, this issue was likely a point of concern (Appendix C). The most significant differences were found among sets of ALK's where disparity due to missing data in directly observed ALKs for handline (HL) and longline (LL) red snapper fisheries was evident (Appendix C). Application of the StALK algorithm to red snapper data for year 2003 demonstrated that incomplete ALK data can generate disparate values of the total mortality rate, Z , relative

to estimated ALK that have data sufficiency (Appendix C). Like any approach sensitive to its principle data, StALK is most likely prone to bias or ineffective in use in length frequencies that exhibit sampling paucity or data deficiency.

Existing Methods of Estimation Age Composition and Estimation of ALKs

Bartoo and Parker (1982) present a means to avoid the biases in deterministic age frequency estimation from the von Bertalanffy growth function by introducing a stochastic age frequency estimation algorithm. This approach is based on variance of length-at-age from a von Bertalanffy relationship such that for any age, the probability of a specific length interval is the probability of that interval taken over all lengths intervals containing that age. Bartoo and Parker (1982) constructed a probability matrix, P , for any length-at-age with corresponding dimensions equaling the number of length intervals by number of age classes. A resulting numbers-at-age vector (with a length equaling corresponding age classes, j), A , is solved via the least squares normal equation from the probability of length-at-age matrix, P , and from a vector of length frequencies (with a length equaling the number of corresponding size intervals, s), L , described by Bartoo and Parker (1982) is a least squares procedure,

$A = (P^T P)^{-1} P^T L$, solving vector A by:

$$SS = \min \sum_{i=\min s}^{\max s} \left[L_i - \sum_{j=0}^{\max j} A_j P_{i,j} \right]^2 \quad (3.19)$$

When comparing the stochastic age estimation versus deterministic age estimation against a control of known observed numbers of age, the authors found their method

significantly reduced bias in age frequency estimation - as much as 50 to 65% in some instances. Parrack and Cummings (2003) argue that this approach is an improvement over LCCC when cohort abundances are markedly variable.

Similarly to using known variability of length-at-age to solve for an unknown vector of numbers of age, size mixture modeling and modal progression analyses can be used to fit discrete predicted length-at-age distributions to an observed length-frequency database. Such methods were adopted by MacDonald and Pitcher (1979) and also found in the widely-used program MULTIFAN-CL (Fournier et al., 1998).

Kimura and Chikuni (1987) developed an iterative age-length key (IALK) algorithm which combined mixture distribution modeling and age-length keys from directly observed ages. The IALK method simply requires that empirically estimated length-at-age distributions be applicable to the population sampled for length frequencies and is flexible to apply age-length data sampled from one statistical population to a length frequency sampled from another (Kimura and Chikuni, 1987). Like the method introduced by Bartoo and Parker (1982), a proportion at age (j) distributions are fitted, \hat{p}_j . Given an observed fraction $q_{i,j}$ of length at age (i,j) the formulation is:

$$\sum_i \left[\frac{L_i q_{i,j}}{\sum_j \hat{p}_j q_{i,j}} \right] = 1 \quad (3.20)$$

Whereas L is the observed length frequency proportion in length category, i. Kimura and Chikuni (1987) fit estimates for \hat{p}_j using the expectation-minimization (EM) algorithm described by Dempster (1977) and maximum likelihood estimation (MLE).

The existing methodologies to assess the distribution of ages in landings in absence of age-length keys present many caveats. The approach by Bartoo and Parker

(1982) does not take into account changes in size-at-age distributions due to exploited conditions that result from size at age specific exploitation patterns. The iterative IALK approach by Kimura and Chikuni (1987) requires prior knowledge of size-at-age without consideration of growth transfer processes from size at an age class to size at the following age class. The IALK method relies on information from prior ALKs which may be a limitation for fisheries that have not had a prior ALK developed. The family of methods that estimate proportions of ages in length frequencies from fitting a mixture of finite discrete distributions information (MacDonald and Pitcher, 1979), which may be based on estimated size-at-age (Fournier et al, 1998), does not take into consideration deformations in size-age distributions that result from selectivity, availability to a fishery, or minimum size due to management. The approaches by Bartoo and Parker (1982), Kimura and Chikuni (1987), and Fournier et al (1998) do not track individuals or groups of individuals through age or size throughout ontogeny. Nor do these methods account for selectivity which may alter size at age distributions. In contrast, the StALK method is based on a conceptual frame that avoids bias by tracking size at age groupings throughout time and estimating distributions of size at age with individuals subjected to a given size-based selectivity pattern through.

The Novelty of StALK

The StALK algorithm makes the simple assumption that each individual's growth deviation is constant over its lifetime, without making any assumptions about the mechanisms behind individual variation in growth. However, growth potential of individuals is commonly a heritable, genetically-imprinted trait in most fishes (Sainsbury,

1980; Russo et al., 2009). Studies have linked growth predisposition to genetic components. Johnson et al. (2011) and Cheverud et al. (1983) determined that genetic covariance between size and growth at different ages is likely due to expressions of single genes that code for growth factors and body sizes at different ages. Furthermore studies on multiple fishes corroborate a linkage between size at early life history stages with size at age in following years by positive genetic covariance: rainbow trout in a laboratory (McKay, 1986), Atlantic silversides (Munch et al., 2005; Walsh et al., 2006), and hatchery-reared salmonids (Heath et al., 1999, Carlson and Simmons, 2008). Growth of offspring is linked to body size of maternal individuals through phenotype correlation (Berkeley et al., 2004). Fishing selectivity of larger individuals may remove or diminish the contribution of larger individuals to procreate the population with heritable traits conducive to larger growth. Kirpatrick (1984) presented an 'assignment-at-birth growth model' and contended that individuals have a predisposition to growth based on an inherent growth trajectory and that individuals in a cohort are theoretically normally distributed by size. Russo et al. (2009) adopted a similar concept for which individuals have a predetermined growth trajectory, but can 'jump' to a different phase of growth and 'jump' back to the original trajectory due to environmental or seasonal factors. Eveson et al. (2011) found that individual fish grow variably and uniquely and tested the impacts of assuming incorrect variance or no variance in growth parameters for individual growth; the authors found that consequences of not accounting for variance in growth parameters were minor.

The distribution for predisposed growth deviance used in StALK can be any given a statistical distribution that reflects phenotypic correlations of size at age for that species

or any assumed mechanism. However, assuming that normally-distributed heritable growth deviances for individuals yield normally distributed size at age is consistent with common assumptions in the literature. Size at age distributions, even with variable growth trajectories, are widely accepted to be normally or lognormally distributed with increases in variance with respect to increases in mean size at age (Sainsbury, 1980; Kirpatrick, 1984, Russo et al, 2009). Hordyk et al. (2014) utilized transfer mechanism of individuals through predetermined normal distributions of size at age with increasing variability of length at age - though this study did not track groups of fish through ontogeny like the StALK algorithm does, nor did that study construct an ALK. Selection of larger individuals by fisheries leads to distributions of size at age being right skewed and the StALK algorithm accounts for these processes.

The StALK algorithm can also be flexible in accounting for extrinsic factors that can impact growth and size at age distributions, such as environmental factors or population processes, by adjusting inputs for size at age parameters with respect to extrinsic factors. Brodziak et al (2008) noted that in the recovery and increase of haddock abundance, mean size at age was reduced for several mature age classes, presumably due to density-dependent limitations. For species such as haddock for which the relationship between abundance and compensatory shifts in size at age can be inferred (Brodziak et al 2008)- the StALK concept can adjust size at age parameters. However, this requires knowledge on abundance, which would likely only be available for species that have sufficient data for an age based assessment. Therefore, StALK should be used with caution for species in which significant compensatory effects on size-at-age are known (or speculated) to be density-dependent.

StALK is a viable option for estimating age distributions in data poor fisheries. However, future research is warranted. Future work that should be conducted with StALK includes the application of StALK with animals with growth trajectories that are not von Bertalanffy in nature or that have multiple growth stanzas. StALK and its operating model, SimCatch, can be used to test whether ALKs should be collected on an annual basis or if ALKs change annually given certain conditions. Often times, ALKs cannot be collected for a particular year or fishery due to personnel limitations or time constraints. StALKS can either provide a temporary alternative in case empirically collected ALKs are not available or test if ALKs can be used from prior years.

Further simulation testing with StALK's operating model can be conducted with species with unknown (or misspecification of) terminal ages. StALK could also be tested in hypothetical data poor scenarios in which older ages are intermittently unavailable due to depletion or seemingly unavailable due to lack of sampling. StALK and its operating model could be applied to estimate optimal sampling for length frequencies of a population and optimal direct estimation used to provide advice on efficient means to develop ALKs. StALK can also be tested and applied on simulated scenarios in which a population withstood a sporadic cataclysmic event(s) (such as oil spills or climate phenomenon) in which specific incoming cohorts withstood dramatic deleterious effects. Sensitivity of StALK, length-based methods, and age slicing to such events should be examined through simulation testing.

Based on StALKs results and known growth information, full recruitment into the purse seine fishery begins at age 4 and 5, though many individuals below 165 cm (and age 4) are exploited in the fishery and not accounted for in estimation of mortality

because they do not lie within the range of full recruitment. Age 4 is the most dominant age group in all observed sailfish (Figure 3.3.11). Age 5 is the most prominent age class on a consistent basis in the waters off Central America where recreational fisheries are most prominent (Figure 3.4.4) and where information on abundance (CPUE) is most available. Ramirez et al. (2011) noted that age 5 was the most prominent in directly estimated ages in southern Mexico. The significance of this age class is underscored in analyses in Chapter 4.

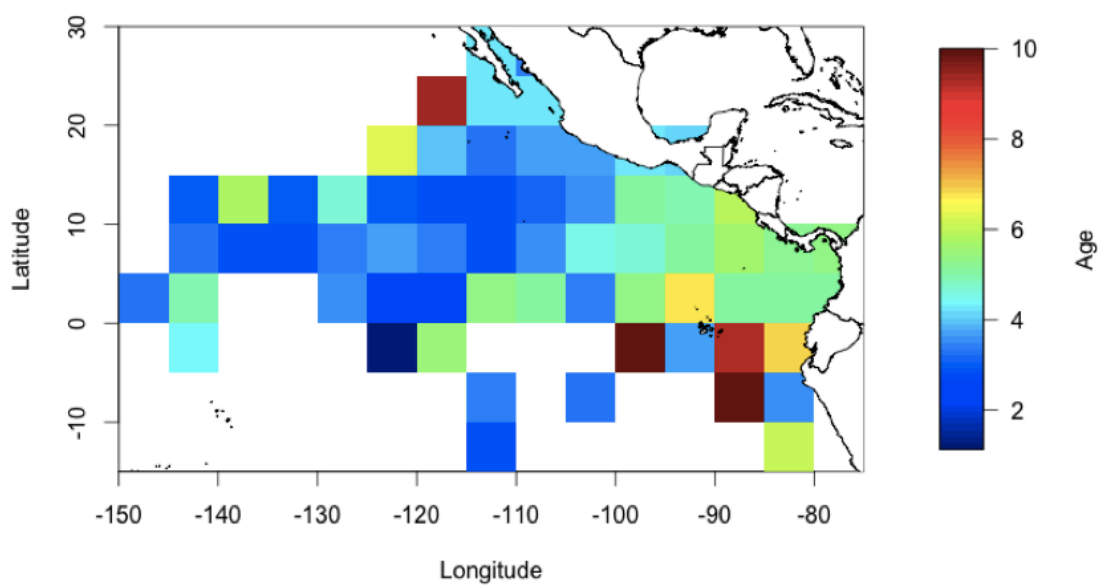


Figure 3.4.4. Average age (years) for sailfish in the EPO by 5°x5° graticule as estimated by StALK algorithm

Chapter 4

Dynamics of Local Availability and Fishing Success of Recreational Fisheries

4.1 Background

Recreational for-hire fisheries are a very significant component of Central American fisheries, both economically and socially. Recreational fisheries targeting billfish in this region rely on a catch-and-release strategy to utilize the resource while minimizing incidental mortality due to fishing. In this way, individual billfish have protracted exploitable life span providing users with a sustainable commodity that has an added economic value. To enhance survival of the caught and released fish, recreational fisheries make exclusive use of circle hooks to prevent unnecessary hook trauma in the esophagus or digestive tracts. Recreational fisheries have developed significantly since the early 1980's; however, it was not until the early 1990's that billfish recreational fishing infrastructure was developed fully in Costa Rica and Guatemala. Such developments are lacking a statistical system that collects mandated or voluntary fishery-dependent data necessary to assess the effects of billfish exploitation. Such a system would facilitate the generation of information that could support management of these important regional fishery resources.

The large recreational multinational fleet carries out thousands of daily fishing operations during a fishing season that usually expands from December to May. A formal fishery statistical system to record the outcome of all fishing operations over large areas of the ocean would require an investment and a multinational institutional set up which would not be feasible. At present, the only data available consist of fishing records

collected by some individuals on their own, and integrating these data is not possible under present day institutional arrangements both within and among countries.

Recreational fisheries may not cover the range of the species due to vessel limitations, but these fisheries are one of the few fisheries actively targeting billfishes and archiving catch and effort statistics.

Along the Pacific Coast of Central America, coastal artisanal and semi-industrial longline fleets targeting tuna and mahi mahi inflict substantial impacts on billfish resources, which are caught incidentally in those minimally regulated fisheries. Historically, information on relative abundance from CPUE indices have been lacking in most capture fisheries that exploit billfishes in the eastern tropical Pacific, especially small-scale and semi-industrial fisheries that have large yet not quantified fishing capacities and sparse records of catch or effort. Over-exploitation of target species in some of the commercial fisheries has prompted the retention of billfish species. Billfish are also caught as bycatch in some of the purse seine fleets targeting yellowfin tuna, where billfish may be integrated in the landings and processed with packed tuna. In addition billfish commercial statistics have been identified as insufficient to formally implement critically needed billfish stock assessments (Hinton, 2013: IATTC 2013 Sailfish Assessment). Based on the lack of statistical information from recreational and commercial fleets, billfish species can be classified as data poor stocks in which formal assessments are not plausible (Pilling et al., 2008).

There is a need to understand the spatial-temporal dynamics of the species to assess the impacts of fishing intensity by the various fleets on the billfish stocks. In billfish recreational fisheries, the lack of knowledge on the spatial temporal

characteristics of the stocks inhibits the ability to optimize recreational fishing time as well as operational costs that effect revenues from fishing. On the other hand, there is a need to understand oceanographic features and processes that drive the dynamics of the billfish resources.

An electronic logbook system that can record billfish caught and released at specific georeferenced places was implemented. This remote data gathering system offers an opportunity to link stock availability to operational tactics of the recreational fleets. For this purpose, in 2010, the University of Miami began partnering with CLS America, Inc, a satellite fishing vessel tracking company, to develop and implement an efficient and cost effective electronic satellite logbook system that would remotely collect catch and effort data in the charter/for-hire billfish sport fishing fleets in Guatemala and Costa Rica. The data collected from the program may be used to estimate relative abundance indices of billfish species as well as to assess spatial and temporal fish availability and operational dynamics of fishing intensity in these fisheries. Information is gathered in real-time to geo-statistically monitor fishing operations relative to the seasonal distribution of billfish.

The goal of this Chapter is to understand the impacts of billfish habitat seasonality and recreational fleet dynamics on local fishing success. The objectives are: 1) to develop spatially explicit catch and effort indices to understand billfish availability to recreational fisheries and to model fishing behavior and vessel interference relative to fishing catch efficiency. 2) To determine ecosystem variables that drive seasonal trends in availability to the recreational fisheries. 3) To determine large-scale ecosystem dynamics that drive availability on an annual and multi-annual level (Figure 4.1.1).

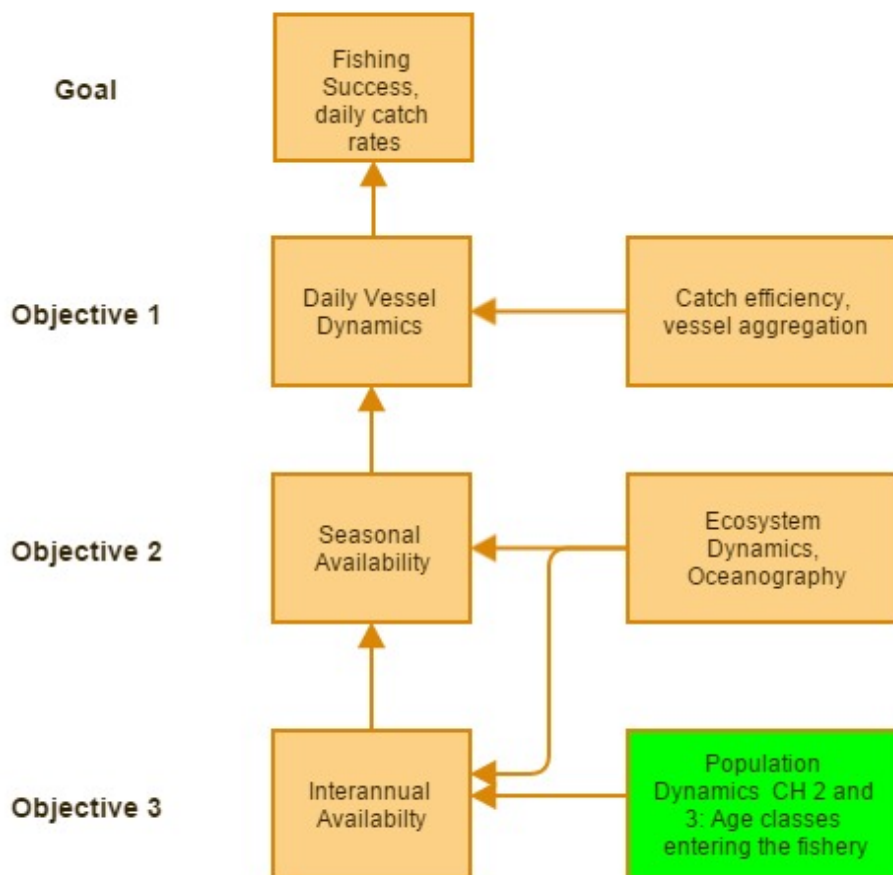


Figure 4.1.1. Flowchart and hierarchy of goal and objectives for this chapter

4.2 Materials and Methods

Description of Data in Recreational Fisheries Targeting Billfish

Data on catch and effort for recreational billfish fisheries in Central America have historically been reported by vessel owners and vessel captains upon returning to port at the end of the fishing day or as monthly reports. These records are by vessel per fishing trip (trips are one day each) and provide information on ‘raises’, ‘bites’, ‘releases’, and gear type (conventional, flyfishing, spinning tackle). Raises indicate the number of billfish visually seen by the crew by ‘teasing’ billfish to the surface with hookless lures

(called ‘teasers’), which alert the crew (a captain operating the vessel and at least one mate) that a biting fish may be imminent. Bites refer to the number of fish that bite a baited hook presented to a teased, raised billfish that get successfully hooked and commence a fight with an angler. Releases refer to the number of hooked fish successfully fought and brought towards the boat. Conventional fishing incorporates the use of teasers pulled behind a boat at a low to moderate speeds. Depending on the vessel and crew, 3 to 6 lines with hook-less teasers are used to attract billfish, sometimes with 1 or 2 lines having a baited hook directly behind the vessel (often called a ‘shotgun’ by anglers). Teasers are set out on port and starboard sides with varying lengths with the use of outriggers to prevent lines from crossing. When a fish is observed by the vessel crew raised towards a teaser at the surface, a baited hook is ‘pitched’ to the fish with the hopes of coaxing that fish into biting the baited hook. Flyfishing encompasses similar techniques to tease fish to the surface but with fewer lines on one side so that an angler may cast to a raised billfish. When a billfish is raised, the captain may put the vessel in neutral and an angler may cast a hooked fly to a billfish with the hopes to hook the fish.

Historical records available for analyses of recreational fisheries in Central America began in the mid 1980’s with surveys of recreational fishermen from Costa Rica, Guatemala, and Panama carried out by NOAA Fisheries. The longest continuous series of billfish data by vessel in Central America spans from 1994 to present in the Pacific coast of Guatemala. For the last two decades, data originating from Artmarina Fins n’ Feathers Lodge (monthly 1994-2005), Sailfish Bay Lodge (monthly 2006), Casa Vieja Lodge (daily 2006-present), and Guatemala Billfishing Adventures (daily 2005-2007) have incorporated into the longest series available. In Costa Rica, data on

billfishing is available on a daily or monthly basis from independent vessels in Flamingo (northern Costa Rica) and Quepos (Central Costa Rica) from 2001 to 2008. These historical records are used to supplement analyses in this chapter, although they do not include latitude and longitude information.

A Satellite Logbook System to Collect Information on Fishing Activity

The satellite logbook system was developed first for Guatemala and later Costa Rica. The system allows the captains to enter species caught-and-released with a touchscreen device. Latitude, longitude and date are automatically drawn from a GPS at the time that a catch is logged. Catch data is automatically transmitted via satellite to an email address. Vessel location data is monitored and relayed at pre-defined time intervals to a server at CLS America called the Iridium Processing Center (IPC) and then transmitted via FTP to the University of Miami. The data are then posted to a web portal called the Iridium Web Portal (IWP, <http://mydata.clsamerica.com>) for use by user groups and fishing operators (Figure 4.2.1). The CLS America system has exclusive use of the Iridium Satellite Constellation owned and operated by Collecte Localisation Satellites, known colloquially as CLS France, the parent company of CLS America. Transmission cost is approximately \$1.75 per KB of data sent, which is approximately 5-10 messages depending on the number of characters sent in data reports. Location services for vessel monitoring costs \$54.99 per vessel per month.

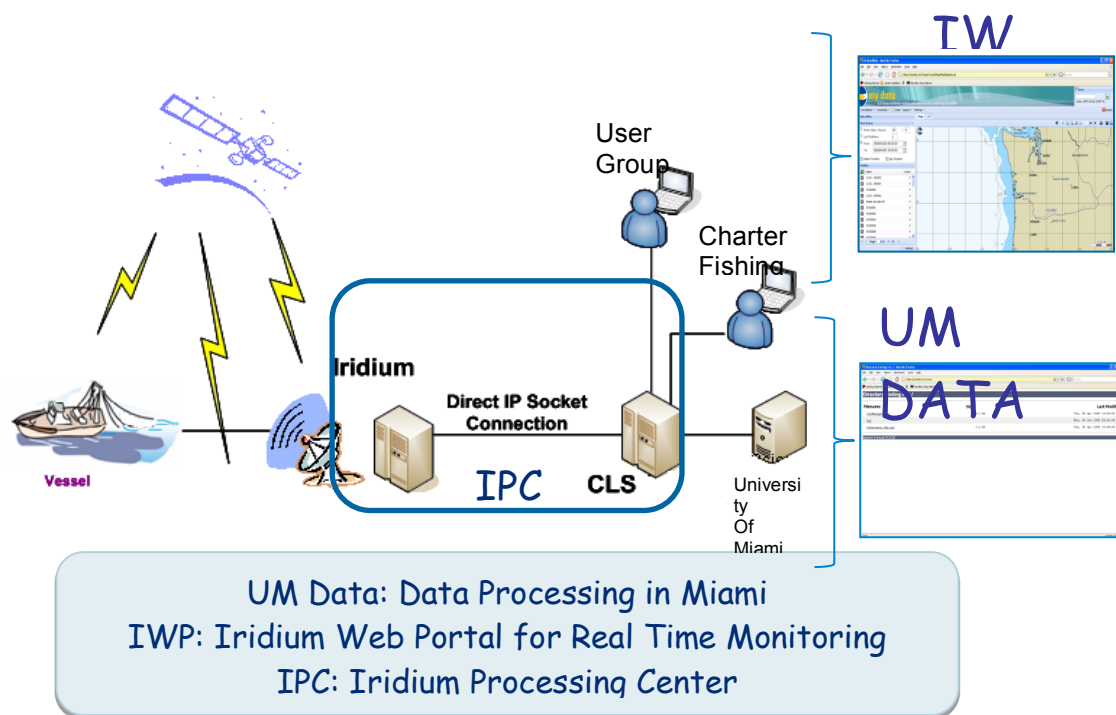


Figure 4.2.1. The Iridium satellite constellation system offers satellite GPS and data transmission capabilities from vessels to the Iridium Processing Center (IPC) and CLS America servers transmit the information to individual users as well as a centralized project laboratory (University of Miami) for data assimilation and integration with oceanographic and habitat data.

The hardware that has been tested and initially used as a satellite logbook system in Guatemala first consisted of a two-way communication satellite dome antenna - the Thorium Satellite Transceiver (TST) that has an integrated GPS antennae as well as the Iridium Short Burst Data (SBD) modem inside, a Junction box to relay data from the Thorium unit, a Central Processing Unit (CPU) that meets IP-65 waterproof standards for the marine environment to process data, and the Data Terminal Equipment (DTE), which provides an easy touch-interface also meeting IP-65 waterproof standards (Figure 4.2.2).

This interface was developed cooperatively with for-hire captains in Guatemala in 2010 to ensure the unit was easy to use and stood up to the rigors of on-board use.

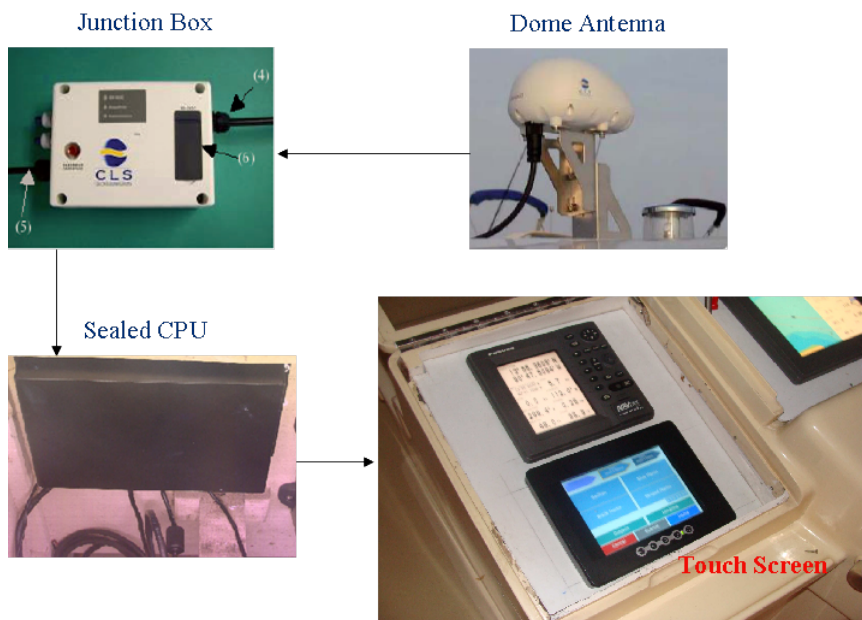


Figure 4.2.2. Components of the hardware necessary to operate an electronic satellite logbook system.

Prior to the 2012 fishing season, an Android device (Motorola Defy) was introduced as a replacement to the touchscreen DTE and joint CPU to reduce hardware needed on vessels, reduce cost, and make data entry more convenient (Figure 4.2.3). Partnering with CLS America and CLS France, a mobile application for recreational billfish data collection was created to process and send user input via Bluetooth connection to the Junction box, which then relayed information to and from the Thorium antennae. This system phased out the use of large hardware systems (CPU and DTE) and has been in use as of the 2012 fishing season to present.

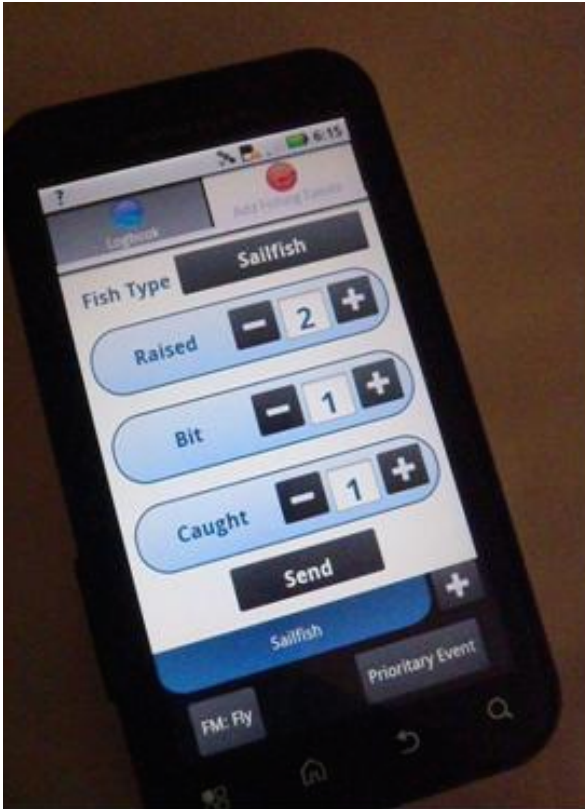


Figure 4.2.3. An Android phone, Motorola Defy, with the Billfish Catch Reporter mobile application, used from Fall 2011 to present.

Data Generated by Satellite Logbook System

Satellite logbook systems generate A) position reports of the vessel for a predetermined time period automatically collected and reported and B) data entered and sent by the fisherman for fishing events that take place. Position reports are collected either on half hour or hour increments depending on movement of the vessel. The data reports include a timestamp, vessel heading (direction in degrees), vessel speed (nm), latitude (decimal degrees) and longitude (decimal degrees). Timestamps are sent in compressed UNIX time, which are milliseconds since January 1, 1970 at 00:00:00.00

GMT. Position reports are available, but for a limited time at the IWP, mydata.clsamerica.com. However, these data were sent from CLS to an FTP server at the University of Miami Computing Facility as *.DAT files. These *.DAT files have a unique 13-digit identifier such as 'DIST-000121-1245803.dat'. Position reports are read, concatenated, and processed in the R Statistical Computing Language (scripts in Appendix). Timestamps are converted to 'YYYY-MM-DD HH:MM' formats using R.

Fishing events are reported by captains or crew as they encounter billfish. These encounters may last several minutes to an hour or more. Each fishing event provides data on geolocation (latitude in decimal degrees and longitude in decimal degrees), timestamp (also in UNIX time), species encountered, predetermined fishing mode, fish raised in a given encounter, how many of those raised fish bite, and the number of fish that bit and were successfully caught and released. Target billfish species and ancillary target species entered include in order of prevalence: sailfish, *Makaira nigricans* (blue marlin), *Istiompax indica* (black marlin), *Kajikia audax* (striped marlin), *Thunnus albacares* (yellowfin tuna), *Coryphaena hippurus* (dorado), *Acanthocybium solandri* (wahoo), and *Sarda chiliensis* (bonita). The logbook system also allows for captains to send a report of dolphins or commercial longliners encountered.

Oceanographic Data and Sources Used to Define Habitat

Georeferenced billfish catch data can be coupled to oceanographic data collected daily via satellite. Such variables may be related to biological productivity, habitat quality, and circulation which may explain variance and presence of billfish and impact

the behavior of fishermen. These oceanographic variables include altimetry (sea surface height, SSH), sea surface temperature (SST in degrees C), geostrophic currents derived from altimetry (u, v, w direction in m/s), and in some cases- chlorophyll (Chla in ml/L).

SSH and geostrophic data were collected through AVISO (<http://www.aviso.altimetry.fr/>) as gridded netCDF files (*.nc). Geostrophic current and altimetry data is in 0.1 degree resolution and are coupled measurements in two orthogonal axes. Geostrophic satellite products come in both meridional (v, south to north) and zonal (u, west to east) components in m/s. Total geostrophic current is calculated as:

$$w = \sqrt{u^2 + v^2} \quad (4.1)$$

resulting in a vector with a magnitude w in m/s with a direction in radians calculated from the arctangent of the u and v axes. These data are processed from gridded netCDF files with dimensions time, latitude, and longitude in the R Computing Language (scripts attached in Appendix) in a function called “GetUVData.r” .

Chlorophyll and temperature are provided as gridded netCDF files through the ERDDAP website (<http://coastwatch.pfeg.noaa.gov/erddap/index.html>). Chlorophyll data originate from NASA satellite MODIS Aqua product and is available as delayed in 0.04 degrees resolution. Sea surface temperature data originate from NOAA Coastwatch Aqua MODIS Pacific Ocean daytime with a resolution of 0.025 degrees. These data are extracted and processed in the R Computing Language in a function called ‘MapExtractOceanData.r’ (scripts attached in Appendix).

Often, oceanographic variables that may drive seasonal dynamics of billfish species are available on a monthly scale only. Mixed layer depth, a variable often used to

estimate vertical habitat, is a depth for which water density changes at any given temperature by 0.0125 kg/cubic meter of seawater (Levitus, 1982). This depth often corresponds to thermocline depth and depth of oxygen declines (Levitus, 1982). Spatially gridded mixed layer depth data (MLD, m depth) is available as netCDF datasets by month from the NOAA National Oceanographic Data Center (NODC) (<https://www.nodc.noaa.gov/OC5/WOA94/mix.html>). Upwelling indices are available through the Pacific Fisheries Environmental Laboratory webpage (<http://www.pfeg.noaa.gov/products/las.html>). Extrapolated dissolved oxygen data (ml/L seawater) is available through the World Ocean Atlas (<http://www.nodc.noaa.gov/OC5/woa13/>) in gridded netCDF formats with dimensions latitude, longitude, depth by increments of 10 m depth and spatial resolution of 1 degree. Oxygen minimum depth, a vertical habitat limit (depth in meters corresponding to 1.0 mL/L O₂) is estimated in the R Statistical Computing Language by interpolating dissolved oxygen at 0.1 m depth increments using a spline function and querying interpolated depth that corresponds to 1.0 mL/L O₂. The University of Hawaii Sea Level Center (<http://ilikai.soest.hawaii.edu/>) provides data on global sea height conditions and large scale tropical currents such as the northern equatorial current (NEC) and equatorial countercurrent (ECC). The northern equatorial current NEC is estimated by the difference in dynamic sea height between the countercurrent trough (~9N) and the north equatorial ridge (~20N) (Wyrтки, 1974). The ECC is estimated by the difference in dynamic sea height between the equatorial ridge (2N) and the countercurrent trough (9N) (Wyrтки, 1974). These current indices are compounded as annual averages of months in which intensity is greatest (October to March) and lagged five years. An annual multivariate

ENSO Index (MEI, data available <http://www.esrl.noaa.gov/psd/enso/mei/>) is used to summarize ocean state on a seasonal basis. It is constructed as the first principal component of observed sea surface temperature, sea level pressure, zonal surface wind (east/west), meridian surface wind (north/south), surface air pressure, and cloud cover fraction over the tropical Pacific Ocean (Wolter and Timlin, 1993).

Billfish observation data from logbooks and historical time series are coupled to oceanographic data through querying data that corresponds to the closest observed latitude and longitudes and times of data being investigated. This data management is done in the R Computing Language (scripts available upon request).

Estimating Vessel Behavior, Aggregation, and Relative Dispersion

Patchiness and aggregation of harvesting entities relative to a resource have been quantified by Clark and Evans (1954, 1955), Pielou (1977) and Uwin (1981) using a set of functions, including the sum of nearest neighbor distances relative to total possible spatial range and the number of entities (or organisms, vessels) utilizing a resource. These families of aggregation and patchiness metrics in spatial ecology test for the assumption that entities are non-random in nature and are aware of other entities, much like the behavior of fishers searching for a resource and having knowledge of where other vessels may be operating. A modified nearest aggregation neighbor index τ_i modified from Clark and Evans (1954) was calculated for each vessel i (from 1 to n vessels reporting) and hour while fishing t , given Euclidean distances r_i in nautical miles from vessel i to the other n vessels reporting that hour, as the mean distance:

$$\tau_{i,j,t} = \frac{\sum_{n=1}^i r_{i,j,t}}{n} \quad (4.2)$$

A small aggregation index, τ , implies that the vessel is relatively aggregated in relation to other vessels. Additionally, the aggregation index and distance searched is used to calculate the Evans and Clark R-ratio to estimate clustering, where R is the ratio of aggregation τ to the P distance searched by that vessel:

$$R_{i,y} = \frac{\tau_{i,j}}{P_{i,j}} \quad (4.3)$$

P is measured by satellite logbook tracks as the distance (in nm) of vessel tracks from home port to where fishing activity occurs for any given hour. The R-ratio determines the relative density in a search area and is a metric for clustering or dispersion of a vessel relative to other fishing vessels. An R-ratio greater than 1.0 implies that the vessel, i , is dispersed relative to its search area, P . That means if a vessel travels a great distance to search for fish that the average nearest neighbor (aggregation) must be greater than distance searched. If the R-ratio is less than 1.0, then that means that the vessel is densely clustered relative to its search area. Even if a vessel does not travel a great distance to search, a low R-ratio means the vessel is quite clustered and its aggregation estimation is less than its distance searched for fishing.

These aggregation and cluster/dispersion indices are then compared to estimated local indices of billfish based on fish raised by the vessel, oceanographic variables, and the proportion of raised fish successfully caught and released to discern the impacts of vessel aggregation on fishing success and the impacts of the ecosystem on fishing vessel

behavior. The relationship of vessel aggregation to local availability (indicated by number of raised fished) is fit to a power function.

Fishing success is a function of local availability, dependent on ocean conditions and reflected in the number of fish raised - but also dependent on the efficiency with which lured fish bite hooks. While daily local availability is evidently dependent on conditions related to ecosystem processes, the success of encountering and then catching sailfish is impacted by crowding of vessels during fishing operations that may impede catchability. Catch reports were placed into hourly increments and separated by fishing mode (conventional or fly). Catchability, $Q_b Q_c$, of sailfish to recreational fishing is equal to the fraction of raised fish hooked and fought by an angler. Numbers of raises, bites, and catches are compiled by hour to examine the impacts of vessel crowding on the catchability of raised fish. Crowding effects (indicated by Aggregation, τ) have impacts on the ratio of fish biting, Q_b , and the ratio of that bite being caught, Q_c . A logit function was fitted to average observed Q_b and Q_c estimates with respect to vessel aggregation, τ . A logit model was fitted to catch efficiencies, limiting outcomes as a probability from 0 to 1:

$$\hat{Q} = \frac{e^{a+b\tau}}{1+e^{a+b\tau}} \quad (4.4)$$

where τ is aggregation (in bins of 0.05nm), and a and b are fitted parameters.

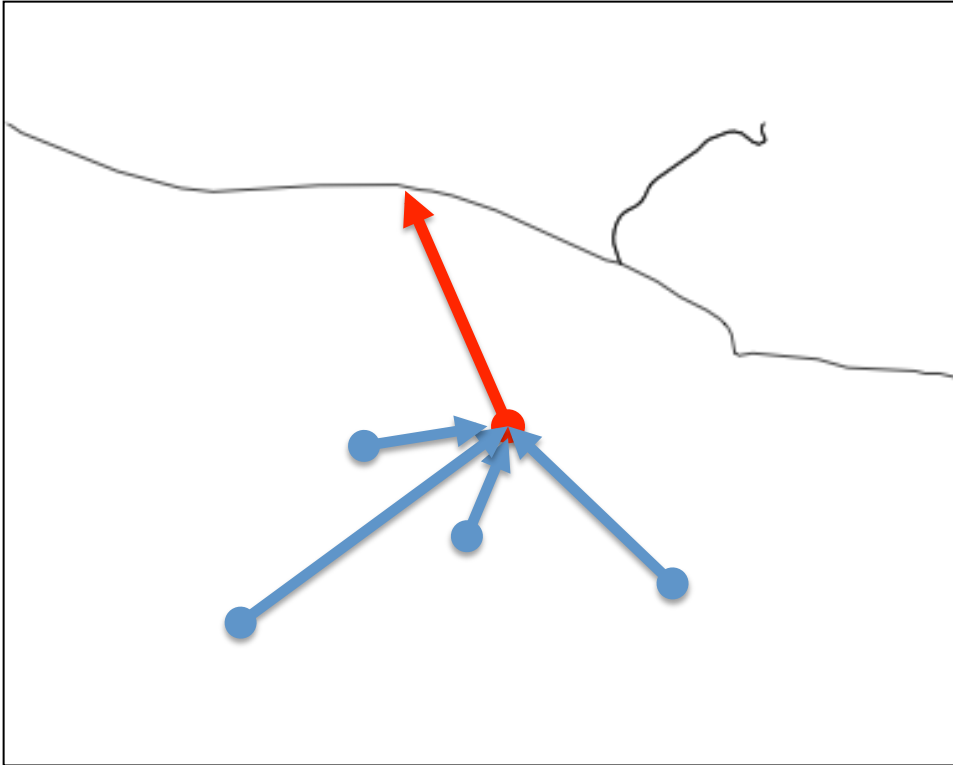


Figure 4.2.4. Depiction of nearest neighbor, averages of r (in blue) and distance searched, P (red) used in determining indices for aggregation and clustering (R-ratio) for the vessel indicated by the red dot.

Estimating Local Availability with Respect to Oceanographic Data and Vessel Effects

Availability is defined as the number of fish raised per unit of time, a direct observation of fish raised to the surface by the vessel's fishing operations. Local availability was estimated on daily and monthly time increments across all fishing boats per day. Availability for examining the effects of fleet dynamics on fishing success is defined on a daily level, however seasonal availability is estimated by month from 1994-2014. Generalized linear models (GLM) are the most commonly used statistical methods

to partition a response variable (often CPUE as a proxy of abundance) into sources of variance that explain a response in abundance or availability (Jones et al., 1998). These methods can determine which variables are most effective in explaining variance of a response variable. For recreational fisheries targeting billfish, the occurrence of fish raised per time (analyzed both daily and monthly) fished is a more robust estimator of local availability than fish caught and released (Ehrhardt and Fitchett, 2006). The number of raised fish, Y , for boat i for time t is estimated through a GLM:

$$Y_{i,t} = \beta_0 + \beta_{1,\text{gear}(i)} + \beta_{2,\text{vessel}(i)} + \beta_{3,i,t}X_{3,i,t} + \dots + \beta_{n,i,t}X_{n,i,t} + e_{it} \quad (4.4)$$

where $\beta_{1,\text{gear}}X_{1,\text{gear}}$ are coefficients and factors for fishing gear/mode (conventional or fly), $\beta_{2,i}X_{2,i}$ denotes coefficients and factor for vessel effects for i vessels, and $\beta_{3,i,t}X_{3,i,t} + \dots + \beta_{n,i,t}X_{n,i,t}$ are coefficients and values for oceanographic variables encountered spatially by vessel i for time period t . Error, $e_{i,t}$, is defined as $N(Y, \sigma_y)$. Interactions are considered through stepwise regression in reduction of model deviance through AIC evaluation. Daily CPUE indices (with respect to raises, bites, and catches per day) are analyzed on daily and monthly (seasonal) basis to discern ecosystem dynamics driving local availability on varying time scales. Oceanographic variables used in explaining local availability on daily levels include zonal (west to east) geostrophic currents (u), meridional (south to north) geostrophic current (v), total current (w), sea surface temperature (SST), sea surface height (SSH), and chlorophyll (chl_a). Sailfish exhibit seasonality in availability off the Guatemala coast that may be due to ecosystem forcing. Environmental variables - sea surface height (SSH), sea surface temperature (SST), and local upwelling indices were used to explain variation in raises/per day/month on a monthly scale using a multiple regression model in the R Statistical language (R

Development Core Team. 2014) with the response (raises/day/month) normalized using the power transform developed by Box and Cox (1964).

Due to cloud cover in the region times and locations may be missing data; these data are interpolated using an autoregressive spline function fit to the previous 5 days and the following 3 days at each gridded point. Each of these variables was georeferenced to match locations of fishing activity from the satellite logbook system. For monthly estimates for which daily georeferenced satellite logbook data was not available (1994-2008), oceanographic variables were estimated as a gridded monthly averages of observations within the gridded range of fishing, 89.5° W to 92.5° W longitudinal range and 12.5° N northward to the coastline. Fishing characteristics used to explain local availability in raises per day include factors of vessel and fishing mode (conventional/fly).

A principal component analysis was conducted on the three oceanographic variables considered most important to defining habitat: sea surface height (SSH), sea surface temperature (SST) and upwelling, to determine synergistic impacts of these variables on sailfish availability. Analyses were carried out in R (R Development Core Team. 2014). This analysis is used to demonstrate shifts in oceanographic variability on a seasonal level.

Inter-annual Processes Determining Availability of Sailfish to Recreational Fisheries

Age 5 is the first fully recruited, most prominent age class estimated from length-frequency data analyzed by the StALK algorithm throughout the Eastern Tropical Pacific and from directly observed ages of sailfish from the Gulf of Tehauntepec near Guatemala

(Cerdenares-Ladron de Guevara et al 2011). An index of Age 5 fish was estimated by multiplying annual proportions of age 5 estimated by StALK times a CPUE from recreational fisheries in Guatemala. Indices of tropical zonal current intensity, the northern equatorial current (NEC) and the equatorial counter current (ECC), are used to describe ecosystem dynamics of the tropical eastern Pacific, lagged five years. The multivariate ENSO Index is also used to explain availability, with no time lag. These indices are available in Table. 4.2.2.

Table 4.2.2. Annual indices (1994-2010) of NEC lagged five years, MEI, catch per trip, proportion of age 5 fish from StALK analyses on length frequencies, and a year 5 strength index.

Year	NEC Index, 5 year lag	MEI	Catch per Trip	Proportion Age 5	Year 5 Strength
1994	227.8	0.413	2.9	0.16	0.47
1995	218	1.095	4.0	0.36	1.42
1996	255.6	-0.513	5.1	0.29	1.44
1997	399.4	-0.372	8.2	0.25	2.04
1998	338	2.568	3.1	0.44	1.50
1999	214.2	-1.129	4.5	0.24	1.09
2000	332	-1.174	10.2	0.35	3.57
2001	287.6	-0.641	4.8	0.42	2.03
2002	255.4	-0.130	7.1	0.23	1.62
2003	385.8	1.017	7.0	0.45	3.20
2004	216.6	0.267	5.8	0.21	1.25
2005	243.4	0.707	9.0	0.17	1.49
2006	181.8	-0.504	4.3	0.34	1.48
2007	215	0.758	8.1	0.15	1.22
2008	322.8	-1.280	7.0	0.45	3.20
2009	250	-0.697	8.3	0.22	2.06
2010	304.2	1.223	18.0	0.19	2.11

4.3 Implementation and Results

Satellite Logbook System

The satellite logbook system was installed in two boats at the end of the 2010 fishing season, the *Finest Kind* and the *Rum Line*, two leading fishing vessels in Guatemala. At the beginning of the 2010-2011 fishing season, the satellite logbook system was installed in the *Spindrift*, the *Release*, the *Makaira*, the *Intensity*, the *Maverick*, the *Gypsy*, and the *Decisive*. Later in 2011, the new android logbook system was then retrofitted on existing vessels and installed in two more vessels, the *Allure* and the *Circle Hook*. At the conclusion of the 2012 season, 5 vessels in southern Costa Rica were outfitted with the logbook system: the *Croc-a-Bye-Baby*, *Croc of Gibraltar*, *Crocodillo*, *Typhoon*, and the *Contender*. Implementing and installing the satellite logbook required about a half a day labor for each unit to install and required training on using the devices. Participation was voluntary. Fishermen were motivated to participate to provide better data collection for assessing a resource financially valuable to them, and to gain better understanding of oceanographic conditions that may impact fishing success.

Between 2011 and 2013, 3892 catch reports were sent from vessels operating with the system. The system transmitted 102,000 vessel position reports during that time. 19,307 of those were while vessels were underway in fishing activities. Vessels are determined to be underway if vessel speed exceeds 2 knots. Vessels are considered underway but not fishing if the vessel is traveling at over 15 knots, a speed too fast for fishing activities.

Daily Availability Determined by Ocean Conditions

The GLM with raises per vessel day as the response variable (Table 4.3.1) found that variables that best explain daily availability are vessel effect, gear type, zonal geostrophic flow, temperature, and an interaction between zonal geostrophic flow and temperature. Sea surface height (SSH) was removed from the analyses because it was correlated ($R=0.81$) with zonal geostrophic current and total absolute geostrophic flow. Meridian (south to northward) geostrophic current did not explain much variance in raises per day, but zonal (west to east) flow did. This is most likely due to the east-west orientation of the coastline in Guatemala. Dominant eastward zonal currents are along the shore and are conducive of convergent zones that promote upwelling along the shoreline, resulting in conditions propitious to fishing. (Figure 4.3.1). The absence of nearshore zonal currents creates conditions that do not promote high catch rates (Figure 4.3.2). In conditions with zonal flow, localized upwelling conditions likely contribute to high densities in a compressed habitat which lead to favorable availability for anglers (Ehrhardt and Fitchett, 2006).

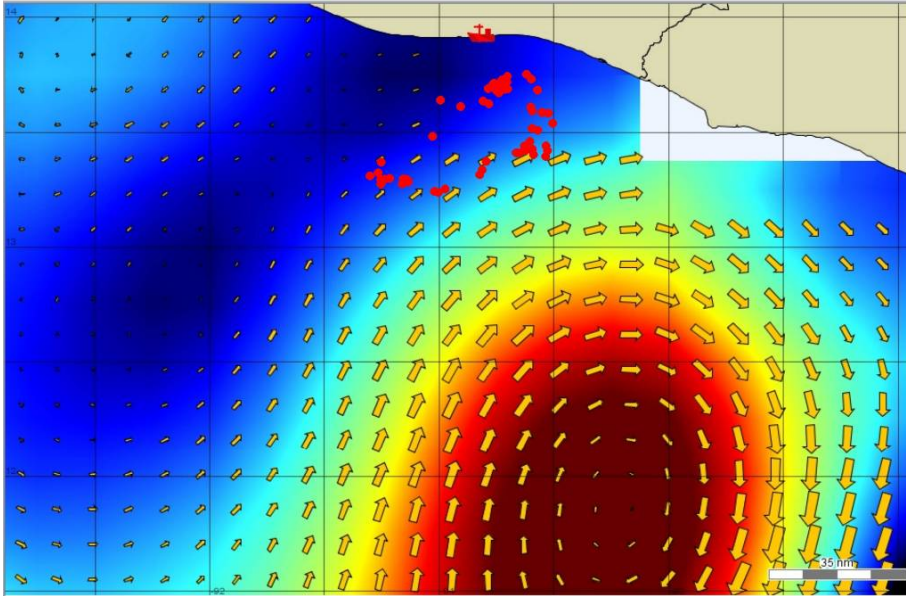


Figure 4.3.1. Oceanographic conditions (SSH and geostrophy) conducive to high catch rates (red dots). February 12-14, 2011, with strong zonal currents and a powerful anticyclonic eddy

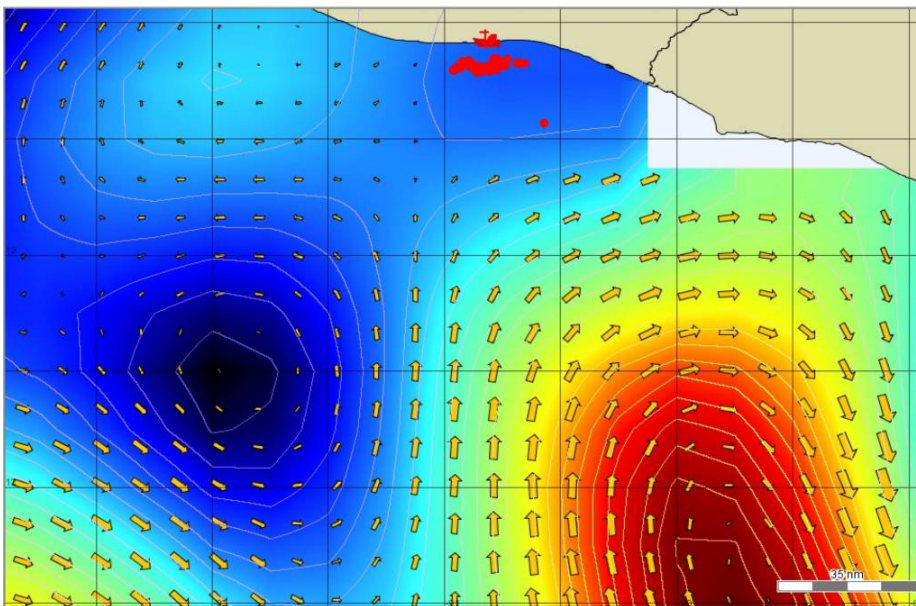


Figure 4.3.2. Oceanographic conditions (SSH and geostrophy) conducive to poorer fishing conditions (catch in red dots), January 31- February 2, 2011, with an absence of dominant zonal current as a divergent transition zone.

Seasonal Availability Due to Ecosystem Dynamics

Sailfish availability in raises per day from the Guatemalan recreational fleet is highly seasonal with the majority of fish raised and caught being in the months of December through April. Figure 4.3.3 shows the influx of sailfish into the recreational fishery and the exiting of sailfish out of the fishery during a typical year. Sea surface height was the best environmental explanatory variable when used on a monthly basis to summarize habitat conducive to availability of sailfish (Table 4.3.1). PCA results of oceanographic variable observations by month from 1994 to 2008 were placed along 3-dimensional orthogonal axis and color coded by months of sailfish entering (red) and exiting (blue) the recreational fishery off Guatemala (Figure 4.3.4). The average monthly first principal component shares a trend with average monthly standardized availability (Figure 4.3.5) estimated from the model described in Table 4.3.1.

Table 4.3.1. Multiple regression ANOVA table of monthly raises per day (1994-2010) power transformed (0.38) to a Normal distribution using Box-Cox Powers (Box and Cox, 1964) and partitioned by month, vessel, sea surface height (SSH) and a month*SSH interaction term. Multiple $R^2 = 0.34$

Component	Df	Sum Sq	Mean Sq	F value	Pr(>F)
Month	11	30.4	2.76	9.54	1.00E-15
Boat	22	19	0.86	2.98	8.20E-06
SSH	1	12.8	12.84	44.4	7.00E-11
Month:SSH	11	12.6	1.14	3.96	1.60E-05
Residuals	504	145.8	0.29		
Total	549	220.6			

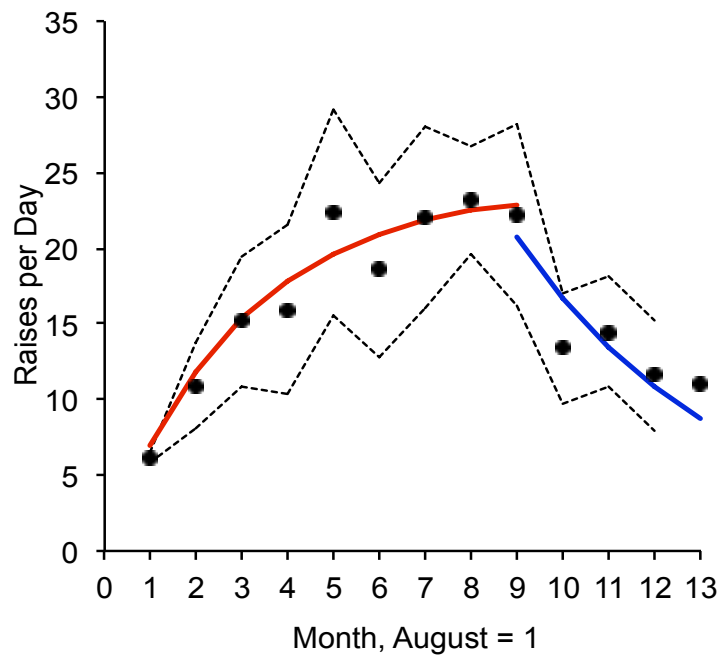


Figure 4.3.3. Seasonal trends in sailfish availability from GLM results, showing a gradual increase in local abundance from August to April (red) with a decrease from May to August (blue).

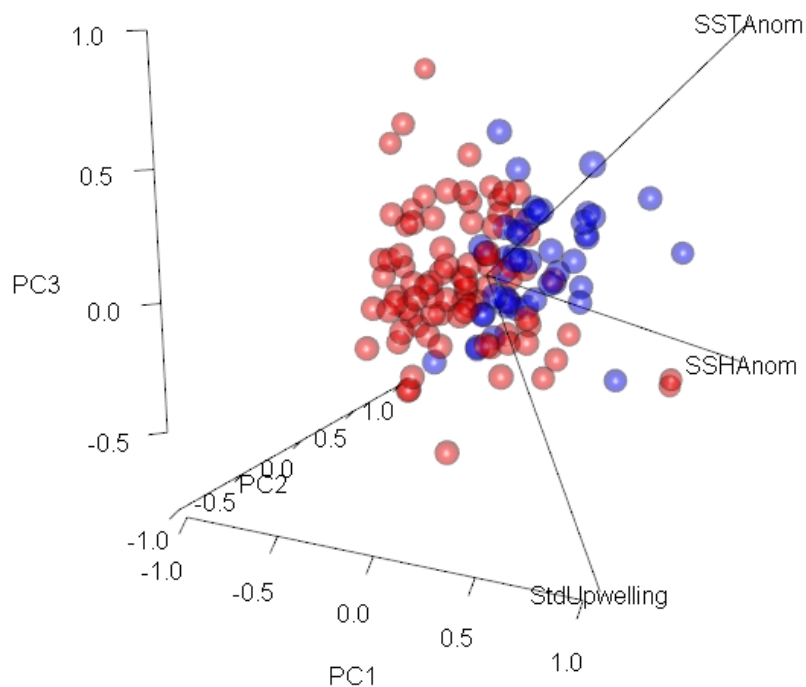


Figure 4.3.4. 3D Principal Component Analyses plot of orthogonal sea surface temperature (SST), sea surface height (SSH), and Upwelling. Red observations denote months in which sailfish are entering the recreational fishery from the late summer and winter (September to April) months and blue denotes observations taken in summer months (May to August) where sailfish are exiting the fishery.

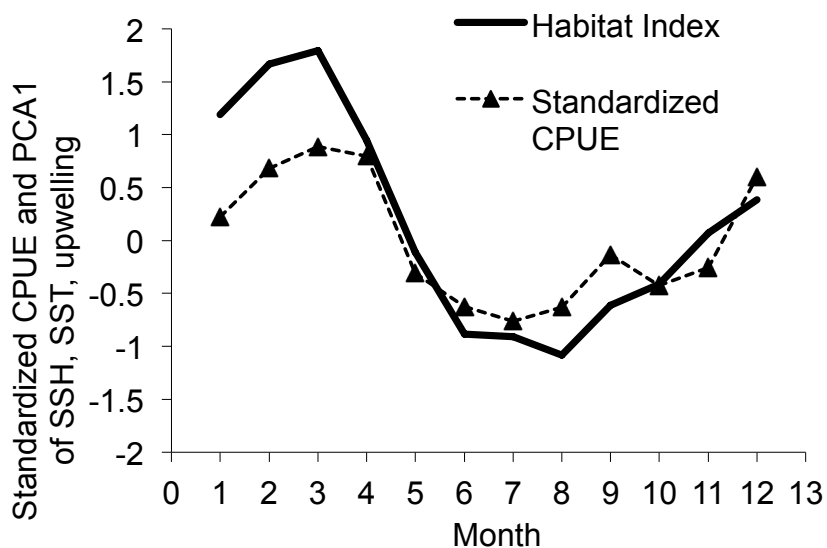


Figure 4.3.5. Monthly averages of standardized availability (CPUE) and the first principal component of a PCA of sea surface height (SSH), sea surface temperature (SST), and upwelling (Habitat Index).

Quantifying Recreational Fishing Vessel Dynamics and Fishing Success

Vessel hourly location reports and catch reports from the satellite logbook system in the 2011-2012 season in Guatemala (2222 catch reports, 4669 hourly position reports in 144 days when at least 3 to 11 vessels were fishing and reporting data, November 8 to March 31) were used to model vessel and fleet behavior and quantify vessel behavioral effects on fishing success- for which fishing success is defined as the number of fish hooked (bites) and subsequently released (caught) by anglers from a given number of fish raised. Under an estimated level of daily sailfish availability, the fleet aggregated in patches when availability was high in areas fished. Vessels seemingly aggregate in their search for fish with respect to resource availability and resource density. In days for which vessels were dispersed, availability of sailfish for fishing was

relatively low – while in days of high availability, vessels were clustered (Figure 4.3.6). Clustering and dispersion of vessels are related to the availability within the exact locality of daily fishing operations. On average for a vessel fishing with bait, Bites = $0.6948 * \text{Raises}$ with an R^2 of 0.754. Likewise, Q_c is on average 0.5875 per fish biting.

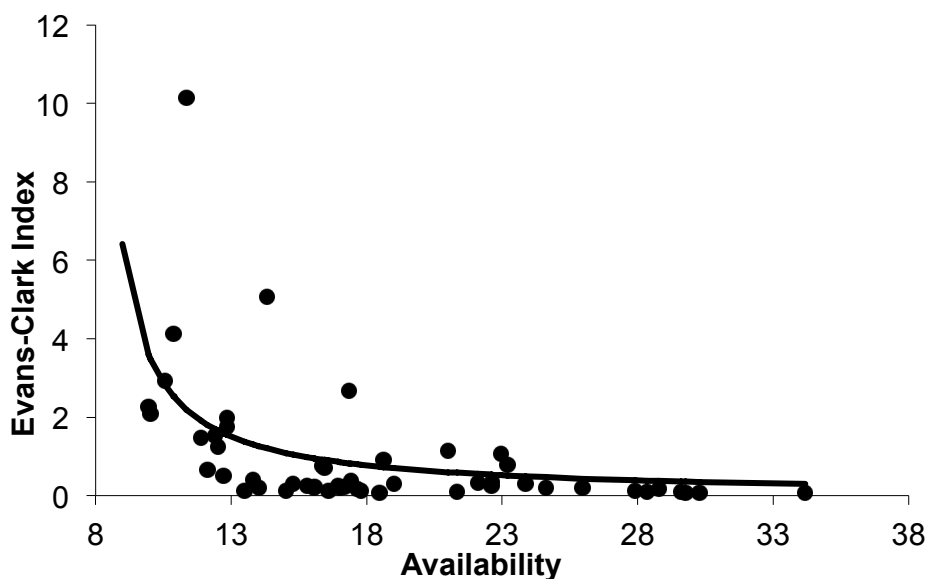


Figure 4.3.6. Evans-Clark R-ratios as a function of average predicted availability (raises per day) for daily vessels fishing 2011-2012 when three or more other vessels were

fishing simultaneously, $R\text{-ratio} = \frac{1}{666.27(1 - e^{-0.00019 * (Y\text{raises} - 7.57)})}$.

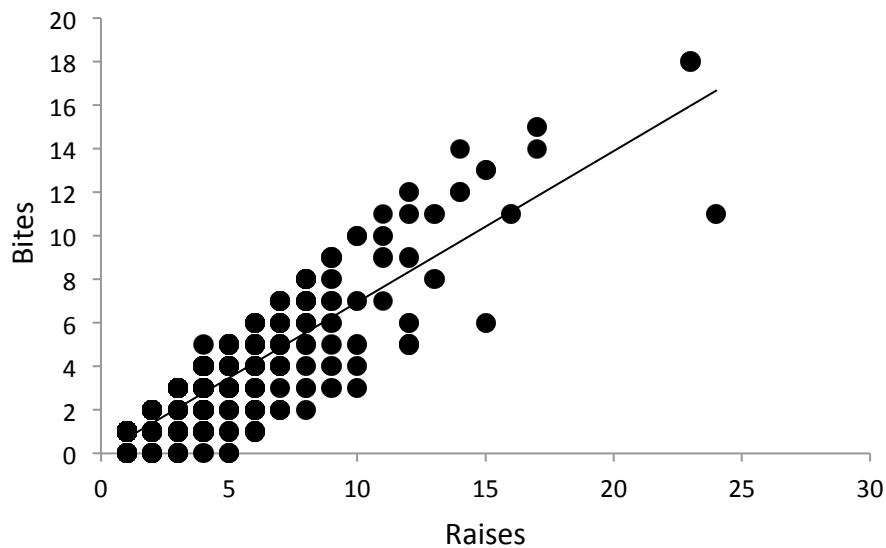


Figure 4.3.7. Estimation of catch efficiency per hour, Q_b as a linear function of bites with respect to raises (discrete). Bites = $0.6948 \cdot \text{Raises}$ with an R^2 of 0.754.

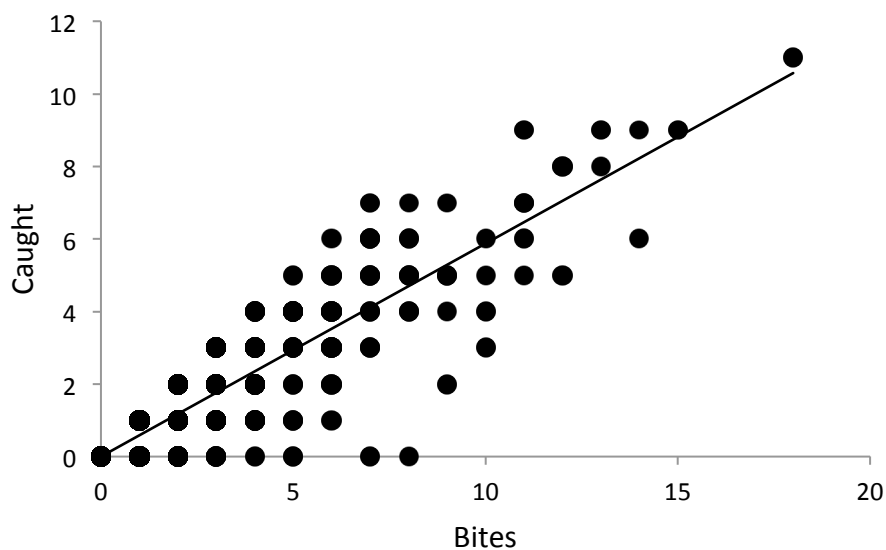


Figure 4.3.8. Estimation of catch efficiency per hour, Q_c as a linear function of caught and released fish (discrete) with respect to Bites. Caught = $0.5875 \cdot \text{Bites}$ with an R^2 of 0.60.

Vessel Aggregation Effects on Catch Efficiency, Q

935 hours of fishing time from 144 days for which conventional tackle was used exclusively were used in analyzing catch efficiency. Figure 4.3.9 depicts in color logarithmic scale differing aggregation values on the upper and lower sides of the average Q_b trendline. Binomial logit curves for predicted catch efficiencies were estimated as a function of aggregation with parameters a and b for Q_b ($a = 0.41$, $b = 2.00$) and Q_c ($a = 0$, $b = 1.93$) and shown in Figure 4.3.10 and 4.3.11, respectively. Standard errors for Q at levels of aggregation are fitted as a power function (Figure 4.3.12). These figures depict an increase in per capita catchability given average distance from other vessels. While aggregating with other boats may facilitate searching for fish to raise, per capita catchability is adversely effected due to vessel interference.

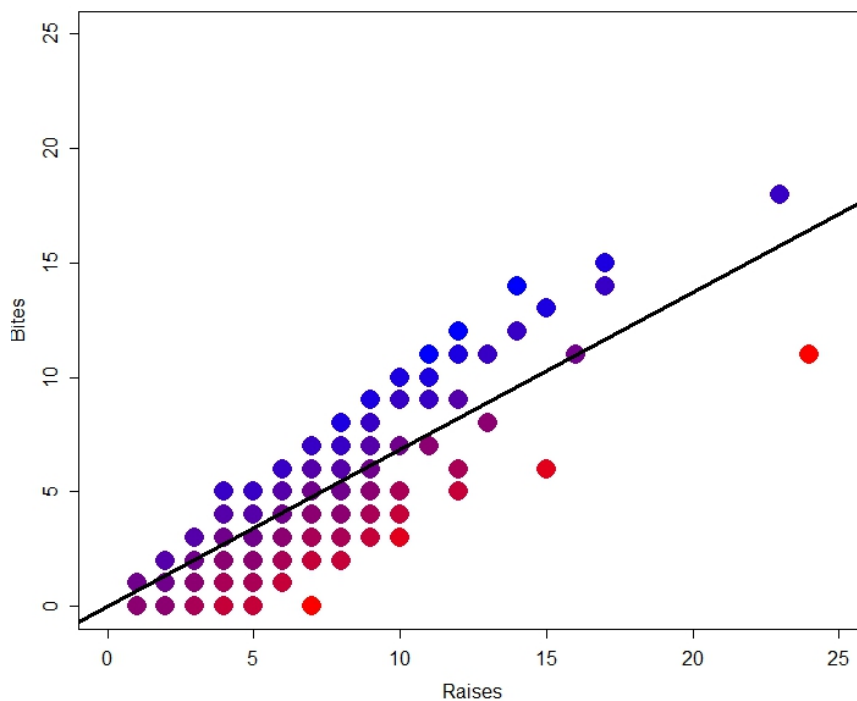


Figure 4.3.9. Relationship of Bites as a function of Raises with discrete points colored relative to natural log scale of aggregation (red = low τ , blue = high τ).

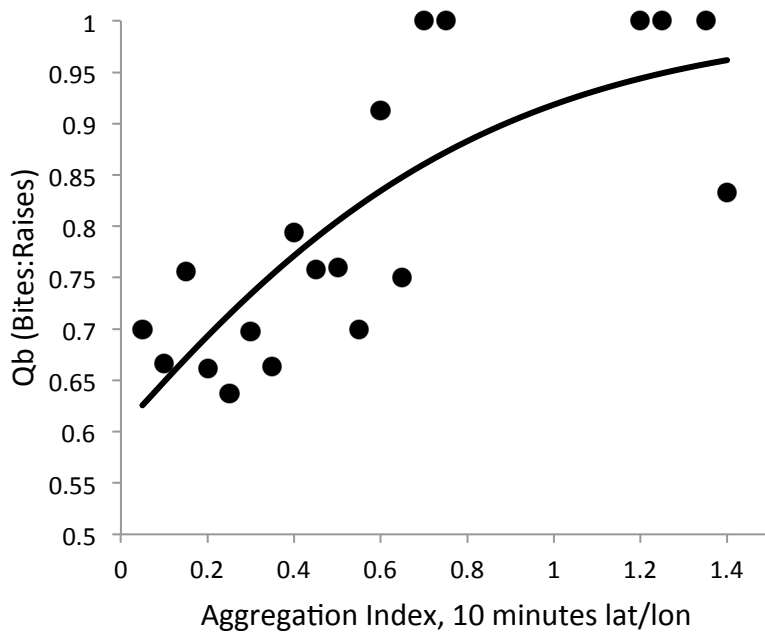


Figure 4.3.10. Estimated Q_b as a function of aggregation, τ

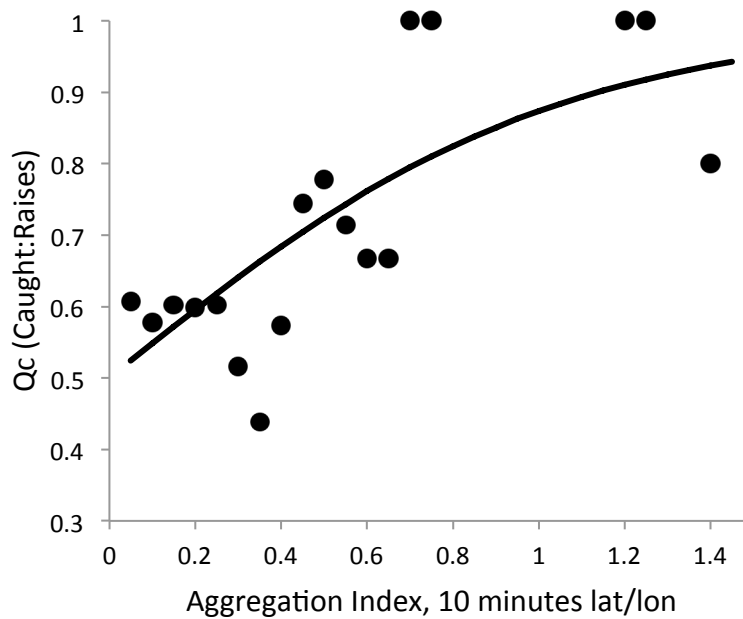


Figure 4.3.11. Estimated Q_c as a function of aggregation, τ

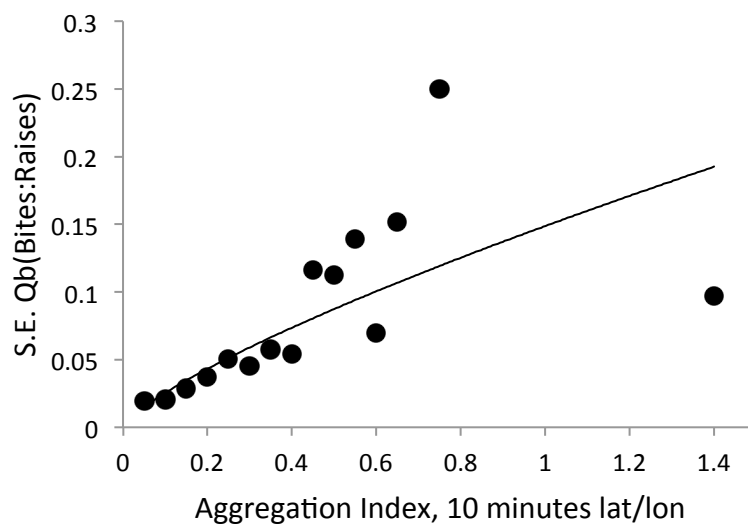


Figure 4.3.12. Standard error of Q as power function of aggregation, τ , $y=0.15\tau^{0.77}$, $R^2=0.75$.

Ocean Circulation and Interannual Availability to Recreational Fisheries

Plotting NEC indices with a five year lag, year 5 year-class strength, and catch per trip as standardized indices, Figure 4.3.13 depicts a shared trend and signal among the three variables, particularly between the five-year lagged NEC index and the year 5 strength index ($R^2=0.48$).

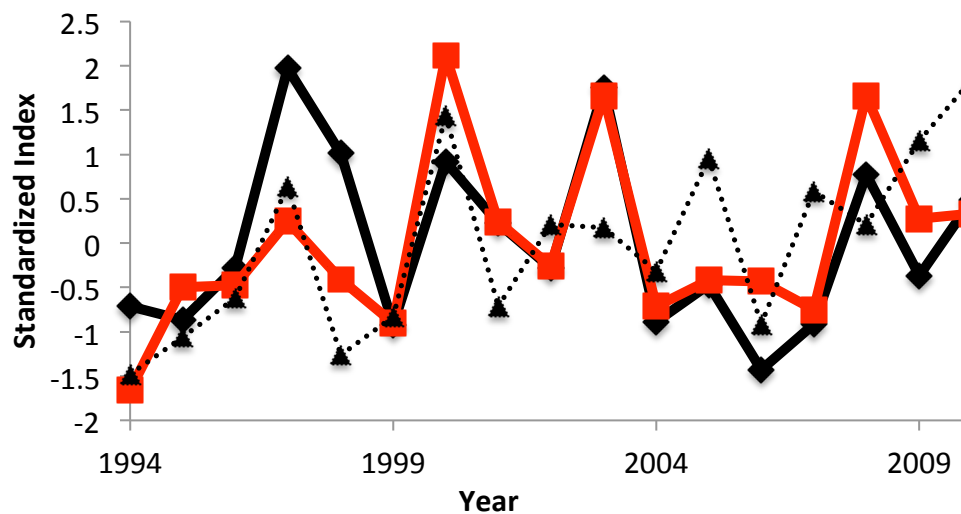


Figure 4.3.13. Plotted time series of standardized indices (mean = 0, standard deviations=1) of five-year lagged NEC (solid black), catch per day (dashed black), and year 5 strength (solid red).

To predict year 5 strength (recruitment) as a function of NEC and MEI, a multiple regression model is fitted with variables (Table 4.3.2) NEC at t-5 and MEI explaining availability of year 5 fish to recreational fisheries. The regression yielded a multiple R^2 of 0.66 and predicted year 5 recruitment values that fall close to estimated values of year 5 strength (Figure 4.3.14).

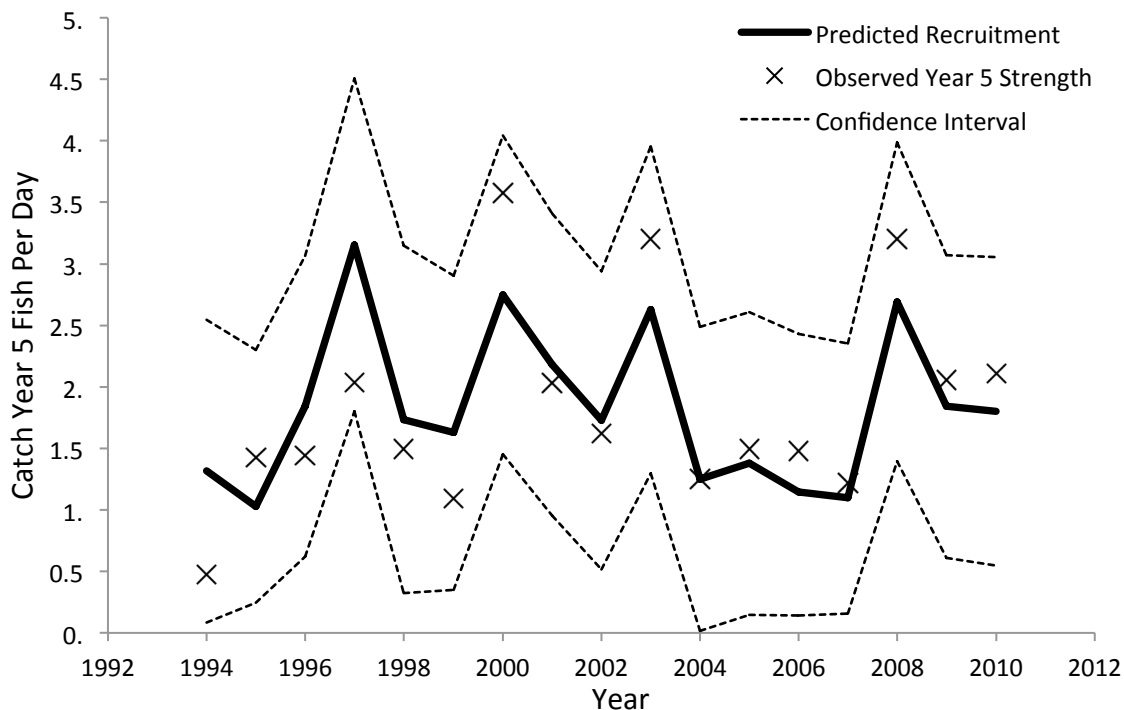


Figure 4.3.14. Predicted recruitment of age 5 sailfish by year as a multiple regression of NEC lagged 5 years and MEI at present with 95% CI (multiple $R^2=0.66$)

Table 4.3.2. ANOVA table of a multiple regression model predicting recruitment of year 5 sailfish as a function of NEC lagged 5 years and MEI at present.

Component	Df	Sum Sq	Mean Sq	F value	Pr(>F)
NEC at t-5	1	4.17	4.17	15.82	0.0022
MEI at t	1	1.5	1.5	5.69	0.0362
Residuals	11	2.9	0.26		
Total	13	8.57			

4.4 Discussion

Catch Efficiency of Recreational Fishing Operations

The satellite logbook system used in this study automatically records time and position to monitor the distribution of fishing effort and to quantify fishing success relative to spatio-temporal ocean conditions. This allowed measurement of the effects of vessel crowding on catch rates. Vessel movements and decisions on where to fish are often dependent on local resource availability, knowledge of which is derived from experience and anecdotal knowledge shared among captains in a recreational fleet. The daily degree of vessel aggregation (R-ratio) relative to daily target fish availability estimated as fish raised per day fishing (Figure 4.3.6) show that fishermen could be categorized as dispersed relative to distance traveled in days when they found lower fish availability, while vessel crowding is significant relative to distance traveled on those days in which local resource availability found by the fleet per day is higher. Fishing vessels readily communicate with one another as a *quid pro quo* relationship such that fishermen know where others are successfully catching fish. Fishermen have access under different platforms (e.g. contracted services or directly from internet websites) to oceanographic data that could help improve catch rates. Prior day's trip results are also incorporated into decision making regarding where to go next.

Recreational fishermen may be fishing under conditions similar to an ideal free distribution (IFD) or ideal free behavior (IFB). In the animal kingdom, an IFD is a situation in which foraging animals select habitat and distribute themselves to maximize biological fitness (Fretwell and Lucas 1972). That is, the encounter rate of a predator with its prey is proportional to the distribution and availability of the prey within an area. In

the case of fishermen (the catch and release predator), they are maximizing their opportunities of raising and subsequently catching as many target fish as possible by aggregating with respect to patches of many available fish within their daily range. Assuming the fishermen have abilities to hone in on billfish locations within their daily vessel range, fishing success is maximizing the number of fish caught by day's end, but with tradeoffs on travel distance (and consumables like fuel) and the risk of vessel interference. An IFD assumes that over relatively short time periods catch rates will be relatively constant and fishing success will be equal among entities as they position and disperse themselves relative to the distribution of a resource. Under free access, competition increases as the number of entities compete for a fixed amount of resource, thus driving down per capita success (Holt, 1985). In situations in which success is not equal among individuals and in which populations are open, entities may still be following ideal free behavior which makes catch rates actively approach equilibrium (Holt and Barfield, 2001).

The principle of IDF has been used to explain fishing effort distribution relative to a resource (Gillis et al, 1993) and cost associated with implementing effort (Gillis and van der Lee, 2012). Gillis and Peterman (1998) modeled interference between fishing entities by increasing nominal effort and density of fishing entities under scenarios of IFD. They found that catchability was grossly impeded by increased and aggregated fishing effort and concluded that catch-per-unit effort indices may not be proportional to resource abundance without considering effort densities and precise effort estimation. Similar cases are found in the literature on passive gear density effects on catchability (Ehrhardt and Deleveaux, 2009).

In the case of recreational fisheries, a satellite logbook system allows estimation of vessel aggregation effects on catchability or catch efficiency. Existing studies of recreational fishing effort and capacity increases in controlled populations of fish have also found deleterious effects on catchability due to competition and interference. Hook-and-line sportfisheries may be considered either active or passive gears depending on the searching nature of the sportfishers. Figure 4.4.1 exhibits the relationship between the numbers of competing hook-and-line sportfishing effort units (anglers or anglers per hectare) versus ensuing catchabilities in four contained freshwater systems. In each of these four cases (walleye in Lake Oneida, NY, largemouth bass in a stocked impoundment, rainbow trout in Mt. Mitchell, NC, and California brown trout in a stocked stream), the area of impoundment, the stocked abundance and density of fish, and fishing effort is completely known. In each of these four cases, catchability is reduced exponentially with an increase in density of competing fishers (Figure 4.4.1). An exponential function is fitted to show the apparent reduction in catchability with respect to fishing capacity. This pattern may be of great concern to those intending to sustain high catch rates within a sportfishery.

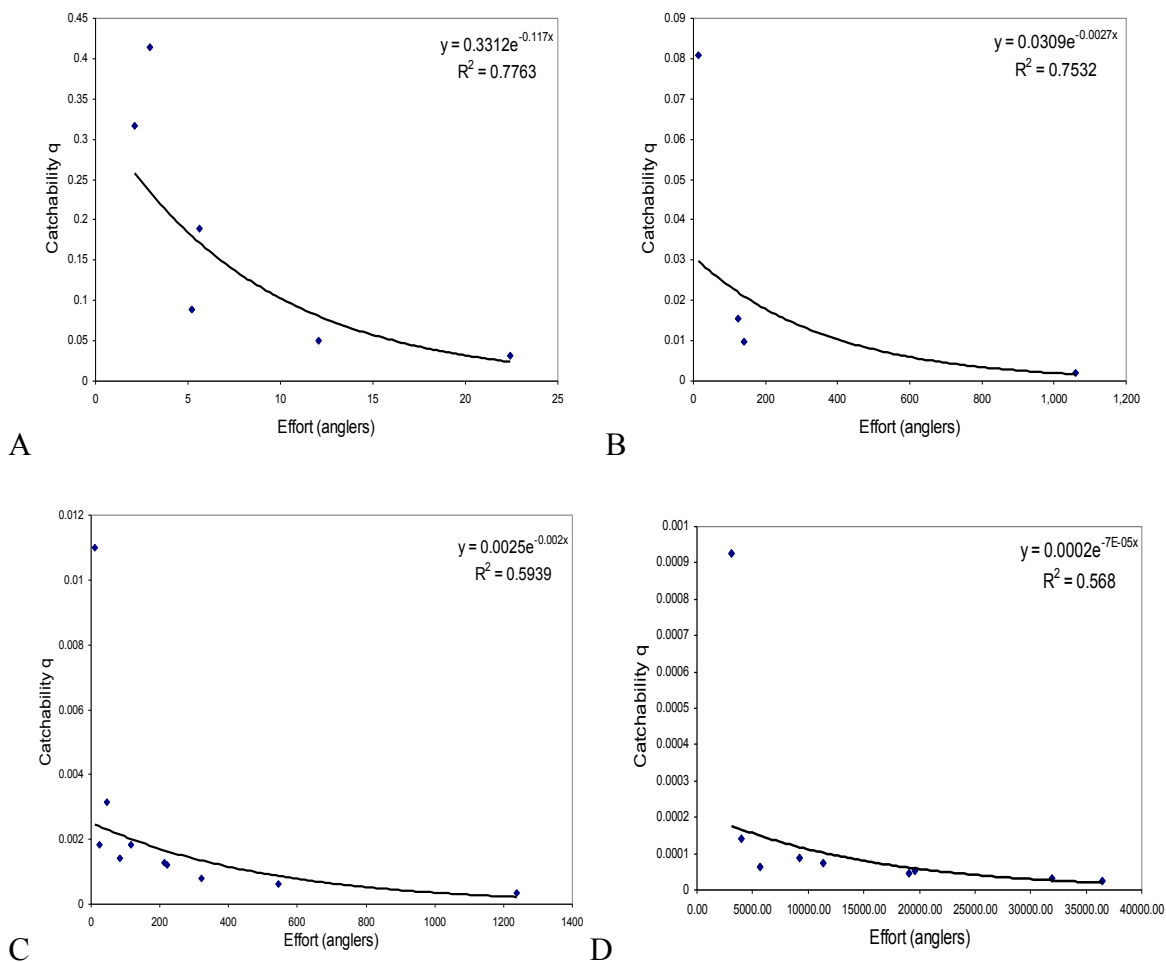


Figure 4.4.1. Catchability versus sportfishing effort capacity in four controlled scenarios in which stock size, effort, impoundment area, density, and catch are known. Data provided is from: A) Walleye Lake Oneida, NY (DeWalk et al, 2005), B) Largemouth bass (Issak et al, 1992), C) Rainbow trout Mt. Mitchell, NC (Ratlidge and Cornell, 1952), D) California brown trout (Vestal et al, 1954; Butler and Kabel, 1959).

Considering Gillis and Peterman (1998) model of vessel interference on catchability, the satellite logbook system generated data that allowed us to analyze vessel interference on catch efficiency. Both Q_b and Q_c expressed as a logit function of aggregation (Figures 4.3.10 and 4.3.11) show that higher aggregation of fishing vessels

have effects on Q_b and Q_c . Like the conclusion of Gillis and Peterman (1998), increasing local fishing intensity would exacerbate vessel crowding, which would negatively impact catch efficiency. For example, billfish recreational vessels move in large, erratic sweeps in any direction when a fish is raised to the surface depending on the behavior of the fish. At this time the crew is involved in multiple tasks like ensuring that the client hooks the teased fish while making sure that navigation is following a proper course with respect to the fish and the other vessels immediately in the neighboring area. If more boats are in close proximity, the vessel may not be operated optimally for catching the fish. Additional vessel noise and fishing activity at the surface may also impact fishing efficiency by causing fish behavior to be more skittish and reticent to pursue baits.

Seasonal and Inter-annual Billfish Availability to Recreational Fisheries Due to Ecosystem Forcing Dynamics

Along the Central American Pacific coast Sailfish are dynamically coupled to ecosystem forcing due to habitat compression affecting distribution of prey species (Ehrhardt and Fitchett, 2006). This unique ecosystem forcing is generated in the region due to wind-driven upwelling as a consequence of seasonal gap winds passing across the Central American Isthmus from the Caribbean and Gulf of Mexico (Wyrski, 1964, 1965, 1966, 1967; Bakun, 1999). The combined effects of wind and Coriolis forcing creates a high frequency of eddy formations that increase productivity in the pelagic environment, including prey for billfishes and tunas (Bakun et al, 1999). These processes operate in synergy with the surfacing of the dissolved oxygen minimum layer that forces the envelope of oxygenated surface waters to be compressed near the surface, thus rendering

predators and prey species vulnerable to capture in fisheries (Ehrhardt and Fitchett, 2006).

Our analyses showed that surface height (SSH) is the most important variable driving seasonal sailfish availability while resultant zonal geostrophic currents were found to be favorable to increased catch rates on the daily level. Sea surface height has been used as a proxy for water circulation, perturbations along the water column, and upwelling (Wyrki, 1974). Satellite-derived sea surface height data is used to calculate ocean circulations and eddy movements (Stammer, 1997, 1998), while serving as a predictor for chlorophyll and primary productivity (Chelton et al, 2011), and can be used to detect eddies not easily identified by most satellite derived products (Mason et al., 2014). Along with SSH, variance in sea surface temperature and upwelling can also explain seasonal differentiation in the availability of those fish resources that are linked to prey compression, such as the sailfish (Figure 4.3.12). These oceanographic features contribute significantly to the surfacing of dissolved oxygen poor deeper waters, which is common in eastern boundary current regions (Bakun et al., 1999). It has been suggested that most commercial pelagic fishery resources found in these DO deprived regions would not inhabit parts of the water column where DO is 1 mL/L or less. Therefore, a minimum DO depth in which dissolved oxygen is 1 mL/L in concentration (Figure 4.4.1) appears to be a distributional boundary. These conditions are especially prominent off the coasts of Central America where recreational fishing operations for billfishes are most productive. Transport of upper ocean dissolved oxygen is often dictated by zonal current regimes in the eastern tropical Pacific (Stramma, 2010, Figure 4.4.2). The northern equatorial countercurrent (ECC) and northern equatorial current (NEC) transport waters

richer in dissolved oxygen into and out of the eastern tropical Pacific, respectively (Stramma, 2010).

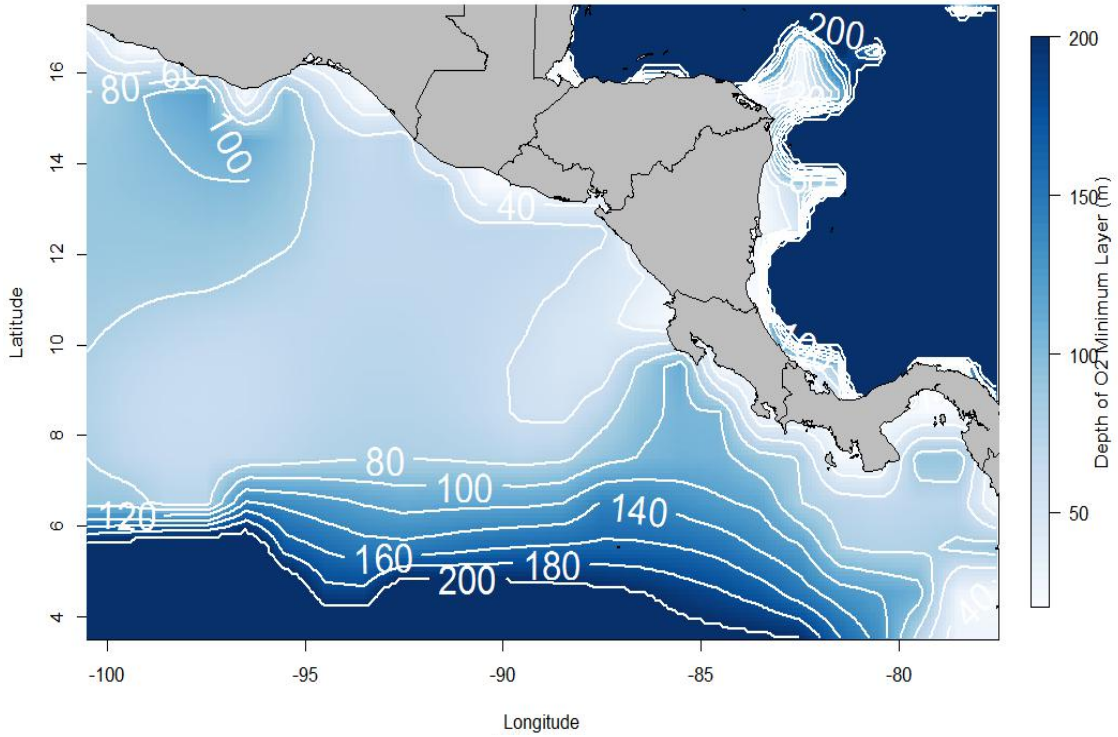


Figure 4.4.2. DO minimum depth (in meters) color shaded in blue hues (deeper) to white (shallower) in the eastern tropical Pacific. Data from World Ocean Atlas 2013, processed in R.

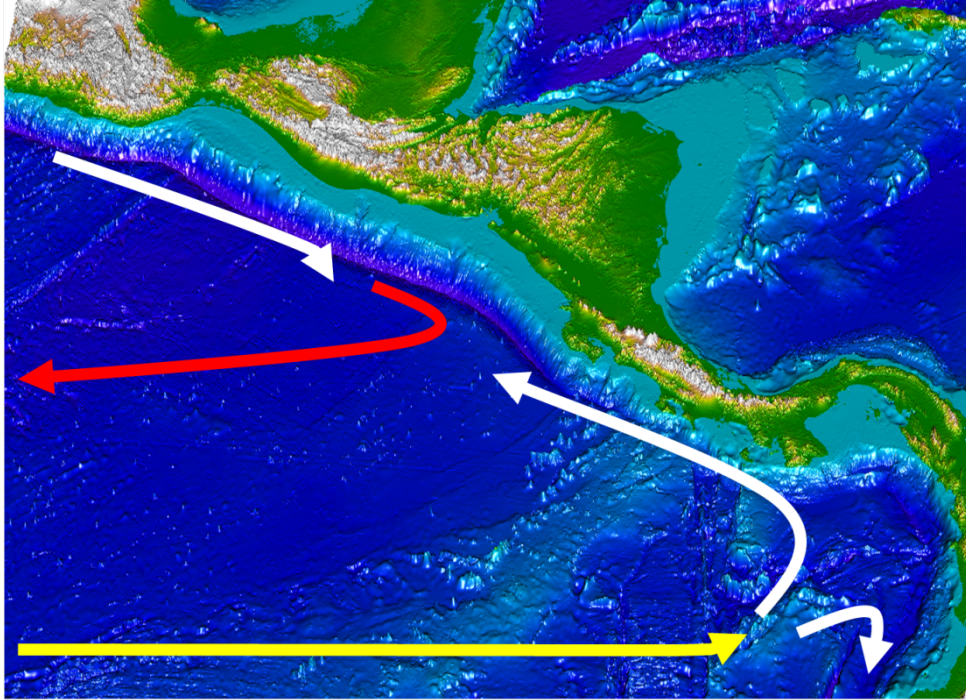


Figure 4.4.3. Illustration of the northern equatorial current (red) and equatorial countercurrent (yellow) with bathymetry of the eastern Pacific basin. Currents in white represent coastal currents, including the Costa Rican Current and California Current,

Analyses suggest that strong zonal currents in the eastern tropical Pacific are likely linked to successful larval sailfish recruitment in certain years that will show as recruits of age 5 in the recreational fisheries five years following strong zonal current events. Conversely, poor cohort abundances are observed five years after a weak zonal current is observed. This is notably linked to the northern equatorial current (NEC) which prevails zonally along latitudes where recreational fishing operations are highest (8°N to 15°N). Forced cyclonic eddies result due to intense zonal currents, which create retention mechanisms favorable to spawning success (Bakun, 2006). Zonal current intensities also drive the formation of eddies which act as prime retention mechanisms and sources of food for marine fishes of varying ages (Bakun, 2006). Figure 4.4.3 shows a time period

of intense NEC and ECC with resulting eddies while Figure 4.4.4 depicts a period of low zonal currents and. Bakun (2006) also suggests that resulting fronts and eddies provide much needed resources for young fishes, but also serve as predator pits where a tradeoff is high mortality for the prey. Cyclonic eddies were found to be prime spawning and retention mechanisms favorable to sailfish off the Florida Current (Richardson et al., 2009) and the mechanism is plausible in the eastern Pacific as well. Success of spawning and recruiting into the fishery as adults is probably dependent on these physical resource retention mechanisms. The intensity of the NEC may serve as a proxy of these processes which drive recruitment of sailfish in the eastern tropical Pacific as demonstrated by the strong correlation between NEC and recruitment. Large scale environmental proxies are often used to predict or estimate recruitment: yellowfin tuna, skipjack tuna, and albacore recruitment are well known to show sensitivity to interannual southern El-Niño Southern Oscillation (ENSO) and Pacific Decadal Oscillation (PDO) indices (Lehodey et al, 2002). Therefore, given knowledge of biological oceanographic dynamics propitious to recruitment, the relationship between northern equatorial currents and success and failure of year 5 sailfish entering recreational fisheries may be biologically significant.

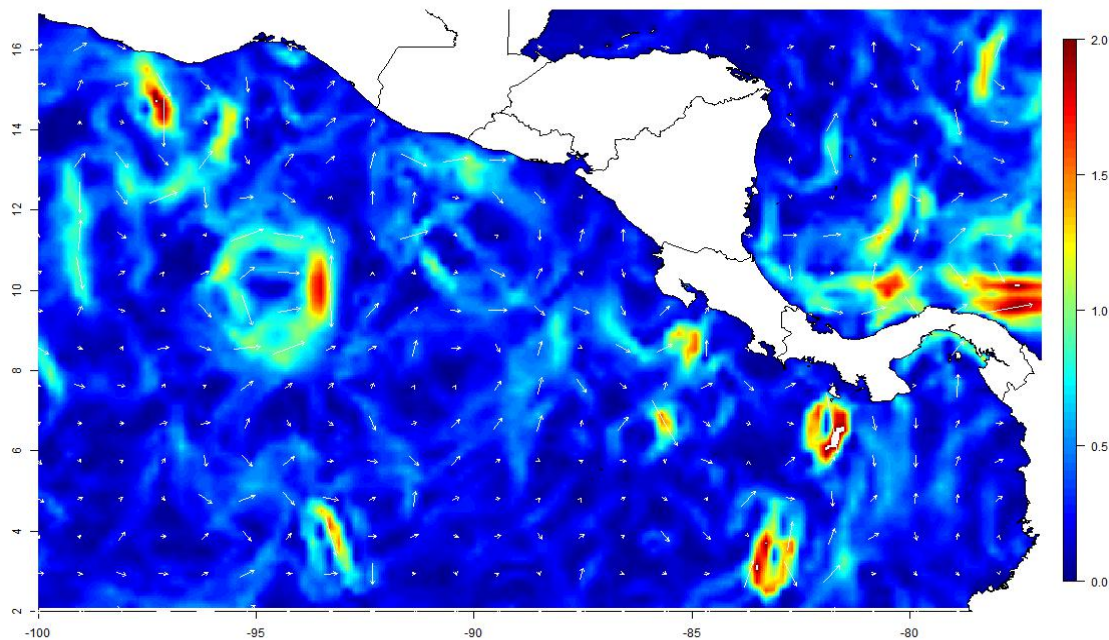


Figure 4.4.4. Geostrophic currents and eddies during a period of high zonal currents.

Data: AVISO, January 2010

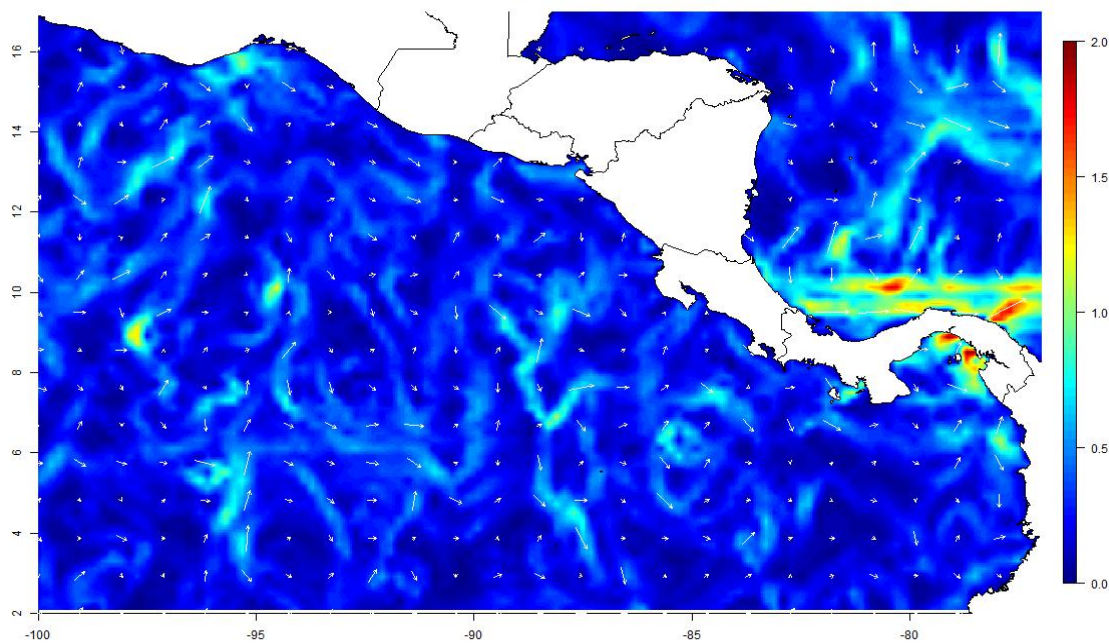


Figure 4.4.5. Geostrophic currents and lessen eddies during a period of low zonal currents. Data: AVISO, June 2010

Chapter 5

Conclusions

The Inter-American Tropical Tuna Commission (IATTC), failed in their 2013 attempt to assess sailfish, for the following reasons: inability to derive parameters from model results used to make determinations of management benchmarks, lack of contrast in indices of abundance in years used to assess the species (1994-2009), data were insufficient for an assessment using the standard stock assessment model -- Stock Synthesis, and significant levels of unreported catch which make assessing the stock unlikely using a surplus production approach (Hinton and Maunder, 2013). The assessment also assumed a natural mortality of $M=0.5$ and growth coefficients from Cerdenares-Ladrón et al. (2010) that yielded an L_{∞} of 180 cm EFL (176-186cm confidence interval) whereas 30-40% of length-frequencies from purse seine fisheries throughout the entire region exceeded the asymptotic length. While the studies directly observing of size-at-age groups and estimating growth parameters in local regions are valid in their findings, their application to the entire habitat range of the species distribution or stock may not be viable.

Analyses presented in Chapter 2 found geographical size stratifications of sailfish throughout the eastern tropical Pacific Ocean which may indicate movement throughout ontogeny. In the absence of hard parts to determine fish age, alternative methods for estimating growth parameters through analyzing mixture distributions of length-frequencies are offered. Assumptions of variance of size at age for mixture distribution analyses were tested on partial regional data of directly observed length at age data and

proportion of ages provided by Cerdenares-Ladrón et al. (2010). Analyses on ecosystem-wide length frequencies suggest that variability of size at age distributions follow a constant coefficient of variation (CV). An improved growth equation was offered in Chapter 2 with an L_{∞} of 207.46 cm EFL, K equal to 0.37 yr^{-1} , and -0.002 years for t_0 with a CV equal to 10.1%. The value estimated for K is similar to the one estimated by Cerdenares-Ladrón et al. (2010) with an L_{∞} and mean size at age that resemble those from an alternative back-calculation estimates offered by Cerdenares-Ladrón et al. (2010). Data from IATTC purse seine length-frequencies yielded only 4% of total observations to be greater than the new L_{∞} . Improvements in growth parameters rendered an opportunity to estimate mortality and met the need to partition a comprehensive database of length-frequencies for sailfish in the region into age classes by year.

In the absence of complete landings and effort data from many fisheries exploiting sailfish in the eastern Pacific Ocean, this Dissertation offers an algorithm to build a numerical solution for age-length keys (ALKs), which are probabilities of age at length, to partition any given observed length frequency into ages and to estimate mortalities. ALKs traditionally require direct observation of age and length of animals through biological sampling. Often due to budget constraints, time, and manpower-building ALKs from biological sampling is not feasible. In Chapter 3 an algorithm is introduced, called Statistical Age-Length Key (StALK), to estimate ALKs from an opportunistic length frequency database that is representative of the stock. The StALK algorithm requires a dependable growth equation (either with a variance-covariance matrix or with mean/standard deviations for size at age) and some knowledge of selectivity/availability which can be estimated from length-frequencies. The novelty of

this new StALK method is that it projects individual size at age groups from assumed known size at age distributions assuming fish are predisposed to grow larger or smaller relative to a fixed growth deviance. Thus StALK has individuals progressing in size at age according to a predisposed growth trajectory. This predisposed growth deviance is seeded in all individuals at age 0 in the algorithm as a deviance score from mean size at age (z-score). As individuals progress in age, they maintain their predisposed growth deviance(z-score) and fall within sizes that correspond with their seeded deviances (or z scores) relative to mean size at age. Fish are removed from the population due to size-specific exploitation and size at age distributions are altered due to mortality processes. StALK adjusts age-specific parameters accounting for mortality and recruitment signals by fitting resulting length-frequencies to observed length-frequencies. StALK's limitations and capabilities were shown by testing it with simulated series of resulting ALKs from fisheries under varying levels of exploitation, recruitment, and error in inputs of mortality and selectivity/availability. StALKs performed well in most simulated instances achieving equality in total mortality estimates among 94% of StALK estimates and simulated ALKs in two 34 year runs, and lost some accuracy in some scenarios in which recruitment varied as much as 30%-40% in consecutive years. Applying StALK to simulated fisheries in which recruitment varied +/-20% found that resulting age distributions are statistically equal even with considerable misspecification error in selectivity inputs (logistic: -10% to +31% error in logistic rate, -7% to +14% error in logistic midpoint, knife-edge: -28% to +4%) and growth inputs (-7% to +16% error in L_{∞}). Mortality estimates for sailfish in the eastern tropical Pacific estimated with age compositions in landings generated by the StALK algorithm follow a similar trend as

other methodologies to estimate mortality with growth parameters- including length-based methods (Beverton and Holt, 1954; Ehrhardt and Ault, 1992) and deterministic length-converted catch curves (Pauly, 1983). However, this approach builds an ALK which can determine total proportions of complete age classes in a length frequency sample, in this case the purse seine fishery. For the first time, sailfish can be assigned an annual mortality rates and age compositions in the eastern Pacific.

Estimates of mortality for sailfish in the eastern Pacific Ocean exceed a mortality benchmark, $F_{0.1}$, which is a precautionary level of fishing mortality in the context of growth overfishing (Gulland and Boerema, 1973), for all but two years in data analyzed from 1991 to 2010. This suggests that sailfish are experiencing overfishing for most of the years analyzed.

Age 5 sailfish is the first fully recruited age class in the tuna purse seine fishery and the predominant age class found in recreational fisheries in Guatemala. In Chapter 4, annual CPUE indices from Guatemala recreational fisheries multiplied by the proportion of age 5 sailfish estimated by StALK for fish caught in the purse seine fishery offers an index for an age 5 year class strength available to recreational fisheries. This age 5 recruitment strength index carries a statistically 5-year delayed signal with the northern equatorial current index (NEC) during winter months when the index peaks and when sailfish catch rates are highest. Intense NEC and equatorial countercurrent (ECC) indices are indicative of intense zonal current movement which bring about eddies. These ocean features serve as mechanism that feed the ‘ocean triad’ mechanisms described by Bakun (1998). These mechanisms include enrichment of the upper ocean for productivity,

concentration of prey and food for fishes, and retention mechanisms conducive to survival of recruits and successful introduction year classes to a fishery (Bakun, 1998).

Ecosystem forcing in the eastern Pacific makes sailfish and other billfishes susceptible to exploitation, but also creates conditions favorable to high catch rates in recreational fisheries. Analyses of CPUE on varying temporal resolution scales found that encounter rates with sailfish in recreational fisheries are driven by zonal geostrophic currents and altimetry. Sailfish are raised by recreational vessels at higher rates when these features create convergence transition zones directly within daily fishing range.

Georeferenced fishing effort and catch data were collected in the first ever billfish satellite logbook system for recreational fishing and implemented on recreational fishing boats in Guatemala and later in southern Costa Rica. Encounters with sailfish and other billfishes were logged, georeferenced, and timestamped. These encounters are fish raised by the fishing vessel, the number of raised fish that bit the baits, and the number of fish successfully caught of those that bit the baits. Fishing vessel, crew, and angler abilities contribute to fishing success but the fleet density relative to searching distance and to other fishing vessels impacts the rate of success and detection of sailfish. On days of higher availability of sailfish in which more fish are raised per boat, fishing vessels are typically clustered in hot spots where the average distance from other vessels is smaller than the distance traveled from port to search for fish. Data from satellite logbook systems suggest that fishing vessels are operating with respect to aggregation of the resource and can hone in on sailfish densities- however a tradeoff and risk exists from maintaining a distance too close to other boats despite the high densities of fish present. Catchabilities of raised sailfish are adversely impacted by vessel aggregation. This can

negatively impact the daily fishing success of a recreational fishing fleet, despite high availabilities. It can be inferred that increasing fishing intensity or fleet capacity could possibly further impede fishing success.

Recommendations and Future Work

Given that sailfish are bycatch in large-scale, highly politicized tuna fisheries and targeted in artisanal fisheries in several developing countries- collecting reliable catch and effort information for sailfish is quite difficult. Recreational fisheries in the region exclusively target sailfish and other billfishes and rely on sailfish as an economically important resource. Hundreds of thousands of sailfish are raised by sportfishing vessels annually off Central America and a portion of those fish are caught and released. Comprehensive collection of recreational fishing effort, encounters with billfishes, and catches is currently underway. This information on regional scales can provide information to infer regional availability and assess recreational fisheries relative to local habitat. As demonstrated in this Dissertation, georeferenced data on catch and effort is important to assess recreational fisheries with respect to oceanographic conditions and vessel dynamics. While satellite logbook systems may be costly, mobile technologies with GPS capabilities are more widely available and decreasing in price- rendering the use of ‘apps’ on mobile devices.

This work was able to add to our understanding of sailfish population dynamics by providing an improved growth equation and by estimating fishing mortality of the sailfish stock in the eastern tropical Pacific. However, significant gaps in the understanding of the stock still persist, such as abundance. Billfish length frequencies

from recreational fisheries do not currently exist. Means to electronically measure lengths of sailfish and other billfishes using mobile technologies without bringing animals out of the water are necessary since billfish are seldom removed from the water in recreational fishing. Automated image processing of photos collected through mobile devices using FiLeDI algorithm can be used to measure fish lengths quickly (Norhaida Abdullah et al., 2009) and has proven to be an inexpensive and accurate method to measure fish lengths (Shafry et al., 2012). This can be used to estimate size of billfishes caught and released by recreational fisheries on a routine and widespread basis to monitor the status of the stock available to recreational fisheries.

Information on the early life history, spawning behavior, and seasonality of maturation of billfish are either lacking or equivocal in nature (Eldridge and Wares, 1974, Hernandez-Herrera et al., 2000, Ramirez Perez et al., 2011). Comprehensive information on the location and peak seasonality of mature female billfish throughout the entire region is needed to draw direct conclusions on spawning behavior and specific ecosystem conditions propitious to spawning. Growth of young billfish, particularly sailfish, is virtually unknown in the region. Age 1 sailfish are rare in direct age observation and information on the growth of juvenile fish in the eastern tropical Pacific is absent. However, the importance of circulatory regimes which form eddies throughout the eastern Pacific driving recruitment of sailfish (as shown in Chapter 4) can be an impetus to test hypotheses regarding the presence of larval and juvenile sailfish utilizing eddies as retention and food mechanisms.

Information on migration patterns and empirical estimation of mortality of sailfish is needed. Tagging of billfishes in the eastern tropical Pacific with conventional spaghetti

tags has been unsuccessful at drawing inferences on long-term migrations, mortality, and growth rates. Much of this is due to the lack of returns, unknown reporting probabilities, and poor quality of data in the few returns reported. However, the implementation of satellite tagging can provide important continuous information of movement and behavior.

Lastly, this Dissertation offers a new methodology, StALK, to estimate ALKs for sailfish in the eastern Pacific with the goal to partition length frequencies into ages. However, further application and research using this methodology is warranted. Testing of StALK through further simulations of stocks with varying longevities, differing growth parameter relationships, and varying length sampling strategies could further test the efficiency of StALK and glean ways to improve the new methodology. As demonstrated by application to two vastly different red snapper fisheries, successfully estimates expected age frequencies from large length frequency databases, but fails to produce age frequencies from ALKs in another fishery of the same species that does not have expansive length-frequencies or known selectivity. Further testing with other species will possibly reveal ways to improve the algorithm, but most importantly, it may also render support in assessing other species.

References

- Aires-da-Silva, A., Maunder, M.N., Schaefer, K.M., Fuller, D.W. 2014. Improved growth estimates from integrated analysis of direct aging and tag-recapture data: an illustration with bigeye tuna (*Thunnus obesus*) of the eastern Pacific Ocean with implications for management. *Fisheries Research*.
- Alvarado-Castillo, R., Felix-Uraga, R., 1998. Growth of *Istiophorus platypterus* (Pisces: Istiophoridae) from the mouth of the Gulf of California. *Rev. Biol. Trop.* 46, 115–118.
- Arregúin-Sánchez, F. 1996. Catchability: a key parameter for fish stock assessment. *Reviews in Fish Biology and Fisheries*, 6: 221–242. 07.
- Ault, J.S., Bohnsack, J.A., and G.A. Meester. 1998. A retrospective (1979-1996) multispecies assessment of coral reef fish stocks in the Florida Keys. *Fishery Bulletin* 96(3):395-414.
- Ault, J.S., Smith, S.G., and Bohnsack, J.A. 2005. Evaluation of average length as an estimator of exploitation status for the Florida coral-reef fish community. *ICES J Mar Sci*, 62: 417:423.
- Ault, J.S., Smith S.G., Browder J.A., Nuttle W., Franklin E.C., Luo J., DiNardo G.T., and J.A. Bohnsack. 2014. Indicators for assessing the ecological dynamics and sustainability of southern Florida’s coral reef and coastal fisheries. *Ecol. Indicat.* dx.doi.org/10.1016/j.ecolind.2014.04.013
- Bakun, A. 2006. Fronts and eddies as key structures in the habitat of marine fish larvae: Opportunity, adaptive response and competitive advantage. *Sci Marina* 70 (S2): 105-122.
- Bakun, A. 2006. Wasp-waist populations and marine ecosystem dynamics: navigating the “predator pit” topographies. *Prog in Oceanog* 68: 271-288.
- Bakun, A., J. Csirke, D. Lluch-Belda and R. Steer-Ruiz. 1999. The Pacific Central American Coastal LME. pp. 268-280. In: K. Sherman and Q. Tang (eds.) *Large Marine Ecosystems of the Pacific Rim: Assessment, Sustainability and Management*. Blackwell Science Inc. Malden, Massachusetts. 465 pp.
- Baranov, F.I .1918. On the question of the biological basis of fisheries *Izvestiya*, 1: 81–128. (Translated from Russian by W.E. Ricker, 1945)
- Bartoo, N. and K. Parker. 1982. Stochastic age-frequency estimation using the von Bertalanffy growth equation. *Coll. Vol. Sci. Pap., Int. Comm. Conserv. Atl. Tunas*, Madrid, Spain (SCRS/81/53), Vol. XVII(1):35-43.

- Bayliff, W.H. 2010. Report of the IATTC observer program Agreement on the International Dolphin Conservation Program. La Jolla, CA.
- Berkeley, S.A., Chapman C., and S.M. Sogard. 2004. Maternal Age as a Determinant of Larval Growth and Survival in a Marine Fish, *Sebastes Melanops*. Publications, Agencies, and Staff of the U.S. Department of Commerce. Paper 429.
- Bendik, A. B., R. G. Bernikov, G. P. Budylenko, Ch. M. Nigmatullin, I. V. Smirnov, N. M. Timoshenko, and G. M. Zakharov. 1987. Report on the Results of the Cooperative Soviet-Nicaraguan Investigations on the Biological Resources in the Maritime Areas of the republic of Nicaragua in 1986. Scientific Institute for Fisheries Research and Oceanography of the Atlantic Ocean (AtlantNIRO). Ministry of the Fishing Industry of the USSR. Kalingrad. 225 p.
- Beverton, R.J.H. and Holt, S.J. 1957. On the dynamics of exploited fish populations. *Fish. Invest. Ser. II, Vol. 19*. 533 pp.
- Bourassa, M. A., L. Zamudio and J. J. O'Brien. 1999. Noninertial flow in NSCAT observations of Tehuantepec winds. *J. Geophysical. Research*, 104, 11,311–11,319.
- Brodziak, J., M.L. Traver, and L.A. Col. 2008. The nascent recovery of the Georges Bank haddock stock. *Fisheries Research* 94:123–132.
- Brothers, E. B. 1980. Age and Growth Studies on Tropical Fishes. In: Saila, S. and Roedel, P. (Eds.): Stock assessment for tropical small-scale fisheries. Intern. Cent. Mar. Res. Management Univ. Rhode Is. 119-136.
- Box, G.E.P. and D.R. Cox. 1964. An analysis of transformations. *Journal of the Royal Statistical Society—Series B* 26(2): 211-252.
- Caddy, J. F. 1979. Some considerations underlying definitions of catchability and fishing effort in shellfish fisheries and their relevance for stock assessment purposes. *Fisheries Marine Service Reports*, 1489, 22 pp.
- Campana, S. E. 2001. Accuracy, precision and quality control in age determination, including a review of the use and abuse of age validation methods. *Journal of Fish Biology*, 59: 197–242.
- Carlson, S.M. and T.R. Seamons. 2008. A review of quantitative genetic components of fitness in salmonids: implications for adaptation to future change. *Evolutionary Applications* 1: 222-238.
- Cerdenares-Ladrón De Guevara, G., Morales-Bojórquez, E., and R. Rodríguez-Sánchez (2011): Age and growth of the sailfish *Istiophorus platypterus* (Istiophoridae) in the Gulf of Tehuantepec, Mexico, *Marine Biology Research*, 7:5, 488-499.

- Chang, Y.-C., G.-Y. Chen, R.-S. Tseng, L. R. Centurioni, and P. C. Chu. 2012. Observed near-surface currents under high wind speeds, *J. Geophys. Res.*, 117.
- Chang, S.-K. and M.N. Maunder. 2012. Aging material matters in the estimation of von Bertalanffy growth parameters for dolphinfish (*Coryphaena hippurus*). *Fisheries Research*, 119–120: 147–153.
- Chelton, D. B., Gaube P., Schlax M. G., Early J. J., and R.M. Samelson. 2011. The influence of nonlinear mesoscale eddies on near-surface oceanic chlorophyll. *Science*, 334: 328–332.
- Cheverud, J., Rutledge J., and W. Atchley. 1983. Quantitative genetics of development: Genetic correlations among age-specific trait values and the evolution of ontogeny. *Evolution*, vol. 37, pp. 895-905
- Chiang, W.-C., Sun, C.-L., Yeh, S.-Z., 2004. Age and growth of sailfish (*Istiophorus platypterus*) in waters off eastern Taiwan. *Fish. Bull.* 102, 251–263.
- Clark, W. G. 1981. Restricted least-squares estimates of age composition from length composition. *Can. J. Fish. Aquat. Sci.* 38:297–307.
- Clark, P.J. and F.C. Evans 1954. Distance to nearest neighbor as a measure of spatial relationships in populations, *Ecology* 35, 445–453.
- Davies, N., Hoyle, S., and J. Hampton. 2012. Stock assessment of striped marlin (*Kajikia audax*) in the southwest Pacific Ocean. In: *The 8th Scientific Committee of the Western and Central Pacific Fisheries Commission*. Busan, Republic of Korea.
- Deleveaux, V.K.W. 2012. On the Growth and Exploitation Pattern Effects on the Recuperation from Overfishing of the Red Snapper, *Lutjanus campechanus*, in the Gulf of Mexico. Dissertation, University of Miami, 132 pp.
- Deriso, R. 1980. Harvesting strategies and parameter estimation for an age-structured model. *Can. J. Fish. Aquat. Sci.* 37: 268–282.
- Dortel, E., Massiot-Granier F., Rivot E., Million J., Hallier J-P., Morize E., Munaron J-M., Bousquet N. and E. Chassot. 2013. Accounting for Age Uncertainty in Growth Modeling, the Case Study of Yellowfin Tuna (*Thunnus albacares*) of the Indian Ocean. *PLoS ONE* 8(4): e60886. doi:10.1371/journal.pone.0060886
- Ehrhardt, N.M. and J.S. Ault. 1992. Analysis of two length-based mortality models applied to bounded catch length frequencies. *Transactions of the American Fisheries Society* 121: 115–122.
- Ehrhardt, N.M. and V.K.W. Deleveaux. 2006, Interpretation of tagging data to study growth of the Atlantic sailfish (*Istiophorus platypterus*). *Bull. Mar. Sci.*, 79:719-726.

Ehrhardt, N.M. and V.K.W. Deleveaux. 2009. Fishing capacity in a trap fishery for *Panulirus argus*. *Fish Bull* 107:186–194.

Ehrhardt, N. M and M.D. Fitchett. 2006. On the seasonal dynamic characteristics of the sailfish, *Istiophorus platypterus*, in the Eastern Pacific off Central America. *Bull. Mar Sci.*, 79(3) 589-606

Ehrhardt, N.M and M. D. Fitchett 2008. Report to the Government of Costa Rica : Evaluation and recommendations regarding recreational sport fisheries targeting billfishes and their exploitation. In Spanish. *Unpublished report*.

Ehrhardt, N. M and M.D. Fitchett. 2009. Socioeconomic analyses of recreational fisheries in Central America. *Unpublished report*.

Ehrhardt, N.M, and M.D. Fitchett. 2015, *in progress*. A dynamic production approach to estimate mortality in fish populations.

Ehrhardt, N. M., R. J. Robbins, and F. Arocha. 1996. Age validation and growth of swordfish, *Xiphias gladius*, in the northwest Atlantic. ICCAT (International Commission for the Conservation of Tunas) Col. Vol. Sci. Pap. 45(2):358–367.

Eldridge, M. B. and P. G. Wares. 1974. Some biological observations of billfishes taken in the eastern Pacific Ocean, 1967-1970. Pages 89-101 in R. S. Shomura and F. Williams (eds.), *Proceedings of the International Billfish Symposium (Kailua-Kona, Hawaii, 9–12 August 1972)*, Part 2: Review and contributed papers, NOAA Tech. Rep. NMFS SSRF-675.

Evans, D. H. and G. P. Wares. 1972. Food habits of the striped marlin and sailfish off México and southern California. *Fish Wildl. Serv. Res. Rep.* 76: 1–10.

Eveson, J.P., Polacheck T., G.M. Laslett. 2007. Consequences of assuming an incorrect error structure in von Bertalanffy growth models: a simulation study. *Can J Fish Aquatic Sci.* 64:602-617

Fiedler, P. C. 2002. The annual cycle and biological effects of the Costa Rica Dome. *Deep-Sea Res.* 49A: 321–338.

Fredricksson, A 1934. On the calculation of age-distribution within a stock of cod by means of relatively few age determinations as a key to measurements on a large scale. *Rapp. B.-V. Reun. Cons. Int. Explor. Mer* 86: 1 - 14.

Fournier, D. A., Sibert, J. R., Majkowski, J., and Hampton, J. 1990. MULTIFAN: a likelihood-based method for estimating growth parameters and age composition from multiple length frequency data sets illustrated using data for southern bluefin tuna (*Thunnus maccoyii*). *Canadian Journal of Fisheries and Aquatic Sciences* 47, 301–317.

Fournier, D. A., Hampton, J., and Sibert, J. R. 1998. MULTIFAN-CL: a length-based, age-structured model for fisheries stock assessment, with application to South Pacific albacore, *Thunnus alalunga*. *Canadian Journal of Fisheries and Aquatic Sciences* 55, 205-16.

Fretwell, S.D. and H.L. 1970. On territorial behaviour and other factors influencing habitat distribution in birds. I. Theoretical development. *Acta Biotheor* 19:16-36.

Gavaris, S., 1988. An adaptive framework for estimation of population size. *Canadian Atl. Fish. sci. Adv. Comm. (CAFSAC) Res. Doc.* 88/29:1 . 12.

Gentner, B. 2008. Economic Analysis of International Billfish Markets. Gentner Consulting Group, Prepared for the International Game Fish Association. 71 pp.

Gerritsen, H.D., D. McGrath, and C. Lordan 2006. A simple method for comparing age-length keys reveals significant regional differences within a single stock of haddock (*Melanogrammus aeglefinus*). *ICES Journal of Marine Science*, 63: 1096-1100.

Gillis D. M., Peterman, R. M., and A.V.Tyler. 1993. Movement dynamics in a fishery: application of the ideal free distribution to spatial allocation of effort. *Can J Fish Aquat Sci.* 50:323-333.

Gillis, D. M., and R.M. Peterman. 1998. Implications of interference among fishing vessels and the ideal free distribution to the interpretation of CPUE. *Can J Fish Aquat Sci*, 55: 37–46.

Gillis, D. M., and A. van der Lee. 2012. Advancing the application of the ideal free distribution to spatial models of fishing effort: the isodar approach. *Can J Fish Aquat Sci*, 69: 1610 – 1620.

Graves, J. E. and J. R. McDowell. 1995. Inter-ocean genetic divergence of istiophorid billfishes. *Mar. Biol.* 122: 193–204.

Gulland, J.A. 1964. Manual of methods for fish population analysis. FAO. Fish. Tech. Pap. No. 40. 60 pp. Gulland, J.A. 1983. Fish Stock Assessment. A Manual for Basic Methods. New York: John Wiley and Sons. 223 pp.

Gulland, J. A. 1965. Survival of the youngest stages of fish, and its relation to year-class strength. *Int. Comm. N. E. AU. Fish.. Spec. Publ.* 6:363-372.

Gulland, J. A. 1978. Manual of methods for fish stock assessment. Part 95 1. Fish population analysis. *FAO Man. Fish. Sci.* 4. 154 p.

Gulland, J.A. and L.K. Borema. 1973. Scientific advice on catch levels. *Fishery Bulletin* 71(2):325-335.

- Gulland, J.A. 1964. Catch per unit effort as a measure of abundance. *Rapports et Procès-Verbaux des Réunions Commission Internationale pour l'Exploration Scientifique de la Mer Méditerranée*, 155, 8-14.
- Gulland, J.A. 1983. Effort and catch per unit effort. In: *Fish Stock Assessment: A Manual of Basic Methods*. Ch.2, Section 2.3, p.30-53.
- Hall, M.A., N. Vogel, and M. Orozco. 2006. Eastern Pacific regional sea turtle program. Final Report (June 2006). Western Pacific Regional Fishery management Council. 67p.
- Hammers, B.E., and Miranda, L.E. 1991. Comparison of methods for estimating age, growth, and related population characteristics of white crappies. *N Am J Fish Manage* 11:492-498.
- Heath, D.D., Fox C.W. and J.W. Heath. 1999. Maternal effects on offspring size: variation through early development of chinook salmon. *Evolution*. 53(5) 1605-1611.
- Hernandez, A., J. Maradiaga, and A. Seko. 1998. Results of an intermediate shelf exploratory fishing survey. Directorate of Fisheries Development. Ministry of Economy and Fisheries. Government of Nicaragua. 45 p.
- Hernández-Herrera, A., and M. Ramírez-Rodríguez. 1998. Spawning seasonality and length at maturity of sail.sh (*Istiophorus platypterus*) off the Pacific coast of Mexico. *Bull. Mar. Sci.* 63:459-467.
- Hill, K. T. 1986. Age and growth of the Pacific blue marlin, *Makaim nigricans*: A comparison of growth zones in otoliths, vertebrae, and dorsal and anal fin spines. M.S. Thesis, California State Univ., Stanislaus, 107 p.
- Hinton, M. G. and M. N. Maunder. 2003. Methods for standardizing CPUE and how to select among them. IATTC SCRS/2003/034. 11p.
- Hinton, M. G. and M. N. Maunder. 2013. Status of salfish in the eastern Pacific Ocean in 2011 and outlook for the future. IATTC SCRS/2013/SAC-04007c, May 2013. 14 p.
- Hinton, M.G. and Nakano, H. 1996. Standardizing catch and effort statistics using physiological, ecological, or behavioral constraints and environmental data, with application to blue marlin (*Makaira nigricans*) catch and effort data from Japanese longline fisheries in the Pacific. *Bull. Inter-Amer. Trop. Tuna Comm. Bull.* 21: 169–200.
- Holt, R.D. 1985. Population dynamics in two-patch environments: some anomalous consequences of an optimal habitat distribution. *Theoretical Population Biology* 28, 181–208.
- Holt, R. D. and M. 2001 On the relationship between the ideal free distribution and the evolution of dispersal (ed. J. Clobert, E. Danchin, A. A. Dhondt & J. D. Nichols), pp. 83–95. New York, NY: Oxford University Press.

Hordyk, A., Ono, K., Valencia, S., Loneragan, N., and J.A. Prince. 2014. novel length-based empirical estimation method of spawning potential ratio (SPR), and tests of its performance, for small-scale, data-poor fisheries. *ICES J Mar Sci*, doi:10.1093/icesjms/fsu004

ISC, 2013. Stock assessment of blue marlin in the Pacific Ocean in 2013, report of the Billfish Working Group, 13th Meeting of the International Scientific Committee for Tuna and Tuna-like Species in the North Pacific Ocean, Busan, Korea, 17-22 July 2013. 118 pp.

Johnson, D. W., Christie, M. R., Moye, J., and M.A. Hixon. 2011. Genetic correlations between adults and larvae in a marine fish: potential effects of fishery selection on population replenishment. *Evolutionary Applications*, 4(5), 621–633

Jones, C.D., M.T. Judge and M. Ortiz. 1998. Standardization of recreational CPUE for blue and white marlin in the western North Atlantic Ocean 1973-1995. Col. Vol. Sci. Pap. ICCAT, 47: 279-287.

Joseph, J., W. L. Klawe, and C. J. Orange. 1974. A review of the longline fishery for billfishes in the Eastern Pacific Ocean. Pages 309–331 in R. S. Shomura and F. Williams (Eds.). *Proceedings of the International Billfish Symposium Kailua-Kona, Hawaii, 9–12 August 1972. Part 2. Review and contributed Papers.* NOAA Tech. Rep. NMFS SSRF-675.

Kimura, D. K. 1977. Statistical assessment of the age-length key. *J. Fish. Res. Board Can.* 34:317-324.

Kimura, D. K., and S. Chikuni. 1987. Mixtures of empirical distributions: an iterative application of the age-length key. *Biometrics* 43:23–35.

Kirkpatrick, M. 1984. Demographic Models Based on Size, Not Age, For Organisms with Indeterminate Growth. *Ecology* 65:1874–1884

Kleiber P, Hinton MG, Uozumi Y. 2003. Stock assessment of blue marlin (*Makaira nigricans*) in the Pacific using MULTIFAN-CL. *Mar Freshw Res* 54(4):349-360.

Kopf R.K., Drew K, and R.L Humphreys Jr. 2010. Age estimation of billfishes (*Kajikia* spp.) using fin spine cross-sections: the need for an international code of practice. *Aquat Living Resour* 23:13–23

Koto, T. and K Kodama. 1962. Some considerations on the growth of marlins, using size-frequencies in commercial catches. I. Attempts to estimate the growth of sailfish. *Rep Nankai Reg Fish Res Lab* 15:97–108

Legault, C.M. 1996. A computer-intensive algorithm to create growth transfer matrices for use in age and size simulation models. *Bull. Mar. Sci.* 59(2):444-449.

- Legault, C.M. 1997. Management of a multigear fishery exploiting a highly migratory stock : Spanish mackerel, *Scomberomorus maculatus*, in the eastern Gulf of Mexico. *Dissertation*, University of Miami Division of Marine Biology and Fisheries, Miami, FL.
- Lehodey, P., Chai F., and J. Hampton. 2003. Modelling the climate-related fluctuations of tuna populations from a coupled ocean-biogeochemical-populations dynamics model. *Fish Oceanog* 13 (4/5):483–494
- Levitus, S. 1982. Climatological Atlas of the World Ocean, NOAA Professional Paper No. 13, pp. 191
- MacDonald, P.D.M., and T.J. Pitcher. Age-groups from size-frequency data: a versatile and efficient method of analyzing distribution mixtures. *J. Fish. Res. Board Can.* 36: 987-1001.
- Macías-Zamora R, Vidaurri-Sotelo AL, Santana-Herna'ndez H, Valdez-Flores JJ, Beltra'n-Pimienta R. 2001. Pez vela. In: SAGARPA, editors. Sustentabilidad y pesca responsable en Me'xico Evaluacio'n y Manejo. Mexico: SAGARPA, p 389-410
- Majkowski, J. & Hampton, J. (1982). Deterministic partitioning the catch value of southern bluefin tuna (*Thunnus maccoyii* (Castlenau)) into age-classes using an age-length relationship. In Proceedings of the International Workshop on ' Age determination of oceanic pelagic fishes-tunas, billfishes and sharks, Miami, Feb 15-1 8th 1982. (E. D. Prince, ed.)
- Manching, H. C., Balint-Kurti, P. J., and A.E. Stapleton. 2014. Southern leaf blight disease severity is correlated with decreased maize leaf epiphytic bacterial species richness and the phyllosphere bacterial diversity decline is enhanced by nitrogen fertilization. *Frontiers in Plant Science*, 5, 403. doi: 10.3389/fpls.2014.00403.
- Mason, E., Pascual A., and J.C. McWilliams, 2014. A New Sea Surface Height–Based Code for Oceanic Mesoscale Eddy Tracking. *J. Atmos. Oceanic Technol.*, 31:1181–1188.
- Maunder M. N., et al. 2006. Interpreting catch per unit effort data to assess the status of individual stocks and communities. *ICES J Mar Sci* 63:1373–1385.
- Maunder, M. N., and K.R. Piner. 2015. Contemporary fisheries stock assessment: many issues still remain. *ICES Jour. Mar. Sci.*, 72 (1): 7-18.
- Maunder, M. N., and A. E. Punt. 2004. Standardizing catch and effort data: a review of recent approaches. *Fish. Res.* 70: 141-159.
- McKay, L.R., Ihssen P.E., and G. W. Friars. 1986. Genetic parameters of growth in rainbow trout, *Salmo gairdneri*, prior to maturation. *Can J Genetics Cytology*. 28:306-312.

Ministry of the Fishing Industry of the USSR. 1988. Description of the Fisheries in the Maritime Areas of Nicaragua. Scientific Institute for Fisheries Research and Oceanography of the Atlantic Ocean (AtlantNIRO). Kalingrad. 167 p.

McClenachan, L. 2009. Documenting loss of large trophy fish from the Florida Keys with historical photographs. *Conservation Biology* 23:636-643.

Methot, R. D., and C. R. Wetzel. 2013. Stock synthesis: A biological and statistical framework for fish stock assessment and fishery management. *Fisheries Research* 142: 86-99.

Miyabe, N. and W.H. Bayliff, 1987. A review of the Japanese longline fishery for tunas and billfishes in the Eastern Pacific Ocean, 1971-1980. *Inter.-Amer. Trop. Tuna Comm., Bull.* V 19, No. 1. 163 p.

Munch, S.B., Walsh M., and D.O. Conover. 2005. Harvest selection, genetic correlations, and recruitment: one less thing to worry about? *Can. J. Fish. Aquat. Sci.* 62:802-810.

Murphy, G. I. 1965. A solution of the catch equation. *J. Fish. Res. Board Can.* 22:191-202.

Musyl, M. K., R. W. Brill, C. H. Boggs, D. S. Curran, T. K. Kazama, and M. P. Seki. 2003. Vertical movements of bigeye tuna (*Thunnus obesus*) associated with islands, buoys, and seamounts near the main Hawaiian Islands from archival tagging data. *Fish. Oceanogr.* 12:152-169.

Myers, R. A. and B. Worm. 2003. Rapid worldwide depletion of predatory fish communities. *Nature* 423: 280-283

Nakamura I. 1985. *FAO Species Catalogue. Vol. 5. Billfishes of the World. An Annotated and Illustrated Catalogue of Marlins, Sailfishes, Spearfishes and Swordfishes known to date.* Rome: FAO Fish Synopsis 5: 65 pages.

NORAD/UNDP/FAO Programme. 1988. Surveys of the fish resources on the Pacific shelf from Colombia to Southern Mexico 1987. Reports on Surveys with R/V Dr. Fridtjof Nansen. Institute of Marine Research. Bergen. 94 p.

Parrack, M., and N.J. Cummings. 2003. Errors in transforming length samples to age frequencies without age samples. *Fisheries Res.* 63:235-243.

Paulik, G. J. 1969. Computer simulation models for fisheries research, management, and teaching. *Trans. Am. Fish. Soc.* 98:551-559

Pauly, D. V. 1980. On the interrelationships between natural mortality, growth parameters, and mean environmental temperature in 175 fish stocks. *J. Cons. Int. Explor Mer* 39, 175-92.

- Pauly D. 1983. Length-converted catch curves: A powerful tool for fisheries research in the tropics (Part 1). *Fishbyte* 1(2): 9–13.
- Pauly, D. 1990. Length-converted catch curves: A powerful tool for fisheries research in the tropics. Part 1. *FISHBYTE* 8 (3), pp. 33–38.
- Pauly, D., and N. David. 1981. ELEFAN I, a basic program for the objective extraction of growth parameters from length frequency data. *Meeresforschung* 26, 205-211.
- Pauly, D. 1987. A review of the ELEFAN system for analysis of length-frequency data in fish and aquatic invertebrates. pp. 7-34. In: D. Pauly & G.R. Morgan (Eds.) *Length-Based Methods in Fisheries Research*, ICLARM, Manila, and Kuwait Institute for Scientific Research, Safat.
- Pauly, D. and G.R. Morgan (eds). 1987. Length-based methods in fisheries research. *ICLARM Conf.Proc.*, 13:468 p.
- Pielou, E. C. 1977. *Mathematical ecology*. Wiley, New York, 385 p.
- Pilling, G. M., Apostolaki, P., Failler, P., Floros, C., Large, P. A., Morales-Nin, B., Reglero, P., Stergiou, K. I. and A.C. Tsikliras. 2008. Assessment and Management of Data-Poor Fisheries, in *Advances in Fisheries Science: 50 years on from Beverton and Holt* (eds A. Payne, J. Cotter and T. Potter), Blackwell Publishing Ltd., Oxford, UK.
- Polacheck, T. 2006. Tuna longline catch rates in the Indian Ocean: Did industrial fishing result in a 90% rapid decline in the abundance of large predatory species? *Mar Policy* 30:470–482.
- Paloheimo, J. E., and E. Cadima. 1964. On statistics of mesh selection. *ICNAF Serial No 1394/Doc. No 98*.
- Pope, J.G. 1972. An investigation of the accuracy of Virtual Population Analysis using cohort analysis. *ICNAF Res. Bull.* 9, 65–74.
- Prince, E. D., and C.P. Goodyear. 2006. Hypoxia-base habitat compression of tropic pelagic fishes. *Fish. Oceanogr.* 15 (6): 451–464.
- Prince, E.D., D. B. Holts, D. Snodgrass, E. S. Orbesen, J. Luo, M. L. Domeier, and J. E. Serafy. 2006. Transboundary movement of sailfish, *Istiophorus platypterus*, off the Pacific coast of Central America. *Bull. Mar. Sci.* 79:827–838.
- Prince, E.D., D. W. Lee, C. A. Wilson, and J. M. Dean. 1986. Longevity and age validation of tag-recaptured Atlantic sailfish, *Istiophorus platypterus*, using dorsal spines and otoliths. *Fish. Bull., U.S.* 84:493--502.

- Quinn, T.J. 1987. Standardization of catch per unit of effort for short-term trends in catchability. *Nat. Resource Modeling* 1, 279-96.
- Quinn, T. J. and R. B. Deriso. 1999. *Quantitative Fish Dynamics*. Oxford University Press, New York, New York. 542 pages.
- R Development Core Team. 2014. R Statistical Computing environment.
- Ramírez-Pérez J.S., C. Quiñónez-Velázquez, A.L. Abitia-Cárdenas, and M.N. Melo-Barrer. 2011. Age and growth of sailfish *Istiophorus platypterus* (Shaw in Shaw and Nodder, 1792) from Mazatlan, Sinaloa, Mexico. *Environ. Biol. Fish.* 92: 187–196.
- Richardson, D.E., Cowen R.K., Prince E.D., and S. Sponaugle. 2009. Importance of Straits of Florida spawning ground to Atlantic sailfish (*Istiophorus platypterus*) and blue marlin (*Makaira nigricans*). *Fish Oceanogr* 18:402–418
- Ricker, W E. 1954. Stock and recruitment. *Journal of the Fisheries Research Board*, 11: 559–623
- Ricker, W. E. 1958. Handbook of computations for biological statistics of fish populations. *Fish. Res. Board Can. Bull.* 119. 300 p.
- Ricker, W.E., 1975. Computation and interpretation of biological statistics of fish populations. *Bull. Fish. Res. Board Can.* 191, 1–382
- Robson, D. S. 1966. Estimation of the relative fishing power of individual ships. *International Commission for the Northwest Atlantic Fisheries Bulletin* 3: 5–15.
- Rosas-Alayola, J., A. Hernandez-Herrera, F. Galvan-Magana, L. Abitia-Cardenas, and A.F. Muhlia-Melo. 2002. Diet composition of sailfish (*Istiophorus platypterus*) from the southern Gulf of California, Mexico. *Fish. Res.* 57: 185–195. Ross, D.A., 1970 ed, "Introduction to Oceanography." Harper Collins College Div., NY.
- Russo, T., Mariani, S., Baldi, P., Parisi, A., Magnifico, G., Clausen, L. W., and S. Cataudella. 2009. Progress in modelling herring populations: an individual-based model of growth. *ICES J Mar Sci* 66: 1718–1725.
- Sainsbury, K.J. 1980. Effect of individual variability on the von Bertalanffy growth equation. *Can. J. Fish. Aquat. Sci.* 3(2): 241-7.
- Shingu, C., P. K. Tomlinson, and C. L. Peterson. 1974. A review of the Japanese longline fishery for tunas and billfishes in the eastern Pacific Ocean, 1967-1970. *IA TTC Bull.*, 16:65-230.
- Shimazaki H. and S. Shinomoto. 2007. A method for selecting the bin size of a time histogram *Neural Computation*. Vol. 19(6): 1503-1527

- Sibert, J., Hampton, J., Kleiber, P., and Maunder, M. 2006. Biomass, size, and trophic status of top predators in the Pacific Ocean. *Science* 314: 1773-1776.
- Siegfried, K. I. and Sanso', B. 2006. Two Bayesian methods for estimating parameters of the von Bertalanffy growth equation. *Environmental Biology of Fishes*
- Sippel, T., Holdsworth, J., Dennis, T., and Montgomery, J. 2011. Investigating behavior and population dynamics of striped marlin (*Kajikia audax*) from the southwest Pacific Ocean with satellite tags. *PLoS ONE* 6, e21087
- Sponaugle S, K.D. Walter, K.L. Denit, J.K. Llopiz, and R.K. Cowen. 2010. Variation in pelagic larval growth of Atlantic billfishes: the role of prey composition and selective mortality. *Mar Biol* 157:839–849
- Stilla, U. and K. Hedman. 2010. Feature fusion based on Bayesian network theory for automatic road extraction; in: Soergel, U. (eds.) *Radar Remote Sensing of Urban Areas, Remote Sensing and Digital Image Processing*, Vol. 15, pp 69-86.
- Stammer, D. 1997. Global characteristics of ocean variability estimated from regional TOPEX/POSEIDON altimeter measurements. *J. Phys. Oceanogr.*, 27: 1743–1769.
- Stammer, D. 1998. On eddy characteristics, eddy transports, and mean flow properties. *J. Phys. Oceanogr*, 28: 727–739.
- Stramma, L., G. C. Johnson, E. Firing, and S. Schmidtko. 2010). Eastern Pacific oxygen minimum zones: Supply paths and multidecadal changes, *J. Geophys. Res.*, 115.
- Stumpf, H.G. 1975: Satellite Detection of Upwelling in the Gulf of Tehuantepec, Mexico. *J. Phys. Oceanogr.*, 5, 383–388.
- Teegavarapu, R. S. V. 2014. Statistical corrections of spatially interpolated missing precipitation data estimates. *Hydrol. Process.*, 28: 3789–3808.
- Unwin, D .1981. *Introductory Spatial Analysis*. Methuen Publishing. New York, USA.
- Xie, S.-P., H. Xu, W.S. Kessler and M. Nonaka (2005): Air-sea interaction over the eastern Pacific warm pool: Gap winds, thermocline dome, and atmospheric convection. *J.Climate*, 18(1), 5-20.
- Walsh, M. R., Munch, S. B., Chiba, S. and D.O. Conover. 2006. Maladaptive changes in multiple traits caused by fishing: impediments to population recovery. *Ecology Letters*, 9: 142–148.
- Ward, P. and R.A. Meyers. 2005. Inferring the depth distribution of catchability for pelagic fishes and correcting for variations in the depth of longline fishing gear. *Can. J. Fish. Aquat. Sci.* 63:1130-1142.

Westrheim, S. J., and W. E. Ricker. 1978. Bias in using an age-length key to estimate age-frequency distributions. *J. Fish. Res. Board Can.* 36:184-189.

Willett, C.S., 1996. A study of anticyclonic eddies in the eastern tropical Pacific Ocean with integrated satellite, in situ, and modeled data. Ph.D. Thesis, University of Colorado, 127pp.

Wolter, K., and M.S. Timlin, 1993. Monitoring ENSO in COADS with a seasonally adjusted principal component index. Proc. of the 17th Climate Diagnostics Workshop, Norman, OK, NOAA/NMC/CAC, NSSL, Oklahoma Clim. Survey, CIMMS and the School of Meteor., Univ. of Oklahoma, 52-57.

World Ocean Atlas. 2013. National Oceanographic Data Center.
<https://www.nodc.noaa.gov>

Wyrtki, K., 1964: Upwelling in the Costa Rica Dome. *Fish. Bull.*, 63 (2), 355-372.

Wyrtki, K., 1964: Surface currents of the eastern tropical Pacific Ocean. *Inter-Amer. Tropical Tuna Comm. Bull.*, 9 (5), 270-304.

Wyrtki, K., 1965: Summary of the physical oceanography of the Eastern Pacific Ocean. Univ. Calif. IMR Ref. 65-10, UCSD-34P99-11, 69 pp.

Wyrtki, K., 1967. Circulation and water masses in the eastern equatorial Pacific Ocean. *Int. J. Oceanol. Limnol.*, 1 (2), 117-147.

Wyrtki, K., and R. Kendall, 1967: Transports of the Pacific equatorial countercurrent. *J. Geophys. Res.*, 72 (8), 2073-2076.

Yurov, V.G and J. C. Gonzales. 1971. Possible catches of the *Histiophorus gladius* in the Eastern region of the Pacific Ocean. (In Russian with summary in Spanish). *Sovetsko-Kubinskie Rybokhoziaistvennye Issledovaniya*, 3:104-110 (translated by W.L. Klawe)

Zhou, S. J., A. D. M. Smith and M. Fuller. 2011. Quantitative ecological risk assessment for fishing effects on diverse data-poor non-target species in a multi-sector and multi-gear fishery. *Fisheries Research* 112(3): 168-178.

Appendix A

Profiles of Residuals by Adjusting Mean Size at Age in MIX Analyses

In Chapter 2, mixture distribution analyses, MIX, was used to partition length frequencies of sailfish in the entire EPO to determine size at age distributions. Ages 3 and 4 were fixed according to Cerdaneres-Ladrón De Guevara et al. (2011) direct observation of size at age. By changing mean size at age from estimates in MIX, error is expected to increase. Figure A1 depicts the profile of squared residuals by changing mean size at age in MIX.

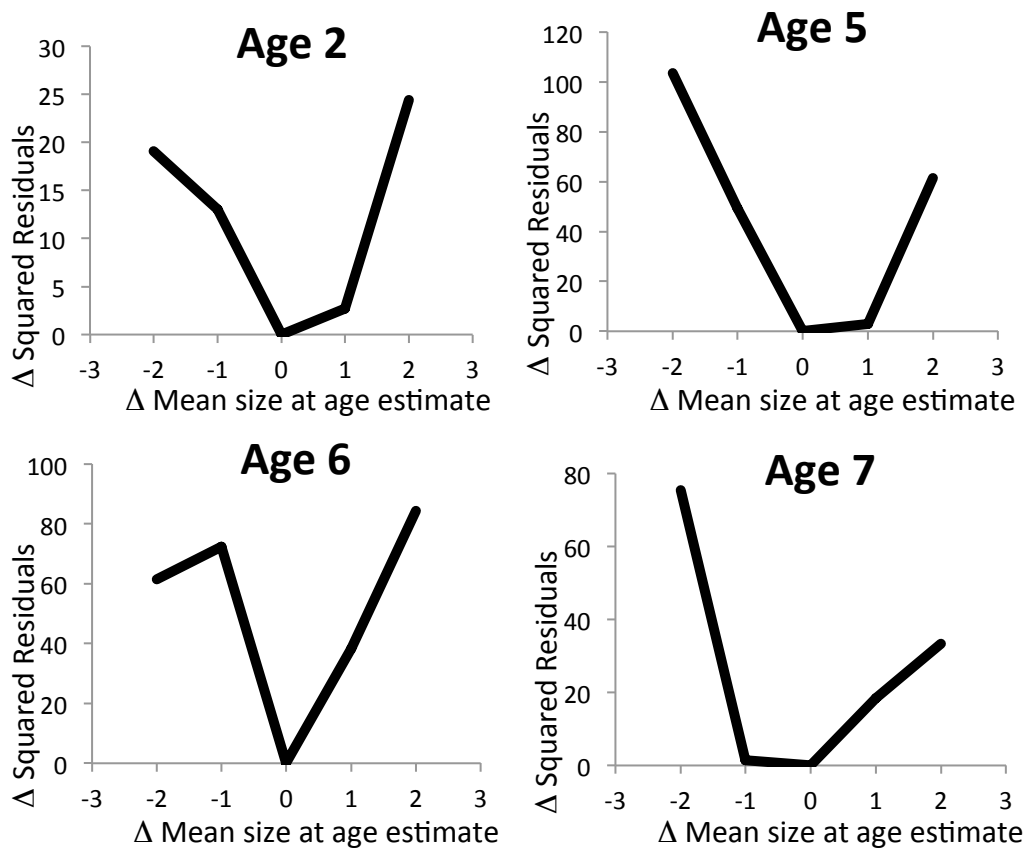


Figure A1. Profiles of change in squared residuals by adjusting mean size at age from mixture distribution analyses of sailfish length-frequencies, 1991-2010.

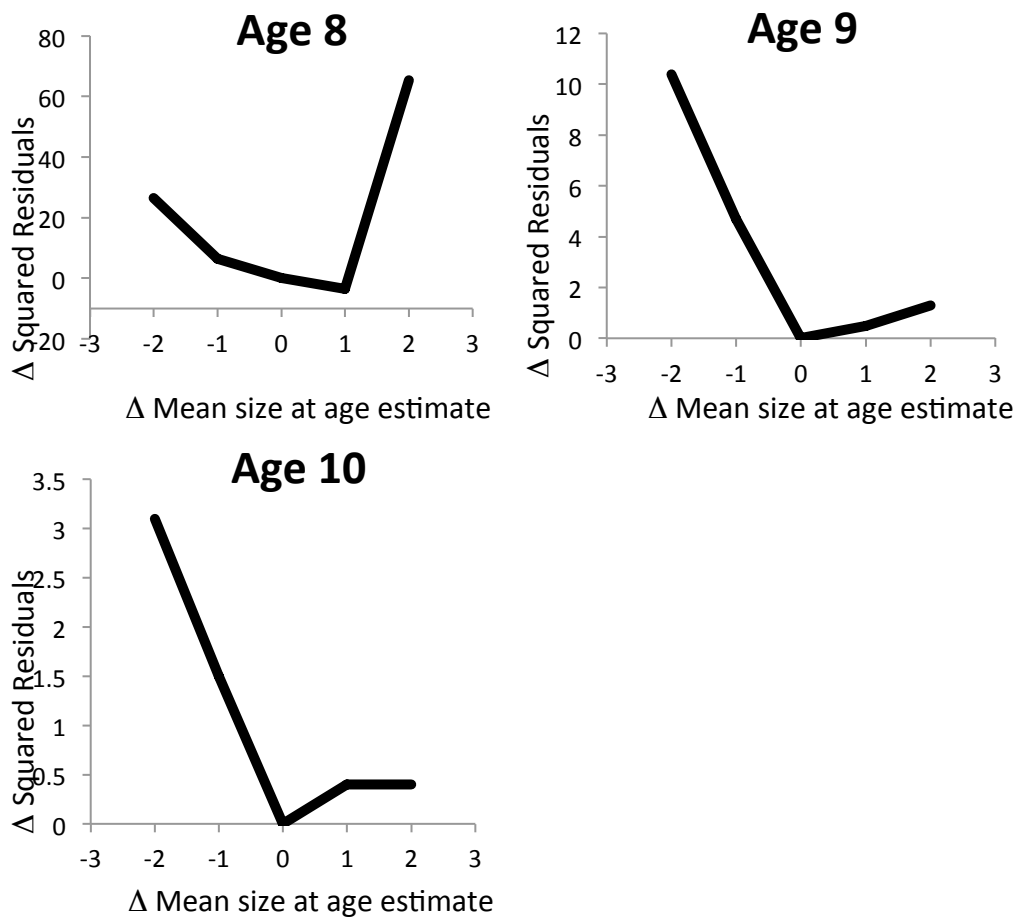


Figure A1 (cont'd). Profiles of change in squared residuals by adjusting mean size at age from mixture distribution analyses of sailfish length-frequencies, 1991-2010.

Appendix B

Introducing a Selectivity Pattern Estimation Methodology

The StALK algorithm may utilize any selectivity pattern, size or age dependent. These can be knife-edge selectivity patterns, polynomials, or any known function. In the following analysis to validate StALKs, a selectivity pattern is derived from length converted catch curve analyses (LCCC, Pauly 1990) by ‘slicing’ ages from length frequencies.

An estimate of the exploitation pattern is important to estimate the age at size from unexploited growth characteristics in the proposed algorithm. Length-converted catch curve analysis provides the means to estimate an approximate relative fishing exploitation pattern because the methodology estimates total instantaneous mortality rate Z for a range of relative ages (a') of fully recruited individuals (t_c to t_λ). Mortality is estimated as the slope of a regression line fitted to the natural log of the catch in numbers (C_j) in a given length class j divided by the time needed to grow through the length class (Δa_j):

$$\log_e\left(\frac{C_j}{\Delta a_j}\right) = b + Za'_j \quad (\text{B1})$$

where Δa_j can be estimated from a von Bertalanffy growth equation as:

$$\Delta a_j = a_{j+1} - a_j = \frac{1}{K} \ln\left(\frac{L_{\infty} - L_j}{L_{\infty} - L_{j+1}}\right). \quad (\text{B2})$$

where a_{j+1} and a_j are the ages corresponding to the upper and lower size limits of a fully recruited size class j . Also, a'_j is the relative age of the animals at the mid-length of the class size j , which is also computed from a von Bertalanffy growth function using the average length in size class j (L_r) as:

$$a' = \frac{\log_e(1 - \frac{L_{t'}}{L_{\infty}})}{-K} \quad (\text{B3})$$

Equations (B2) and (B3) are inserted in equation (B1), which is fitted to annual fully recruited length frequency data. Therefore, a least squares linear regression estimates the slope of a line over the age/size range indicative of full availability.

To determine the selectivity pattern from LCCC fitting, the linear model parameter estimates (b and Z) fitted from age of full recruitment to age of exit from the fishery are used to predict numbers at age from the age of first capture to age of full recruitment (Figure A1) N_a^* . The selectivity values at age, B_a , from age of partial recruitment to the fishery to age of first full recruitment is given by:

$$B_a = \frac{\text{Ln} \left[\frac{C_j}{\Delta a_j} \right]}{\text{Ln} \left[\frac{\hat{C}_j}{\Delta a_j} \right]} = \frac{\text{Ln} \left[\frac{C_j}{\Delta a_j} \right]}{a + Za_j'} \quad (\text{B4})$$

B_a for fully recruited ages is = 1 given that $B_a = \frac{a + Za_j'}{a + Za_j'}$ for any a_j' .

For selectivities of ages beyond the age of full recruitment there is a need to fit another LCCC. This is to estimate selectivity for fish which availability to selection may change (decrease) with size and age. If the trend is non linear then another function (e.g., exponential) may be fitted. The last functions fitted for the range of older not fully recruited ages are used in the same manner as in equation (B4).

To make selectivity at age, B_a , size-specific selectivity, B_a is converted back to lengths j (B_j)

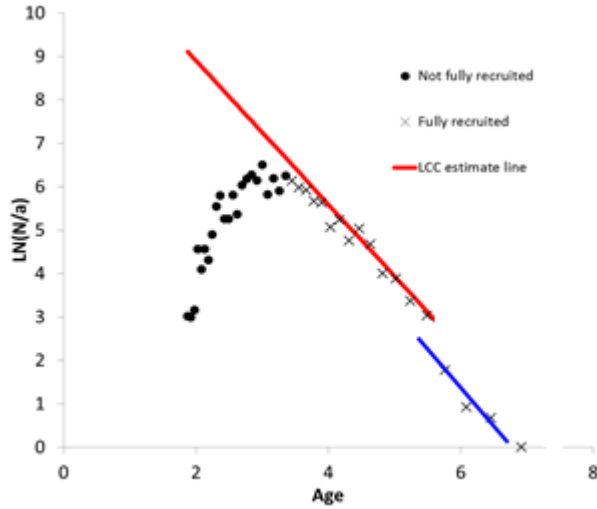


Figure B1. Selectivity in the non-fully recruited stage is estimated as being the ratio between \hat{N}_a the non-fully recruited stock (solid black circles) to the LCCC line estimates for fully recruited fish N_a^* (red line) and fish not fully available (blue line).

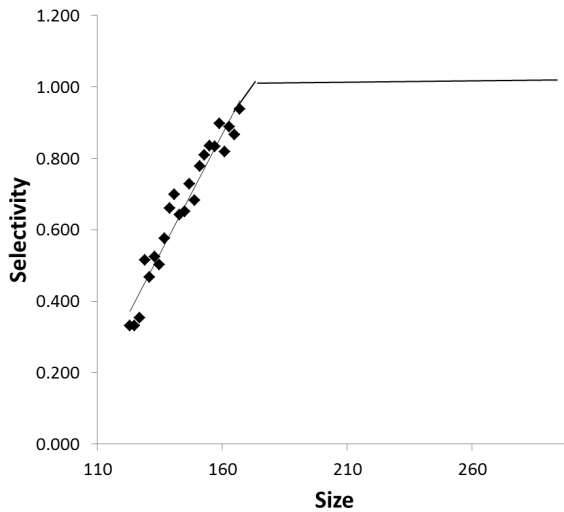


Figure B2. Following application of equation (4) selectivity at length are estimated and a linear relationship fitted (solid black line) and selectivity is equal to equal 1 at fully recruited lengths.

This approach to estimate a selectivity pattern estimates selectivity linearly from size at entry into a fishery to size at full recruitment and assumes selectivity equal 1 from size of full recruitment to maximum size (Figure A2). However, this approach can also estimate linear or non-linear decreasing trends of selectivity from fully exploited sizes to sizes recruited out of the fishery. This method is demonstrated and applied to estimate selectivity of a fishery (2003 red snapper handline and longline fisheries) with known ALKs for validation of the StALK algorithm in Appendix C

Appendix C

Red Snapper Growth, ALKs, and Estimated ALKs

The StALK Algorithm was applied to length frequencies in landings of the US Gulf of Mexico Red Snapper for which extensive ALKs are available. This is done in order to assess the statistical merits and accuracy of the numerical solution to ALK estimation to a case where ALKs are known and, therefore, catch at age are available from direct sampling of landings. This is accomplished by comparing numerically estimated ALKs against the known observed ALK. The Red Snapper ALKs and length-frequencies are for two very contrasting fisheries with very different selectivity patterns with differing size/age recruitment processes, therefore, very different length frequency distributions. Those fisheries are the Hand Line (HL) recreational and commercial fisheries and the longline (LL) commercial fishery. Data for this analysis were obtained from the National Marine Fisheries Service, Southeast Fishery Science Center through MARFIN Project NA10NMF4330116 entitled: “Development of an algorithm to estimate age structures in landings precluding the routine use of age-length-keys for applications in data-poor fisheries and with species that cannot be aged directly”.

Age frequencies at length (ALK) and length frequency data for 2003 represent the most complete database for the species and fisheries. Additionally, 2466 otolith readings for the HL fisheries were made available for this analysis by National Marine Fisheries Service, Panama City Laboratory. Natural mortality estimates for red snapper at age a , M_a , used in the SEDAR 2009 assessment are used as such: $M_0 = 0.5$; $M_1 = 0.3$; $M_2 = 0.2$; $M_3 = 0.2$; $M_4, M_5 \dots M_{20} = 0.1$.

StALK was applied to length frequencies from handline fishery with known means, μ , and standard deviations, σ , at size obtained by Deleveaux (2012)(Table B1).

Table B1. Mean size μ (mm total length) and standard deviation σ for each age class (Estimated from parameters in Deleveaux (2012) Table 2.5, Annex I).

Age	μ	σ
0	15.3	3.8
1	168.4	44.9
2	295.6	54.6
3	401.5	59.9
4	489.5	63.3
5	562.8	65.7
6	623.7	67.5
7	674.5	68.8
8	716.7	69.9
9	751.8	70.7
10	781.0	71.3
11	805.3	71.9
12	825.5	72.3
13	842.3	72.6
14	856.3	72.9
15	868.0	73.2
16	877.7	73.3
17	885.7	73.5
18	892.4	73.6
19	898.0	73.7
20	902.7	73.8

Because of extremely high levels of exploitation observed in these fisheries, fish older than 20 years of age are a rarity; however, it is known that Red Snapper may live close to 50 years (Deleveaux, 2012). In the implementation of StALK a maximum age of 20 years was adopted as potentially present in landings. Seeded recruitment at age 0 was 100,000,000 individuals such that the algorithm can transfer sufficient number of individuals to older age classes even when fishing mortality rates are very high. Size of

recruitment is assumed to be the legal size limit of 15 inches (375 mm) total length. Size frequencies from the fisheries show that 385 mm total length is the smallest fish landed in the LL fishery and 375 mm in the HL fishery. Maximum sizes are assumed to be maximum sizes observed in length frequencies (940 mm for LL and 935 mm for HL).

Table C3. Estimated ALK for Gulf of Mexico red snapper HL fishery using StALK algorithm

	1	2	3	4	5	6	7	8	9	10	11	12	13	14	15	16	17	18	19	20
380	0.286	0.604	0.101	0.008																
390	0.221	0.636	0.132	0.011																
400	0.168	0.649	0.167	0.017																
410	0.112	0.653	0.210	0.025																
420	0.081	0.635	0.252	0.032																
430	0.055	0.630	0.273	0.038	0.004															
440	0.036	0.628	0.279	0.050	0.006															
450	0.026	0.595	0.296	0.073	0.010															
460	0.017	0.566	0.308	0.093	0.016															
470		0.525	0.320	0.132	0.022	0.001														
480		0.443	0.346	0.173	0.033	0.005														
490		0.360	0.354	0.229	0.049	0.008														
500		0.304	0.334	0.281	0.068	0.013														
510		0.246	0.327	0.308	0.099	0.020	0.001													
520		0.178	0.322	0.339	0.126	0.030	0.005													
530		0.127	0.341	0.329	0.161	0.034	0.007													
540		0.084	0.327	0.337	0.193	0.048	0.010	0.000												
550		0.061	0.297	0.318	0.242	0.063	0.017	0.003												
560		0.049	0.256	0.308	0.271	0.090	0.021	0.005												
570		0.037	0.209	0.301	0.303	0.113	0.029	0.008	0.001											
580		0.026	0.184	0.278	0.300	0.154	0.043	0.011	0.003											
590		0.001	0.144	0.276	0.328	0.177	0.054	0.016	0.004	0.000										
600			0.107	0.262	0.317	0.220	0.068	0.020	0.006	0.002										
610			0.077	0.262	0.299	0.233	0.091	0.027	0.009	0.002	0.000									
620			0.055	0.253	0.293	0.239	0.109	0.035	0.012	0.004	0.001									
630			0.041	0.229	0.268	0.262	0.132	0.046	0.015	0.005	0.002	0.000								
640			0.031	0.193	0.245	0.266	0.169	0.063	0.021	0.008	0.003	0.001	0.000							
650			0.023	0.154	0.235	0.275	0.192	0.077	0.028	0.010	0.004	0.001	0.000	0.000						
660			0.017	0.127	0.247	0.254	0.197	0.098	0.038	0.014	0.005	0.002	0.001	0.000	0.000					
670			0.011	0.096	0.243	0.251	0.199	0.124	0.047	0.018	0.007	0.003	0.001	0.000	0.000	0.000				
680			0.008	0.078	0.235	0.223	0.221	0.134	0.060	0.024	0.010	0.004	0.002	0.001	0.000	0.000	0.000	0.000	0.000	
690				0.056	0.205	0.231	0.218	0.152	0.079	0.033	0.014	0.005	0.003	0.001	0.001	0.000	0.000	0.000	0.000	0.000
700				0.043	0.193	0.202	0.219	0.166	0.099	0.044	0.019	0.008	0.004	0.002	0.001	0.000	0.000	0.000	0.000	0.000
710				0.030	0.156	0.217	0.220	0.169	0.109	0.054	0.023	0.011	0.005	0.002	0.001	0.001	0.000	0.000	0.000	0.000
720				0.024	0.130	0.214	0.200	0.178	0.121	0.070	0.033	0.016	0.007	0.004	0.002	0.001	0.001	0.000	0.000	0.000
730				0.017	0.102	0.225	0.187	0.177	0.131	0.076	0.042	0.021	0.010	0.005	0.003	0.001	0.001	0.001	0.001	0.000
740				0.014	0.080	0.191	0.186	0.189	0.140	0.092	0.054	0.025	0.014	0.007	0.004	0.002	0.001	0.001	0.001	0.001
750				0.010	0.058	0.182	0.180	0.175	0.147	0.104	0.066	0.036	0.018	0.010	0.005	0.004	0.002	0.001	0.001	0.001
760				0.007	0.047	0.153	0.188	0.167	0.149	0.111	0.074	0.045	0.025	0.014	0.008	0.005	0.003	0.002	0.002	0.002
770					0.036	0.121	0.208	0.158	0.150	0.119	0.077	0.054	0.033	0.017	0.010	0.007	0.005	0.003	0.002	0.002
780					0.027	0.107	0.183	0.154	0.150	0.125	0.092	0.058	0.041	0.025	0.015	0.009	0.006	0.004	0.003	0.003
790					0.021	0.080	0.164	0.165	0.146	0.127	0.099	0.070	0.044	0.032	0.020	0.013	0.009	0.007	0.005	0.005
800					0.016	0.066	0.150	0.171	0.136	0.126	0.103	0.076	0.054	0.034	0.023	0.018	0.013	0.008	0.006	0.006
810					0.012	0.047	0.120	0.184	0.134	0.125	0.106	0.083	0.061	0.043	0.029	0.021	0.016	0.012	0.009	0.009
820					0.010	0.039	0.102	0.160	0.148	0.124	0.110	0.083	0.063	0.050	0.036	0.027	0.021	0.015	0.012	0.012
830					0.005	0.028	0.085	0.146	0.160	0.121	0.104	0.094	0.075	0.053	0.039	0.031	0.024	0.020	0.016	0.016
840						0.023	0.071	0.125	0.158	0.127	0.109	0.095	0.077	0.061	0.047	0.037	0.030	0.022	0.018	0.018
850						0.017	0.053	0.110	0.150	0.131	0.108	0.098	0.083	0.067	0.049	0.044	0.036	0.029	0.024	0.024
860						0.015	0.042	0.093	0.137	0.150	0.116	0.098	0.080	0.067	0.058	0.046	0.038	0.034	0.026	0.026
870						0.011	0.034	0.077	0.121	0.145	0.128	0.091	0.087	0.076	0.063	0.054	0.046	0.036	0.032	0.032
880						0.009	0.024	0.066	0.107	0.136	0.139	0.110	0.088	0.079	0.063	0.055	0.047	0.043	0.034	0.034
890						0.001	0.021	0.050	0.093	0.128	0.131	0.126	0.092	0.076	0.073	0.065	0.057	0.046	0.042	0.042
900							0.017	0.039	0.076	0.111	0.131	0.133	0.110	0.087	0.073	0.067	0.055	0.053	0.046	0.046
910							0.013	0.031	0.064	0.100	0.125	0.124	0.127	0.104	0.078	0.066	0.065	0.054	0.048	0.048
920							0.010	0.024	0.051	0.085	0.112	0.127	0.120	0.109	0.098	0.081	0.068	0.060	0.055	0.055
930							0.005	0.020	0.041	0.071	0.099	0.118	0.126	0.124	0.112	0.088	0.074	0.068	0.054	0.054
940								0.018	0.035	0.062	0.090	0.111	0.123	0.125	0.104	0.107	0.091	0.067	0.068	0.068

Table C5. Estimated ALK for Gulf of Mexico red snapper LL fishery for StALK

algorithm	Age																			
	1	2	3	4	5	6	7	8	9	10	11	12	13	14	15	16	17	18	19	20
380	0.286	0.604	0.101	0.008																
390	0.221	0.636	0.132	0.011																
400	0.168	0.649	0.167	0.017																
410	0.112	0.652	0.210	0.026																
420	0.081	0.631	0.251	0.037																
430	0.052	0.597	0.298	0.048	0.005															
440	0.031	0.550	0.346	0.065	0.008															
450	0.020	0.474	0.399	0.094	0.013															
460	0.011	0.407	0.407	0.158	0.018															
470		0.341	0.406	0.229	0.024	0.001														
480		0.242	0.476	0.246	0.030	0.005														
490		0.176	0.489	0.289	0.040	0.007														
500		0.132	0.460	0.347	0.051	0.011														
510		0.066	0.460	0.390	0.068	0.015	0.001													
520		0.043	0.388	0.419	0.124	0.021	0.005													
530		0.030	0.351	0.426	0.162	0.025	0.006													
540		0.019	0.294	0.458	0.187	0.033	0.009	0.000												
550		0.011	0.239	0.488	0.209	0.038	0.013	0.003												
560		0.007	0.188	0.508	0.228	0.048	0.016	0.004												
570		0.004	0.140	0.487	0.249	0.093	0.021	0.006	0.000											
580		0.002	0.118	0.467	0.254	0.120	0.029	0.008	0.002											
590		0.000	0.088	0.453	0.282	0.130	0.034	0.011	0.002	0.000										
600			0.050	0.407	0.309	0.169	0.044	0.015	0.004	0.001										
610			0.029	0.338	0.336	0.180	0.090	0.020	0.005	0.001	0.000									
620			0.019	0.292	0.369	0.185	0.103	0.024	0.007	0.002	0.000									
630			0.014	0.260	0.355	0.211	0.120	0.029	0.009	0.002	0.001	0.000								
640			0.010	0.214	0.337	0.223	0.147	0.053	0.012	0.003	0.001	0.000	0.000							
650			0.006	0.166	0.324	0.238	0.172	0.074	0.014	0.004	0.001	0.000	0.000	0.000						
660			0.004	0.135	0.302	0.261	0.182	0.090	0.018	0.005	0.002	0.001	0.000	0.000	0.000					
670			0.002	0.100	0.259	0.299	0.190	0.108	0.033	0.006	0.002	0.001	0.000	0.000	0.000	0.000				
680			0.001	0.053	0.241	0.291	0.232	0.123	0.046	0.008	0.003	0.001	0.000	0.000	0.000	0.000	0.000	0.000	0.000	
690				0.038	0.200	0.310	0.235	0.142	0.056	0.014	0.003	0.001	0.000	0.000	0.000	0.000	0.000	0.000	0.000	0.000
700				0.027	0.183	0.276	0.262	0.158	0.065	0.022	0.004	0.002	0.001	0.000	0.000	0.000	0.000	0.000	0.000	0.000
710				0.018	0.142	0.259	0.316	0.162	0.070	0.024	0.006	0.002	0.001	0.000	0.000	0.000	0.000	0.000	0.000	0.000
720				0.014	0.123	0.235	0.315	0.184	0.084	0.030	0.010	0.002	0.001	0.000	0.000	0.000	0.000	0.000	0.000	0.000
730				0.009	0.100	0.231	0.316	0.197	0.094	0.033	0.013	0.005	0.001	0.001	0.000	0.000	0.000	0.000	0.000	0.000
740				0.006	0.059	0.187	0.323	0.262	0.101	0.039	0.014	0.005	0.002	0.001	0.000	0.000	0.000	0.000	0.000	0.000
750				0.004	0.037	0.185	0.306	0.277	0.115	0.046	0.018	0.007	0.003	0.001	0.000	0.000	0.000	0.000	0.000	0.000
760				0.003	0.031	0.163	0.298	0.290	0.127	0.053	0.021	0.008	0.004	0.002	0.001	0.000	0.000	0.000	0.000	0.000
770					0.023	0.129	0.296	0.290	0.165	0.058	0.022	0.010	0.004	0.002	0.001	0.001	0.000	0.000	0.000	0.000
780					0.017	0.120	0.265	0.299	0.183	0.066	0.027	0.011	0.005	0.003	0.001	0.001	0.000	0.000	0.000	0.000
790					0.013	0.085	0.253	0.307	0.199	0.084	0.032	0.014	0.006	0.003	0.002	0.001	0.001	0.001	0.000	0.000
800					0.010	0.054	0.249	0.305	0.210	0.103	0.036	0.016	0.008	0.004	0.002	0.001	0.001	0.000	0.000	0.000
810					0.007	0.042	0.211	0.322	0.220	0.113	0.046	0.019	0.009	0.005	0.003	0.001	0.001	0.001	0.000	0.000
820					0.005	0.037	0.196	0.299	0.233	0.125	0.059	0.021	0.010	0.006	0.003	0.002	0.001	0.001	0.001	0.000
830					0.002	0.028	0.177	0.292	0.241	0.136	0.062	0.031	0.013	0.007	0.004	0.002	0.001	0.001	0.001	0.001
840						0.025	0.115	0.293	0.258	0.153	0.078	0.039	0.018	0.009	0.005	0.003	0.002	0.001	0.001	0.001
850						0.019	0.091	0.284	0.266	0.154	0.089	0.046	0.025	0.012	0.006	0.004	0.002	0.002	0.001	0.001
860						0.016	0.078	0.264	0.263	0.173	0.096	0.051	0.026	0.015	0.008	0.004	0.003	0.002	0.001	0.001
870						0.012	0.072	0.227	0.266	0.184	0.106	0.055	0.033	0.019	0.012	0.007	0.004	0.002	0.002	0.002
880						0.010	0.060	0.163	0.276	0.202	0.121	0.070	0.040	0.024	0.014	0.009	0.005	0.003	0.002	0.002
890						0.001	0.052	0.141	0.277	0.212	0.124	0.079	0.043	0.026	0.018	0.012	0.008	0.005	0.003	0.003
900							0.046	0.127	0.242	0.216	0.142	0.087	0.053	0.033	0.021	0.014	0.009	0.006	0.004	0.004
910							0.038	0.123	0.174	0.236	0.162	0.095	0.064	0.041	0.025	0.016	0.012	0.008	0.005	0.005
920							0.031	0.108	0.161	0.233	0.166	0.110	0.066	0.043	0.031	0.021	0.014	0.010	0.007	0.007
930							0.019	0.101	0.161	0.175	0.183	0.125	0.083	0.055	0.037	0.024	0.016	0.012	0.008	0.008
940								0.094	0.157	0.156	0.193	0.135	0.092	0.062	0.037	0.030	0.021	0.013	0.010	0.010

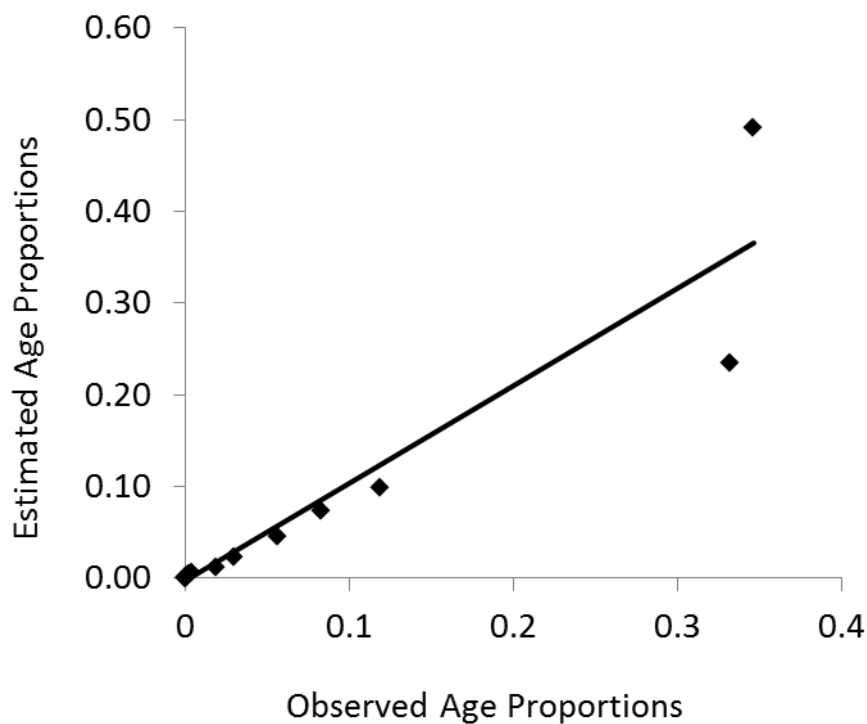


Figure C1. Regression of total age proportions from a known observed ALK versus those of an estimated ALK using the StALK algorithm for Gulf of Mexico red snapper hook and line fishery.

Table C6. ANOVA table and parameter estimate confidence intervals for linear regression of age proportions from a known observed ALK versus those of an estimated ALK using the StALK algorithm for red snapper HL fishery.

	<i>d.f.</i>	<i>SS</i>	<i>MS</i>	<i>F</i>	<i>p-level</i>
<i>Regression</i>	1.	1,367,989.13424	1,367,989.13424	163.36831	0.
<i>Residual</i>	18.	150,725.71101	8,373.65061		
<i>Total</i>	19.	1,518,714.84525			

	<i>Coefficients</i>	<i>Standard Error</i>	<i>LCL</i>	<i>UCL</i>	<i>t Stat</i>	<i>p-level</i>	<i>H0 (5%) rejected?</i>
Intercept	-4.05852	22.80709	-51.97444	43.8574	-0.17795	0.86075	No
OBS	1.03379	0.08088	0.86386	1.20372	12.78156	0.0000000002	Yes

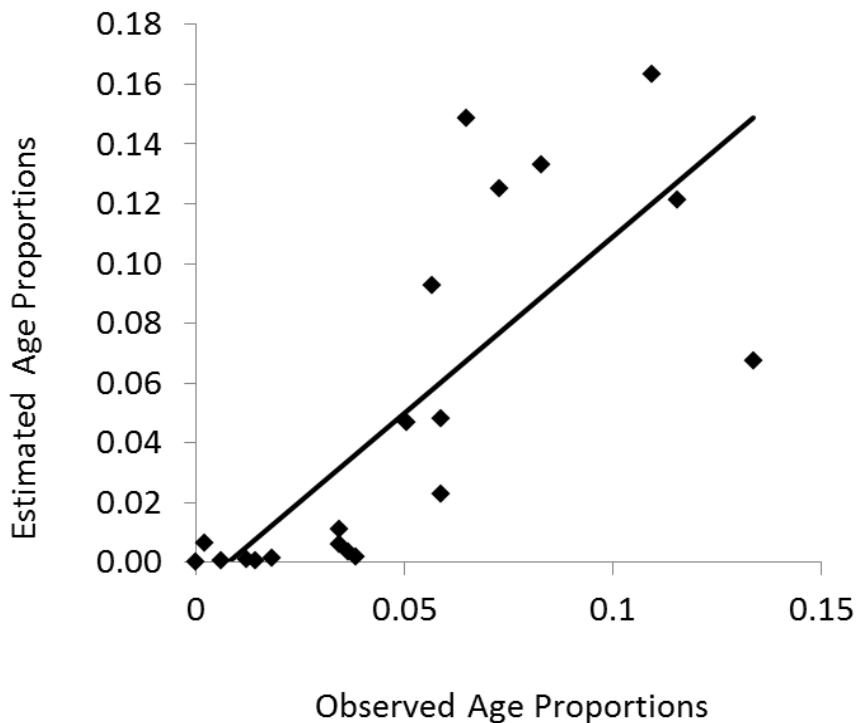


Figure C2. Regression of age proportions from a known observed ALK versus those of an estimated ALK using the StALK algorithm for Gulf of Mexico red snapper longline fishery.

Table C7. ANOVA table and parameter estimate confidence intervals for linear regression of age proportions from a known observed ALK versus those of an estimated ALK using the StALK algorithm for Gulf of Mexico red snapper longline fishery.

	<i>d.f.</i>	<i>SS</i>	<i>MS</i>	<i>F</i>	<i>p-level</i>		
<i>Regression</i>	1.	11,584.2245	11,584.2245	25.47604	0.00008		
<i>Residual</i>	18.	8,184.78898	454.7105				
<i>Total</i>	19.	19,769.01347					

	<i>Coefficients</i>	<i>Standard Error</i>	<i>LCL</i>	<i>UCL</i>	<i>t Stat</i>	<i>p-level</i>	<i>H0 (5%) rejected?</i>
Intercept	-7.96121	8.3521	-25.50832	9.5859	-0.9532	0.35312	No
OBS	1.30117	0.25779	0.75957	1.84277	5.04738	0.00008	Yes

Length frequencies for the HL fisheries are shown in Figure C3. Selectivities for red snapper HL fisheries (C4) are estimated using an LCCC approximation method (Appendix B). Directly estimated ALKs for both red snapper fisheries are given. The numerous empty cells observed in the NMFS database are due to incomplete ALK data collected from landings.. The estimated ALK for the longline fishery contrasts significantly with the observed ALK. One significant advantage of using StALK is that it generates a numerically complete matrix of values. It is also observed that ages older than 9 years are rare in the HL fisheries while much more conspicuous in the LL fishery- presumably due to differing selectivities. Such unbalances in sample allocations do not happen in the numerically estimated ALK.

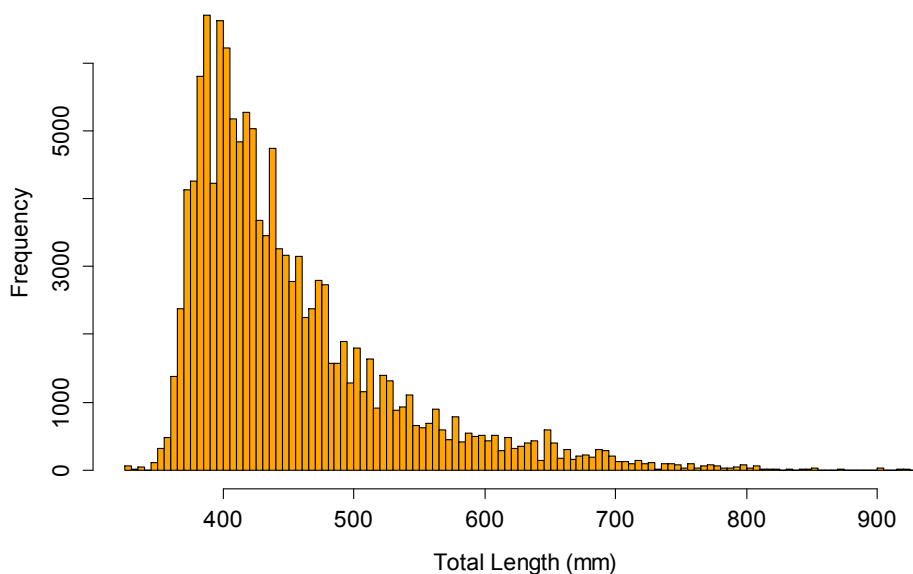


Figure C3. Length frequencies for A) red snapper recreational and commercial hand line fisheries and B) longline fishery for 2003.

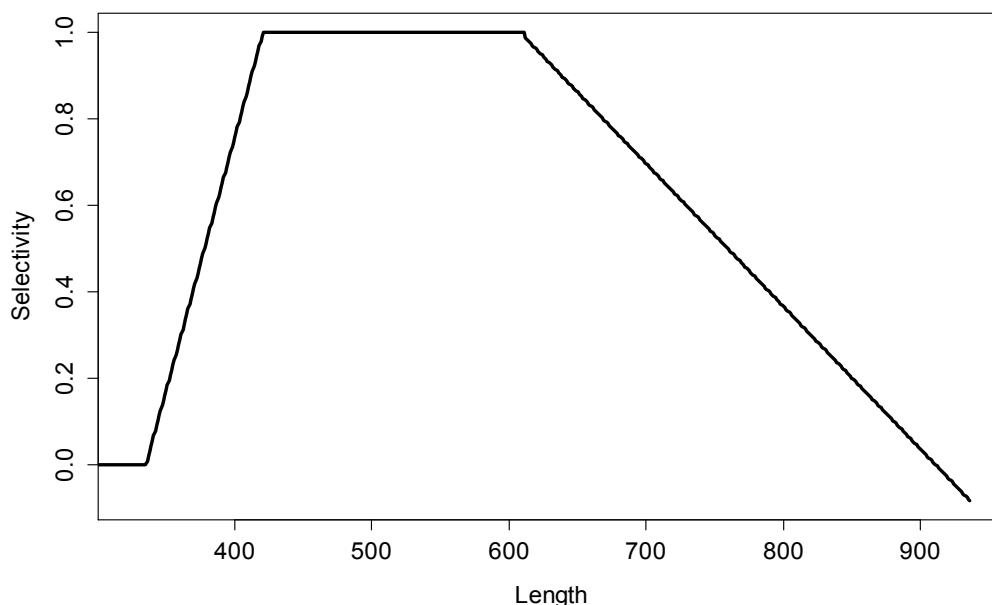


Figure C4. Selectivity for handline (HL) red snapper fishery using a LCCC differential method described in Appendix c.

Linear regression was used to test hypotheses concerning differences between directly observed age at length from samples and the ages at length estimated by the new algorithm. Such hypotheses are based on the idea that if both methodologies on average generate similar age compositions at age, then the slope correlating each data set should have a slope approximately equal to 1. Such comparison for HL fisheries yielded a significant regression ($p < .0001$) with a high coefficient of determination ($R^2 = 0.98$), and a 95% confidence interval for slope that encompasses a slope = 1.0 (Figure C5). The results also show that the intercept is not different than zero (t-test 5% $P = 0.86$). These results show that the estimated ALK from StALK yield proportions of ages at size similar to that of the directly observed ALK for red snapper HL fisheries.

The catch at age data were subjected to a simple age-structured catch curve analysis (ACC) to explore for differences obtained in the assessment of the total instantaneous mortality rate, Z , generated by such model. The results for the HL fisheries are presented in Figure C5. The fitted catch curves are statistical identical and both estimated very similar Z -values of 0.445 for the directly observed ALK and 0.455 for the numerically estimated ALK. This result is expected due to the more complete data set observed in the directly observed ALK, which allowed a better representation of the probabilities of age distributions at size over a wide size range for intermediate size fish. Analysis of covariance (ANCOVA) between age-structure catch curves (ACC) found no significant difference of slopes (Z , total mortality) between StALK estimates and empirical estimates of age frequencies ($P = 0.8$). ACC results and striking similarities of empirical estimates and StALK estimates are in Figure C5.

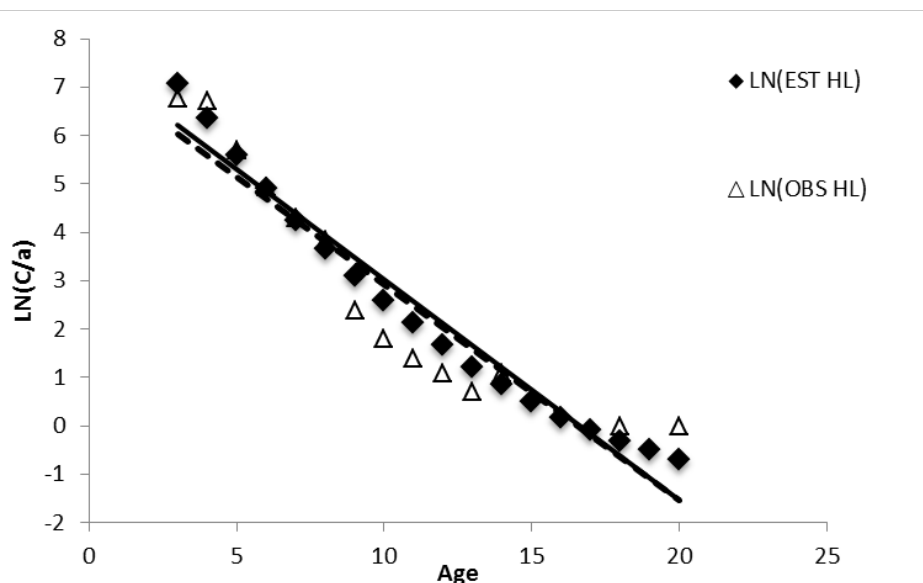


Figure C5. Catch curves for direct observed ALK (dashed line) and numerically estimated ALK (solid line) for the Hand Line Gulf of Mexico Red snapper fishery.

VITA

Mark Daniel Fitchett was born in Burlington, North Carolina on September 19, 1981. He is the son of Walter Reid Fitchett, Jr. and Donna Graven Fitchett of Cary, North Carolina. He has one elder brother, Paul Graven Fitchett of Charlotte, North Carolina. He received his elementary and middle school education from Penny Road Elementary and East Cary Junior High School. From 1996 to 2000, he received his secondary education at Athens Drive High School in Raleigh, North Carolina. In August of 2000, he entered North Carolina State University and graduated with honors and a 3.5 grade point average in May 2004. He holds two degrees from North Carolina State University: a B.S. in Natural Resources with a concentration in Marine and Coastal Resources and a B.S. in Zoology.

In August of 2004, he was admitted to the University of Miami Rosenstiel School of Marine and Atmospheric Science under the academic advising of Professor Nelson M. Ehrhardt. In May 2007, he was granted the degree of Master of Science in Marine Biology and Fisheries. In 2010, he was awarded the prestigious NOAA Fisheries Sea Grant Marine Population Dynamics Fellowship for a three year term. In August 2015, he was granted the degree of Doctor of Philosophy in Marine Biology and Fisheries at the University of Miami.

Permanent Address:

Mark D. Fitchett

301 Kelso Court

Cary, North Carolina 27511